Identification and characterization of key regulatory elements involved in virulence modulations of *Pseudomonas aeruginosa*

by

Maryam Dadashi

A Thesis Submitted to the Faculty of Graduate studies

The University of Manitoba

In partial fulfillment of the requirements for the degree of

Doctor of Philosophy

Department of Oral Biology

Dr. Gerald Niznick College of Dentistry

University of Manitoba

Winnipeg, Manitoba, Canada

Abstract

The opportunistic pathogen *Pseudomonas aeruginosa* is a significant cause of infection in immunocompromised individuals, cystic fibrosis patients, and burn victims. For its survival advantage, the bacterium adapts to a motile or sessile lifestyle when infecting the host. The active type III secretion system in motile bacterial cells enables a cytotoxic effect on the host. In contrast, an operative type VI secretion in sessile bacterial cells embedded in biofilms helps survive against bacterial competitors. *P. aeruginosa* switches between the lifestyles through regulatory pathways, including Gac-Rsm and secondary messengers like c-di-GMP. In this thesis, different molecular techniques were applied to understand the regulatory pathways of H1-T6SS, and the newly identified modulators were characterized.

The results revealed the RNA binding protein RtcB as a switch controller of a motile and sessile bacterial lifestyle. Wildtype PAO1 in in-vitro conditions, armed with an active T3SS and inactive T6SS. In contrast, PAO1(Δ*retS*) bears an active T6SS and repressed T3SS. Deletion of *rtcB* led to simultaneous expression of T3SS and T6SS in both PAO1 and PAO1(Δ*retS*). Furthermore, the deletion of *rtcB* increased the biofilm formation in PAO1(Δ*rtcB*) and restored the motility of PAO1(Δ*rtcB*Δ*retS*). The killing assay showed that H1-T6SS was activated in PAO1(Δ*rtcB*) and could compete against *Escherichia coli*.

Transcriptome analysis was performed for PAO1, PAO1(Δ*rtcB*), PAO1(Δ*retS*), and PAO1(Δ*rtcB*Δ*retS*). It revealed 370 genes of PAO1(Δ*rtcB*) and 1030 genes in PAO1(Δ*rtcB*Δ*retS*) were differentially expressed. That includes genes encoding various virulence factors and the four types of secretion systems. Quantification of c-di-GMP

showed elevated levels in PAO1(Δ*rtcB*), which contributed to the altered phenotype and characteristics of PAO1(Δ*rtcB*).

The long-chain-fatty-acid—CoA ligase FadD1 was also identified as a new player in H1-T6SS regulation in this thesis. It deactivated the expression of H1-T6SS in the absence of sensor kinase RetS. In PAO1(Δ*fadD1*Δ*retS*), the expression of sRNAs RsmY and RsmZ which was essential for activation of H1-T6SS, was repressed, and the intracellular concentrations of c-di-GMP diminished. This alteration led to an elevation in swarming motility, higher cAMP, and restoration of T3SS, wherein PAO1(Δ*retS*) was inactive, indicating that fadD1 plays a role in influencing both H1-T6SS and other virulence factors.

In summary, work from this thesis has revealed a pivotal role of RtcB and FadD1 in the virulence of *P. aeruginosa*. Furthermore, it gives new insights into the complex regulatory network that modulates the switch between T6SS and T3SS in *P. aeruginosa*.

Acknowledgment

I would first like to express my profound gratefulness and appreciation to my thesis advisor, Dr. Kangmin Duan. His encouragement, support, and advice helped me throughout my academic journey. Words cannot say it all but, thank you for everything you have done for me and the patience you had with me. Thank you for all the time you have spent helping me learn and grow.

I would also like to extend my deepest gratitude to my committee members Dr. Prashen Chelikani, Dr. Ayush Kumar, and Dr. Raj Bhullar, for their continuous help and constructive feedback. Your warm and cheerful comments were great motivation to continue the journey.

I am also thankful for the kind and honest mentorship of Dr. Ghavami and Dr. Uzonna. Thank you for your insightful and scientific comments and guidance. I will never forget your help.

Thank you to Dr. Kirouac and Dr. Sa, and Ms. Lisa Chrush for your support, help, and kind friendship.

Thank you to the lab members from Dr. Duan's lab for being helpful, thoughtful, honest, and fun friends throughout my doctorate journey.

I would also thank the College of Dentistry, the Department of Oral Biology, and the funding agencies that supported my academic endeavors and research.

To my lovely friends, I could not be here without your support. Aida, Kathy, Paria, Farnaz, Dr. Shahla, and the late Dr. Forough, thank you for always being there for me.

I would also like to respectfully acknowledge my colleagues from my past clinical work in Laleh hospital. Thank you, Dr. Sajadi, Dr. Tofighi, and Dr. Khandani, for showing me

the most resounding support and motivation; it was such an honor to work with all of you.

Thank you to my family. I am thankful to my cousin Hossein and his wife Somayeh, who took me under their wings and helped me when I first came to Canada. I thank my aunt, Dr. Marzieh Danesh, who mentored me through my academic journey and the challenging days I faced during my life; you are a kind, considerate, caring, and the most knowledgeable physician specialist I know.

My most genuine heartfelt gratitude goes to my sophisticated and open-minded parents, who taught me to grow into the strong, determined person I am today. They showed me how to be persistent and keep working towards my goal even when I experienced challenges and setbacks. Thank you.

A big thank you to my brothers Babak, Maziar, and Mahyar; you always stood up for me and made my life beautiful and meaningful.

To my spouse, soulmate, best friend, and my one and only Yasser, you have made my dreams come true, and you are one of the best things that have happened to me. You have the purest and most innocent heart that gives me everything I have ever wanted. Thank you for choosing me to walk through life with, side by side.

And finally, I am so incredibly thankful for my son Radin, who brings me ultimate joy and happiness every day. I love you, sweetheart, so very much!

Dedication

To my wonderful **parents** for their endless love and support,

who taught me to believe that anything was possible;

And to my beloved son, **Liam**,

who didn't see the beauty of the world;

never got the chance to go to school and learn, dance, sing and laugh.

You will remain in our heart forever, sweetheart

See you on the other side, baby

List of Manuscripts in preparation or published related to this study

---

Manuscripts in preparation

1. **Dadashi, M.**, Chen, L., Duan, K., (2021). Putative RNA ligase RtcB affects the switch between T6SS and T3SS in *Pseudomonas aeruginosa* through c-di-GMP signaling.

   Research Article **(Under Review)**.
2. **Dadashi, M.**, Duan, K., (2021). Presence of circular RNAs in bacterial model *Pseudomonas aeruginosa*.

   Research Report **(Under Review)**.
3. **Dadashi, M.**, Yerex, K., Duan, K., (2021). Long-chain-fatty-acid-CoA--ligase FadD1 modulates T6SS and T3SS through c-di-GMP and cAMP in *Pseudomonas aeruginosa*.

   Research Article **(Drafted)**.
4. **Dadashi, M.**, Duan, K., (2021). The role of stress response regulators on virulence factors of *Pseudomonas aeruginosa*.

   Article Review **(In preparation)**.

Published manuscripts

1. Zhou, C.-M., **Dadashi, M.**, & Wu, Min. (2020). Expanding Roles and Regulatory Networks of LadS/RetS in *Pseudomonas aeruginosa*.

   https://doi.org/10.1201/9780429274817-1

2. Bhagirath, A. Y., Li, Y., Somayajula, D., **Dadashi, M.**, Badr, S., & Duan, K. (2016). Cystic fibrosis lung environment and *Pseudomonas aeruginosa* infection. *BMC Pulmonary Medicine, 16*(1), 174. doi:10.1186/s12890-016-0339-5.

Table of contents

List of Figures

List of Tables

List of Abbreviations

1-2-heptyl-3-hydroxy-4-quinolone	PQS
2-(2-hydroxyphenyl)-thiazole-4 carbaldehyde)	IQS
3-oxo-C12- Homoserine lactone	C12-HSL
Acyl-homoserine lactones	AHLs
Adenylyl cyclases	ACs
Arbitrary primed-PCR	AP-PCR
Autoinducers	AIs
Circular RNA	cRNA
Cyclic AMP	cAMP
Cyclic adenosine monophosphate	cAMP
Cyclic diguanylate	c-di-GMP
Cystic fibrosis	CF
Cystic fibrosis transmembrane regulator	CFTR
Diguanylate cyclase	DGC
Dimethyl sulfoxide	DMSO

Extracellular polymeric substances	EPS
GC-FID	GC-Flame ionization detector
Gas chromatography	GC
Genomic DNA	gDNA
Guanosine monophosphate	GMP
Guanosine triphosphate	GTP
Hydrolytic phosphodiesterases	PDE
Inoue transformation buffer	ITB
Long-chain fatty acids	LCFA
Medium-chain fatty acid	MCFA
Multidrug resistant	MDR
N-butanoyl-L-Homoserine lactone	C4-HSL
Non-coding RNA	ncRNA
Nucleoside diphosphate kinase	NDK
Phenazine-1 carboxylic acid	PCA
Phosphoguanylyl guanosine	pGpG
Polymerase chain reaction	PCR

Pyocyanin	PYO
Quorum sensing	QS
RNA sequencing	RNA-seq
RNase R	RR
Reverse Transcriptase PCR	RT-PCR
Relative centrifugal force or G-force	xg
Short-chain fatty acid	SCFA
Small RNAs	sRNAs
Super optimal broth	SOB
Super optimal broth with catabolite repression	SOC
Threonine phosphorylation	TPP
Two component system	TCS
Type IV pili	TFP

Chapter 1

Introduction

Bacterial pathogens affect a broad host species and cause diseases with significantly diverse symptoms and severities. The pathogens possess virulence traits that facilitate the bacterial establishment, colonization, and infection in the host. To fight against bacterial infections, the first step is to understand and apprehend bacterial virulence and its regulatory network and modulators. Antimicrobial agents' development is left futile by the emersion of multidrug resistance (MDR) bacteria. To overcome this, novel anti-virulence therapeutic agents are a promising way of combating antibiotic resistance by controlling the pathogenicity of bacterial pathogens (Hauser, 2011).

1.1 Characteristics of *Pseudomonas aeruginosa* bacterium

The bacterium *Pseudomonas aeruginosa* belongs to the Gram-negative genus of *Pseudomonas*, which contains 144 species (Gomila et al., 2015). *Pseudomonas* strains can thrive in numerous environmental habitats; plants, animals, and humans, to live and/or cause infection where they find the opportunity (Ramos, 2004). It is a motile, rod-shaped, heterotrophic, and facultative aerobic (Diggle et al., 2020) bacterium. Under an anaerobic environment, the bacterium survives using nitrate as the terminal electron acceptor and arginine (Diggle et al., 2020). It grows well in a wide temperature range of 4 - 42˚C with optimum growth at 37˚C on a medium with minimal salts and a sole carbon source (Diggle et al., 2020). Its large genome (5.5-7 Mbp) supports the bacterium with versatile metabolic needs to encode multiple pathway-related enzymes and transcriptional regulators, virulence factors, and two-component systems (Stover et al., 2000; Klockgether et al., 2011). Over 500 regulatory elements participate in the regulation of virulence factors (Stover et al., 2000). Besides the core genome, the accessory genome (acquired by horizontal gene transfer) and individual mosaics make ongoing changes that

contribute to a continuous modification of the bacterial genome (Klockgether et al., 2011).

1.2 *P. aeruginosa* pathogenicity and its virulence traits

To establish the infection, a variety of virulence factors are produced by *P. aeruginosa*. They are cell-associated structural features like lipopolysaccharides, flagellum, and pili or extracellular effectors, including exotoxins, phenazines, proteases, and pyocyanin (Kipnis et al., 2006). These exotoxins are secreted to the environment, directly to the host, and/or other bacteria (Sharma et al., 2017; Green and Mecsas, 2016; Kepseu, Van Gijsegem et al., 2012). The arsenal of virulence factors ultimately attributes to host-pathogen interaction's fate (do Vale et al., 2016). During the early stages of infection, the bacterium with a planktonic and motile lifestyle induces tissue damage and inflammation in the host tissue (Valentini et al., 2018). By the expression of flagella and pili, the bacteria gets in contact with the host and embarks the translocation of toxins directly to the host tissue through the type three secretion system (T3SS) (Berube et al., 2016). Together with LasB protease, T3SS effectors damage host cells' integrity, lead to rapid bacterial growth and spread, and acute infection in the host (Valentini et al., 2018). When the disease becomes chronic, the bacterium forms a mucoid matrix and loses its motility and T3SS activity, characteristics of planktonic cells. The chronic infection features a sessile biofilm-forming bacterial phenotype (Lam et al., 1980). The biofilm formation promotes the long-term survival and persistent strains, resistant to clearance by the host immune system and drugs (Valentini et al. 2018). The quorum sensing (QS) system has a vital role in the maintenance and elevation of inflammation and biofilm formation (Kievit 2009). The signaling molecule, cyclic diguanylate (c-di-GMP), mediates the switch

between the two *P. aeruginosa* lifestyles (Merritt et al. 2007). The nosocomial infection by *P. aeruginosa*, an increased incidence of multidrug-resistant strains, and the adaptive antibacterial resistance during chronic illnesses entail significant risks to patient's health worldwide. Therefore, it is inevitable to develop novel therapeutic agents against its virulence. To do so, it is necessary to elaborate on the regulatory elements of the bacterium's survival and pathogenicity aspects. **Figure 1.1** represents the virulence factors and the regulatory elements discussed in this study.

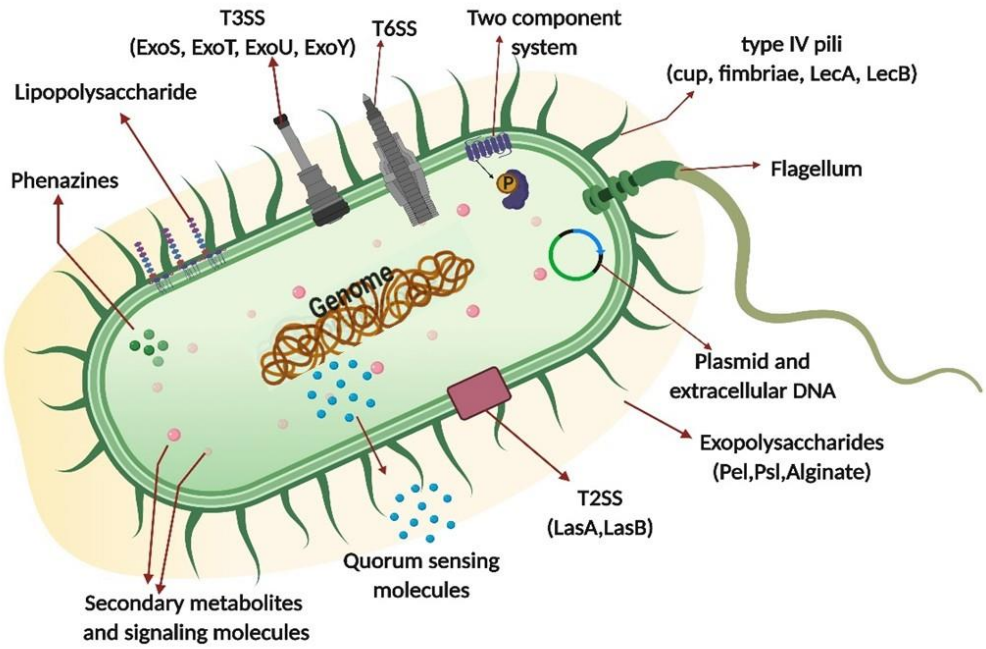

Figure 1.1 The key virulence factors and regulators of *P. aeruginosa* pathogenicity.

The virulence factors of *P. aeruginosa* during acute and chronic infections are modulated through signaling molecules and regulatory networks. The schematic diagram points to some of the cell-associated virulence traits like T3SS, T6SS, lipopolysaccharide, type IV pili, T2SS, and extracellular toxins like phenazines, QS molecules, and exopolysaccharides. The figure represents examples of regulatory elements like two-component systems, secondary metabolites, and quorum sensing molecules. The figure is created with BioRender at BioRender.Com.

1.2.1 **Protein secretory systems**

Prokaryotes have several strategies for protein secretion. Secretion systems are essential for manipulating the host, competing with adjacent prokaryotes, nutrient acquisition, and defense against antimicrobial agents (Green et al., 2016). In diderm (containing two cellular membranes) bacteria, six types of secretion systems (T1SS- T6SS) have been characterized. In contrast, a specific ESX system (T7SS) secretion system is found only in *Mycobacteria* (Abdallah et al. 2007), and a T9SS (Por secretion system) is recently reported in *Bacteroidetes* (Sato et al. 2010). The secretion systems deliver bacterial toxins, so-called effectors, to manipulate the host's fitness (L. Boyer et al. 2012).

Generally, three cargo delivery classes are specified based on the final localization of effectors, crossing only the inner membrane of the bacterium, or both inner and outer membrane, or bacterium membranes and host membrane. (Green et al., 2016). Sec, Tat, and holins, the general secretory machinery, are present in Gram-negative and Gram-positive bacteria and deliver the cargo across the inner membrane (Hutcheon et al., 2003; Denks et al. 2014; Saier et al., 2015). In Gram-negative bacteria, other diverse systems deliver effectors through the outer membrane (Thanassi et al., 2000; Yen et al. 2002). T1, T3, T4, and T6SS transport the proteins through the cell envelope of the bacteria in a single-energy coupled step, although T4SS perhaps does the transport in a two-step process (Tseng et al., 2009; Llosa et al. 2002; Baron, O´Callaghan et al., 2002; Ma et al. 2003; Pantoja et al. 2002). The T2 and T5SS deliver the protein in a two-step process (Tseng et al., 2009). Not all secretion systems are present in a single bacterium.

In *P. aeruginosa*, five out of six secretion systems of Gram-negative's exist. The bacterium harbors Type 1, Type 2, Type 3, Type 5, and Type 6 secretion systems, enabling a wide range of toxin secretion (Bleves et al. 2010). T1SS consists of Apr (Guzzo et al. 1991; Duong et al. 2001) and Has systems (Wandersman et al., 2004). Apr involves the transport of AprA and AprX to the extracellular milieu (Matsumoto 2004). Has system secrets a haemophore HasAP, an essential player in bacterium's fitness at the early stage of infection (Wandersman et al., 2004). Two T2SS are known in *P. aeruginosa*; Xcp (extracellular proteins) and Hxc (homologs to Xcp) (Ruer et al., 2007; Ball et al., 2002). Some Xcp-dependent proteolytic enzymes are LasB, LasA, PaAP, which play an essential role in the bacterium's pathogenicity (Olson et al., 1992; L. S. Engel et al., 1998; Cahan et al., 2001). The LapA effector is produced by the Hxc system in a phosphate-limiting environment (Ball et al., 2002). T2SS is mainly regulated by QS, cell surface signaling system PUMA3, and two-component system (TCS) PhoB/R (Llamas et al., 2009; A. Filloux et al., 1988; Chapon-Hervé et al., 1997). T5SS exists in two subtypes in gram-negative bacteria, the autotransporters (Ats; T5aSS and T5cSS) and two-partner systems T5bSS). EstA is an autotransporter in *P. aeruginosa*, which is required to produce rhamnolipids. The EstA deletion mutant was shown defective in biofilm formation and motility (Wilhelm et al., 2007). AaaA is an autotransporter, important for establishing *P. aeruginosa* infection with arginine-specific aminopeptidase activity (Luckett et al., 2012). EprS is another proposed autotransporter of the bacterium that modulates host inflammatory response in a PAAR-dependent manner and thereby crucial in the virulence of the *P. aeruginosa* (Kida et al., 2013). T3SS and T6SS are

emphasized more in detail and are part of the investigation of this study. T3SS is crucial in killing the host, and T6SS involves killing the eukaryotes and prokaryotes.

1.2.1.1 Type 6 secretion system

Thirteen genes make up the core components of T6SS in *P. aeruginosa,* and they are tightly clustered together (F. Boyer et al., 2009). Three T6SS-dependent loci are present in the bacterium; Called Hcp secretion Island (HSI). HSI-1 (H1- T6SS), HSI-2 (H2-T6SS), HSI-3 (H3-T6SS), was proposed to be acquired horizontally (Filloux et al., 2008). PA0074-PA0091 genes encode H1-T6SS proteins, H2-T6SS by the genes PA1656-PA1671. H3-T6SS proteins, which are located in two divergent operons, are transcribed by the genes PA2359-PA2371 (Alain Filloux et al., 2008). Several toxin effectors of T6SSs were identified, and their mode of action was well characterized. (Sana et al., 2016). In general, H1-T6SS has been studied in more detail, and it is associated with the killing of prokaryotic targets, playing a pivotal role in a multifactorial environment. The H2 and H3- T6SS exert their toxins to both prokaryotes and eukaryotes (Allsopp et al., 2017).

***T6SS structural characteristics*:**

T6SS apparatus resembles an inverted tailed bacteriophage, and its components are categorized in function-specific groups. The genes encoding for TssL, TssJ, TssM proteins make the platform for baseplate assembly and are embedded in the membrane (Zoued et al., 2013). The baseplate proteins are encoded by *tssEFKG,* which supports the biogenesis of the T6SS apparatus (Brunet et al., 2015). The phage-like tail's inner tube is made up of Hcp hexamers (Ballister et al., 2008), wrapped by a contractile sheath of

TssB and TssC proteins (Kudryashev et al., 2015). The TssA protein has a crucial role in docking the baseplate complex and embarks the sheath and inner tube polymerization (Zoued et al., 2017). The puncturing device at the tip of the apparatus is a trimer of VgrG protein, sharpened by a cap-like PAAR protein (Basler et al., 2013; Brunet et al., 2014; Shneider et al., 2013). ClpV is an essential AAA+ ATPase of the system, provides the energy required for the function and needle contraction (Records, 2011). ClpV is also necessary for the depolymerization and polymerization of the T6SS (Planamente et al., 2016). The structural features of the T6SS are depicted in **Figure 1.2**.

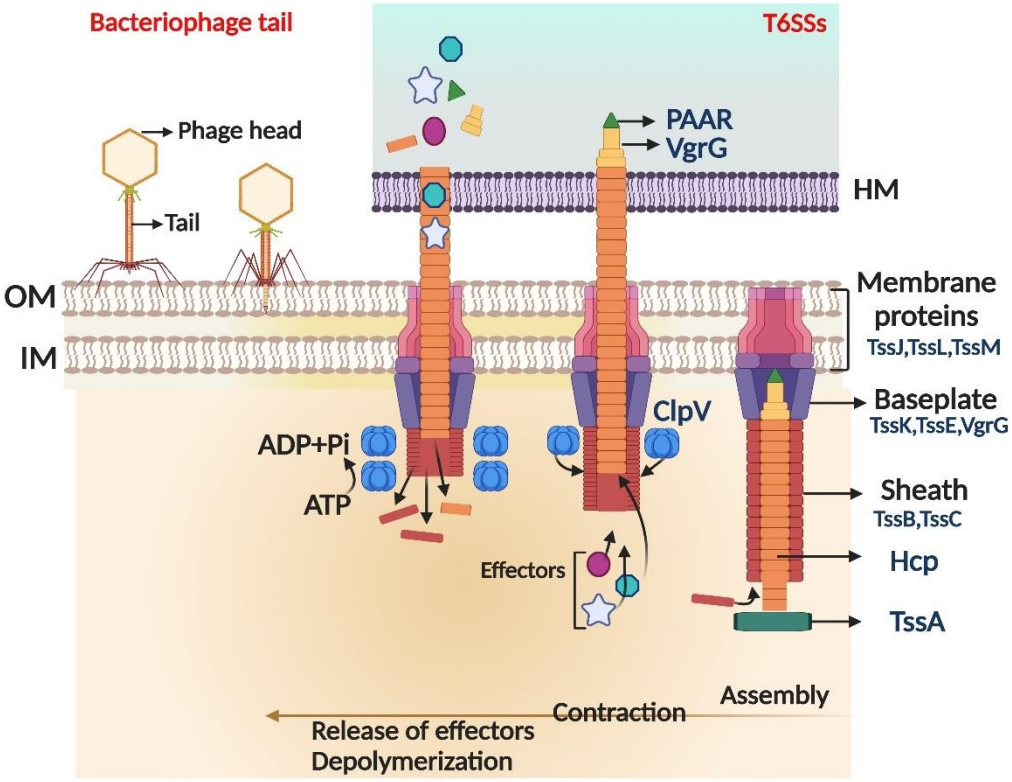

Figure 1.2 Structural features of T6SS and its resemblance to bacteriophage.

T6SS apparatus resembles the contractile tail of bacteriophage (the top left corner) at protein composition, structural and functional level. It consists of membrane-embedded complex, baseplate, and tail components. The proteins composing each part are specified in dark blue. Hcp proteins provide a lumen for the transport of effector proteins through the sheath complex and Hcp. The polymerization of Hcp is initiated upon docking of the TssA to the baseplates. The VgrG spike is sharpened with a PAAR protein as a puncturing device. When releasing the toxins by an unknown cue, ClpV provides the required energy for the sheath subunits' depolymerization to be available for the next depolymerization. HM, host membrane; OM, Outer membrane; IN, inner membrane. The Figure is created at BioRender.Com.

Regulation of T6SS:

Generally, T6SSs are regulated at three levels, including transcriptional, post-transcriptional, and post-translational. At the transcriptional level, the QS system controls the expression of T6SS. While *las, pqs,* and MvfR (PqsR) suppress the H1-T6SS, they promote the expression of H2- and H3-TSS. The *las* cascade affects H1- and H3 indirectly as there is no binding site present on those loci. Moreover, the *rhl* and *pqs* of the QS system positively regulate H2- and H3T6SS but not H1-T6SS (Lasica et al., 2017; Sana, Berni, and Bleves, 2016; Sana et al., 2012).

RsmA is a global regulator of all T6SS at the post-transcriptional level. In the RsmA mutant of *P. aeruginosa* PAK strain, *ppkA*, *pppA*, *hcp1, clpV1,* and *fhA* genes of H1-T6SS were upregulated. RsmA is under the effect of the Gac-Rsm pathway, which will be discussed later. In a study by Allsopp *et al.*, the inhibitory role of RsmA on all T6SS was explained (Allsopp et al., 2017).

Post-translationally, H1-T6SS is regulated by the threonine phosphorylation (TPP)-dependent and TPP-independent pathways. In the TPP-dependent pathway, the serine-threonine kinase PppA dimerizes upon receiving unknown environmental cues and subsequently phosphorylates Fha1 protein. Phosphorylated Fha1 is required for the secretion of Hcp1 (Mougous et al., 2007). The TPP-independent pathway recruits TagR, a protein upstream of the secretion system operon, to suppress the activation of H1-T6SS.

The sigma factor (δ^{54}) RpoN, regulates T6SSs divergently. H3-T6SS has two putative right and left operons. H2- and left H3-T6SS are negatively coregulated by RpoN while H1- and right H3-T6SS are upregulated (Sana et al., 2013).

An exogenous factor that affects the T6SSs is iron, influencing the system through ferric-uptake (Fur) protein. Iron has an essential role in the virulence and metabolism of *P. aeruginosa*. Fur protein is a repressor for both H2- and H3-T6SS in this bacterium (Lin et al., 2017; Sana et al., 2012). These regulatory elements are depicted in **Figure 1.3**.

Effectors and functions of T6SS:

T6SSs are enriched with diverse effectors both structurally and functionally. H1-T6SS exports seven anti-prokaryotic toxins of *tse1- tse7* directly to the nearby bacteria. Their cognate immunity proteins are encoded in their proximity by *tsi1- tsi7* genes. This is to block their toxicity before delivery (Hachani et al., 2014; Whitney et al., 2014; Hood et al., 2010; Sana, Berni, and Bleves, 2016; Pissaridou et al., 2018). H2-T6SS translocate several toxins to prokaryotes and eukaryotes and H3-T6SS uses PldB and TseF to damage the cell wall integrity and to affect the virulence factors (Jiang et al., 2014; Russell et al., 2013; Lu et al., 2013; Barret et al., 2011; Alcoforado Diniz et al., 2015; Hu et al., 2014; Russell et al., 2014; Lin et al., 2017). The effectors of T6SSs are represented in **Figure 1.3**. Type six injectosome is required for successful infection of the host. Sana et al. showed that the survival of *C. elegans* infected with ClpV2 and ClpV3 mutant strains of *P. aeruginosa* PAO1 was higher (Sana et al., 2012; 2013), and mutation of HIS-I from H1-T6SS impaired the pathogenicity of *P. aeruginosa* in a rat model of chronic respiratory infection (Potvin et al., 2003).

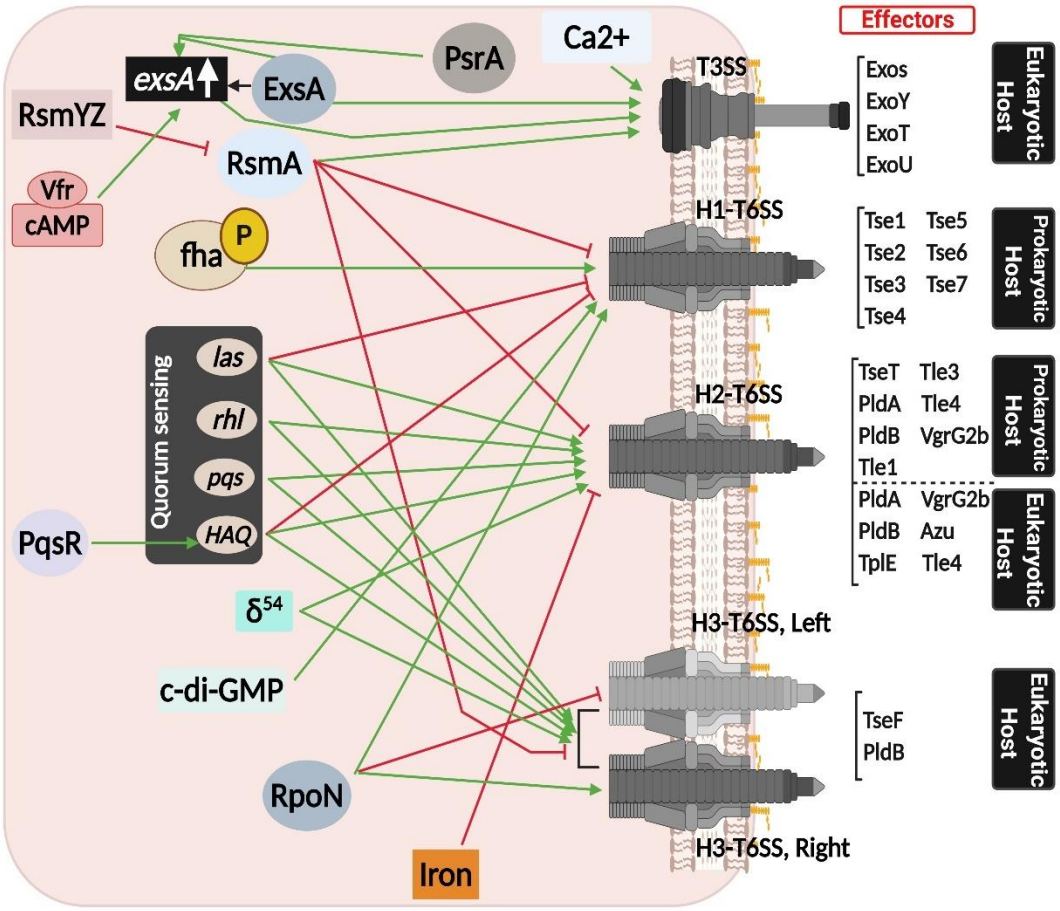

Figure 1.3 An overview of the regulators of T6SS and T3SS in *P. aeruginosa*

P. aeruginosa encodes for three T6SSs (H1-, H2-, H3-T6SS) and T3SS with distinct regulatory pathways. The expression or induction is shown by green arrows, and repressive controls are shown in red. Each T6SSs exports a set of effector proteins to the prokaryotes or eukaryotes. T3SS targets the eukaryotic host cells and induces cytotoxicity and inflammatory response. H1-T6SS effectors exclusively are anti-prokaryotic, while H2-T6SS exports the toxins inter-, and intraspecies. H3-T3SS controls the virulence factors through TseF and PldB. The Figure is created at BioRender.Com.

1.2.1.2 T3SS

Type three secretion system (T3SS) stands as one of the critical virulence determinants of *P. aeruginosa* (Hauser et al., 2003). The syringe-like apparatus is embedded in the bacterium's inner membrane, which infects the host cells through a contact-dependent injection.

Structural features of T3SS:

T3SS syringe comprises a set of proteins for needle complex and a proteinaceous membrane pore to translocate the T3SS effectors by needle complex (Sundin et al., 2004). The shaft of the needle is made up of PscF proteins, which provide a lumen for transportation of the effectors and to sense whether the host cell is in contact with the bacterium (Pastor et al., 2005). PscN is an ATPase of the system and is controlled by PscL (Burghout et al., 2004; Koster et al., 1997). PscC with PscW lipoprotein forms a channel across the outer membrane (Koster et al., 1997; Burghout et al., 2004). PscP regulates the needle's length, and PscJ protein is a basal component of the needle complex (Burns et al., 2008; Journet et al., 2003). The translocation apparatus consists of PcrV, PopB, and PopD proteins (Dacheux et al., 2001), which also contribute as a host cell contact sensor (Armentrout et al., 2016).

Regulation of T3SS:

A two-phase regulation of T3SS occurs at the transcription and secretion level. ExsA is a transcriptional master regulator of T3SS that binds to the promoter of T3SS genes and upregulates the transcription (Brutinel et al., 2008a). ExsCDE modulates it in a "catch

and release" manner. ExcD is an anti-activator that represses ExsA binding to the promoter (McCaw et al., 2002). ExsC binds directly to ExcD and antagonizes its function (Dasgupta et al., 2004).

ExcE inhibits the function of ExsC on ExsD protein by binding to the ExcC when T3SS is not in the secretion phase (Rietsch et al., 2005). When the needle is induced for secretory conditions, ExsE is delivered through the needle and is depleted from the cell. This results in the release of ExsC. Free ExsC sequesters ExsD, and consequently, ExsA is free to bind to its putative ExsA binding site on the promoter of the T3SS genes (Urbanowski et al., 2007).

Other regulatory mechanisms of T3SS include intracellular 3′,5′-cyclic AMP (cAMP), and the Gac system, which is discussed in the future sections. Indeed, in the presence of glutamate, calcium depletion condition, is a trigger for upregulation of T3SS (Rietsch and Mekalanos, 2006; Vallis et al., 1999). Besides, PsrA is involved in the regulation of T3SS. Long-chain fatty acids (LCFA) binds to PsrA and sequester the protein from binding to the promoter region of *exsC* (*exsCp*), lowering the transcription of T3SS-related genes. The regulation of T3SS is represented in **Figure 1.3**.

Effectors and functions of T3SS:

Four toxins were previously reported for T3SS; ExoS, ExoY, ExoT, and ExoU (Hauser, 2009). They interfere with the inflammatory response of the host and promote phagocytosis evasion. Their cytotoxic effect causes host cell damage and tissue destruction (Engel et al., 2009). In 2014, Neeld et al. introduced a nucleoside diphosphate kinase (NDK) exported through a T3SS needle (Neeld et al., 2014). PemA and PemB

effectors were discovered by a machine learning approach and were confirmed in *P. aeruginosa*, where their expression is not essential for the virulence efficacy of the T3SS (Burstein et al., 2015). Although T3SS is the hallmark of acute infections caused by *P. aeruginosa* antibodies (Moss et al., 2001), its functionality is attenuated in chronically infected patients, such as cystic fibrosis patients.

The toxins of T3SS are listed in **Figure 1.3**.

1.2.2 Biofilm formation and social behavior of *P. aeruginosa* in biofilms

Biofilms are sophisticated, resilient structured scaffolds formed on varieties of biological and nonbiological surfaces. More than 90% of biofilm is made by the EPS matrix composed of proteins, extracellular proteins, and polysaccharides (Maurice et al., 2018).

Biofilm formation is the progressive teamwork of different microorganisms in a well-harmonized endless cycle depicted in **Figure 1.4**. In in-vivo conditions, patients suffer from chronic infections of *P. aeruginosa*, caused by a mucoid biofilm-forming bacterium with the progression of the disease (Høiby et al., 2010). Consequently, response to treatments is inadequate, and the pathogen resists eradication by antibiotics and host defense (Bjarnsholt, 2013). By attachment of free-floating cells to the surface, the cells aggregate together and form the biofilm layer. By maturing this layer, cells disperse as a clump or single cells to free-floating planktonic microorganisms and start another cycle (Kostakioti et al., 2013). Several regulatory factors control the transition between the planktonic lifestyle to the multicellular biofilm lifestyle. This is to cope with the environmental changes and as a protective barrier against the host and antibiotics (Kostakioti et al., 2013). sRNAs, two-component systems (TCSs), c-di-GMP, and

quorum sensing (QS) molecules are major regulatory determinants controlling biofilm formation (Yi et al., 2019), which is discussed later. c-di-GMP; controls biofilm production through regulation of flagella and type IV pili, extracellular polymeric substances (EPS) production, stress response, and antimicrobial resistance, biofilm dispersion, expression of surface adhesins, and production of other secondary metabolites (Römling et al., 2013). Interestingly, Bouillet et al., showed that activation of T6SS is an essential cause of RpoS and SoxR stress response system expression, and in the regulation of biofilm ultrastructure by different bacterial species (Dong et al. 2015; Bouillet et al. 2019).

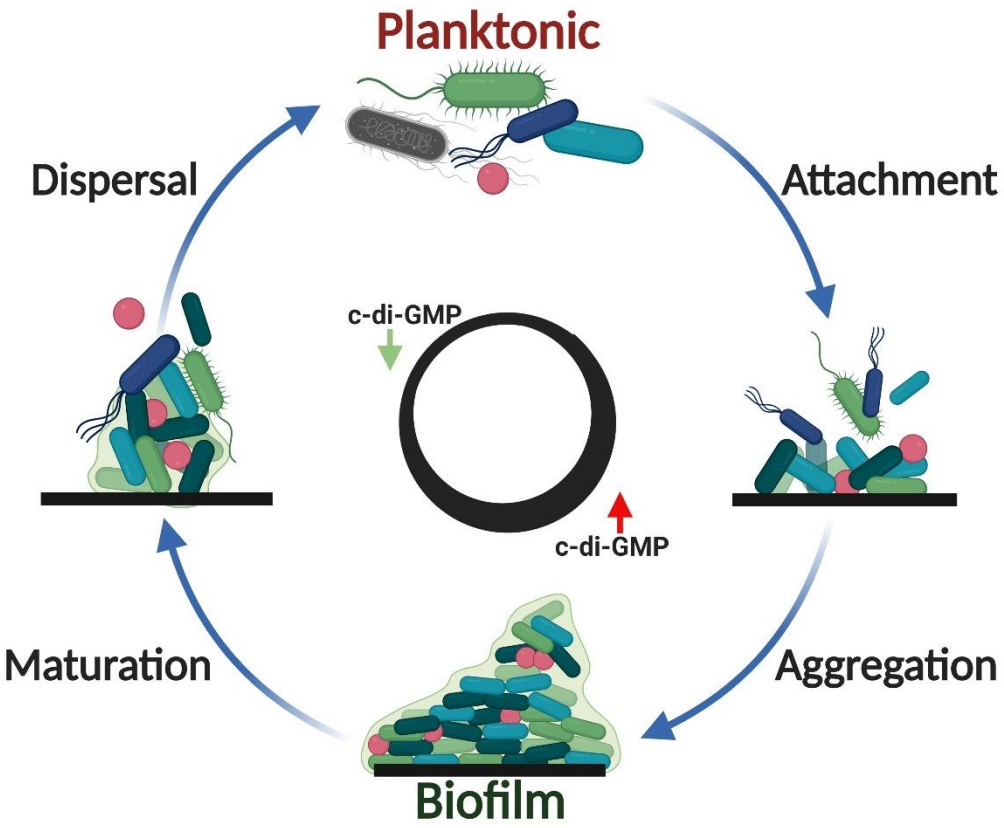

Figure 1.4 The life cycle of *P. aeruginosa*

The formation of biofilms starts with the attachment of the planktonic cells to a suitable surface. This is followed by an aggregation step when bacteria produce EPS and forming a multilayer structured community. After the biofilm matures, some cells or clumps of cells disperse and start another biofilm production cycle, in favorable conditions. With some exceptions, the intracellular concentrations of c-di-GMP control the biofilm cycle. Higher levels of c-di-GMP lead to biofilm formation while lower levels initiate the biofilm dispersal. The Figure is created with BioRender.Com.

1.2.3 **Motility**

Motility plays a pivotal role in the life cycle of *P. aeruginosa* and is necessary for its virulence, biofilm formation/dispersal, and chemotaxis (Vater et al., 2014). *P. aeruginosa* is featured with a single polar flagellum and polar type IV pili (TFP), which give the bacterium the ability of swimming and twitching motilities, respectively (Murray et al., 2008). The swimming motility requires a highly moist surface. It appears like a radial translucent halo zone on the medium (Ha et al., 2014). Loss of functional polar flagellum results in a decreased swimming motility. The direction of swimming is controlled by the chemotactic behavior of the bacteria towards chemoattractant and chemorepellent. Thus, a lack of chemotaxis demonstrates a similar phenotype to the loss of flagellum (Watari et al., 2010; Ha et al., 2014). The twitching motility is independent of swimming and relies on TFP filamentous proteins (Burrows, 2012; Talà et al., 2019). The cell adheres through the adhesins at the tips of TFP and moves the bacteria towards the attachment site. Functional TFP is essential for biofilm formation and dispersal (Burrows, 2012). The bacterium also exhibits swarming motility on semi-solid surfaces, with the aid of TFP and flagellum, in the presence of carbon and nitrogen sources like glucose and glutamate (Köhler et al. 2000; M. Harunur et al., 2000). Generally, swarming motility behavior is correlated with an elevation of adaptive resistance and virulence factors production (Overhage et al., 2008). Moreover, it is dependent on the production of rhamnolipids and its precursor 3-(3-hydroxy alkanoyl oxy) alkanoic acid (HAA), which is synthesized by *rhlABC* genes under the regulation of the RhlR QS regulator (Caiazza et al., 2005). Though a study in 2006 showed that HAA deficient strains of *rhlAB* mutants are still able to swarm in the presence of glutamate and succinate and are dependent on the medium's

nutritional composition (Shrout et al., 2006). When swarming behavior is induced, hundreds of genes related to the virulence and adaptive resistance is overexpressed. At least 35 gene regulators participate in the modulation of swarming, showing the complexity of swarming as a lifestyle change other than merely a physical movement of bacteria (Yeung et al., 2012). In addition to swimming, twitching, and swarming, sliding and surfing motility of *P. aeruginosa* contributes to the displacement of the bacterium in surfactants and mucin, respectively (Yeung et al., 2012; Fall, Kearns et al., 2006).

1.3 Regulation of the transition between chronic and acute infection

P. aeruginosa adapts to the environment by sensing and responding to the availability of its survival requisites. Its large genome and numerous regulatory elements support the bacterium's reaction to the conditions threatening its fitness. Below, the regulatory aspects related to this thesis are discussed.

1.3.1 Gac-Rsm pathway

The two-component system (TCS) GacA/S comprises a sensor kinase (GacS) and a response regulator (GacA). By unknown environmental cues, GacS is autophosphorylated and activates its cognate response regulator GacA in a phosphotransfer manner. The phosphorylation of GacA leads to an upregulation of two small RNAs (sRNAs) RsmY and RsmZ. RsmYZ sRNAs bind to the global transcriptional regulator RsmA and sequester the protein. When not antagonized by sRNAs, RsmA promotes the expression of T3SS genes and negatively affects T6SS (Brencic et al., 2009; Goodman et al., 2004; Allsopp et al., 2017). It involves downregulation of exopolysaccharide-related genes, *pel* and *psl* (Allsopp et al., 2017),

modulation of flagella, type IV pili, T2SS, and rhamnolipids (Valentini et al., 2018). RsmA mutant strains were persistent during chronic infections and were less cytotoxic to epithelial cells during acute infection in mice (Mulcahy et al., 2006).

Hybrid sensor kinase-response regulator RetS is a regulator of several virulence phenotypes of the bacterium as a repressor of T6SS and biofilm; and activator of T3SS (Goodman et al., 2004; Allsopp et al., 2017). It exerts its function through a direct modulatory effect on GacS (Goodman et al., 2009), prevents its autophosphorylation (Brencic et al., 2009). The hybrid sensor kinase PA1611, when expressed, inhibits the negative regulation of RetS on the GacS pathway (Kong et al., 2013). This leads to activation of GacS/A and production of sRNAs RsmYZ. HptB controls the expression of RetS positively and directs the production of virulence factors and T3SS (Bordi et al., 2010) (**Figure 1.4**). In turn, the calcium responsive kinase Lads reciprocally controls the expression of T3SS through interaction with GacA/S TCS. Consequently, the Gac-Rsm pathway functions in transition between acute and chronic infection, although regulators could participate or interfere in this signaling play. Those are independent modulators that affect the transition between the two-phase of infections.

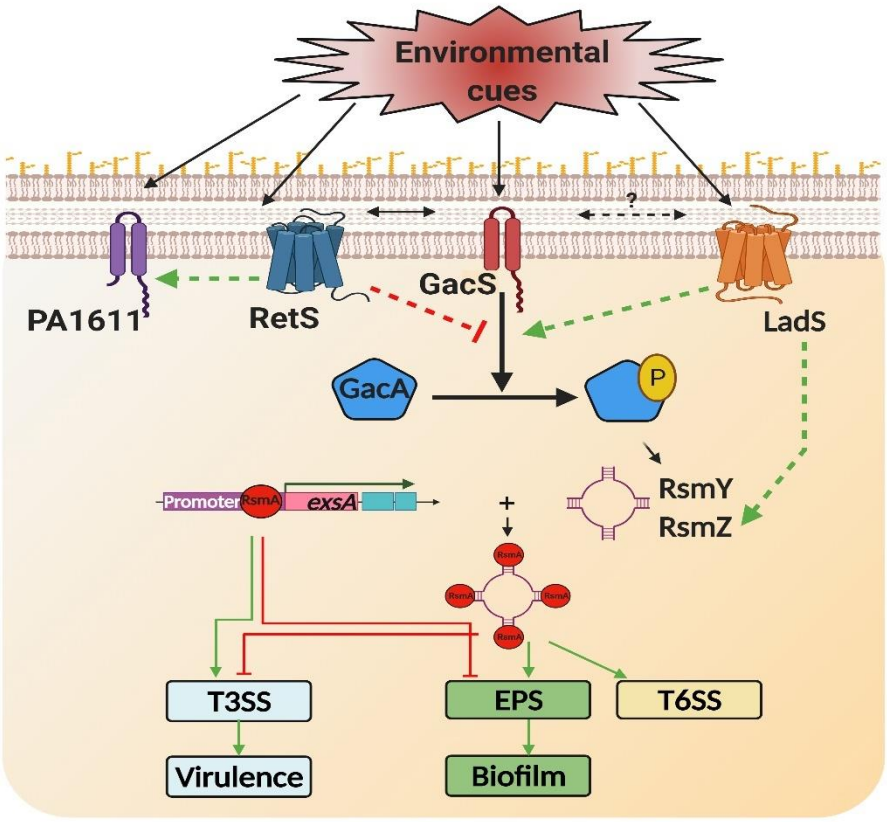

Figure 1.5 Gac-Rsm pathway in *P. aeruginosa*.

The signaling pathway is composed of GacS/GacA TCS, RetS, and LadS membrane proteins that respond to unknown environmental cues. RetS represses phosphorylation of GacA by forming a heterodimer with GacS, while LadS antagonizes RetS function. Also, the direct interaction of RetS with PA1611 removes its inhibitory effect on GacS. When GacS is not inhibited, it upregulates the expression of two sRNAs, RsmY and RsmZ. The RsmY and RsmZ sequester RsmA protein, the translational repressor of many chronic phase-related genes like *pel* exopolysaccharide production and T3SS downregulation. By sequestration of RsmA, the infection switches in favor of a persistent chronic phase, and bacteria enter a sessile biofilm lifestyle. The Figure is created at BioRender.Com.

1.3.2 **Secondary messengers and small regulatory molecules**

Secondary messengers mediate a myriad of cellular functions and signaling cascades in eukaryotes and prokaryotes. In bacteria, cyclic nucleotides play a crucial role from exopolysaccharide production and biofilm formation to cell differentiation, growth, and survival (Ryan et al., 2006; Hee et al., 2020). Below, three important secondary messengers related to this study are discussed.

1.3.2.1 c-di-GMP

The signaling molecule c-di-GMP is a mediator of significant bacterial processes and tunes the transition between mobile and sessile lifestyles (Römling, Galperin, and Gomelsky, 2013). The correlation between high intracellular concentrations of c-di-GMP and biofilm formation versus lower concentrations and motility has been confirmed previously (Simm et al., 2004). The molecule regulates multiple virulences and metabolic determinants such as TFP retraction, flagella rotation, antibiotic resistance and stress responses, adhesin expression, production of secondary metabolites (Römling, Galperin, and Gomelsky, 2013). *P. aeruginosa* biofilms bear approximately 75-110 pmol mg $^{-1}$ c-di-GMP. In contrast, the planktonic cells are estimated to contain $\leq$ 30 pmol mg $^{-1}$ (Basu Roy and Sauer, 2014). These levels are maintained by the antagonistic activity of diguanylate cyclase (DGC) enzymes carrying a GGDEF domain for the biogenesis of c-di-GMP and hydrolytic phosphodiesterases (PDE) enzymes containing EAL or HD-GYP domains (Schirmer and Jenal, 2009). Proteins bearing both GGDEF and EAL domains in tandem, function with the dominant role of one domain (Tamayo, Pratt, and Camilli 2007). C-di-GMP is synthesized from two Guanosine triphosphate (GTP) substrates and

degrades into guanosine monophosphate (GMP) and/or phosphoguanylyl guanosine (pGpG). Cellular receptors of c-di-GMP are an essential part of the signaling cascade to translate the effect of c-di-GMP into a cellular response. In bacteria, these receptors are proteins with the PilZ domain, inactive GGDEF/ EAL/ HD-GYP domain-containing proteins, transcriptional factors, riboswitches, and some RNA processing proteins (Ryan, Groot, and Smith, 2012; Sondermann, Shikuma, and Yildiz, 2012). A strong link between the Gac-Rsm pathway and the c-di-GMP signaling network exists (Moscoso et al., 2014). A functional RsmYZ is required for the effect of c-di-GMP on the Gac-Rsm pathway, wherein *rsmYZ* mutants; low cellular concentrations of c-di-GMP were reported (Moscoso et al., 2014). In turn, RsmA mutants showed a higher concentration of c-di-GMP (Moscoso et al., 2014). C-di-GMP biogenesis is responsive to cellular stress to promote or prevent planktonic/biofilm life (Chua et al., 2015). Moreover, it affects the QS-dependent regulation of motility and biofilms through *las* system response (Petrova et al., 2017).

1.3.2.2 cAMP

The signaling molecule cAMP is synthesized by Adenylyl cyclases (ACs) from ATP, and degradation is carried out by phosphodiesterase (PDE). There are three ACs in *P. aeruginosa*; CyaA, CyaB, ExoY (Yahr et al. 1998a), and one PDE (CpdA). The molecule receives by cAMP-binding proteins CbpA and Vfr, to execute the message (Smith et al. 2004; Wolfgang et al., 2003; Fuchs et al., 2010). CyaB contributes to cAMP's biosynthesis, where CyaB and Vfr mutant showed a lower cellular content of cAMP and virulence attenuation in mice (Smith et al., 2004). In *P. aeruginosa*, CyaAB modulates 181 genes, which 162 of them are under Vfr's regulatory effect (Wolfgang et al., 2003).

Upon receiving cAMP molecules, Vfr functions as a transcriptional activator of virulence factors such as T3-, T2SS, and TFP and represses several genes, *e.g.*, Flagellar biogenesis-related genes (Dasgupta et al., 2002; Wolfgang et al., 2003). Interestingly, the effector protein of T3SS, ExoY, is an AC, which does its adenylyl cyclase activity in the targeted host cells after delivery (Yahr et al., 1998).

1.3.2.3 Phenazines and pyocyanin

Phenazines are diffusible, redox-active small molecules involved in virulence, biofilm formation, and gene expression modulation of the bacteria (Lazdunski, Ventre, and Sturgis, 2004; Hernandez and Newman, 2001). When recognized by neighboring cells, they alter the host gene expression pattern and induce cytotoxicity (Rahme et al., 1995; Caldwell et al., 2009; Ran, Hassett, and Lau, 2003; Dietrich et al., 2008). *P. aeruginosa* harbors two redundant operons of seven genes, *phz1* and *phz2*, which produce enzymes for biosynthesis of phenazine-1 carboxylic acid (PCA) (Mavrodi et al., 2001). Phz1 is flanked by *phzM* and *phzS* genes, encoding enzymes for the conversion of PCA to pyocyanin (PYO). Pyocyanin is an end signaling molecule sufficient and essential for the activation of genes involved in efflux, iron acquisition, and redox processes (Dietrich et al., 2006). A third segregated *phzH* gene encodes an enzyme to modify PCA to phenazine-1-carbamide (Hansford, Holliman, and Herbert, 1972; Byng, Eustice, and Jensen, 1979). Phz1 and Phz2 are under the control of separate promoters (*p*). The *phz1p* contains a *las*-box, recruiting LasR and RhlR transcriptional regulators of the QS system for its regulation (Schuster, Urbanowski, and Greenberg, 2004; Whiteley, Lee, and Greenberg, 1999). Moreover, binding of quinolone signal PQS to the PqsR transcriptional regulator is required for PYO production in *P. aeruginosa* (Xiao et al., 2006; Déziel et

al., 2005). A LasR-RhlR homolog, QscR regulon, negatively regulates Phz2 operon in a GacA-dependent manner (Chugani et al., 2001; Lequette et al., 2006). The major phenazine of *P. aeruginosa* is pyocyanin, which governs at least 22 genes as a final signal of the QS system in the PA14 strains (Dietrich et al., 2006). The expression levels of *phz1* and *phz2* differ in liquid culture vs. biofilm. Although *phz1* is upregulated in aerobic liquid cultures, *phz2* showed a higher contribution to phenazine production. Conversely, *phz2* was highly expressed in biofilms and was almost the solo-producer of phenazines (Recinos et al., 2012). The *phz2* mutant strains were less virulent in the murine model of lung infection. The differential modulation of phenazines supports the bacterium for better adaption to the various environmental conditions (Recinos et al., 2012).

1.4 Quorum sensing

Quorum sensing is a density-dependent chemical communication between a group of synchronized bacteria that contribute to gene expression regulation (Rutherford and Bassler, 2012). Generally, bacteria produce signaling molecules called autoinducers (AIs), which are released into the environment. By accumulating AIs, the threshold concentration is achieved and detected by the response regulator protein (Abisado et al., 2018). The response regulators are transcriptional regulators present in cytoplasm or histidine sensor kinases bound to the membrane (Papenfort and Bassler, 2016). The response process is feed-forward feedback, which increases the production of AIs. This is one of the key roles in maintaining the pathogenicity of bacteria, such as virulence factors production, biofilm formation, and the individual's conjugative behaviors (Abisado et al., 2018). In Gram-positive species, modified short oligopeptides are used as the AIs

signaling molecules wherein Gram-negatives, the main AIs molecules, are acyl-homoserine lactones (AHLs) (Abisado et al., 2018). In *P. aeruginosa* at least four multi-level QS systems have been identified, including Las, Rhl, PQS, and IQS systems, which hierarchically exert their function (Lee et al., 2015). The *las* system consists of *lasI* and *lasR*, present at the top of the hierarchy, and produces 3-oxo-C12-HSL signals. The signal activates the expression of *lasI*, *rhlI*, and *rhlR* of the *rhl* system. Transcriptional activation of the *rhl* system leads to N-butanoyl-L-homoserine lactone production (C4-HSL) with the same positive feedback on *rhlI*. The two other networks, PqsABCDH and AmbBCDE are also regulated by *lasI* and release One-2-heptyl-3-hydroxy-4-quinolone (PQS) and 2-(2-hydroxyphenyl)-thiazole-4 carbaldehyde) (IQS) when expressed (Lee and Zhang, 2015). The interdisciplinary regulation of the QS system of *P. aeruginosa* is depicted in **Figure 1.6**. Moreover, RpoN directly regulates QS-related genes (*lasI*, *rhlI*, *pqsR*) and T6SS genes (*hcpA* and *hcpB*) (Shao et al., 2018).

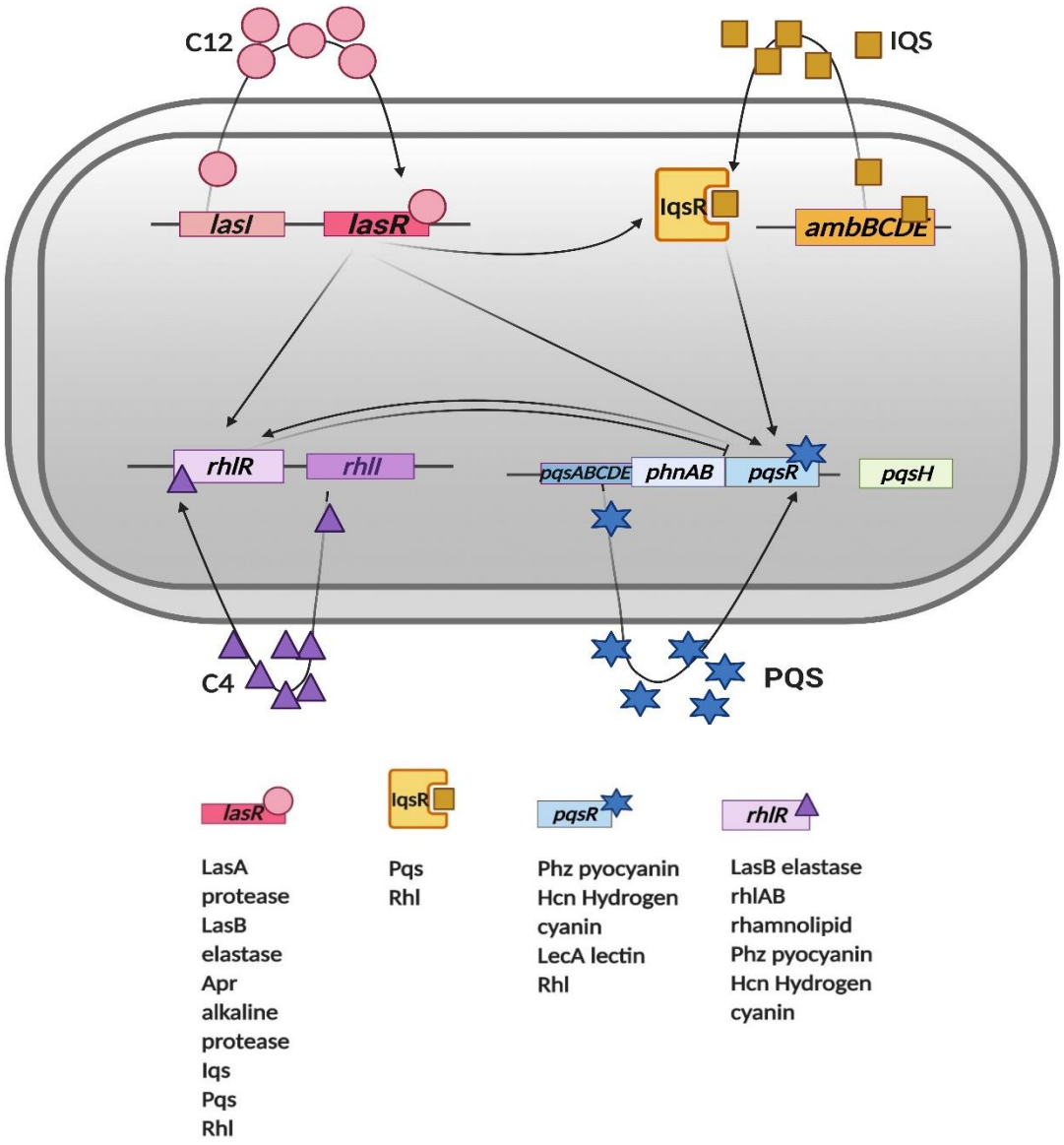

Figure 1.6 Schematic representation of QS signaling network in *P. aeruginosa*.

C12, 3-oxo-C12-HSL; C4, N-butanoyl-L-homoserine lactone; PQS, *Pseudomonas* quinolone signal; IQS, integrating quorum-sensing signal. The arrows show a stimulatory effect. The perpendicular lines indicate the inhibitory effect. Affected virulence factors are shown at the bottom. The Figure is created at BioRender.Com.

1.5 *P. aeruginosa* and polymicrobial infection in the lungs of cystic fibrosis patients

Bacteria thrive in complex polymicrobial communities and often engage in highly sophisticated social, inter- and intraspecies interactions. They live in dynamic biofilms rather than the planktonic form of a single species (Pierson, Wang, and Pierson III, 2013; Peters et al., 2012). The lungs of cystic fibrosis (CF) patients, with a diverse heterogeneous microenvironment (varied pH, oxygen level, nutrients, and antibiotics), is a well-known model of a multi-bacterial organ (Magalhães, Lopes, and Pereira, 2017). A group of phylogenetically distant bacteria makes up the CF lungs' ecosystem (Yang, Jelsbak, and Molin, 2011).

Cystic fibrosis is an autosomal recessive genetic disease that resulted from more than 1500 possible mutations of the cystic fibrosis transmembrane regulator (CFTR) gene (Oliver et al., 2000; Folkesson et al., 2012). The CFTR is a cAMP-regulated chloride ion channel, and its mutations cause dysregulation in electrolyte levels of epithelial surfaces, *e.g.*, lung epithelium (Gellatly and Hancock, 2013). Consequently, the fluid retention decreases and the dehydration leads to a thick and sticky mucus with impaired mucociliary motion (Gellatly and Hancock, 2013; Folkesson et al., 2012). This results in low efficacy clearance of exogenous microbes and provides a rich thickened medium (mucus) promoting bacterial growth (Folkesson et al., 2012).

The pathogens *Staphylococcus aureus, Haemophilus influenzae, P. aeruginosa, Stenotrophomonas maltophilia,* and *Burkholderia cepacia* complex dominantly contribute to colonization in CF lungs and disease progression from birth until an

established chronic infection (Lyczak, Cannon, and Pier, 2002; Hutchison and Govan, 1999; Karpati and Jonasson, 1996; Høiby, 1982). Thus, the CF airways are almost always colonized by bacteria, with a significant contribution of *P. aeruginosa* in CF patients' morbidity and mortality (Folkesson et al., 2012). The introduction of exogenous antibiotics for treatment boosts drug-resistant *P. aeruginosa* compared to other microbes (Folkesson et al., 2012). Yet, *P. aeruginosa* must face the physiochemical variation, challenges by host immune system, and competition from other prokaryotic and eukaryotic species (Williams, Ranjendran, and Ramage, 2016; Bleves et al., 2010; Lyczak, Cannon, and Pier, 2002; Hutchison and Govan, 1999; Folkesson et al., 2012; Chen et al., 2015). Expression of virulence factors like protein secretion systems promotes the competencies and competitiveness of bacterium in the lungs of CF patients, and attenuation of the virulence factors can lower the fitness of *P. aeruginosa* for better therapeutic outcomes.

1.5 Hypothesis and objectives

1.5.1 Study rationale

The bacteria in their natural habitat or inside their host live in a polymicrobial community with social interspecies and trans-kingdom interaction. They adapt, live, and thrive in such environments by the alternation of their gene expression pattern. *P. aeruginosa* is an opportunistic pathogen causing disease in patients with an immunocompromised health condition, cystic fibrosis patients, and individuals with a burnt wound. In CF patients' lungs, it is one of the primary colonizing bacterium entailing the lung function to decline and results in the patient's morbidity and mortality. They induce chronic infection with

the formation of biofilms and resistance to the host defenses. *P. aeruginosa* dedicates an arsenal of virulence factors to induce cytotoxicity in the host or fight back against other prokaryotic and eukaryotic competitors. To do so, more than 500 regulatory elements are known to support the bacteria for its survival fitness (Klockgether et al., 2011).

T6SS is a protein secretory injectosome secreting toxins detrimental to other microorganisms and the host in a contact-dependent manner. In *P. aeruginosa*, three clusters of T6SS are present and encode for H1-, H2-, H3-T6SS, each with distinct and complex regulatory pathways. H1-T6SS injects the antibacterial effectors to the neighboring bacteria (Hood et al., 2010), which is crucial to deal with other prokaryotes in a multi-microbial environment. Some regulators of H1-T6SS were elaborated previously, but our knowledge about its master regulators remains limited.

1.5.2 **Hypothesis**

Although the primary regulatory pathways of T6SSs in *P. aeruginosa* have been investigated, little is known about the global modulators of the T6SS systems. We hypothesize that Gac-Rsm is not the only major regulator of T6SS. Other regulators exist in *P. aeruginosa,* and they can be identified by a robust screening technique like transposon mutagenesis. In addition, potential regulators may not only affect the expression of T6SSs but also influence other virulence factors to alter bacterial pathogenicity.

1.5.3 **Objectives**

To test the above hypothesis, I designed three objectives:

1. To screen and identify probable unknown modulators of H1-T6SS

H1-T6SS plays a vital role in the fitness of *P. aeruginosa* in competition with other bacteria. The novel modulators of H1-T6SS are to be elucidated, and their role in the bacterial competition is to be examined.

2. To determine the role of RNA ligase RtcB on the virulence determinants of *Pseudomonas aeruginosa*

The RNA binding protein RtcB is a stress response regulator in *Escherichia coli*. However, its role in *P. aeruginosa* is not yet understood. The connection between RtcB and significant virulence determinants of *P. aeruginosa* will be elucidated in this objective.

3. To characterize the role of long-chain fatty acid ligase *fadD1* in the regulation of H1-T6SS

To investigate the modulatory effect of FadD1 and characterize the pathway affected by FadD1. FadD1 is a long-chain-fatty acid ligase that involves the transport of exogenous long-chain fatty acids to the cell. The role of FadD1 on T6SS was not previously investigated. This is to elaborate through which mechanism FadD1 controls the expression of T6SS and whether it is connected to the Gac-Rsm pathway of *P. aeruginosa.*

Chapter 2

2 General material and methods

2.1 Materials and equipment

This study's general culture media and antibiotics were purchased from Sigma Aldrich (St. Louis, MO) or Fisher scientific (Toronto, Canada). The antibiotics used: Gentamicin **(**Cat# 355815**),** Tetracycline (Cat # T7660), Ampicillin (Cat # A9393), Carbenicillin (Cat # 10177012),Trimethoprim (Cat # T7883), Kanamycin (Cat # K1377), Carbenicillin (Cat # 10177012). Compounds and kits used: EGTA (Cat# 324626), IPTG(Cat# 15529019), Anaerobic gaspacks (BD, Cat# 260001, 260680), Bacterial Genomic DNA kit (Geneaid, Cat# GBB300), Presto mini plasmid kit (Geneaid, Cat# PDH300), Gel/PCR DNA fragments kit (Geneaid, Cat# DF300), TRIzol™ Plus RNA purification kit (Thermofisher Scientific, Cat#12183555), RNA cleanup kit (Geneaid, Cat# PR050), Pierce™ Coomassie (Bradford) Protein Assay Kit (Thermofisher Scientific, Cat#23200), Clarity MaxWestern ECL Substrate (Bio-Rad, Cat#1705062), Cyclic AMP Select ELISA kit (Cayman Chemical, Cat# 581001), CdiGMP Elisa kit (MyBioSource, Cat# MBS288159).

For Gel-Documentation, Blook LED transilluminator were purchased from Bio-Rad (Mississauga, Canada). For quantitative Real-Time PCR, EcoTM Real-Time PCR System was purchased from MBI (Montreal, Canada); For PCR, LifePro Thermal Cycler was purchased from Bioer Serves Life (Tokyo, Japan). Fusion FX Vilber Lourmat was used for imaging purposes and was purchased from MBI Lab Equipment (Montreal, Canada). For centrifugation, Ultracentrifuge Optima XE-90 purchased from Beckman Coulter (US), Sorvall ST 8R Benchtop Centrifuge purchased from Thermofisher Scientific (Toronto, Canada), and SIGMA 1-14 microcentrifuge purchased from MBI (Montreal, Canada). For electroporation, Pak machine was purchased from BTX Harward Apparatus (US). For electrophoresis, the apparatus was purchased from Bio-Rad (Mississauga,

Canada). For ultrasonic cleaning, FisherbrandTM M Series Mechanical Ultrasonic Cleaning Bath (Cat# 15-337-416) was purchased from Fisher Scientific (Ottawa, Canada). The water bath used was polyscience general-purpose digital water bath, purchased from Scientific Ca (Canada). For sterilization and Autoclave, LV 250 Laboratory Steam Sterilizer was purchased from Steris (Mississauga, Canada). For contamination-free and work safety, 1300 Series Class II, Type A2 Biological Safety Cabinet was purchased from Thermofisher Scientific (Ottawa, Canada).

2.1.1 **Bacterial media and antibiotics**

Pseudomonas Isolation Agar (PIA) (pH 7.0): 20 gl^{-1} Peptone, 1.4 gl^{-1} $MgCl_2$, 10 gl^{-1} K_2SO_4, 25 mgl^{-1} Irgasan™, 2% Glycerol, 13.6 gl^{-1} Agar

Luria-Bertani (LB) Agar: 10 gl^{-1} Tryptone, 5 gl^{-1} Yeast extract, NaCl 5 gl^{-1}, and Agar 15 gl^{-1}

LB broth (pH 7.0): 10 gl^{-1} Tryptone, 5 gl^{-1} Yeast extract, and NaCl 5 gl^{-1}

S**alt-free LB agar:** 10 gl^{-1} Tryptone, 5 gl^{-1} Yeast extract, and Agar 15 gl^{-1}

2X M9 Media salts: 25.6 gl^{-1} Na_2HPO_4, 6 gl^{-1} KH_2PO_4, 2 gl^{-1} NH_4Cl, and 1 gl^{-1} NaCl

SOC media (pH 7.0): 20 gl^{-1} Tryptone, 5 gl^{-1} Yeast extract, 2.5 mM KCl, 10 mM NaCl, 10 mM MgCl2, 20 mM Glucose, 10 mM MgSO4

Swarming media: 8 gl^{-1} Nutrient broth, 5 gl^{-1} Glucose, and 5 gl^{-1} Agar

Swimming media: 10 gl^{-1} Tryptone, 5 gl^{-1} NaCl, and 3 gl^{-1} Agar

Proteolytic agar media: 10 gl^{-1} Tryptone, 5 gl^{-1}Yeast extract, NaCl 5 gl^{-1}, Agar 15 gl^{-1}, 2.5% skim milk

Antibiotics were used at final concentrations (µg/ml):

For *P. aeruginosa*, in PIA agar: Gentamicin (Gm) at 150, Tetracycline (Tc) at 200

For *P. aeruginosa*, in LB agar/broth: Gentamicin (Gm) at 50, Tetracycline (Tc) at 70, Carbenicillin (Cb) at 250, Trimethoprim (TMP) at 300

For *E. coli* in LB Agar/broth: Gentamicin (Gm) at 15, Tetracycline (Tc) at 12.5, Kanamycin (Kn) at 50, Ampicillin (Amp) at 50

2.1.2 Buffers

TAE 50X buffer: 2 M Tris-base, 1M Glacial acetic acid, 50 mM Ethylenediaminetetraacetic acid (EDTA) disodium salt

Agarose loading buffer: 25mg Bromophenol blue, 150mM Tris 3.3ml, Glycerol 6ml, Water up to 10 ml

TBE 10X buffer: 1 M Tris base, 1M Boric acid, 20 mM EDTA

SDS-PAGE 10X Running buffer: 30.3 gl^{-1} Tris base, 144.4 gl^{-1} Glycine, 10 gl^{-1} SDS

SDS-PAGE transfer buffer: 100 ml 10X running buffer, 200 ml Methanol, 700 ml Water

TBS buffer: 6.05 g Tris base, 8.76 g NaCl, adjust pH to 7.5 by HCl, up to 1l Water

TBST: 1l TBS, 1ml Tween20

Loading buffer (2X): 4% SDS, 20% Glycerol, 2-mercaptoethanol 10%, Tris-HCl (pH 6.8) 125mM, Bromophenol blue 0.02%

PBS: 8 g/l NaCl, 200 mg/l KCl, 1.44 g/l Na_2HPO_4, 240 mg/l KH_2PO_4 (pH 7.4)

PIPES 0.5 M (PH 6.7): 15.1g PIPES, pH adjustment 5 M KOH, Milli-Q-Water up to 100 ml

Inoue transformation buffer (ITB): 10.88 g MnCl2 4 H2O, 2.2 g CaCl2 2 H2O, 18.65 g KCl, 20 ml PIPES (0.5 M, pH 6.7), Milli-Q-Water up to 1l

HEPES 1M stock: 238.30 g HEPES, 10 N NaOH for pH adjustment, Water up to 1 l

2.2 Molecular biology techniques

2.2.1 Isolation of Genomic DNA

Bacterial Genomic DNA kit from Geneaid was used for the isolation of bacterial gDNA. A single colony of *Pseudomonas aeruginosa* (PAO1) was cultured into LB broth and incubated overnight at 37˚C with vigorous shaking on a shaker at 225 rpm. A 2 ml of overnight cultured bacteria were pelleted down with centrifugation at 6164 xg for 3 min. The supernatant is discarded, and 180 µl of GT buffer from the kit was added to the pellet. After resuspending the pellet, 20 µl of Proteinase K was added to the suspension and incubated at 60˚C for 10 min. The mixture was inverted slowly during the incubation. Then, 200 µl of GB buffer was added to the sample and vortexed for 10 min. The sample is incubated at 70˚C for more 10 min with occasional inversion during incubation. To

remove the RNA contaminant, 5 µl of RNase A was added to the sample and vortexed, following 5 min incubation. In the DNA binding step, 200 µl of absolute ethanol was added to the sample and shook vigorously. The whole mixture was transferred to the GD column, placed on a collection tube, and centrifuged at 18879 xg for 2 min. The follow-through was discarded. The sample was washed with 600 µl Wash buffer. Wash buffer was discarded after centrifugation, and the column was dried with additional centrifugation for 3 min. GD column was transferred to a fresh and clean microcentrifuge tube, and 100 µl of heated elution buffer was added to the GD column. After 3 min incubation at room temperature (RT), the gDNA was eluted by centrifugation at 14000 for 3 min. The concentration and quality of gDNA were measured with nanodrop, and gDNA elution was aliquoted in 15 µl quantity and kept in -20˚C for further use.

2.2.2 **Isolation of plasmids**

Presto^{TM} mini plasmid kit from Geneaid was used to isolate plasmids. A single colony from plasmid-bearing strain was cultured into LB broth with an appropriate antibiotic(s), incubated overnight at 37˚C on a shaker at 225 rpm speed. The next day, 1ml of culture is harvested by centrifuge at 6164 xg for 3 min. The supernatant was discarded, and the cell pellet was resuspended in 200 µl of PD1 buffer. A 200 µl of PD2 buffer was added, and the sample, vortexed and incubated for 2 min at RT. Later, 300 µl PD3 buffer was added to the tube, and the mixture was neutralized by inverting the tube 10 times gently. The sample was centrifuged for 3 min at 18879 xg, and the supernatant was transferred to the PDH column, which was placed on a collection tube. The PDH column was centrifuged briefly for 30 sec, and the follow-through was discarded. In the wash step, 600 µl of wash buffer was added to the PDH column, following brief centrifugation as mentioned. A

longer centrifuge of 3 min at maximum speed was applied to dry the column. A 30-50 µl of elution buffer was added to the center of PDH columns to elute the plasmid DNA. Plasmid DNA was checked for quality and quantity with nanodrop and confirmed by gel electrophoresis or/and sequencing were necessary, and the aliquots were kept in -20˚C for future use.

2.2.3 **Preparation of chemically competent cells**

2.2.3.1 $CaCl_2$ competent cells of *E. coli*

A colony from *E. coli* DH5α strain was grown overnight in 2 ml LB broth at 37˚C following the protocol by Mandel and Higa (Mandel and Higa, 1970). The following day, a subculture from overnight culture was made into 5 ml LB broth and grown for 5 h or until the optical density reaches 0.5 (OD_{600}). The subcultured samples were placed on ice for 10 min, and cells were harvested at 1541 xg for 7 min. The supernatant was discarded, the pellet was re-suspended in 20 ml ice-cold 100 mM $CaCl_2$ gently, following a 10 min incubation on ice. The cells were harvested once more, and the pellet was suspended in 4 ml 100 mM $CaCl_2$ and another incubation of 30 min on ice. A 1 ml of 80% cold glycerol was added to the suspension (final concertation of glycerol 15%). The competent cells were aliquoted in 100 µl quantity into microcentrifuge tubes and stored in a -80˚C freezer. Ice-cold $CaCl_2$ probably causes a bridge between DNA and the bacterial cell surface and uptake of exogenous DNA.

2.2.3.2 Ultra-competent cells of *E. coli*

Ultracompetent cells were prepared based on the protocol described by Sambrook et al. (Sambrook and Russell 2006). It is crucial to make the buffers used in this method with high-quality water (pure Milli-Q water) and avoid any contaminant to maintain the competent cells' efficiency and transformation rate. A 0.5 M PIPES was made and sterilized by a 0.45-mm Nalgene syringe filter. Aliquots of PIPES were stored at -20˚C. Inoue transformation buffer (ITB) was prepared by adding chemicals and PIPES, listed earlier in the buffer section. The buffer was sterilized with a Nalgene syringe filter (0.45-mm). A single colony from pure and freshly cultured *E.coli* cells was transferred to a 5 ml LB broth and grown for 7 h at 37˚C on a shaker at 225 rpm speed.

A 50 ml of SOB media was used for sub-culturing 1 ml of the starter culture. The subculture was incubated at room temperature for 12 h. This was an approximate time that OD_{600} of the culture reached 0.55nm. The flask was placed on ice for 10 min. Then, the culture was transferred to three 50 ml falcon tubes (each 15 ml), and cells were harvested at 1465 xg for 10 min at 4˚C. The supernatant was discarded, and the tubes were stored upside down on a paper towel for 2 min for removal of the remaining media. Pellets were re-suspended gently by swirling in 45 ml of ice-cold Inoue transformation buffer. Cells were harvested at the same condition; buffer was decanted, and excess buffer was removed on a paper towel. 3 ml of ITB was added, and cells were gently resuspended by swirling. A 0.3 ml of DMSO was added to the mix, and the whole mixture was stored on ice for 10 min. Then, ultracompetent cells were immediately aliquoted into fresh pre-chilled microcentrifuge tubes and stored in a -80˚C freezer.

2.2.4 **Preparation of electrocompetent cells**

2.2.4.1 Electrocompetent cells of *E. coli*

An appropriate strain of *E. coli* cells was grown in 2 ml LB broth at 37˚C overnight (Dower et al., 1988). The next day, 10 ml LB broth was inoculated with 100 µl of overnight culture and was grown for 3 h until the cells reached the log phase of growth. The cells were harvested at 1541 xg for 7 min at 4˚C. The supernatant was decanted, cells were re-suspended in 25 ml of 10 mM HEPES and centrifuged again at the same condition. The wash step was repeated once more, and 10% glycerol was added for the last wash step. The cells were gently harvested, and approximately 1 ml of 10% glycerol was added to the cell pellet (the amount of glycerol added depends on the density of the bacterial pellet). The electrocompetent cells were aliquoted in 100 µl quantity and stored in a -80 freezer.

2.2.4.2 Electrocompetent cells of *P. aeruginosa*

A single colony of *P. aeruginosa* cells was transferred to a 6 ml LB broth with appropriate antibiotics and grown overnight at 37˚C (Choi, Kumar, and Schweizer, 2006). The following day, cells were aliquoted into six microcentrifuge tubes, and the process was continued at room temperature. Cultured cells were harvested at 6164 xg for 3 min following the addition of 1 ml of 0.3 M sucrose to each tube for re-suspension and washing the cell. The mixture was pelleted down at 6164 xg for 3 min, and sucrose wash was repeated two more times. Lately, cells were washed with 10% glycerol and harvested by centrifuge. An appropriate amount of 10% glycerol was added to each tube based on

the cell density. A 100 µl aliquots of the competent cells were frozen at -80˚C for future use.

2.2.5 **Chemical transformation**

Chemically competent *E. coli* cells were taken from the -80 freezer and thawed gradually on ice (Pope and Kent, 1996). A total of 3-5 µl of plasmid/ligation mix was added to the thawed cells and incubated on ice for 30 min. The mixture was heat-shocked at 42˚C for 30 sec and immediately placed on ice for 2 min after heat shock. 900 µl of pre-warmed super optimal broth (SOC) media was added into the tubes and incubated for 90 min at 37˚C on a shaker. After incubation, 200 µl of the transformed bacteria were spread on selective media (agar plates with appropriate antibiotics), and plates were placed in a 37˚C warm room for 12-16 h. For the transformation of ultracompetent cells, the heat shock step was 90 sec (Sambrook and Russell, 2006). The remaining transformation mix was stored at 4˚C.

2.2.6 **Electroporation**

For electroporation of *E. coli* and *P. aeruginosa* cells, 2 mm universal fit cuvettes were used. The cuvettes were placed into an ice bucket for 1 hour (Choi, Kumar, and Schweizer, 2006). Electrocompetent cells were thawed on ice. 3-4 µl of plasmid or ligation mix was added to the cells and mixed gently by flicking. The entire mixture was transferred to the center of the cuvette with a broad tip gently to avoid any bubble formation. Electroporation was carried quickly at 1250 V for *E. coli* and 2500 V for *P. aeruginosa*. Then, 500 µl of pre-warmed SOC media was added to the cuvette and mixed by tapping the cuvette. The whole suspension was transferred to a microcentrifuge and

incubated at 37˚C for 90 min. A 200 ml of transformed cells were spread on selective plates and left at 37˚C for 12-16 h until visible colonies appear. The remaining transformation mix was stored at 4˚C.

2.2.7 **Construction of gene expression reporter system and measurement of the expression**

Initially, the promoterless plasmid pMS402 carrying the *luxCDABE* reporter cluster was used to construct chromosomal reporter fusion (Duan et al., 2003). The desired gene promoter (*p*) was PCR-amplified and cloned into the *BamH*I-*Xho*I site upstream of the *lux*-Box on pMS402. The resultant plasmid is called pKD*p*- reporter, which bears the kanamycin resistance marker, was grown on kanamycin plates and was confirmed with PCR and agarose gel electrophoresis. *Pac*I digested fragment of pKD*p* cloned into the digested integration plasmid CTX6.1, originated from mini-CTX-*lux*; to generate a chromosomally integrated reporter (Becher and Schweizer, 2000). CTX*p* was transferred to *E. coli* SM10-λ *pir* (Simon, Priefer, and Pühler, 1983), and biparental-mating between *E. coli* SM10-λ *pir* and *P. aeruginosa* was set up to construct the x-reporter strain *Pseudomonas* (Hoang et al. 2000; Liang et al., 2008). Gene expression measurements were carried out by quantifying the light production (luminescence per second-LPS) of the reporter strain using Synergy2 Multimode Microplate Reader (BioTek). Bacterial growth indeed was recorded at OD_{600} during the luminescence readout. The measurement continued for 24h with 30 min intervals at 37˚C.

2.2.8 **Bi-parental mating**

Bi-parental mating was used to produce a *P. aeruginosa lux*-based integration reporter (Liang et al., 2008) with brief modification. SM10λ*pir* strain of *E. coli* (Simon, Priefer, and Pühler, 1983) bore mobilizing element and was used for conjugation with *P. aeruginosa*. A clone of integration plasmid CTX6.1 (Becher and Schweizer, 2000); originated from plasmid mini-CTX-*lux*, with the desired insert were transferred to the SM10λ*pir* strain. Both *E. coli* and *P. aeruginosa* were grown overnight at 37˚C with agitation at 225 pm. The next day, 35 µl of *E. coli* SM10λ*pir* was spotted on an LB plate, air-dried, and incubated at 37˚C for 2 h. During this time, *P. aeruginosa* was placed at 42˚C for 2 h to deactivate the recipient's restriction-modification enzymes, which inhibit the cells from the uptake of exogenous DNA. After 2 h, 35 µl of *P. aeruginosa* was placed on the *E. coli* strain, spotted before, and left for 6-12 h of incubation in 37˚C. The inoculant was scraped after incubation time, re-suspended in LB broth, and grown for 1 h at 37˚C. 200 µl of culture was spread on selective media and was grown overnight until colonies appeared. The grown colonies bear the plasmid construct in their chromosome, which makes a stable recombinant strain. The colonies were confirmed with colony-PCR and agarose gel electrophoresis.

2.2.9 **Tri-parental mating**

To generate knockout mutants, the *sacB*-based method was applied as described previously (Hoang et al., 1998) with brief modification. *P. aeruginosa* recipient cells, *E. coli* donor cells (bearing pEX18Tc suicide vector construct for the generation of mutant strains), and *E. coli* helper strain containing mobilizing plasmid pRK2013 (Figurski and Helinski, 1979) was used. The bacteria were grown in LB broth with appropriate antibiotics and at 37˚C for 12-16 h. The next day, 35 µl of donor and 35 µl of helper

strain were mixed by flicking in a fresh microcentrifuge tube, and the whole mixture was spotted gently on a well-dried LB plate. The plate was incubated at 37˚C. At the same time, the recipient strain was placed at 42˚C for 2 h. After incubation time, 35 µl of recipient strain was spotted on top of donor and helper strain. It was air-dried and left at 37˚C for 6-12h. Later, the co-culture was scraped from the LB plate, re-suspended in 1 ml LB broth, and grown for 90 min at 37˚C with 225 rpm agitation. Next, 200 µl of the mixture was spread on plates containing Tetracycline at 200 µg ml^{-1} and grown overnight for the appearance of first crossed colonies. Ultimately, strains with the second crossover even were selected on salt-free LB plates supplemented with 8-10 % sucrose (Hmelo et al., 2015).

2.2.10 **Transposon mutagenesis library construction**

Transposon mutant library was constructed following a published protocol (Kulasekara, 2014). The transposon vector used was pBT20, bearing Himar1C9 transposase with 50-fold higher transposition activity (Lampe et al., 1999) and gentamicin resistance marker (Gm^r). For conjugation, the *E. coli* strain SM10λ*pir* was used (donor). LB media was used to grow *E. coli* and *P. aeruginosa* CTX-H1-Δ*retS* strain (recipient). H1 system is one of the three types 6 secretion systems (T6SSs) in *P. aeruginosa* and is consecutively active in PAO1(Δ*retS*), while it is not expressed in wild type *P. aeruginosa* PAO1. PAO1(Δ*retS*) was used as a T6SS dynamic strain ($T6SS^+$) for transposon library construction. Donor and recipient bacteria were streaked with a sterile cotton swab on a LB plate and grown overnight at 37˚C. Next day, cultures were scraped and transferred to 2 ml of LB broth separately and resuspended for dissolving any auto-aggregation specifically in recipient strain. Bacterial density was measured by adding 10 µl of each

strain to 990 µl of LB and measured OD at 600nm with spectrophotometer. The OD of original suspension was acquired by multiplying the OD_{600} of cultures by 100. A 500 µl of each strain were aliquoted and OD were adjusted by following equation to set up a conjugation between donor and recipient in 2:1 ratio.

Donor : (OD_{600} of SM10λ*pir*×500 ÷ 40) −500 = **p** (Dilution factor, µl)

Recipient : (OD_{600} of *P. aeruginosa*×500 ÷ 20) −500 = **q** (Dilution factor, µl)

→ **p** µl of LB broth was added to the donor, and **q** µl of LB broth was added to the recipient.

The final OD of donor and recipient were measured again to confirm the desired OD reached 40 and 20, respectively. A 300 µl of each donor and recipient with adjusted OD were mixed gently, and multiple spots of 50 µl were placed on well-dried LB plates. The plates were incubated for 2 h at 37˚C. After 2 h, the culture spots were scraped and diluted in cold PBS buffer and plated in PIA plates containing 150 µg ml^{-1} gentamicin with the aid of glass beads. Total 500 plates were spread, and a minimum of 60000 colonies was screened; colonies with altered reporter activity were selected under Fusion FX imaging machine for further PCR and sequencing.

2.2.11 **Polymerase chain reaction (PCR)**

The widely used molecular biology technique, Polymerase Chain Reaction (PCR), relies on a thermal cycler machine (LifePro in this thesis) and a thermostable DNA polymerase enzyme to generate a million copies of the desired DNA fragment. The cycles of a PCR reaction include denaturation of template, annealing of primers, and extension of amplicons. Templates were gDNA or plasmid DNA. At 95˚C, the two strands of DNA

template were denatured, and at 58-62˚C, the primers were annealed to relaxed strands. At 72˚C, extension occurred at 1 min for the first 2 kb, and for any additional kb, 1 min was added. Per every 50 µl reaction mix 5 µl of 10X Taq buffer, 5 µl dNTP mix (Thermofisher), 1 µl of each10mM forward and reverse primers, 100ng DNA template, 1 µl Taq DNA Polymerase (Thermofisher), 1 µl of 25mM MgCl2 and nuclease-free water up to 50 µl, were added. The amplicons were analyzed for size accuracy by agarose gel electrophoresis. To load the agarose gel containing SYBR Safe DNA Gel Stain (Invitrogen), 2 µl of DNA loading buffer were mixed with 2 µl of PCR product. The mixture was loaded into a well with a 2 µl DNA ladder (Thermofisher) loaded on the side. The gel percentile and run time depending on the fragment size. For up to 10 kb, the gel was running at 70 V for 75 min. The gel image was taken using the Vilber Lourmat Fusion FX7 imaging machine.

2.2.12 **Arbitrary primed-PCR (AP-PCR)**

For a quicker identification of transposon mutants' insertion sites, the single-primer AP-PCR technique was applied with brief modification (Karlyshev, Pallen, and Wren, 2000). The cell lysate was prepared by the suspension of a touch of bacteria from a single colony in 10 µl nuclease-free water and heated in a Thermal cycler for 10 min at 95˚C. The first step of PCR was to amplify a linear single-stranded transposon-specific amplicon from the cell lysate, using a T7 forward primer. In the second step, the reverse random primer and dNTPs were added to the same tube, and the cycler was set up for another round of PCR. The amplicons were cleaned up and sent for sequencing.

2.2.13 **Agarose gel electrophoresis**

Nucleic acids were separated, quantified, and visualized with agarose gel electrophoresis. For DNA stain, 2 µl SYBR safe DNA gel stain was used for a total volume of 40 ml 1X TAE buffer and 8% agarose. Gel-documentation was performed under Fusion FX imaging machine or BLook LED Transilluminator.

2.2.14 **DNA sequencing**

Constructs, plasmids, and PCR products were sequenced using the MICB facility service of the University of Manitoba, Winnipeg, Manitoba.

2.2.15 **RNA isolation**

Total RNA was isolated with a TRIzol™ Plus RNA purification kit. A single colony of fresh bacterial plates made from glycerol stocks, transferred into 2 ml LB broth and grown overnight on a shaker at 37˚C and 225 rpm speed. The following day, subcultures were made in 3 ml LB broth and grown for 3 h or lag phase of bacterial growth. A 1 ml of culture was harvested by centrifugation, and RNA was isolated following the kit manufacturer's instructions. After elution of total RNA. Eluted total RNA was purified a second time by RNA Cleanup Kit (Geneaid) with a residual DNA elimination treatment step. DNase was deactivated by the addition of ethylene diamine tetra-acetic acid (EDTA), and samples were tested by formaldehyde/agarose gel electrophoresis for confirmation of RNA quality and elimination of residual DNA.

2.2.16 **cDNA synthesis and Reverse Transcriptase PCR (RT-PCR)**

cDNA was synthesized using Maxima First Strand can Synthesis Kit for RT-qPCR with dsDNase (#K1642, Thermofisher) and 500 ng of the RNA template, according to the

manufacturer's instructions. cDNA was aliquoted and stored at -20˚C for a maximum of 1 month. To ensure the quality of cDNA is gDNA-free, a set of reverse transcriptase minus (RT-) negative controls were amplified to confirm the lack of gDNA contamination. The mRNA levels were measured using the PowerSYBR® Green Master Mix (#4368577, Thermofisher) in Illumina real-time PCR system by following the manufacturer's instructions. For total 20 µl reaction mixture, 1 µl of synthesized cDNA, 500nM of forward and reverse primer mix, 1x PowerSYBR® Green PCR Master Mix and nuclease-free up to 20 µl was added. qPCR cycles were selected based on the manufacturer's protocol. The melt curve confirmed only one fragment was amplified in each well. Expression fold changes were calculated using the ΔΔCt method (Livak and Schmittgen, 2001). Ct values were normalized to the expression of the *rpoD* housekeeping gene in the same sample. Data were shown as a percent change relative to gene expression of their background strain.

2.2.17 **Preparation of RNA-sequencing library**

The purity of RNA was assessed by NanoPhotometer® spectrophotometer (IMPLEN, CA, USA). RNA integrity was checked by Bioanalyzer 2100 (Agilent, Santa Clara, CA). rRNA was depleted from 1 microgram of total RNA using the Ribo-Zero Magnetic Gold Kit (Epicentre Biotechnologies, Madison, WI, USA). For RNA-sequencing library construction, TruSeq RNA

Sample Prep Kit v2 (Illumina, San Diego, CA, USA) was used. rRNA-free RNA samples were fragmented into small pieces using Elute Prime Fragment Mix. First Strand Master Mix and SuperScript II (Invitrogen, Carlsbad, CA, USA) reverse transcription (25 °C for

10 min; 42 °C for 50 min; 70 °C for 15 min) was used for First-strand cDNA synthesis. The product was purified with Agencourt RNAClean XP Beads (Beckman Coulter, CA, USA), and the second-strand cDNA library was synthesized using Second Strand Master Mix and dATP, dGTP, dCTP, dUTP mix (1 h at 16 °C). Fragmented cDNA was purified and underwent end-repair (30 min at 30 °C) with AMPureXP Beads (Beckman Coulter, CA, USA). The poly (A) tail was added to the fragments with A-tailing Mix (30 min at 37 °C) before ligating sequencing adapters (10 min at 30 °C). The second-strand cDNA was degraded by the Uracil-N-Glycosylase enzyme (10 min at 37 °C), and the product was purified by AMPureXP Beads. cDNA fragments were enriched by multiple rounds of PCR amplification with PCR Primer Cocktail. Ultimately the PCR products were purified with AMPureXP Beads. The index-coded samples were clustered in a cBot Cluster Generation System based on manufacturers protocol. Sequencing was performed using the Illumina HiSeq™ 2500 platform with pair-end 150 base reads.

2.2.18 **Bioinformatics analysis**

In three standard steps, the raw data of RNA-sequencing has filtered: A) the reads with more than 10% unidentified nucleotides (N) were removed; B) the reads that more than 50 % of their bases had Phred quality scores of ≤ 20, were removed; C) the reads aligned to the barcode adapter using FASTP (https://github.com/OpenGene/fastp) were voided. Quality trimmed reads were aligned using Bowtie2 (Langmead and Salzberg, 2012) (version 2.2.8) to the *P. aeruginosa* PAO1 reference genome to identify known genes and calculated gene expression by RSEM (B. Li and Dewey, 2011). The level of gene expression was calculated and normalized by using the fragments per kb of transcript per million (FPKM) mapped reads method to eliminate the influence of different gene

lengths and amounts of sequencing data on the calculation of gene expression. The edgeR package (http://www.r-project.org/) was used to identify differentially expressed genes (DEGs) across samples with fold changes ≥ 2 and with a false discovery rate adjusted P (*q* value) < 0.05. Go terms and the KEGG pathway was defined as being significantly enriched when the *q* value ≤ 0.05.

2.2.19 **Total protein isolation**

P. aeruginosa strains were grown in 2ml LB broth at 37˚C for 12 h. Bacteria were spanned down with centrifugation, and the pellet was washed 3 times with cold 1X PBS. A 20 µl protease inhibitor cocktail (# ab65621, Abcam) and 1 ml of 0.6 M perchloric acid were added (Irie et al., 2010; Gudapaty et al., 2001), cells were re-suspended and stored on a rotatory shaker for 30 min at 4˚C. Precipitated proteins for separated by centrifugation at 15000G for 10 min at 4˚C. Pellets were resuspended in 6 M urea and stored at -80˚C for further analysis.

2.2.20 **Quantitation of Proteins**

The protein concentration was determined by the Bradford assay (Harlow and Lane, 2006). The Pierce™ Coomassie (Bradford) Protein Assay Kit (#23200, Thermofisher) was purchased, and protein concentration was measured following the kit instructions. The standard curve was made by bovine serum albumin (BSA) standard, purchased from Sigma.

2.2.20.1 SDS-PAGE gel electrophoresis of proteins

SDS-PAGE was used for the separation of proteins by their mass (Laemmli, 1970), and the gels were made based on the molecular weight of target proteins. Overnight cultures of PAO1 and mutant strains were collected and washed three times with cold PBS buffer. A protease inhibitor cocktail and 1 ml of 0.6 M perchloric acid were added to lyse the cells, followed by centrifugation to pellet down the proteins. In 6 M urea, pellets were resuspended, and the total protein concentration of each sample was quantified by Bradford protein assay. Isolated proteins were boiled for 10 min with 2X loading buffer. Prepared samples were run at 100 V on 15% SDS-PAGE for approximately 1 hour.

2.2.20.2 Western blot

Proteins were transferred to PVDF membranes (#1620174, Bio-Rad) by western blot procedure (Mahmood and Yang, 2012). PVDF membranes were activated in methanol and placed in a transfer buffer. SDS Page gel, filter papers, and sponges were placed in transfer buffer too for equilibration. The transfer sandwich was prepared, and proteins were transferred to the membrane at 150 mA current. When the transfer was completed, membranes were soaked in TBST buffer containing 5% nonfat milk to block the membranes for 1 h. Later, the membrane was washed with TBST buffer and probed using 1:500 dilution (TBST+5% nonfat milk) of CsrA- *E. coli* antibody (Rabbit) during the night at 4˚C. After incubation, membranes were washed 3 times, each time for 20 min with TBST buffer. Membranes were placed incubated with secondary antibody, anti-rabbit IgG antibody 1:1000 dilution (diluted in TBST+1% nonfat milk) for 1 h and were washed 3 times, 20 min each time on a rotatory shaker. Just before imaging, detection of the proteins was performed by ECL kit. For loading control, membranes were stained

with Ponceau S for 10 min. The Fusion FX imaging system was used to obtain images. The antibody used in this research is listed in Table 2.1.

Table 2.1 Antibodies used in this study

Target	Antibody source	Dilution	Cat #	company
CsrA	Rabbit	1:5000	CSB-PA543019HA01ENT	Cedarlane
Rabbit IgG	Goat	1:1000	Ab6702	Abcam

2.2.21 **Biofilm formation quantification**

Static biofilm formation was assessed as previously described method (O'Toole and Kolter, 1998) with brief modifications. Bacteria were grown overnight at 37°C in 2 ml LB broth. A dilution ratio of 1:100 was made from overnight culture into 96-well polystyrene microtiter plates (Costar), incubated for 24 h at 37°C. Then, the cultures were rinsed with PBS three times and stained with 1% crystal violet for 20 min at room temperature. Wells were rinsed with distilled water, and 150 µl 2mM acetic acid was added to each well to dissolve the remaining crystal violet. 100 µl of this latest solution was transferred to a new microtiter plate, and the absorbance was read at 550 nm (OD_{550}).

2.2.22 **Motility assay**

The swarming and swimming and twitching motility of bacteria was assessed as described by Rashid and Kornberg (M. H. Rashid and Kornberg, 2000). The media

compositions for swarming motility contain 0.5% agar, 5 gl^{-1} glucose, 8 gl^{-1} nutrient broth mix. For swimming motility, 0.3% agar, 5 gl^{-1} NaCl, 10 gl^{-1} tryptone were added to the water and sterilized for 15 at 115 psi. Twitching motility media consisted of LB broth with 1% agar and sterilized. Bacteria were grown overnight in 2 ml LB broth at 37˚C and on a shaker. A 2µl of overnight cultures were spotted on the surface of swarming and swimming plates, and for twitching motility, it stabbed into twitching plates. Swarm plates were incubated at 37˚C, swim plates at 30˚C for 15h, and twitch plates at 37˚C for 24h. Twitching motility zone were stained for better visualization, after removal of agar and by 1% crystal violet. Plates were imaged using the Fusion FX imaging system. The zone of migration was measured and compared between strains where migration was not easily differentiated.

2.2.23 **Statistical analysis**

Statistical analysis was performed using unpaired student's *t*-test or one-way analysis of variance (ANOVA) with Turkey or Dunnett post-hoc from three independent experiments. Where applicable, the statistical significance is: ****$p < 0.0001$; ***$p < 0.001$**;** **$p < 0.01$; *$p < 0.05$.

Chapter 3

3 Characterization of Putative RNA Ligase RtcB Affecting the Switch Between T6SS and T3SS and Involving the Stress Response of *Pseudomonas aeruginosa*

3.1 Introduction

T6SSs of *P. aeruginosa* are regulated through different regulatory pathways. For instance, H1-T6SS is negatively regulated by QS components, while H2-T6SS and H3-T6SS are positively regulated by QS (Sana et al., 2012; Lesic et al., 2009). In the study by Allsopp et al., AmrZ was shown to be a global regulator of T6SS and binds to the promoter region of T6SS genes. The regulatory effect of AmrZ on T6SSs is selective, whereas RsmA is the repressor of all three T6SSs apparatus (Allsopp et al., 2017). In *P. aeruginosa*, H1-T6SS is mainly regulated at the post-translational level (Mougous et al., 2006), and the cues activating this regulation are poorly understood (Basler, Ho, and Mekalanos, 2013). However, membrane damage caused by bacterial conjugation or chelation of membrane-bound cations by EDTA or extracellular DNA, and antibiotics targeting the membrane are known to be some of the activator signals for T6SSs, (Wilton et al., 2016; Ho, Basler, and Mekalanos, 2013). Though, several questions remained to be investigated. These include the factors that control the abundance of T6SSs- related proteins, other pathways that activate T6SSs, the correlation between T3SS and T6SSs, and whether there is a common modulator for all the secretion systems. Considering the large genome of *P. aeruginosa*, the proteins of unknown function coded in its genome, and the bacterium's strong ability to adapt to different environments, it is possible the regulatory elements controlling the virulence of *P. aeruginosa* are existed and yet to be manifested. In this objective, I characterized the regulation of H1-T6SS by using the transposon mutagenesis strategy. The potential modulatory elements of H1-T6SS identified were investigated by genetic and biochemical methodologies in the context of

T3SS regulation, role of secondary metabolites and other virulence factors in this bacterium.

3.2 Specific materials and methods used in this section

3.2.1 **Bacterial strains and plasmids**

Bacterial strains and plasmids used in this study are presented in **Table 3.1**. *E. coli* and *P. aeruginosa* were routinely grown at 37˚C on LB agar or LB broth unless otherwise explained. Antibiotics' final concentrations are explained in chapter 2.

Table 3.1 bacterial strains and plasmids of this study

Bacterial strains or plasmid	**Relevant characteristics/sequence**	**Source**
***E. coli* strains**		
DH5α	F$^-$ φ80*lac*ZΔM15 Δ(*lacZYA-argF*) U169 *recA*1 *endA*1 *hsdR*17 (r_k^-, m_k^+) phoA supE44 λ^- *thi*$^-$1 *gyrA*96 *relA*1	Invitrogen
SM10-λ *pir*	Mobilizing strain, RP4 integrated into the chromosome; Kn^r	(Simon et al., 1983)
Mach1™-T1^R	F- Φ80*lac*ZΔM15 Δ*lac*X74 *hsd*R(rK- mK+) Δ*rec*A1398 *end*A1 *ton*A	Invitrogen
***P. aeruginosa* strains**		
PAO1	Wild type, lab strain	This lab
PAO1 (Δ*retS*)	*retS* replacement mutant of PAO1	This lab
PAO1 (Δ*rtcB*)	*rtcB* replacement mutant of PAO1	This study

PAO1 (Δ*rtcB*Δ*retS*)	*rtcB retS* replacement mutant of PAO1	This study
Plasmids		
pMS402	Expression reporter plasmid carrying the promoterless *luxCDABE*; Kn^r Tmp^r	(Duan et al. 2003)
CTX-6.1	Integration plasmid origins of plasmid mini-CTX-*lux*; Tc^r	This lab
pRK2013	Broad-host-range helper vector; Tra^+, Kn^r	(Ditta et al. 1980)
pEX18Tc	*oriT*$^+$ *sacB*$^+$ gene replacement vector with multiple-cloning site from pUC18; Tc^r	(Hoang et al. 1998b)
pAK1900	*E. coli-P. aeruginosa* shuttle cloning vector, Amp^r	(Sharp et al. 1996)
pAK-*rtcB*	pAK1900 with a 1260 bp fragment of PA4583 between *Bam*HI and *Hin*dIII; Amp^r, Cb^r	This study
pEX18Tc-*rtcB*	pEX18Tc carrying the upstream and downstream fragment of *rtcB*	This study

pKD-H1T6SS	pMS402 containing H1-T6SS promoter region; Kn^r, Tmp^r	This lab
pKD-*tssA1*	pMS402 containing *tssA1* promoter region; Kn^r, Tmp^r	This study
CTX-H1T6SS	Integration plasmid, CTX6.1 with a fragment of pKD-H1-T6SS containing H1 promoter region and *luxCDABE* gene; Kn^r, Tmp^r, Tc^r	This study
CTX-ExoS	Integration plasmid, CTX6.1 with a fragment of pKD-ExoS containing *exoS* promoter region and *luxCDABE* gene; Kn^r, Tmp^r, Tc^r	This lab
pAK-*rsmY*	pAK1900 with a 124 bp fragment of *rsmY* between *Bam*HI and *Hin*dIII; Amp^r, Cb^r	This study
pAK-*rsmZ*	pAK1900 with a 116 bp fragment of *rsmZ* between *Bam*HI and *Hin*dIII; Amp^r, Cb^r	This study
pKD-*rtcB*	pMS402 containing *rtcB* promoter region; Kn^r, Tmp^r	This study
pET SUMO	A bacterial protein expression vector containing ubiquitin-like modifier (SUMO); Kn^r	Invitrogen

3.2.2 **Construction of gene expression reporters**

The promoter region of the H1-T6SS operon containing *clpV1* was PCR-amplified and cloned into the *Bam*HI-*Xho*I site, upstream of the *lux*-Box on pMS402; resulting in the so-called pKD-H1 reporter. *Pac*I digested fragment of pKD-H1 cloned into integration plasmid CTX6.1 originated from mini-CTX-*lux* to construct a chromosomally integrated reporter (Becher and Schweizer 2000a). CTX-H1 transferred to *E. coli* SM10-λ *pir* (Simon, Priefer, and Pühler, 1983) following a biparental-mating between strains; *E. coli* SM10-λ *pir*:: PAO1(Δ*retS*), *E. coli* SM10-λ *pir*:: PAO1. The biparent-mating led to the construction of a stable chromosomally integrated pKD-H1 reporter in PAO1(Δ*retS*) and PAO1 (Hoang et al. 2000; Liang et al. 2008a). For all other reporters, the same strategy was applied. Gene expression measurements are outlined in chapter 2. The primers used in this study are listed in **Table 3.2**.

Table 3.2 Primers used in this study

Primer	Sequence (5'→3') [a]	Restriction site
rtcB -UP-S	acagcgGAATTCCTGGTGGAGCGCTACTTCACC	*Eco*RI
rtcB -UP-AS	acagcgGGATCCGTCCAGAGCTTGATCGGCTT	*Bam*HI
rtcB -DW-S	acagcgGGATCCCGATGGCCTACAAGGACATCG	*Bam*HI
rtcB -DW-AS	acagcgAAGCTTGATGTTGCGGATGCGCAGC	*Hin*dIII
pAK-*rtcB*-S	acagcgAAGCTTGGAGCACAAGGAAAGCACGATG	*Hin*dIII
pAK-*rtcB*-AS	acagcgGGATCCCGTCATCCTTTCACGCACACC	*Bam*HI
pKD-*tssA1*-S	acagtgCTCGAGGACCGATGGTCAGCTGTCC	*Xho*I
pKD-*tssA1*-AS	acagcgGGATCCCGATGCGTTCGAGTTCGAG	*Bam*HI
pKD-*rtcB*-S	acagcgCTCGAGGCTCGAACGTTGCCTTAACGGC	*Xho*I
pKD-*rtcB*-AS	acagcgGGATCCGGAATACAGCAGGCCGCGTTCG	*Bam*HI
pAK-*rsmY*-S	acagcgAAGCTTCATGCTGGGAAGGCTCGCGATG	*Xho*I
pAK-*rsmY*-AS	acagcgGAATTCCTGAAGGTCGGCCTGGTCTACC	*Bam*HI

pAK-*rsmZ*-S	acagcgGGATCCGTGACGCGCTGTTCCAGTGACG	*Xho*I
pAK-*rsmZ*-AS	acagcgGGAATTCATCGAGCTGAACAGC	*Bam*HI
rpoD-S	GATCTCCATGGAAACCCCGATC	
rpoD-AS	GAGGACTTCGCGGGTGGATTC	
exsA-S	TTCTGCTCGAGGGCGAACTGAC	
exsA-AS	CGGCTGTCCTTTCCCTTGGTAC	
clpv1-S	CTGAACAGCCTGGCCTACAAGG	
clpv1-AS	GAGTCCGGCAACTGGAGGATC	
hcp1-S	GACGTCAAGGGTGAGTCCAAGG	
hcp1-AS	CAGGTTGGGCGTGGACTTGTC	
exsC-S	CAAGGTCAACCGACTGCTTGC	
exsC-AS	CATCGGCCTCCAGCAACAGAC	
Div-*rpoD*-S	GAGCACCTTCGCTCCTTCCTCG	
Div-*rpoD*-AS	AGACGAGATTGCTGTTGCGCT	
Div-*rsmY*-S	GATGTCAGGATAGAGGTCTGC	

Div-*rsmY*-AS	TCCGTATTGTCTTTGGCGCT
Div-*rsmZ*-S	GATCCTTCGGGGTTGCGTGTT
Div-*rsmZ*-AS	ATGATGACGAGGGACTGAAGAG
rsmY-S	TCAGGACATTGCGCAGGAAGCG
rsmY-AS	AGACCTCTATCCTGACATCCGTGCTAC
rsmZ-S	GAAGGATCGGGGAAGGGACGTC
rsmZ-AS	GTATTACCCCGCCCACTCTTCA

Note: [a], underlined are restriction site sequences

The over-hanged base pairs are shown with lower case

3.2.3 **Random transposon library construction, screening, and identification of Tn mutants by arbitrarily primed-PCR and sequencing**

A transposon library was constructed as previously described (Kulasekara et al., 2005). Briefly, pBT20 was mobilized to the CTXH1-PAO1(Δ*retS*) reporter strain using *E. coli* SM10λ*pir* strain as the donor. The donor and recipient were mixed by the ratio of 2:1 and spotted on LB agar plates for 2hr. The colony spots were collected after incubation, washed, diluted, and plated on PIA plates containing 150 μg ml^{-1} Gm. After overnight incubation, mutants with altered H1-T6SS promoter activity were selected under the Fusion-FX imaging system. The selected colonies were tested with Synergy2 Multimode Microplate Reader (BioTek) to measure their promoter activity. Once the change in promoter activity was confirmed, the insertion site was amplified by an arbitrarily primed PCR (ap-PCR), followed by subsequent sequencing of amplicons.

3.2.4 **Construction of unmarked gene knockout mutants**

The *sacB*-based method was applied to construct the knockout mutants by allelic exchange with the pEX18Tc sucrose counter-selection system (Hoang et al., 1998b). The region 1080 bp of upstream and 1078 bp downstream of the *rtcB* gene were PCR-amplified with the incorporation of restriction sites (the primers are listed in **Table 3.2**). The PCR products were cloned to suicide vector pEX18Tc. Triparental mating was set up using *E. coli* strains carrying helper plasmid pRK2013, pEX18Tc-$rtcB_{up+down}$ carrier, and *Pseudomonas* PAO1 wild type and PAO1(Δ*retS*) to build mutant strains (Ditta et al., 1980). PCR and agarose gel electrophoresis confirmed the mutants PAO1(Δ*rtcB*) PAO1(Δ*rtcB*Δ*retS*).

3.2.5 **Construction of complementing vector**

The multi-copy-number *E. coli-P. aeruginosa* shuttle vector pAK1900 carrying a *lac* promoter was used to express the RtcB in trans (Poole et al., 1993). The DNA region of *rtcB* was PCR-amplified in-frame, incorporating restriction sites (the primers used are listed in **Table 3.2**). PCR products were cloned into the *Bam*HI and *Hin*dIII site of pAK1900 and transferred into *Pseudomonas* by electroporation.

3.2.6 **Coliform agar plate assay and CFU counting**

Bacterial competition assay was carried out as described previously, with brief modification (Hachani et al., 2013). The prey is *E. coli* DH5α expressing β-galactosidase. PAO1, PAO1(Δ*retS*), PAO1(Δ*rtcB*), PAO1(Δ*rtcB*Δ*retS*) strains were co-incubated with prey cells, on filter-papers (total of 10 µl) placed on LB agar plates. The plates were incubated at 37°C for 5 hr. Later, each filter paper was resuspended in cold, sterile phosphate-buffered saline (PBS) and washed three times. Samples were serially diluted 10 to 10^{-5}. A 5µl of each dilution was spotted on coliform agar plates for the visual essay. Plates were incubated at 37°C for 16 h and then 2 days at 4°C. The *lacZ*-positive *E. coli* was assessed by the number of blue color colonies. Besides, diluted samples were spread in plates containing coliform agar, and the blue colonies were counted after incubation.

3.2.7 **Fluorescent microscopy**

The fluorometric competition assay was performed using *E.coli* harboring the *pilG*-DsRed expressing vector, emitting red fluorescence. The same set of competitions was applied for the experiment, and slides were prepared from post-co-incubation of prey and

predators. The resultant slides were observed by an inverted microscope (Nikon ECLIPSE T*i*-E).

3.2.8 **Circular RNA discovery, TA cloning, and validation by sequencing**

The existence of circular RNA (cRNA) was investigated following Panda and Gorospe to modify bacterial samples (Panda and Gorospe, 2018). Divergent primers were designed for the small RNAs, *rsmY*, and *rsmZ*; also, for *rpoD* as a housekeeping gene and probable negative control. Total RNA was isolated, as explained earlier. RNA from each sample was aliquoted into two sets. A set of samples were treated with a final concentration of 1U RNase R (Lucigen) for 10 min at 37˚C to digest total linear RNAs. To inactivate the RNase R, samples were incubated at 65˚C for 10 min, following an RNA clean-up step. cDNA was constructed from both sets of samples. The qPCR was performed using Power SYBR^{TM} Green PCR Master Mix based on manufacturer instructions to detect cRNAs. PCR amplicons were subjected to agarose gel electrophoresis on 2% agarose gel made with 1X TAE concentration. After the run, the amplicons were cut and purified. The amplicons were cloned into a Sumo vector (#K30001, Invitrogen) by TA cloning and analyzed by sequencing. Primers used in this assay are available in **Table 3.2.**

3.3 Results

3.3.1 Screening of the transposon insertion mutants with altered expression of H1-T6SS in PAO1(Δ*retS*)

To elaborate on the regulatory pathway of H1-T6SS of *P. aeruginosa*, a transposon mutagenesis library was constructed. A *lux*-based transcriptional reporter (*luxCDABE*) was generated and integrated into the chromosome of PAO1(Δ*retS*), resulting in reporter strain PAO1(Δ*retS*) CTX::H1-T6SS. The transposon library's preparation was performed using PAO1(Δ*retS*) CTX::H1-T6SS, and approximately 50,000 Tn mutants were screened (**Figure 3.1A)**. The colonies showing altered luminescence were selected and further confirmed using a Synergy H4 Multimode Microplate Reader (**Figure 3.1B**). Mutants with altered reporter activity compared to PAO1(Δ*retS*) were selected. The transposon insertion site was defined by arbitrary primed PCR followed by sequencing of the PCR products. DNA sequences obtained were blasted against the *P. aeruginosa* genome sequence to determine the interrupted genes. A total of 13 genes were identified and listed in **Table 3.3**. Among them, insertions in the T6SS genes *tssC1*, *tssB1,* and *hcp1* have entirely repressed the expression of H1-T6SS. Also, interruption of *fadD1*, *ynfM*, and PA5185 resulted in repression of T6SS. FadD1 is a fatty acid degradase with more substrate specificity to long-chain fatty acids. *ynfM* encodes a membrane transport protein, and PA5185 encodes a conserved protein of unknown function. The Tn mutants which demonstrated increased activity of T6SS were: *trpF,* an N-(5'phosphoribosyl) anthranilate (PRA) isomerase that is involved in amino acid metabolism; *rtcB;* and *pnp*, functions in RNA processing; an intergenic region with putative RsmA binding site; *yfgB*; PA5182; and PA4115. The product of *rtcB* is a conserved RNA ligase, a member of

a four-gene operon. The four genes are PA4582 (conserved protein), PA4583 (RtcB, conserved hypothetical protein), PA4584 (conserved protein), and PA4585 (RtcA, RNA3'-terminal phosphate cyclase). RtcB is previously reported as a member of RNA repair in bacteria at stress-induced conditions (Manwar et al., 2019; Tanaka and Shuman, 2011; Kurasz et al., 2018). Considering the variety of unfavorable and stressed conditions in which *P. aeruginosa* establishes the infection, like CF patients' lungs, I selected RtcB to further investigate its potential regulatory role on H1-T6SS.

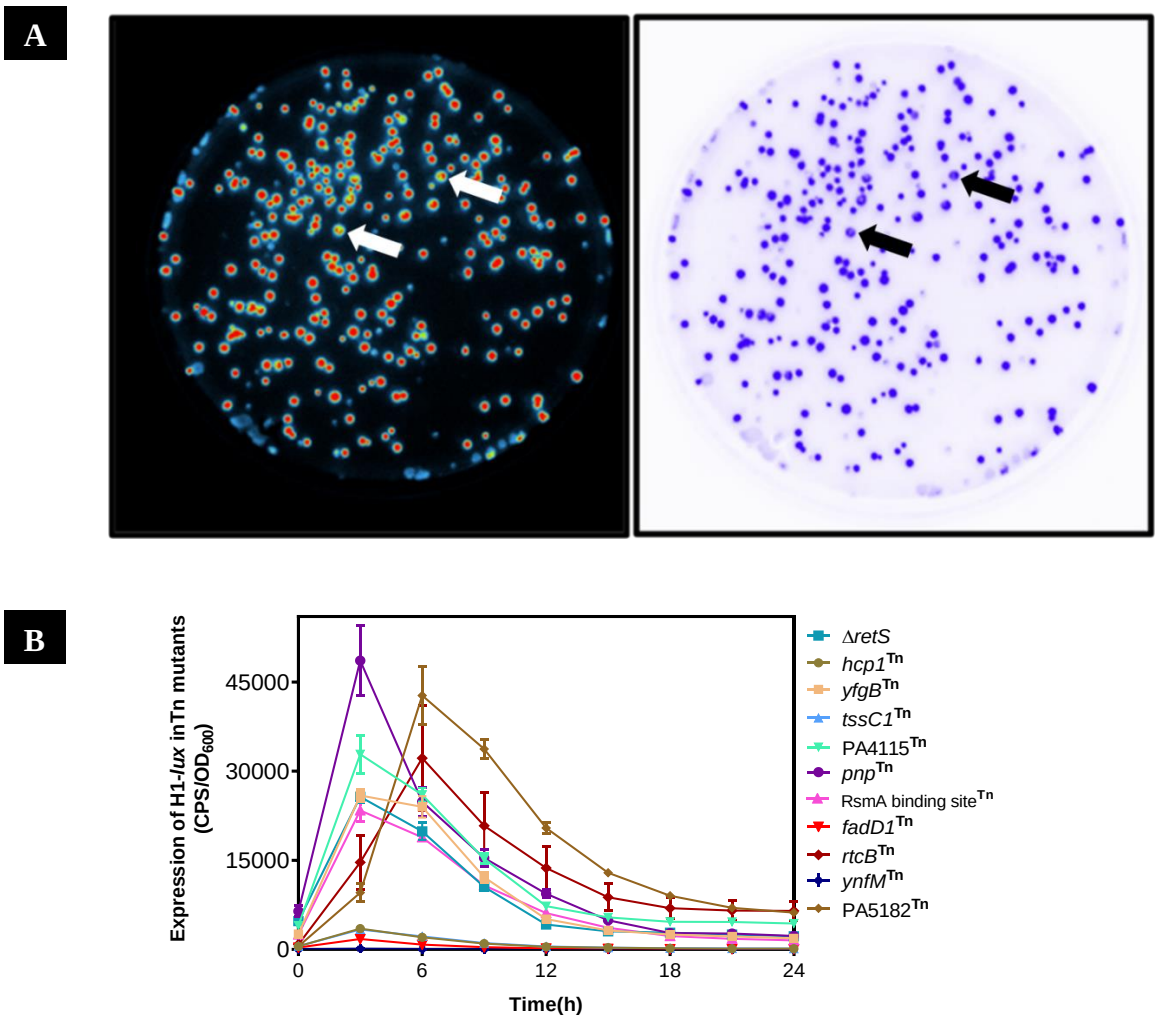

Figure 3.1 Colony screening and quantification of Tn mutants with altered luminescence. A. Colonies harboring H1-*lux* reporters were imaged, and colonies of the same size but with altered luminescence were selected. Colonies with lower light production are shown by arrows in polychrome and monochrome images. **B.** Relative expression of H1-*lux* to growth in Tn mutants compared with PAO1(Δ*retS*) is measured over 24 h. Relative expression in Y-axis is normalized luminescence to the growth of the bacterium. The X-axis represents the duration of data collection. Experiments was performed two times independently. Error bars indicate the standard deviations.

Table 3.3 Potential regulators of H1-T3SS

Gene ID	Protein description	Max fold[a]
PA5182	Hypothetical protein	**4**
trpF	PRA isomerase	**2**
tssB1	T6SS protein	**-5**
tssC1	T6SS protein	**-9**
PA5185	Hypothetical protein	**-9**
hcp1	T6SS protein	**-5**
fadD1	Long-chain-fatty-acid--CoA ligase	**-5**
5028235-5028243	Putative RsmA binding site intergenic region	**1.5**
yfgB	Conserved hypothetical protein	**1.2**
ynfM	MFS transporter	**-9**
rtcB	Conserved hypothetical protein	**3.2**
PA4115	Hypothetical protein	**2**

pnp	Polyribonucleotide nucleotidyltransferase	**2.2**

Note: max fold[a], maximal ratio expression of H1-T6SS in Tn mutant to the PAO1(Δ*retS*)

3.3.2 **Deletion of *rtcB* increased the expression H1-T6SS in *P. aeruginosa***

A mutant with an insertion in the gene PA4583 (*rtcB*) showed an increased expression of H1-T6SS on the agar plate. To confirm the role of RtcB in H1-T6SS, we constructed the *rtcB* knockout mutant in both PAO1 and PAO1(Δ*retS*) backgrounds. The promoter activity *clpV1,* which represents H1-T6SS expression, was compared in PAO1(Δ*rtcB*) and PAO1(Δ*rtcB*Δ*retS*). As shown in **Figures 3.2 A, B**, the expression of *clpV1* significantly increased in PAO1(Δ*rtcB*). No noticeable change in PAO1(Δ*rtcB*Δ*retS*) was observed. Perhaps in transposon insertion mutant polar effect caused higher reporter activity compared with PAO1(Δ*rtcB*Δ*retS*). This indicates that the inactivation of *rtcB* upregulates H1-T6SS in PAO1, and it is a negative regulator of H1-T6SS in *P. aeruginosa* wild type. To verify if the higher expression of H1 in PAO1 is accompanied by an expression of *tssA1*, an essential component of H1, I measured reporter activity of *tssA1* using pKD-*tssA1*. The transcription of *tssA1* was positively regulated in Δ*rtcB* compared to the PAO1 wild type (**Figure 3.2 C**).

A

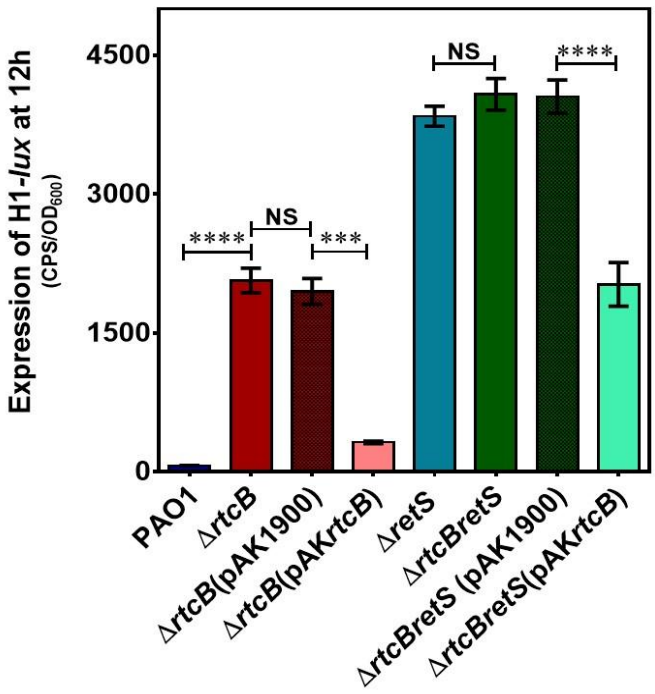
Expression of H1-lux at 12h
(CPS/OD600)
4500
3000
1500
0
****
NS
***
NS
****
PAO1
ΔrtcB
ΔrtcB(pAK1900)
ΔrtcB(pAKrtcB)
ΔretS
ΔrtcBretS
ΔrtcBretS (pAK1900)
ΔrtcBretS(pAKrtcB)

B

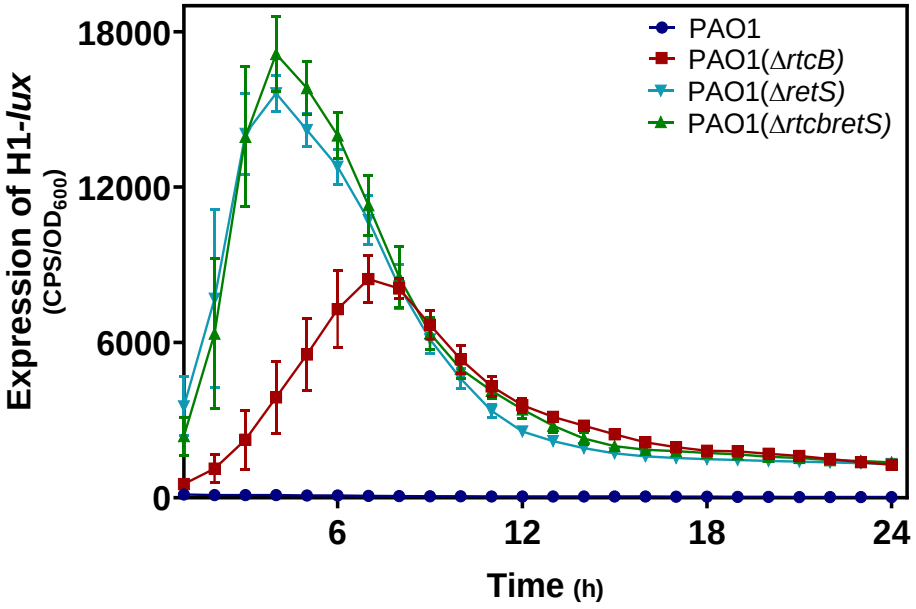
Expression of H1-lux
(CPS/OD600)
18000
12000
6000
0
6
12
18
24
Time (h)
PAO1
PAO1(ΔrtcB)
PAO1(ΔretS)
PAO1(ΔrtcbretS)

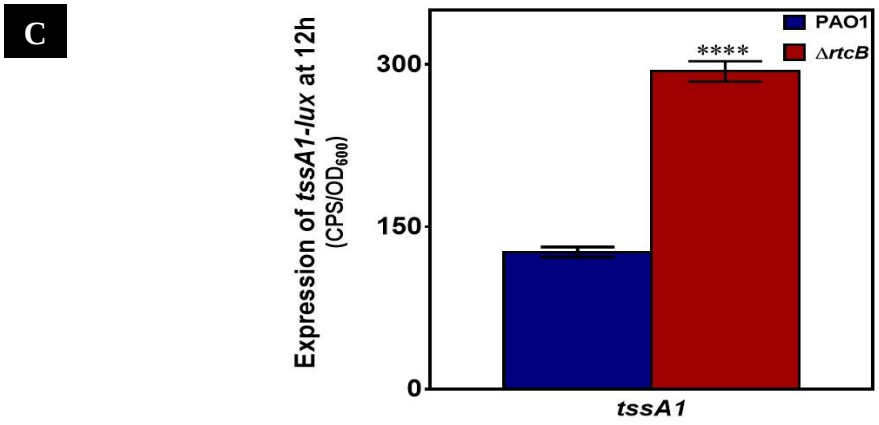

Figure 3.2 Increased expression of H1-T6SS and *tssA1* in PAO1(Δ*rtcB*)

A. CTX-H1 reporter fusion integrated into the chromosome was used to assess promoter activity of H1-T6SS in PAO1 and mutants. A significant increase was observed in the expression of H1-T6SS in PAO1(Δ*rtcB*) compared to PAO1. Data are shown as a relative change of promoter activity to growth (OD_{600}) during a course of 24h readout. One-way Anova was used to analyze the data. These results are the average of three independent experiments. Error bars indicate standard deviations. NS $p > 0.05$, ***$p < 0.001$, and ****$p< 0.0001$ **B.** complementing vector pAK1900-*rtcB* was introduced to mutant strains PAO1(Δ*rtcB*) and PAO1(Δ*rtcB*Δ*retS*). The RtcB expression vector restored the expression of H1-T6SS close to the native level. Data are shown at 12 h (for better observation) and plotted as the relative change of luminescence to growth. These results are the average of three independent experiments. Error bars indicate standard deviations. **C.** The reporter vector pKD-*tssA1* was constructed to measure the promoter activity of *tssA1* in PAO1(Δ*rtcB*) compared to PAO1. TssA1 was highly upregulated in PAO1(Δ*rtcB*). Unpaired student's *t*-test was used to analyze the data. These results are the average of three independent experiments. Error bars indicate standard deviations. ****$p< 0.0001$.

3.3.3 **The effect of RtcB deletion on *P. aeruginosa* anti-prokaryotic pathogenicity**

H1-T6SS delivers toxins into bacterial prey (Hood et al., 2010). To determine PAO1(Δ*rtcB*) pathogenicity against other bacteria in comparison with PAO1, I performed a killing assay (Hachani, Lossi, and Filloux, 2013). The survived live *E. coli* prey cells that were not killed by *P. aeruginosa* appeared blue in the colonies. The higher blue color intensity showed the increased survival rate of *E. coli* due to a less virulent strain of *P. aeruginosa*. PAO1 (Δ*retS*) harbors consecutively active T6SS ($T6SS^{+}$) and is used as a positive control. Compared to PAO1, PAO1(Δ*retS*) exhibited significantly higher virulence, resulted in a lower survival rate of *E. coli* cells. The same behavior was observed in PAO1(Δ*rtcB*) with a higher killing potential than PAO1, confirming that T6SS in PAO1(Δ*rtcB*) is activated (**Figure 3.3A**). To verify this observation, we set up a fluorometric killing assay. Prey *E. coli* cells were transformed with a vector harboring *pilG*-DsRed fluorescent reporter. The density of red fluorescent reflects the viable *E. coli* cells versus dead *E. coli* cells. Indeed, PAO1(Δ*rtcB*) demonstrated a similar killing force as PAO1(Δ*retS*). The obtained result showed that T6SS is functionally activated in PAO1(Δ*rtcB*) and able to kill *E. coli* cells at a higher rate than PAO1 (**Figure 3.3 B**).

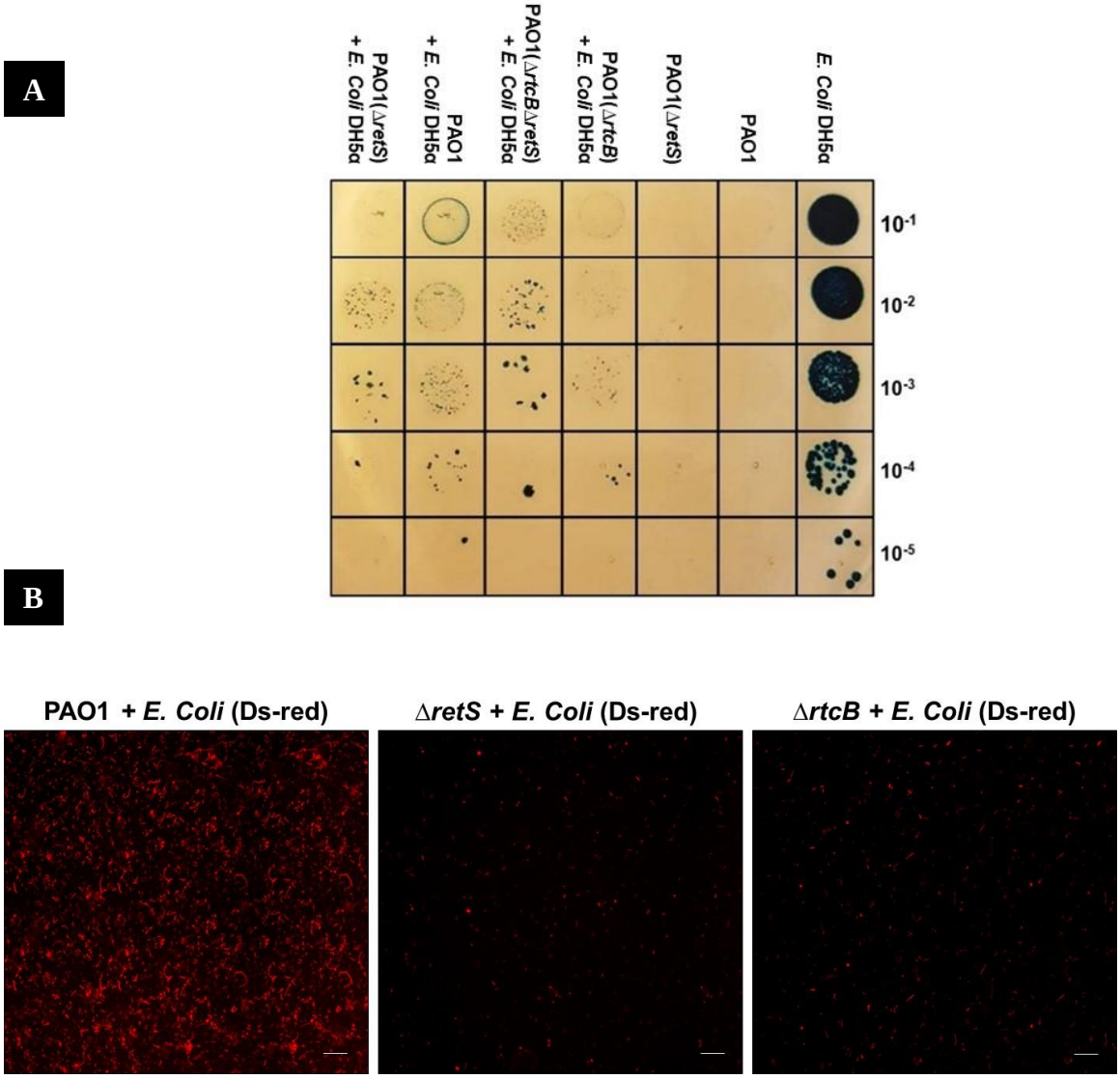

Figure 3.3 Functional H1-T6SS in Δ*rtcB* participates in the killing of prey cells.

A. Coliform agar plate competition assay. The result of co-cultures of *E. coli* with predator *Pseudomonas* strains were spotted on coliform agar plates. Blue color represents *E. coli* cells and is formed by β-galactosidase production that cleaved X-gal. **B.** Fluorescence competition assay. *E. coli* harboring *pilG*-DsRed fluorescent reporter is shown in red color. Scale bar: 100μm. The red color density corresponds to live *E.coli*, not killed by *P. aeruginosa* during co-culture incubation.

3.3.4 **RtcB alters biofilm formation and motility phenotypes**

Expression of T6SS occurs during the chronic phase of *Pseudomonas* infection with an increased biofilm formation rate and lower motility (K. Li et al., 2017). The biofilms hamper host immune defense and antibiotic therapy as a defensive tactic of the bacterial cells (Drenkard, 2003). To examine whether aligned with the upregulation of T6SS in PAO1(Δ*rtcB*), the biofilm formation-related genes are also upregulated, a biofilm formation assay was performed under static conditions. As expected, we found that PAO1(Δ*rtcB*) forms slightly more but statistically not significantly biofilms than PAO1. Interestingly, our results showed that the PAO1(Δ*rtcB*Δ*retS*) strain forms significantly less biofilm compared to PAO1(Δ*retS*) (**Figure 3.4A**).

Then, we examined the effect of *rtcB* deletion on the three forms of bacterial motility. The bacterial mobility tests included swarming, swimming, and twitching for the bacterial migration on semi-solid, liquid, and solid surfaces. Motility is the hallmark of the acute phase of infection with the complex regulatory interplay of flagellar assembly, chemotaxis, type four pili (TFP), Gac-Rsm two-component system (TCS), and QS (Tamar, Koler, and Vaknin, 2016; Kilmury and Burrows, 2018; Joge et al., 2018; Miller et al., 2008; Pletzer et al., 2020). As shown in **Figure 3.4B**, the twitching motility did not show a noticeable change in PAO1(Δ*rtcB*), but it increased in PAO1(Δ*rtcB*Δ*retS*) compared to PAO1(Δ*retS*). Swarming and swimming of PAO1(Δ*rtcB*) were decreased compared to the PAO1 and were significantly elevated in PAO1(Δ*rtcB*Δ*retS*) compared to its background PAO1(Δ*retS*). The lower biofilm formation and higher motility in PAO1(Δ*rtcB*Δ*retS*) could indicate the activation of the motile planktonic phase and the expression of T3SS.

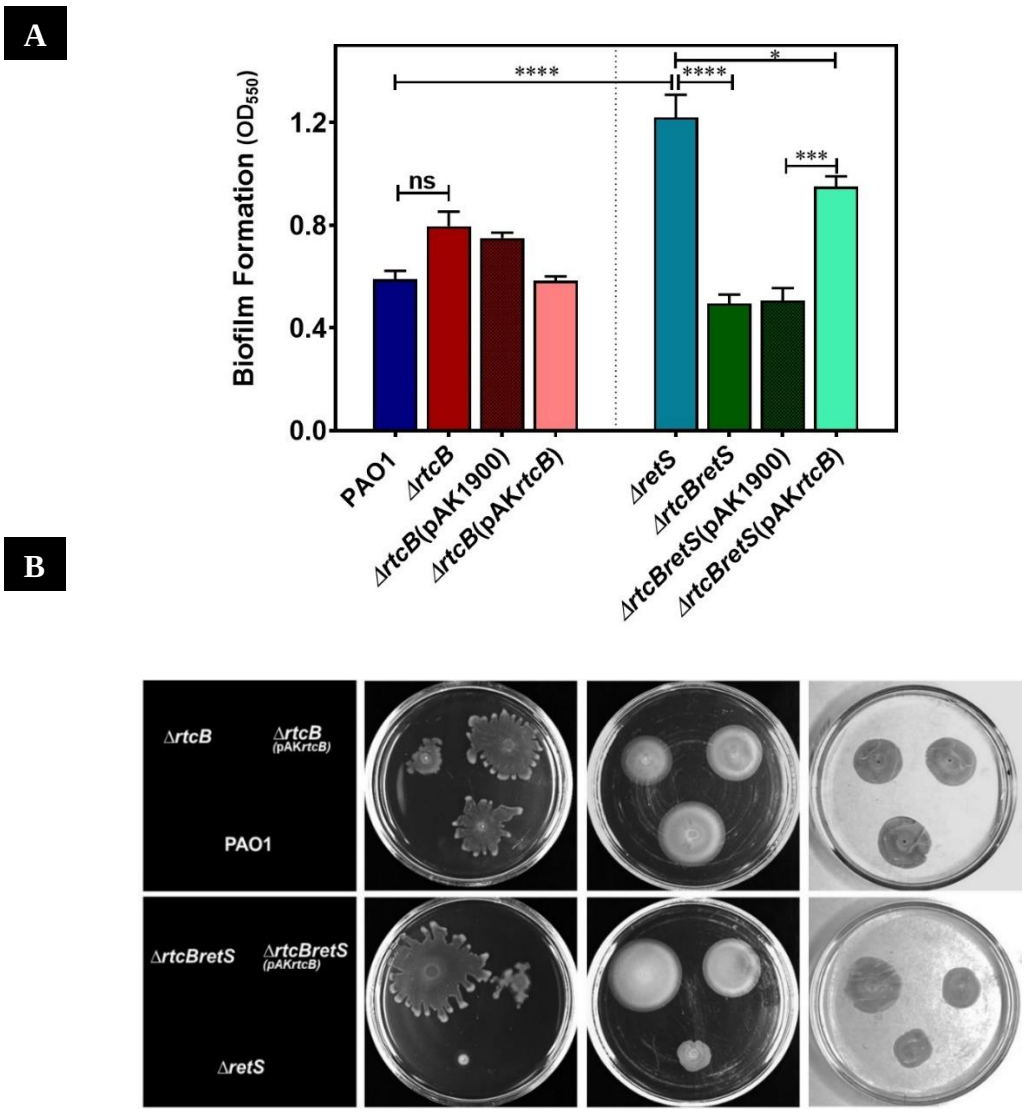

Figure 3.4 Deletion of *rtcB* modulated virulence factors of *P. aeruginosa*.

Complemented strains with RtcB expression vectors are shown with a (+) sign. **A.** Biofilm formation was assayed in a 96-multi-well plate. The PAO1(Δ*rtcB*Δ*retS*) formed significantly fewer biofilms compared with PAO1(Δ*retS*) and its complemented strain. **B**. Swarming and swimming motility of the PAO1(Δ*rtcB*) were decreased compared with PAO1. Swarming, swimming, and twitching were upregulated in PAO1(Δ*rtcB*Δ*retS*) in

comparison to PAO1(Δ*retS*). The experiments were repeated at least 3 independent times. Where applicable, NS $p > 0.05$, *$p < 0.05$,***$p < 0.001$ and ****$p < 0.0001$.

3.3.5 **Deletion of *rtcB* inactivated the switch between T3 and T6SS**

In PAO1(Δ*retS*), T3SS and motility are repressed, but biofilm formation and T6SS are upregulated (Ventre et al., 2006; Moscoso et al., 2011). Since PAO1(Δ*rtcB*Δ*retS*) showed increased motility and lower biofilms, we suspected that the expression of T3SS in PAO1(Δ*rtcB*Δ*retS*) might also be reversed. We generated the PAO1(Δ*rtcB*) and PAO1(Δ*rtcB*Δ*retS*) strains carrying the CTX-*exoS* reporter to examine this. ExoS is an effector protein of the type three secretion system (T3SS) and is used as an indicator of active T3SS. Interestingly, while T6SS was expressed in PAO1(Δ*rtcB*) (**Figure 3.5A**, **B**), the promoter activity of *exoS* remained active. Surprisingly, our data revealed that the expression of *exoS* was restored in PAO1(Δ*rtcB*Δ*retS*) compared to PAO1(Δ*retS*), where T6SS was too expressed. These results represent the upregulation of both T6SS and T3SS in both PAO1(Δ*rtcB*) and PAO1(Δ*rtcB*Δ*retS*); upon deletion of *rtcB*, the conventional switch between these secretion systems no longer exists.

Considering the central role of the Gac-Rsm regulatory pathway in controlling both T3SS and T6SS and the switch between them, we examined Gac-Rsm TCS's role in the modulation of H1-T6SS and T3SS by RtcB. We generated the strains of PAO1(Δ*rtcB*), PAO1(Δ*rtcB*Δ*retS*), PAO1(Δ*retS*) overexpressing *rsmY,* and *rsmZ* sRNAs to assess the reporter activity of H1-T6SS and T3SS. Overexpression of RsmYZ lowered the reporter activity of H1-T6SS in PAO1(Δ*rtcB*). This suggests that the upregulation of H1-T6SS in PAO1(Δ*rtcB*) is possibly not through a lower cellular content of RsmA protein, as more RsmYZ could sequester the RsmA proteins and upregulates H1-T6SS (**Figure 3.5C, D**). On the other hand, complementation of PAO1(Δ*rtcB*Δ*retS*) with RsmYZ overexpression vectors repressed the expression of T3SS. The upregulation of T3SS in

PAO1(Δ*rtcB*Δ*retS*) could be through direct or indirect downregulation of RsmYZ by deletion of *rtcB*, which led to increased RsmA, resulting in more expression of T3SS. The results suggest that RtcB protein possibly exerts its function on the modulation of H1-T6SS and T3SS through at least two different pathways. Maybe this is why both H1-T6SS and T3SS secretion systems remain active in PAO1(Δ*rtcB*) and PAO1(Δ*rtcB*Δ*retS*) simultaneously.

A

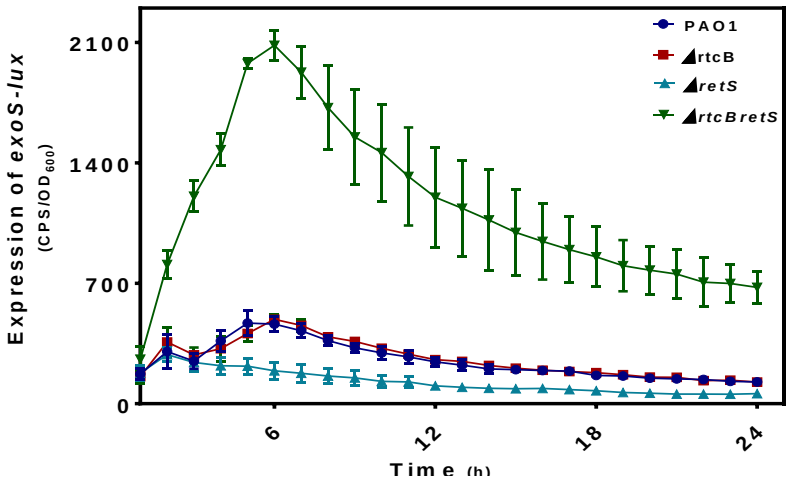
PAO1
ΔrtcB
ΔretS
ΔrtcBretS
Expression of exoS-lux (CPS/OD600)
2100
1400
700
0
6
12
18
24
Time (h)

B

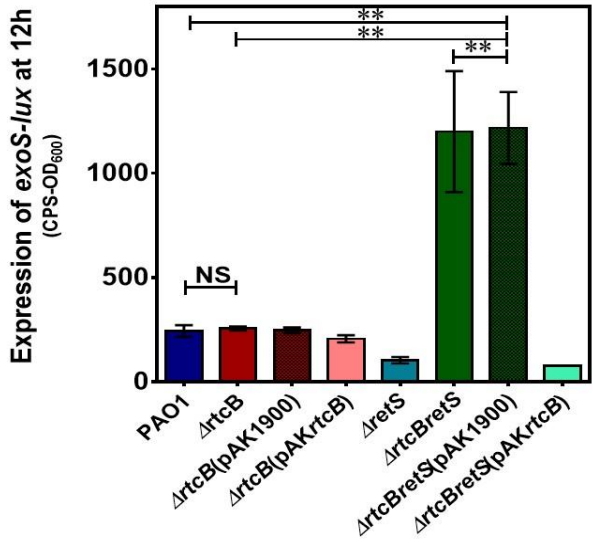
Expression of exoS-lux at 12h (CPS-OD600)
1500
1000
500
0
**
**
**
NS
PAO1
ΔrtcB
ΔrtcB(pAK1900)
ΔrtcB(pAKrtcB)
ΔretS
ΔrtcBretS
ΔrtcBretS(pAK1900)
ΔrtcBretS(pAKrtcB)

C

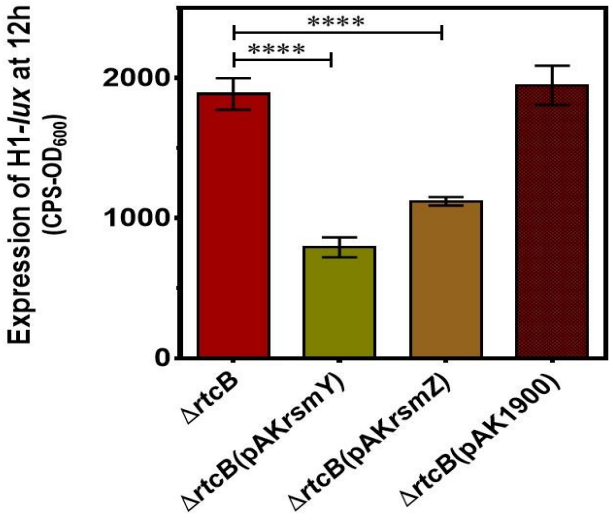
Expression of H1-lux at 12h (CPS-OD600)
2000
1000
0
****
****
ΔrtcB
ΔrtcB(pAKrsmY)
ΔrtcB(pAKrsmZ)
ΔrtcB(pAK1900)

D

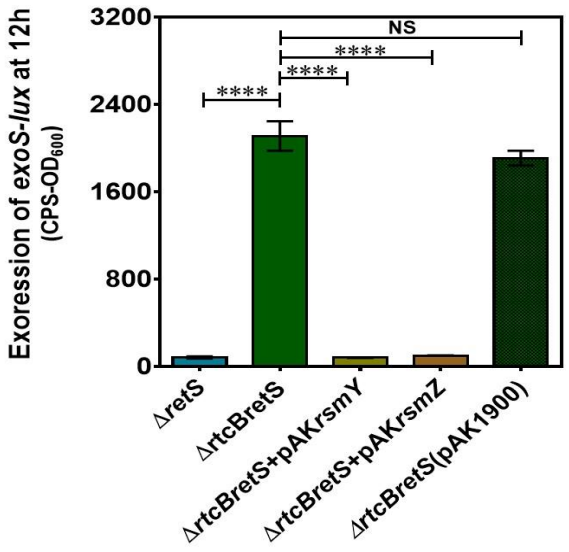

Figure 3.5 The promoter activity of *exoS* was significantly increased in PAO1(Δ*rtcB*Δ*retS*) compared with PAO1(Δ*retS*), and complementation of *rtcB* mutants RsmYZ altered H1-T6SS and *exoS* expression. A. Expression of *exoS*, the effector of T3SS, was restored in PAO1(Δ*rtcB*Δ*retS*). Data are shown as a relative change of promoter activity to growth (OD_{600}) during a course of 24h readout. The results are the average of three independent experiments. Error bars indicate standard deviations. **B.** Complementation of mutants restored the expression of *exoS*. Data is plotted at 12 h of growth. One-way Anova was used to analyze the data. The results are the average of three independent experiments. Error bars indicate standard deviations. NS $p > 0.05$, $^{**}p < 0.01$. **C, D**. Promoter activity of H1 and T3SS, respectively, are measured with and without complementation of mutants by overexpression vectors; pAK*rsmY* or pAK*rsmZ*. Expression of H1-T6SS was reduced in PAO1(Δ*rtcB*), but the expression of *exoS* was repressed to that of PAO1(Δ*retS*)in PAO1(Δ*rtcB*Δ*retS*). One-way Anova was used to analyze the data. These results are the average of three independent experiments. Error bars indicate standard deviations. NS $p > 0.05$, and $^{****}p < 0.0001$.

3.3.6 **Expression of RsmA was increased in *rtcB* deletion strains**

To confirm the activation of T3SS in PAO1(Δ*rtcB*Δ*retS*) was through RsmA, I performed Western blot analysis. In PAO1(Δ*retS*), the expression of RsmA was slightly less than that of PAO1. The expression of RsmYZ is elevated in PAO1(Δ*retS*). They bear multiple RsmA consensus binding sites consisting of a GGA sequence. RsmA is titrated upon binding to those recognition sites (Lapouge et al., 2013). Perhaps the interaction of RsmYZ and RsmA in PAO1(Δ*retS*) lowered the recognition of RsmA protein by CrsA (RsmA) antibody for *E. coli*. Interestingly, in *rtcB* knockout mutants PAO1(Δ*rtcB*) and PAO1(Δ*rtcB*Δ*retS*), the expression of RsmA showed a significant increase. As reported earlier, the upregulation of T3SS is under the control of the RsmA transcriptional regulator (Janssen et al., 2018; Moscoso et al., 2011a), and the Western blot result could explain the restoration of T3SS in PAO1(Δ*rtcB*Δ*retS*). However, in PAO1(Δ*rtcB*), the result was unexpected, where the outcome of an increased RsmA in PAO1(Δ*rtcB*) as a repressor of T6SSs, should have downregulated the H1-T6SS. This supports the notion that RtcB exerts its function on secretion systems through multiple pathways. Western blot result is shown in **Figure 3.6**.

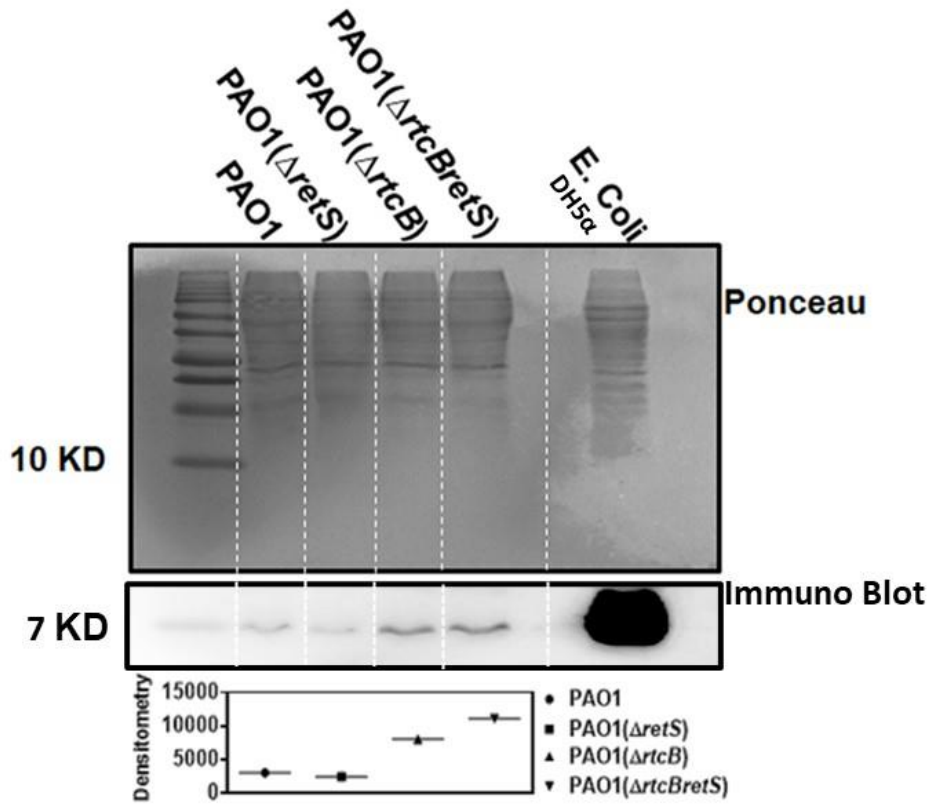

Figure 3.6. RsmA protein concentration was increased in RtcB deletion strain PAO1(Δ*rtcB*) and PAO1(Δ*rtcB*Δ*retS*). The total protein of each strain was normalized by Bradford assay and run by SDS-PAGE, and probed by the *E. coli* CsrA antibody. Ponceau staining was used as a loading control. Densitometry of Immunoblot shows that the expression of RsmA in PAO1(Δ*rtcB*) was increased 2.6-fold compared to PAO1, wherein PAO1(Δ*rtcB*Δ*retS*) showed a 4.4-fold increase compared to PAO1(Δ*retS*).

3.2.2 Deletion of *rtcB* upregulated the expression of *clpV1*, *hcp1*, *exsC,* and *exsA*

Regulations of H1-T6SS and T3SS are complex. The previous data confirmed that the activation of H1-T6SS in PAO1(Δ*rtcB*) and T3SS in PAO1(Δ*rtcB*Δ*retS*) is probably not through the same regulatory pathway. However, to verify whether the master regulators of these secretion systems were involved in RtcB modulation's interplay, I performed quantitative RT-PCR to determine whether the previously known regulators of T3SS and H1-T6SS are affected by deletion of *rtcB*. The qPCR was set up for quantification of selected genes, *hcp1*, *clpV1*in PAO1(Δ*rtcB*) compared to PAO1; and *exsA*, *exsC* in PAO1(Δ*rtcB*Δ*retS*) compared to PAO1(Δ*retS*). Hcp1 secretion is an indication of active H1-T6SS (Hachani et al., 2011). ClpV1 is the ATPase of H1-T6SS, required for the phosphorylation-dependent secretion of H1-T6SS (Hsu, Schwarz, and Mougous, 2009). ExsA is the master regulator of T3SS, and its docking to the consensus sequence of T3SS related-operon activates its transcription (Brutinel et al., 2008; Galle, Carpentier, and Beyaert, 2012). ExsD is an anti-activator, which directly binds to ExsA and represses its function. ExsC is an anti-anti-activator that sequesters ExsD and releases ExsA, which leads to the upregulation of T3SS (Urbanowski, Lykken, and Yahr, 2005). Gene expression relative to the *rpoD* housekeeping gene was analyzed and shown in **Figure 3.7**. The results showed the mRNA levels of *clpV1* and *hcp1* were increased more than 3 and 3.5-fold respectively in PAO1(Δ*rtcB*) compared to PAO1. Indeed, the expression of *exsA* and *exsC* were upregulated more than 4.5 and 5.5-fold compared with that in PAO1(Δ*rtcB*Δ*retS*).

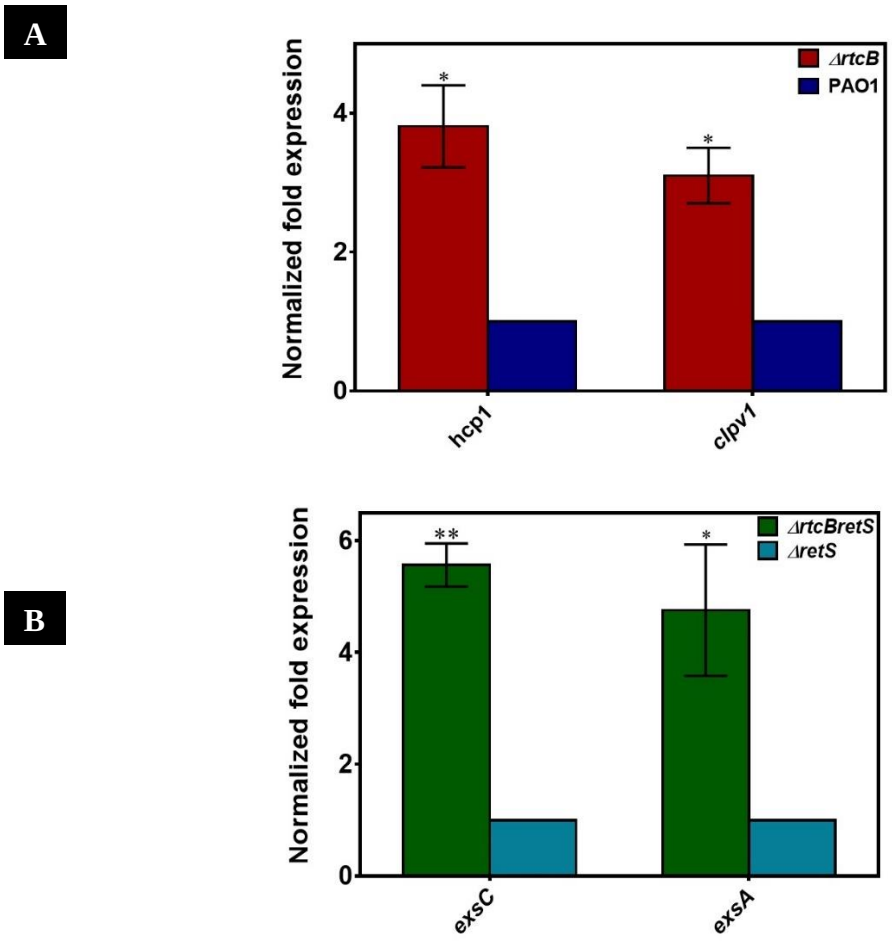

Figure 3.7 RtcB modulates H1-T6SS and T3SS through the cytoplasmic ATPase *clpV1* and master regulator *exsA*. The mRNA levels of essential components of H1-T6SS (*clpV1* and *hcp1*) and T3SS (*exsA* and *exsC*) were quantified by qPCR. **A.** The transcription of *clpV1* and *hcp1* showed a significant increase in PAO1(Δ*rtcB*) than PAO1. **B.** The expression of *exsA* and *exsC* were highly upregulated in PAO1(Δ*rtcB*Δ*retS*) compared to PAO1(Δ*retS*). Graphs presented as a percent change relative to the control (=1). Data were normalized to the levels of housekeeping gene *rpoD*. For A and B; Student's *t*-test was used to analyze the data. These results are the average of two independent experiments. Error bars indicate standard deviations. NS $p > 0.05$, *$p < 0.05$, **$p < 0.01$.

3.3.7 **RtcB is a member of stress response players in *P. aeruginosa*.**

3.3.7.1 ***rtcB*** **expression is higher in a stressed environment**

RtcB protein of *E. coli* functions in the heal and seal of damaged RNA after a stress-induced condition (Manwar et al., 2020; Tanaka et al., 2011; Tanaka and Shuman, 2011). To understand if it plays the same role in *P. aeruginosa*, first, I assessed the RtcB sequence similarity of *P. aeruginosa* to that of *E. coli* with protein blast (**Figure 3.8A**). The blast result showed that RtcB of *E. coli* and *P. aeruginosa* are 70% identical, and they probably function in similar processes. The similarity was further assessed by testing the expression of *rtcB* in stressed growth conditions (LB broth pH 5 versus LB broth pH 7). We constructed an *rtcB-lux* reporter, introduced it into PAO1, and measured reporter activities in a different condition. A significant elevation in reporter activity of *rtcB* in PAO1 was recorded in an acidic pH medium compared with LB pH 7 (**Figure 3.8B**). The data suggested that RNA ligase RtcB of *P. aeruginosa* somewhat plays a role in a stressed environment like RtcB protein of *E.coli* (Manwar et al., 2019) and perhaps through RNA healing or modifications (Engl et al., 2016).

A

```
RtcB E. coli          1 MNY-EL-LTTENAPVKMWTKGVPVEADARQQLINTAKMPFIFKHIAVMPDVHLGKGSTIG
RtcB P. aeruginosa    1 MKDMNILEVAGGKPIKLWTQGVPVEEEARQQLLNTAKMPFIFKHLAVMPDVHLGKGSTIG

RtcB E. coli         59 SVIPTKGAIIPAAVGVDIGCGMNALRTALTAEDLPENLAELRQAIETAVPHGRTTGRCKR
RtcB P. aeruginosa   61 SVIPTLGAIIPAAVGVDIGCGMIAARTSLVAADLPDNLHGLRSAIEQAVPHGKTFGR--R

RtcB E. coli        119 DKGAWENPPVNVDAKWAELEAGYQWLTQKYPRFLNTNNYKHLGTLGTGNHFIEICLDESD
RtcB P. aeruginosa  119 DRGAWHEVPEAADQAWKALAGRFKAITDKHPRLEKTNNRQHLGTLGTGNHFIEVCLDEAD

RtcB E. coli        179 QVWIMLHSGSRGIGNAIGTYFIDLAQKEMQETLETLPSRDLAYFMEGTEYFDDYLKAVAW
RtcB P. aeruginosa  179 RVWFMLHSGSRGVGNAIGNLFIELAKADMRQHIANLPDKDLAYFEEGSRNFDDYVEAVGW

RtcB E. coli        239 AQLFASLNRDAMMENVVTALQSITQKTVRQPQTLAMEEINCHHNYVQKEQHFGEEIYVTR
RtcB P. aeruginosa  239 AQDFARQNRALMMHAVIEAA----RQVIRKPFEANLEAVDCHHNYVQKERHFGQEVLVTR

RtcB E. coli        299 KGAVSARAGQYGIIPGSMGAKSFIVRGLGNEESFCSCSHGAGRVMSRTKAKKLFSVEDQI
RtcB P. aeruginosa  295 KGAVSAQKGQLGIIPGSMGAKSFIVRGLGNQEAFCSCSHGAGRTMSRTKAKKVFSVADQA

RtcB E. coli        359 RATAHVECRKDAEVIDEIPMAYKDIDAVMAAQSDLVEVIYTLRQVVCVKG
RtcB P. aeruginosa  355 RATAHVECRKDADVIDEIPMAYKDIDRVMEAQRELVEVLHTLRQVVCVKG
```

Identities: 277/397(70%), Positives:325/397(81%), Gaps:6/397(1%)
Method: Compositional matrix adjust

B

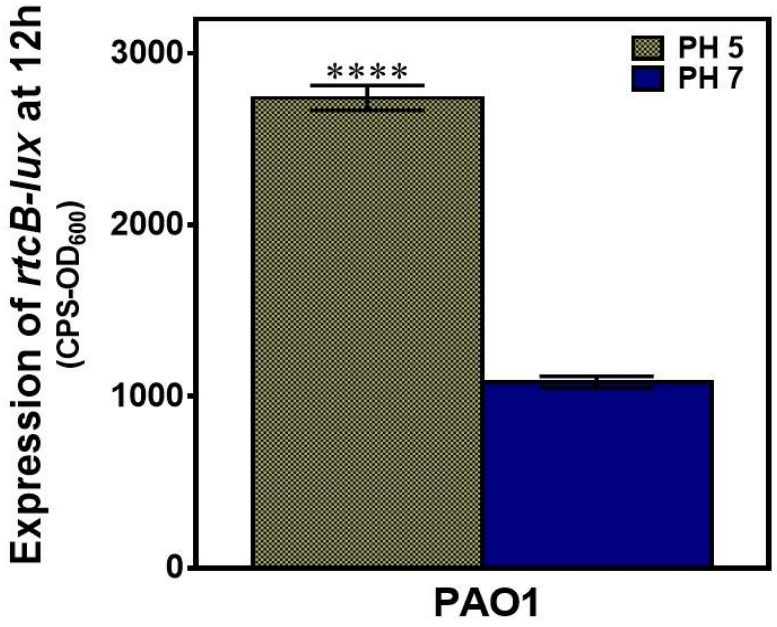

Figure 3.8 RtcB expression increases in the stress-induced environment. A. Sequence similarity of RtcB between *E. coli* and *P. aeruginosa* is shown, and a highly conserved sequence is color-coded as red. **B.** Reporter activity of pKD-*rtcB* was increased in a low pH medium (pH 5) compared to pH 7 in PAO1. Data are shown as a relative change of promoter activity to growth (OD_{600}) at 12 h. The student's *t*-test was used to analyze the data. These results are the average of three independent experiments. Error bars indicate standard deviations. ****$p < 0.0001$.

3.3.8 **Existence of cRNAs in *P. aeruginosa***

It has been shown that RNA ligase RtcB can circularize RNA in-vivo and in-vitro and produced stable circular RNAs (cRNAs) (Petkovic and Müller, 2015; Litke and Jaffrey, 2019; Holdt, Kohlmaier, and Teupser, 2018; Filipowicz, 2014; Englert et al., 2011). The stable cRNAs participate in the stress response of the cell (Fischer and Leung, 2017). Given the enzymatic activity of RtcB and its role in other bacteria's stressed conditions, I investigated the slim probability of cRNAs existence in *Pseudomonas*. I assessed the presence of cRNAs in PAO1 and PAO1(Δ*rtcB*) strains. The small RNAs RsmY and RsmZ play an essential role in the Gac-Rsm pathway and in switching between T6SS and T3SS. Hence the presence of a circular form of these small RNAs was tested. PAO1(Δ*retS*) was selected as a positive control considering the high expression and functionality of RsmYZ in this strain. RNAse R (**RR**) is used to digest the linear RNAs where applicable. Samples treated with RR are shown as $RR^{+,}$ and non-treated samples are noted as RR^{-}. Divergent primers used for the two sRNAs, RsmY and RsmZ, were designed as previously described (Panda and Gorospe, 2018). The divergent primers are facing outward and are expected not to amplify any linear RNA or genomic region. Before the RNA experiment was set up, the divergent primers on genomic DNA of PAO1 were tested to confirm no amplification was observed. For calibration (normalization) of the results, the housekeeping gene *rpoD* was used where applicable.

Besides, linear *rpoD* primer construct was used to

1) normalize the non-treated RNase R samples (**RR^{-}**; 1^{st} set samples: mixed linear and circular RNAs)

2) to guarantee that the PCR Master Mix set up is optimized and leads to amplification of the template

3) to provide the control to assess the proper digestion of linear *rpoD* after RNase R digestion (**RR**$^{+}$; 2nd set samples: circular RNAs), where no amplification of linear RNAs was expected in RNase R-treated samples

4) to confirm that the resultant positive amplification of cRNAs is not a false positive.

No expression of *rpoD* in RR^{+} (with high expression profile) would indicate that linear RNAs were completely digested with RNase R.

On the other hand, the *rpoD* region's divergent primers were designed to calibrate the RR^{+} and used as a negative control for the amplification of cRNA from *rpoD*.

RT-PCR was performed with combinations of primers and templates as controls. The setup, experiment's controls, and results of this study are briefed in **Table 3.4**. In RR^{+} (digested with RNase R), no linear RNA has existed to be used for normalization and relative expression comparison. Here, the existence of cRNAs was the focus of the study and not measuring the expression levels of cRNAs between strains. However, calibration is performed wherever applicable.

The result showed that cRNAs exist in *P. aeruginosa* bacterial cells. cRNAs were present in both RR^{+} and RR^{-} samples as the RNase R digests only the linear RNAs. The concentration of cRNAs in RR^{-} is higher for both *rsmY* and *rsmZ*; perhaps the cleanup step after RR treatment resulted in the loss of samples or the shear forces in the purification step caused nicks in cRNAs. Interestingly, cRsmY showed no significant

difference in RR^- and RR^+ groups and between the same group strains; however, it had slightly more abundance in PAO1(Δ*retS*). Moreover, and expectedly, PAO1(Δ*retS*) harbors considerably higher cRsmZ content compared to other strains. The cRNAs results are shown in **Figure 3.9**.

Table 3.4 PCR setups, controls, and results. Study controls are highlighted in red.

Primers	Template	Results
rpoD, convergent	gDNA	expressed
rpoD, convergent	No template (master mix contamination control)	Not detected
rpoD, divergent	gDNA	Not detected
rpoD, convergent	1st and 2nd set, -RT of all four strains	Not detected
rpoD, convergent	1st set of cDNA (RR^-)	expressed
rpoD, convergent	2nd set of cDNA (RR^+)	Not detected
rpoD, divergent	1st set of cDNA (RR^-)	Not detected
rpoD, divergent	2nd set of cDNA (RR^+)	Not detected
rsmY, divergent	gDNA	Not detected
rsmY, convergent	No template (master mix contamination control)	Not detected
rsmY, convergent	gDNA	expressed
rsmY, convergent	1st and 2nd set, -RT of all four strains	Not detected
rsmY, convergent	1st set of cDNA (RR^-)	expressed

rsmY, convergent	2nd set of cDNA (RR^+)	Not detected
rsmY, divergent	1st set of cDNA (RR^-)	expressed
rsmY, divergent	2nd set of cDNA (RR^+)	expressed
rsmZ, divergent	gDNA	Not detected
rsmZ, convergent	No template (master mix contamination control)	Not detected
rsmZ, convergent	gDNA	expressed
rsmZ, convergent	1st and 2nd set, -RT of all four strains	Not detected
rsmZ, convergent	1st set of cDNA (RR^-)	expressed
rsmZ, convergent	2nd set of cDNA (RR^+)	Not detected
rsmZ, divergent	1st set of cDNA (RR^-)	expressed
rsmZ, divergent	2nd set of cDNA (RR^+)	expressed

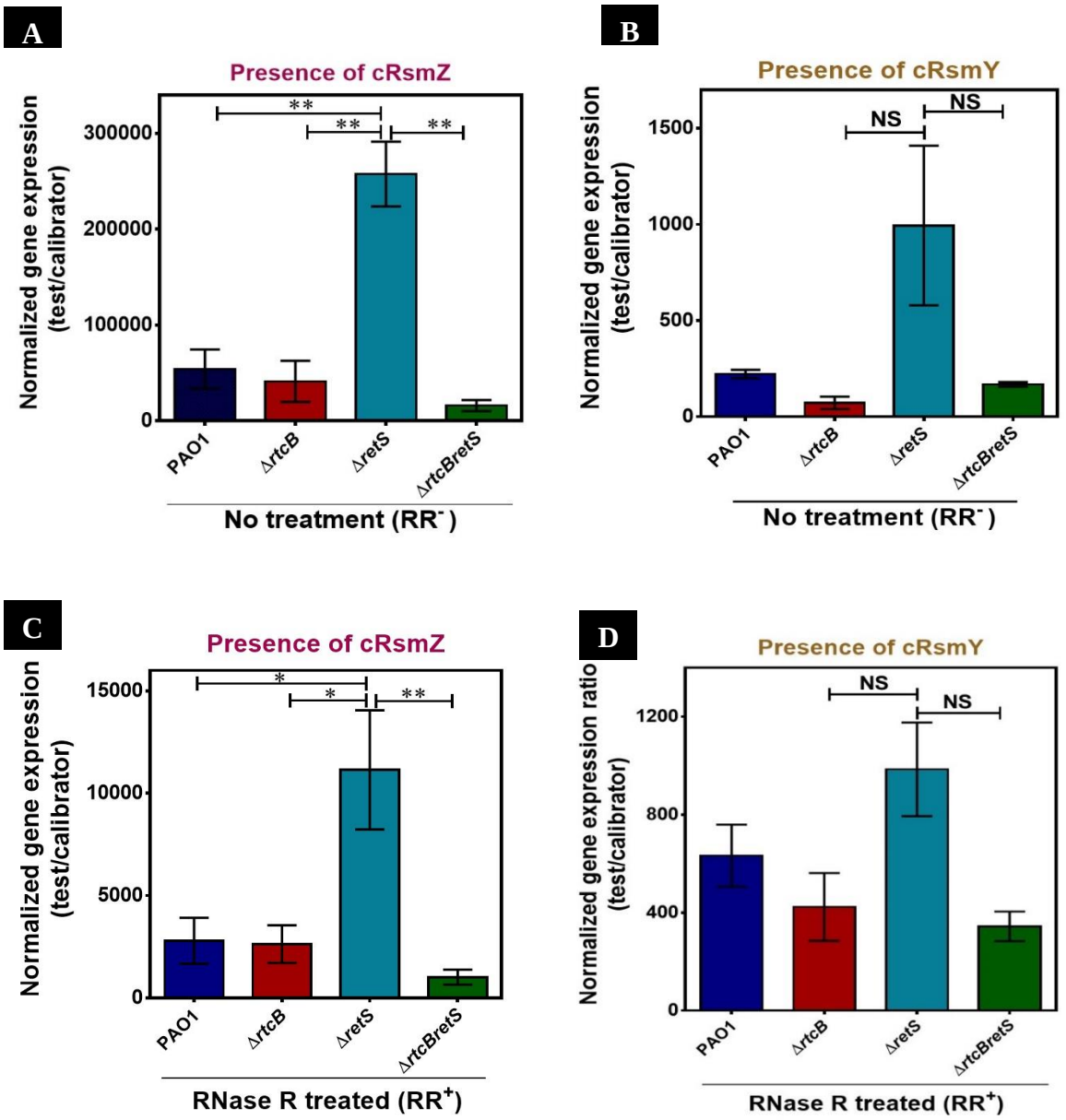

Figure 3.9 Confirmation of the presence of cRNAs in *P. aeruginosa*. A, B, C, D. Presence of cRsmZ and RsmY in PAO1 and mutant strains of *rtcB* and *retS* in RNase R treated and non-treated samples are shown. The cellular content of cRsmZ is significantly higher than cRsmY. In PAO1(Δ*rtcB*), the cRsmYZ are expressed significantly lower than PAO1(Δ*retS*). The experiments were performed three times independently. One-way

Anova was used to analyze the data. Error bars indicate standard deviations. NS $p > 0.05$, *$p < 0.05$, **$p < 0.01$.

Finally, to further confirm the RT-PCR data, the amplicons were cloned to the pET SUMO vector by TA cloning. The constructed plasmids were sequenced, and the result was aligned with RT-PCR observations. As seen in **Figure 3.10A**, amplification of the 5' extremity of cRNA is aligned with the 3' divergent primer and the 3' extremity, back spliced to the 5' end (blue-coded line) (**Figure 3.10A, B**).

As seen in the picture, five cytosines are connecting the 3' and 5' ends, which are highlighted with a red-coded line. The nature of the additional five cytosines linking the two divergent primers is uncertain and needs more studies. Perhaps, a post-transcriptional modification, a capping-like RNA processing step, or a tag as a recognition site for further processing. The unsequenced base pairs reduced the cRNA strand's length from 116 bp to 94 bp. The excised nucleotide from the RNA strand is underlined with Blue-coded color in **Figure 3.10B.** More investigation needs to be performed to confirm and highlight this modification/processing's nature before the back-splicing event. A primary proposed model of cRsmZ is depicted in Figure **3.10C**.

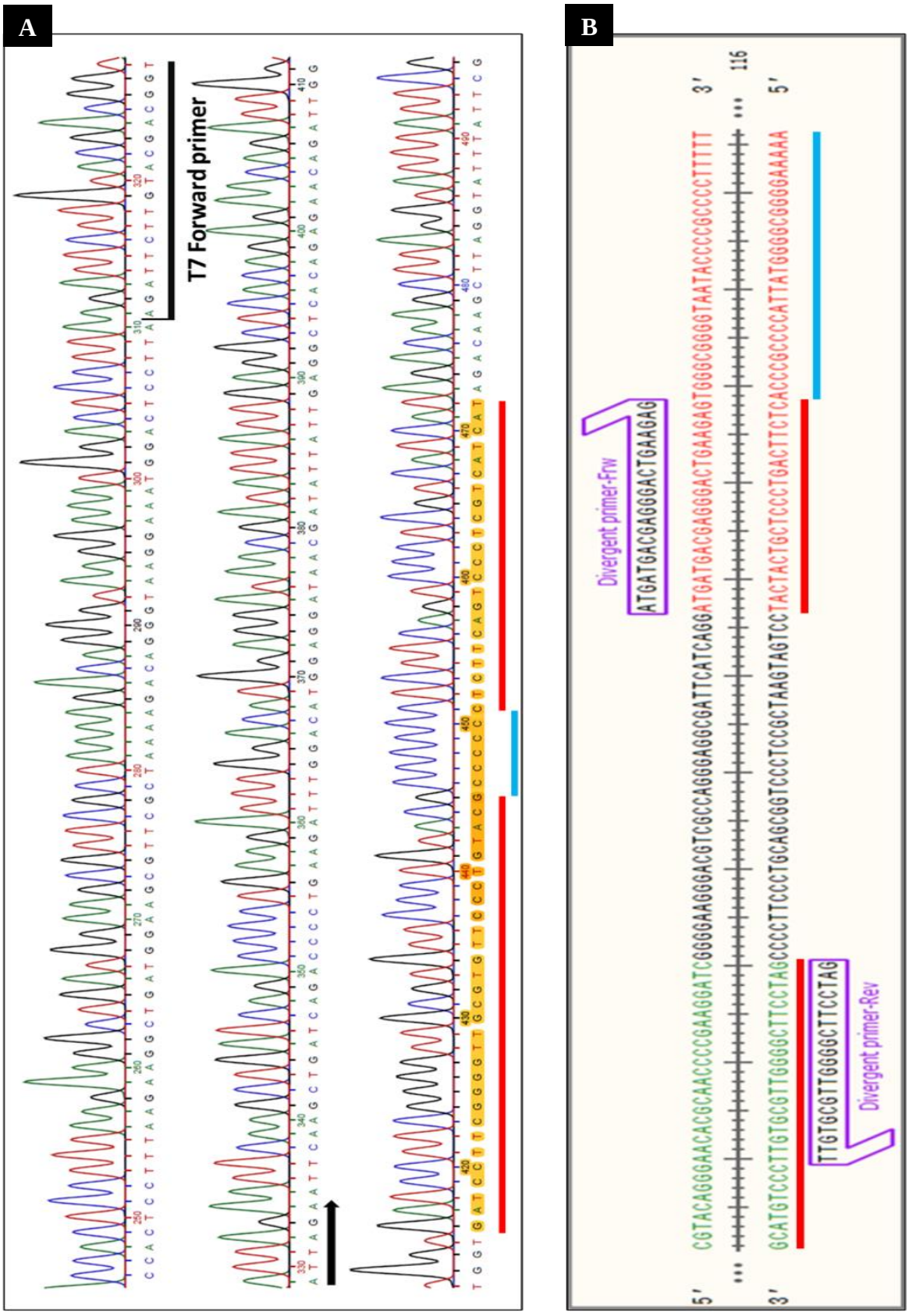
A
T7 Forward primer
B
Divergent primer-Frw
ATGATGACGAGGGACTGAAGAG
5′ CGTACAGGGAACACGCAACCCCGAAGGATCGGGGAAGGGACGTCGCCAGGGAGGCGATTCATCAGGATGATGACGAGGGACTGAAGAGTGGGCGGGGTAATACCCCGCCCCTTTTT 3′
3′ GCATGTCCTTGTGCGTTGGGGCTTCCTAGCCCCTTCCCTGCAGCGGTCCCTCCGCTAAGTAGTCCTACTACTGCTCCCTGACTTCTCACCCGCCCCATTATGGGGCGGGGAAAAA 5′
TTGTGCGTTGGGGCTTCCTAG
Divergent primer-Rev

C

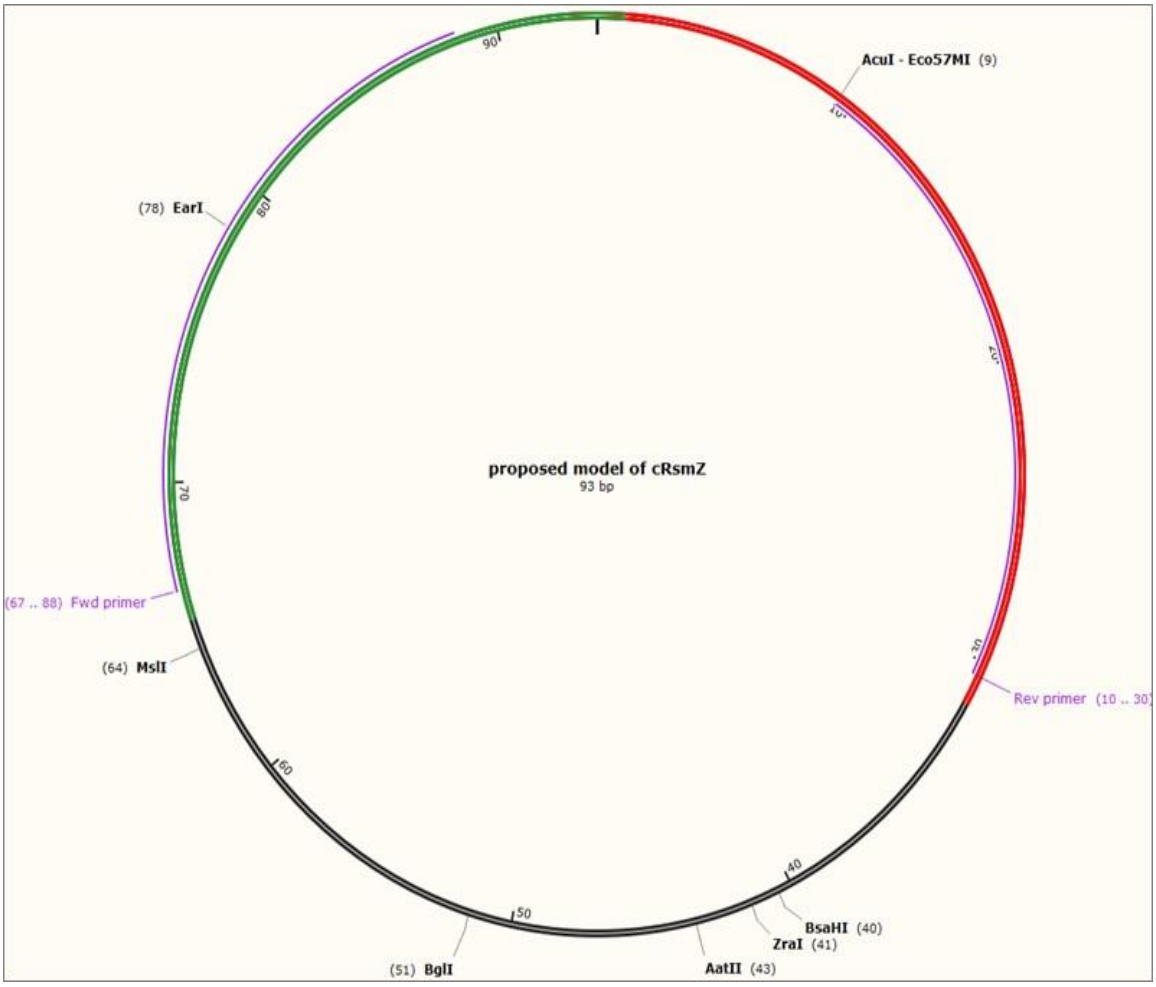

Figure 3.10 Sequencing result confirmed the back-splicing event of RsmZ, and the proposed circular RsmZ is depicted.

A. The sequencing result confirming the amplification of cRsmZ by RT-PCR. The region amplified between divergent primers is highlighted in yellow color. The sequenced base pairs are underlined with red color, and unsequenced base pairs are emphasized with a blue line. The Sumo forward priming site is underlined by a black line. **B.** The DNA sequence of *rsmZ*. Divergent primers are shown in purple. The 3' tail is shown in green,

and the 5’ head is shown in red. The sequenced region is underlined with red color, and the non-sequenced region is underlined with a blue line. **C.** The proposed model of cRsmZ is depicted, and circularization is shown. The 3’ end is highlighted in green, and the 5’ end is colored in red.

3.4 Discussion

In polymicrobial environments, *e.g*., cystic fibrosis patients' lungs, *P. aeruginosa* competes against other colonizing bacteria for its survival (Bhagirath et al., 2016; Sibley et al., 2008; Filkins and O'Toole, 2015). H1-T6SS in *P. aeruginosa* specifically exerts toxins to other prokaryotes living in its proximity. The results I obtained showed that the transposon insertion in PA4583 (*rtcB*) increased the expression of H1-T6SS in PAO1(Δ*rtcB*). This is the first report that shows RNA ligase RtcB participates in the regulation of secretion systems.

Also, higher expression of *tssA1* in PAO1(Δ*rtcB*) suggested not only *clpV1* reporter showed increased activity, but other components of H1-T6SS are also upregulated (Zoued et al., 2017; Planamente et al., 2016), which aided *P. aeruginosa* in killing the prokaryotic prey *E. coli*. Also, *rtcB* was shown to modulate different virulence phenotypes like biofilm formation and motility. In PAO1(Δ*rtcB*) formation of biofilm was slightly higher, whereas motility was reduced. The observation was reversed in PAO1(Δ*rtcB*Δ*retS*) with abolished biofilm production and a significantly higher motility rate than the PAO1(Δ*retS*). With an increase in biofilm formation and expression of T6SS in PAO1(Δ*rtcB*), we expected a pronounced switch from the motile lifestyle to the sessile phase in the PAO1(Δ*rtcB*). Generally, T3SS is active in PAO1 with no T6SS expression. The activation of T3SS and T6SS is modulated in a reverse manner. We expect only T3SS or T6SS is active at a time in a *P. aeruginosa* strain. Interestingly, in PAO1(Δ*rtcB*), both T6SS and T3SS were active and did not make a significant change in T3SS. We concluded that RtcB acts as a modulator of switch between T3SS and T6SS in which, lack of RtcB caused both T3SS and T6SS to be expressed. Also, T3SS expression in

PAO1(Δ*rtcB*Δ*retS*) was restored, where T6SS is yet significantly active. This data confirms that T3SS and H1-T6SS are simultaneously functional in PAO1(Δ*rtcB*) and PAO1(Δ*rtcB*Δ*retS*) without a significant switch between these secretion systems. RtcB affects the switch between secretion systems probably through different regulators and/or mechanisms. This is supported by the observation that an increase in the cellular concentration of free RsmA in PAO1(Δ*rtcB*) and PAO1(Δ*rtcB*Δ*retS*), shown with immune blotting. This increase should have resulted in a lower H1-T6SS expression in PAO1(Δ*rtcB*). Also, the presence of more free RsmA is not a consequence of the lower expression of RsmYZ. The overexpression of RsmYZ should lead to sequestration of RsmA and an even higher expression of H1-T6SS (Janssen et al., 2018). In contrast, overexpression of RsmYZ lowered H1-T6SS expression in PAO1(Δ*rtcB*). This confirms RtcB controls the expression of H1-T6SS in PAO1(Δ*rtcB*) through a different regulator than RsmA/Y/Z. On the other hand, activation of T3SS in PAO1(Δ*rtcB*Δ*retS*) appears to be through upregulation of RsmA where the overexpression of RsmYZ could repress the T3SS. Together, it is confirmed that RtcB controls the expression of RsmA directly or indirectly and modulates the expression of H1-T6SS and T3SS through RsmA and other different mechanisms. RtcB ultimately modulated the master regulators and essential partners of H1-T6SS and T3SS; *clpV1*, *hcp1*, *exsA*, and *exsC*. *ClpV1* is the cytoplasmic AAA+ ATPase of the H1-T6SS and is necessary for toxin delivery and disassembly of T6SS (Hachani et al., 2011; A et al., 2014). In *Burkholderia thailandensis*, localization of ClpV-5 in dynamic and discrete foci suggested the roles beyond solely being an energy provider for the T6SS (Lennings et al., 2019). ExsA is the global regulator of T3SS, binds to the promoters of T3SS-related genes, and upregulates their expression (Hauser,

2009). ExsC titrates the anti-ExsA protein, ExsD, and releases the ExsA. The higher expression of ExsC contributes to the antagonistic activity against ExsD and Free ExsA for higher expression of T3SS genes (Lykken et al., 2006).

I also examined if RtcB takes a role in response to stress conditions. *P. aeruginosa* cells without functional *rtcB* grew slower in a low pH medium, and low pH upregulated the RtcB protein production. Considering the role of RtcB in stress-inducing conditions as a part of the RNA repair operon (Manwar et al., 2019; Tanaka and Shuman, 2011), I explored the role of RtcB in the modification of sRNAs.

The investigation of transcriptional and post-transcriptional control of gene expression is advancing rapidly while RNA processors like RNA ligases in bacteria are less studied. These proteins are highly conserved and present in all three domains of life (Manwar et al., 2020). They are used for ligation and circularization of nicked RNAs in-vitro (Turunen et al., 2014).

Other than the RNA ligases, tRNA ligases can circularize the RNAs like the tRNA ligase of wheat and *Saccharomyces cerevisiae* (Konarska et al., 1981). Also, tRNA ligase RtcB showed RNA circularization activity in-vitro (Petkovic and Müller, 2015b; Englert et al., 2011). RtcB joins the 3’ -phosphate and 5'-OH termini of damaged and/or broken RNA in a GTP-dependent manner (Tanaka and Shuman, 2011). Also, more GTP concentrations resulted in higher levels of RNA circularization (Petkovic and Müller, 2015). The result acquired from testing the presence of circular RNA in *P. aeruginosa* found that RsmZ/Y could present in a circular and linear pattern, where cRNAs are less abundant. Indeed, the cellular content of cRsmZ was notably higher than cRsmY.

In *P. aeruginosa*, at least one other protein encoded by the gene PA5471, ArmZ, has an RNA ligase activity. ArmZ may contribute or partner with the RtcB protein's functioning (this gene not tested in this thesis). It is unclear whether cRNAs are formed at a specific phase of cell growth. The end modifications are part of circularization or appear in linear RNAs as well, or perhaps it plays a molecular tag for targeting the RNAs for circularization. The cRNA experiments could certainly be performed with different time point RNA isolations or in different growth conditions to observe whether the end modification is transient or remain constant and whether the growth phase affects the cellular concentration or expression of cRNAs. The findings are novel and require more studies to reveal the expression pattern and functionality of cRNAs. Collectively, this study identified a novel modulator of H1-T6SS, T3SS, and RsmA/Y/Z protein. The result showed RtcB plays a role in stress-response and RNA processing. The conserved protein RtcB may play diverse roles in the cell.

Chapter 4

4 Transcriptomic analysis of the role of the ribo-repair system in *Pseudomonas aeruginosa*

4.1 Introduction

The three T6SS in *P. aeruginosa* are not redundant nor identical. Each cluster of T6SS is encoded separately under complex modulations (Filloux et al., 2008). In the transposon mutagenesis screening (Chapter 3), the *rtcB*::Tn mutant was identified that showed altered H1-T6SS expression. RtcB is a conserved protein in all three domains of life (Manwar et al., 2020). In addition to its role in the RNA repair after damage by ribotoxins (Tanaka et al., 2011), RtcB catalyzes tRNA splicing (Tanaka et al., 2011). In bacteria, the role of RtcB is yet to be elucidated as the tRNA of the bacteria does not undergo a tRNA splicing event (Manwar et al., 2020). It was suggested that the highly conserved RtcB might play a vital role in the bacteria's homeostasis (Manwar et al., 2020). As indicated in the previous chapter of this thesis, the deletion of *rtcB* not only affected the expression of T6SS and biofilm formation but also restored the motility and the expression of T3SS in the PAO1(Δ*retS*) background. The master regulators of T3SS and T6SS, *exsA* and *clpV1,* respectively, were also affected significantly by *rtcB* deletion. Moreover, higher expression of *rtcB* in stress-induced conditions like low pH environments suggests a role of RtcB in the bacterium's survival in adverse conditions. Therefore, I hypothesized that RtcB is a global regulator of several major virulence factors necessary to the bacterium's fitness. To understand the potential broad roles of RtcB at the whole genomic level, RNAseq was used to compare the transcriptomics of the APO1, *rtcB,* and *retS* deletion mutants. The genes with different expression profiles were selected and further examined.

4.2 Materials and methods

4.2.1 Bacterial strains and plasmids

Bacterial strains and plasmids used in this study are presented in **Table 4.1**. *E. coli* and *P. aeruginosa* were grown at 37˚C on LB agar or LB broth. The concentrations of antibiotics used in this study are addressed in chapter 2.

Table 4.1 bacterial strains and plasmids of this study

Bacterial strains or plasmid	**Relevant characteristics/sequence**	**Source**
***P. aeruginosa* strains**		
PAO1	Wild type, lab strain	This lab
PAO1 (Δ*retS*)	*retS* replacement mutant of PAO1	This lab
PAO1 (Δ*rtcB*)	*rtcB* replacement mutant of PAO1	This thesis
PAO1 (Δ*rtcB*Δ*retS*)	*rtcB retS* replacement mutant of PAO1	This thesis
Plasmids		
pAK1900	*E. coli-P. aeruginosa* shuttle cloning vector, Amp^r	(Sharp et al. 1996)
pAK-*rtcB*	pAK1900 with a 1260 bp fragment of PA4583 between *Bam*HI and *Hind*III; Amp^r, Cb^r	This thesis

4.2.2 **RNA-seq and analysis of differentially expressed genes**

Total RNA was isolated in three independent experiments, and the integrity of RNA samples was assessed by Bioanalyzer 2100 (Aligent, Santa Clara, CA, United States). The rRNAs were depleted from 1 µg of the total RNA using the Ribo-Zero Magnetic Gold Kit (Epicentre Biotechnologies, Madison, WI, USA). TruSeq RNA Sample Prep Kit v2 (Illumina San Diego, CA, United States) was used to construct the RNAseq library. rRNA-free RNA samples were fragmented using Elute Prime Fragment Mix. The first-Strand cDNA was constructed with First Strand Master Mix, and SuperScript II reverse transcriptase (Invitrogen, Carlsbad, CA, United States) and purified by Agencourt RNAClean XP beads (Beckman Coulter, CA, United States). The second-strand cDNA library was synthesized using Second Strand Master Mix and dATP, dGTP, dCTP, dUTP mix. The final cDNAs were end-repaired (30 min at 37˚C) and proceeded to ligate sequencing adapters. AMPureXP Beads was used to purify the RNA-Seq libraries. The clustering of the index-coded samples was performed on a cBot Cluster Generation System based on the manufacturer's protocol, and the sequencing was performed using the Illumina Hiseq TM 2500 platform with pair-end 150 base reads

4.2.3 **Bioinformatics analysis**

The raw data obtained from RNAseq were filtered, and reproducibility between samples was evaluated. The reads with ≥10% unidentified nucleotides (N) and the reads with >50% bases having Phred quality scores of ≤20 were removed. To compensate for the sample number (less than 12) data were filtered with the Edge R package and adjustment of *p* values after FDR to *q* values (Schurch et al., 2016). The reads aligned to the barcode

adapter using FASTP. Quality trimmed reads were matched using Bowtie2 (Langmead and Salzberg, 2012) (version 2.2.8) to the *P. aeruginosa* PAO1 reference genome to determine the genes and calculate the gene expression by RSEM (B. Li and Dewey, 2011). The gene expression level was normalized using the fragments per kb of transcript per million (FPKM) mapped reads method for eliminating the influence of different gene lengths and amount of sequencing data on the calculation of gene expression. Differentially expressed genes (DEGs) in samples with a fold change ≥ 2 and a false discovery rate adjusted *p*-value (*q*-value) <0.05 were identified using the Edge R package (www.r-project.org). The KEGG pathway and GO terms were defined as significant when *q* value ≤ 0.05. To show the difference between the categorized gene expression, Heatmap; MATLAB was used.

4.2.4 **Pyocyanin assay**

Bacteria were grown overnight for 16 h, and the supernatant was harvested. According to the previously described protocol by Essar et al. (Essar et al., 1990), the pyocyanin content was measured. A 5 ml of supernatant was mixed with 3 ml of chloroform. The chloroform layer was separated by centrifugation and transferred to a fresh tube. Then, 1 ml of 0.2 N HCL was added to the falcon tubs and mixed well, following a centrifuge at 4720 xg for 10 min. The top layer was separated, and its absorbance at 520 nm was measured. The cellular content of pyocyanin was presented as micrograms of pyocyanin per milliliter of supernatant, calculated by multiplying the extinction coefficient of 17.072 at 520 nm.

4.2.5 **Proteolytic activity assay**

The strains' protein activity was determined through skim milk (SM) agar plate assay described previously with brief modifications (Gupta, Gobble, and Schuster, 2009). LB plates were supplemented with 2% skim milk. 2 µl of overnight cultures were spotted on the SM plates and were incubated overnight at 37˚C. The clear zone surrounding the bacterial cells was measured as an indicator of the bacterial strain's proteolytic activity.

4.2.6 **Quantification of c-di-GMP**

C-di-GMP was quantified with CdiGMP Elisa Kit from Mybiosource (#MBS288159) with alternation in the extraction of c-di-GMP from bacterial cells, following Irie et al. protocol with brief modifications (Irie and Parsek, 2014). Bacterial strains were grown in 5 ml LB broth for 24 hours at 37°C (biofilm formation condition was applied earlier). Bacterial density was adjusted to 3 ml of OD_{600}=1.8. Bacterial cells were pelleted down for 7 min at 1541 xg and washed three times with PBS buffer. 250 µl of 0.6 M perchloric acid was added to the washed pellet and left on the rotatory shaker for 30 min at 4°C. The supernatant was transferred to a fresh Eppendorf tube following a centrifuge at 18879 xg for 10 min. 200 µl of 1M KOH was added to the tubes, and the salt byproduct was settled by centrifuging at 14000 for 10 min. The clear supernatant was used for the quantification of c-di-GMP following the kit manual. The remaining extracts were aliquoted and stored at -80°C.

4.2.7 **Plant virulence assay**

The plant infection assay was performed in lettuce leaves as described previously (Rahme et al., 1997). Overnight-grown bacterial cultures were adjusted to OD_{600} = 0.01 and washed three times with cold PBS buffer. The pellets were resuspended in 10 mM

MgSO4 and were used to inoculate the mid-ribs of the romaine lettuce leaves. The inoculated leaves were incubated at room temperature for 2 days in plates containing a Whatman filter paper, soaked with 10 mM MgSO4. The leaves were monitored during the incubation and imaged at 48 hr.

4.3 Results

4.3.1 Transcriptional profiling of the *rtcB* knockout mutant

To further investigate the global role of RtcB, RNAseq analysis was carried out with the *rtcB* deletion mutant. The experiments were carried in two groups;

Group 1) PAO1 vs. **PAO1(Δ*rtcB*)**

Group 2) PAO1(Δ*retS*) vs. **PAO1(Δ*rtcB*Δ*retS*)**.

In group 1, 370 genes were differentially expressed, in which 271 genes were upregulated, and 99 genes were downregulated.

In group 2, 1030 genes were differentially expressed; 498 genes were upregulated, and 532 genes were downregulated (**Figure 4.1A**).

The differentially expressed genes (DEGs) were specified based on the sequence homology and the gene ontology (GO) of those that were significantly enriched ($q < 0.05$), which are plotted in **Figure 4.1B, C**. Comparing the DEGs shows the transcription of genes participating in the metabolic process of the cell in both groups like; global pathways, the metabolism of carbohydrates and amino acids, and xenobiotics biodegradation; has significantly altered, which indicates that RtcB takes a key role in

modulation of cell metabolome. Also, DEGs show that RtcB affects the secondary metabolites, bacterial secretion systems, signal transduction pathway, and cell motility considerably. The fifth most affected DEGs were membrane transport proteins, as seen in the pie chart. The expression of bacterial secretion systems as a subcategory of transmembrane proteins was remarkably changed, of which T2SS, T5SS, T3SS, T6SS, and Sec-SRP were affected. Members of the signal transduction pathway and cell motility network are modulated least by deletion of RtcB. The top 20 DEGs affected by deletion of RtcB are represented in **Figure 4.1D, E**.

A

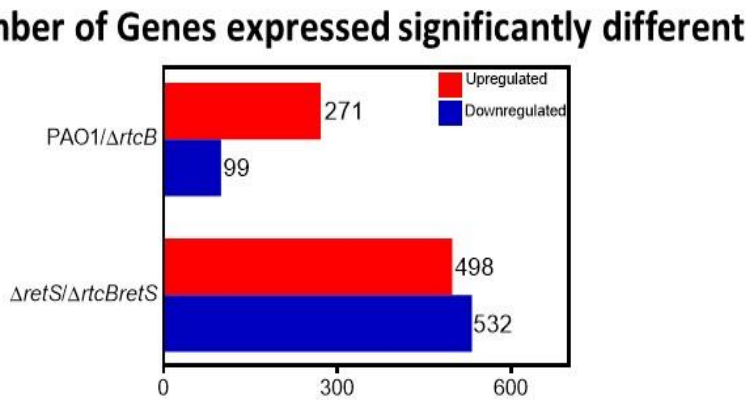
Number of Genes expressed significantly different
Upregulated
Downregulated
PAO1/ΔrtcB
271
99
ΔretS/ΔrtcBretS
498
532
0
300
600

B

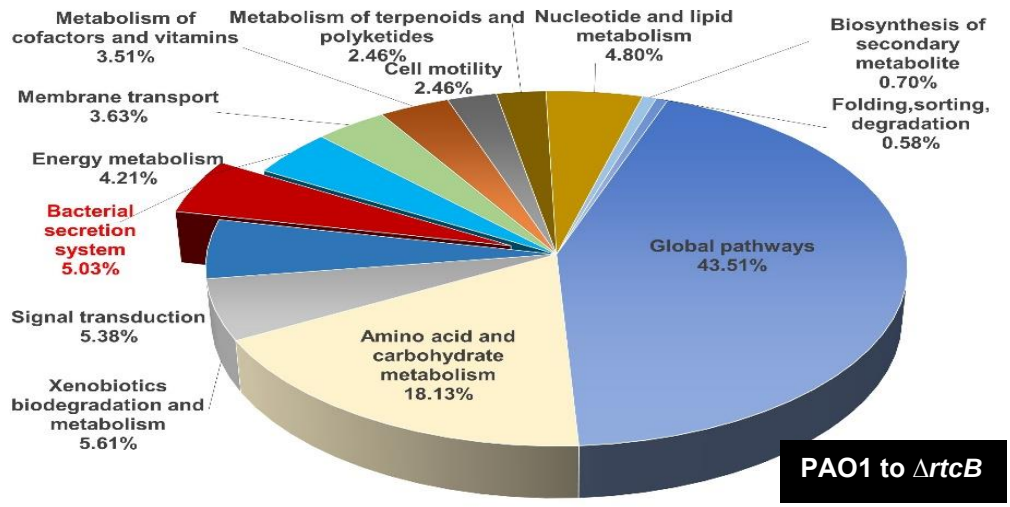
Metabolism of cofactors and vitamins 3.51%
Metabolism of terpenoids and polyketides 2.46%
Nucleotide and lipid metabolism 4.80%
Biosynthesis of secondary metabolite 0.70%
Folding,sorting, degradation 0.58%
Cell motility 2.46%
Membrane transport 3.63%
Energy metabolism 4.21%
Bacterial secretion system 5.03%
Global pathways 43.51%
Signal transduction 5.38%
Amino acid and carbohydrate metabolism 18.13%
Xenobiotics biodegradation and metabolism 5.61%
PAO1 to ΔrtcB

C

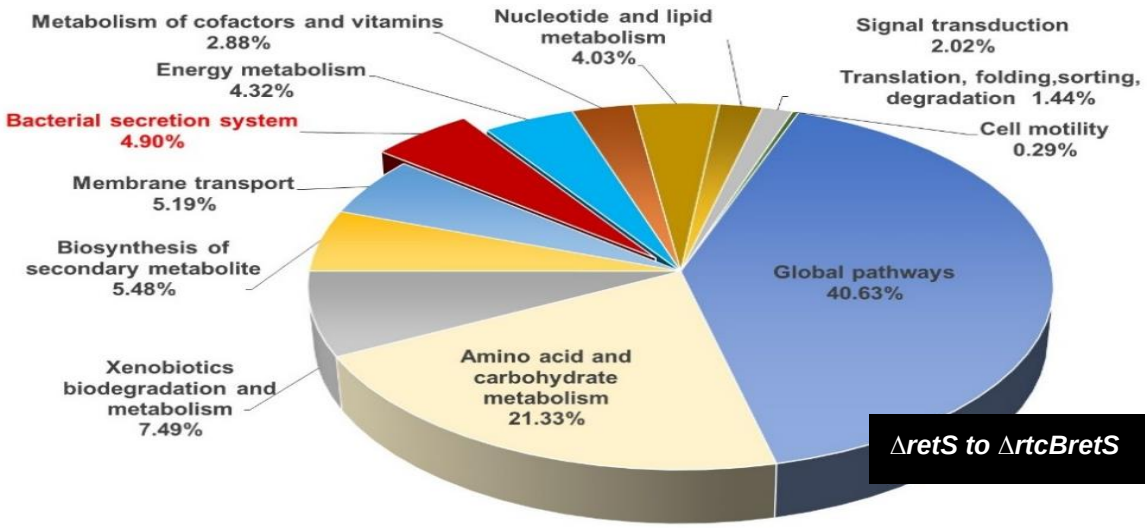
Metabolism of cofactors and vitamins 2.88%
Nucleotide and lipid metabolism 4.03%
Signal transduction 2.02%
Translation, folding,sorting, degradation 1.44%
Energy metabolism 4.32%
Cell motility 0.29%
Bacterial secretion system 4.90%
Membrane transport 5.19%
Biosynthesis of secondary metabolite 5.48%
Global pathways 40.63%
Amino acid and carbohydrate metabolism 21.33%
Xenobiotics biodegradation and metabolism 7.49%
ΔretS to ΔrtcBretS

D

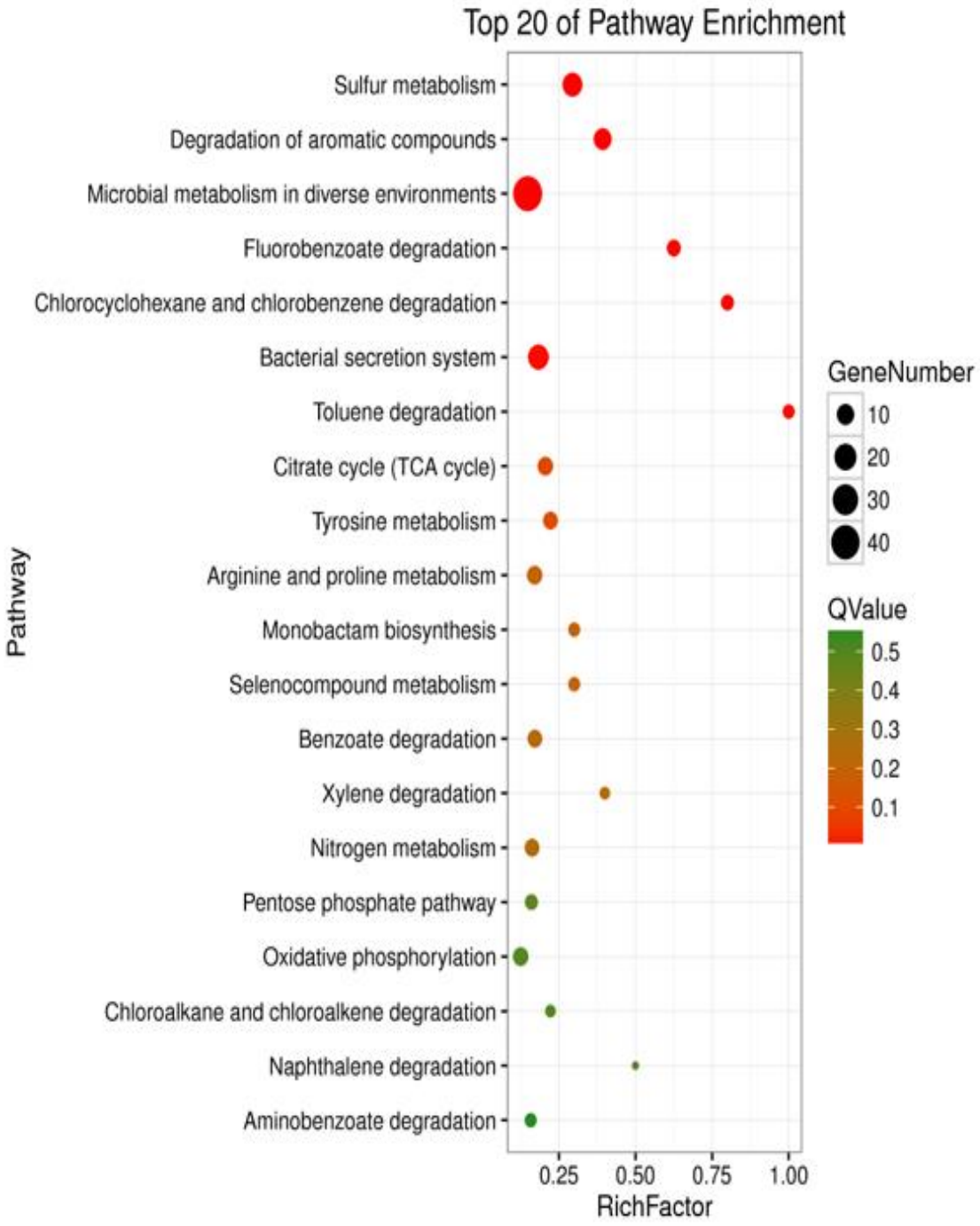

PAO1 to Δ*rtcB*

E

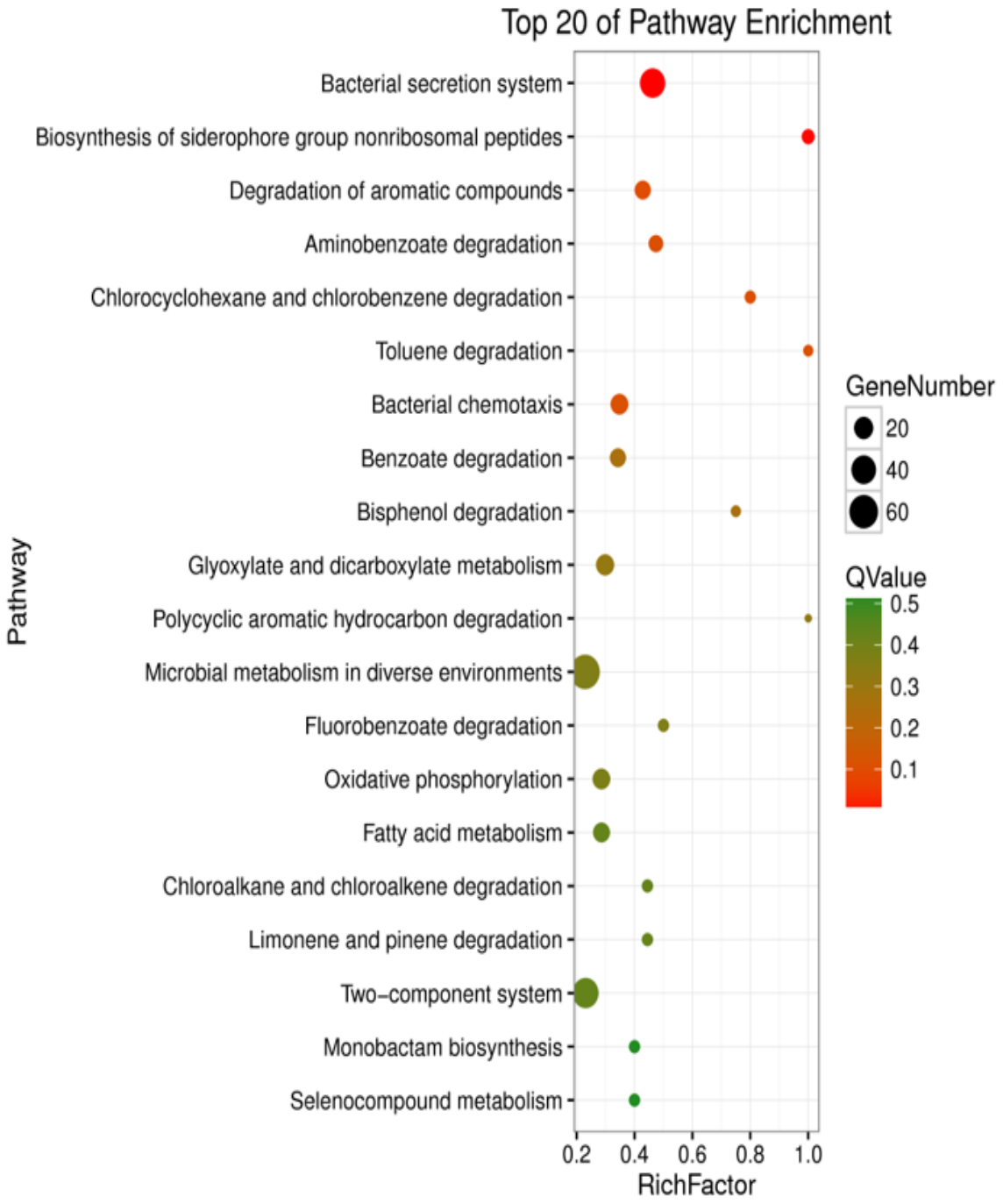

ΔretS to ΔrtcBretS

Figure 4.1 The effect of *rtcB* deletion on the global transcriptome of *P. aeruginosa*. **A.** A total of 370 genes showed significantly different expressed genes in PAO1(Δ*rtcB*)compared to PAO1, and 1030 genes in PAO1(Δ*rtcB*Δ*retS*) compared to PAO1(Δ*retS*). **B, C.** The pie charts presenting the Gene Ontology analysis of differentially expressed genes between groups 1(B) and 2(C). **D, E.** KEGG enrichments between groups 1 and 2, respectively. Y-axis shows the top 20 pathways affected by deletion of *rtcB*. The X-axis represents the ratio of the number of enriched DEGs in the categorized KEGG to the total genes of that category. Dot size represents the number of DEGs of the pathway, and dot color indicates the Q-value. Q-value is the enrichment level of each category.

4.3.2 **Influence of *rtcB* deletion on quorum sensing and pyocyanin production**

Secondary metabolites were significantly differentially expressed between the *rtcB* mutant, and their background as outlined in GO analysis. To examine the effect of RtcB on QS and phenazine metabolites, the expression of genes involved in the QS network and QS-dependent virulence determinants were compared.

In **group 1**, transcripts of 26 genes out of 52 QS genes (50%) were upregulated, wherein in **group 2**, only 14 genes were upregulated (26%).

Additionally, the expression of phenazine biosynthesis genes was increased in group 1. The heatmap graph represents the varied QS-related genes and the selected proteins under direct regulation of QS (**Figure 4.2A**). The raw Z-score was calculated for three biological replicates by processing FPKM values of the significantly differentially expressed genes in **groups 1 and 2**, represented as a color-coded box.

To validate these data, I used the quantification of pyocyanin as a phenotypic marker for assessing the QS system and activity of *phz* operons (Frank and DeMoss, 1959). Production of pyocyanin was increased in PAO1(Δ*rtcB*) compared to PAO1, following higher expression of QS-related genes and *phzA2B2C2*. There was no significant change in pyocyanin production of PAO1(Δ*rtcB*Δ*retS*) and PAO1(Δ*retS*) was observed (**Figure 4.2B**). Moreover, this metabolite was slightly higher in PAO1(Δ*rtcB*Δ*retS*) than PAO1(Δ*rtcB*) aligned with our RNAseq data, with probably more contribution of *phz1* operon in PAO1(Δ*rtcB*Δ*retS*).

4.3.3 **Proteolytic activity was elevated significantly in PAO1(Δ*rtcB*Δ*retS*)**

The expression of *lasB* gene was affected by the deletion of *rtcB*. In PAO1(Δ*rtcB*), the transcription of *lasB* and *lasA* were decreased, and inversely, their transcription increased in PAO1(Δ*rtcB*Δ*retS*) compared with PAO1 and PAO1(Δ*retS*), respectively. The transcription of alkaline protease AprA was also significantly higher in the PAO1(Δ*rtcB*Δ*retS*). Since *lasR* and *rhlR* in PAO1(Δ*rtcB*Δ*retS*) show lower expression, the proteinases' upregulation was not under the effect of *lasR* and *rhlR* (Brint and Ohman, 1995; Gambello and Iglewski, 1991; Toder, Gambello, and Iglewski, 1991). To confirm the higher proteolytic activity of the PAO1(Δ*rtcB*Δ*retS*), the proteolytic assay was performed, and the results are shown in **Figure 4.2C, D**. Expectedly, PAO1(Δ*rtcB*Δ*retS*) showed higher proteolytic activity than PAO1(Δ*retS*).

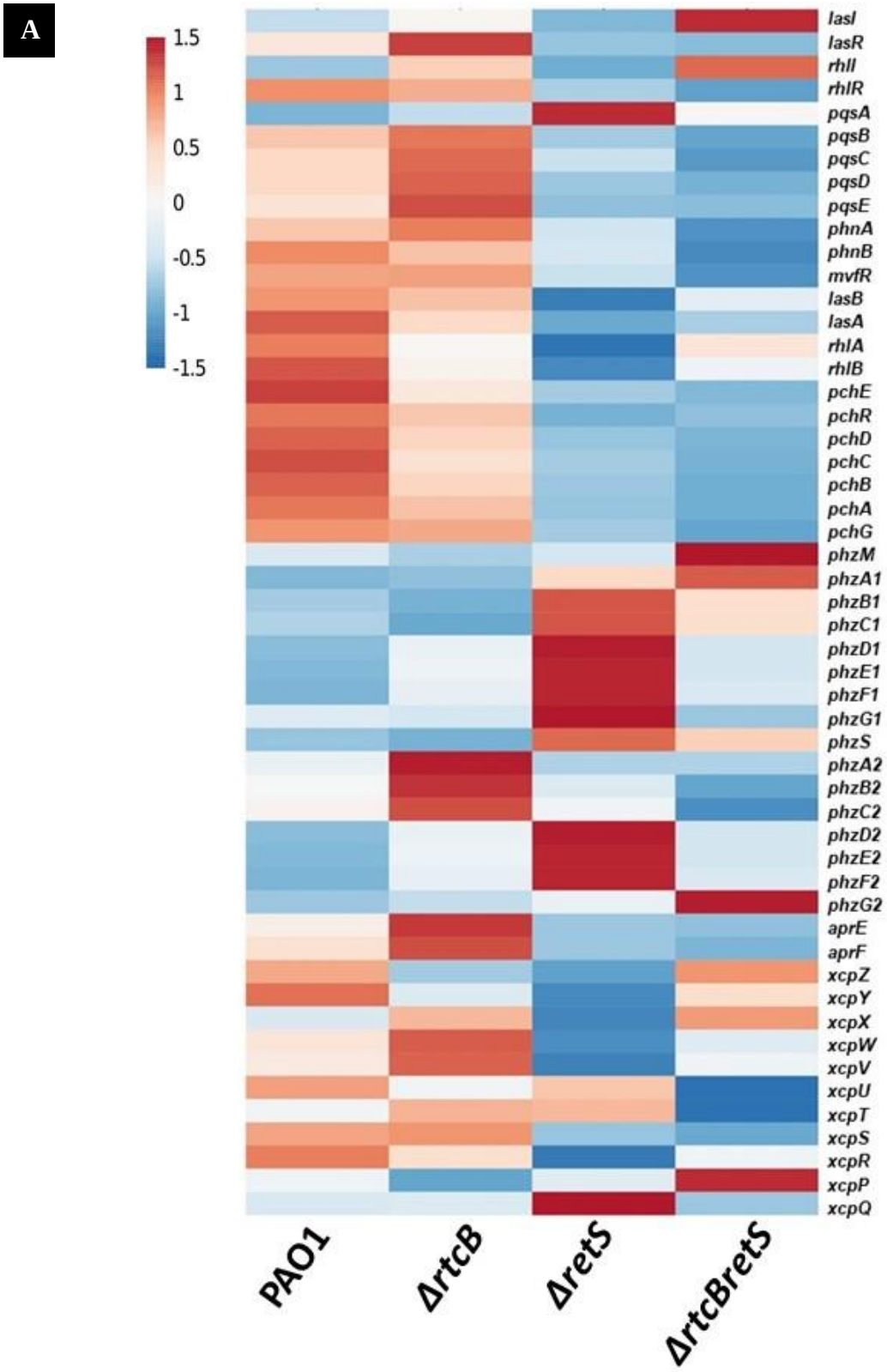
A
1.5
1
0.5
0
-0.5
-1
-1.5
lasI
lasR
rhlI
rhlR
pqsA
pqsB
pqsC
pqsD
pqsE
phnA
phnB
mvfR
lasB
lasA
rhlA
rhlB
pchE
pchR
pchD
pchC
pchB
pchA
pchG
phzM
phzA1
phzB1
phzC1
phzD1
phzE1
phzF1
phzG1
phzS
phzA2
phzB2
phzC2
phzD2
phzE2
phzF2
phzG2
aprE
aprF
xcpZ
xcpY
xcpX
xcpW
xcpV
xcpU
xcpT
xcpS
xcpR
xcpP
xcpQ
PAO1
ΔrtcB
ΔretS
ΔrtcBretS

B

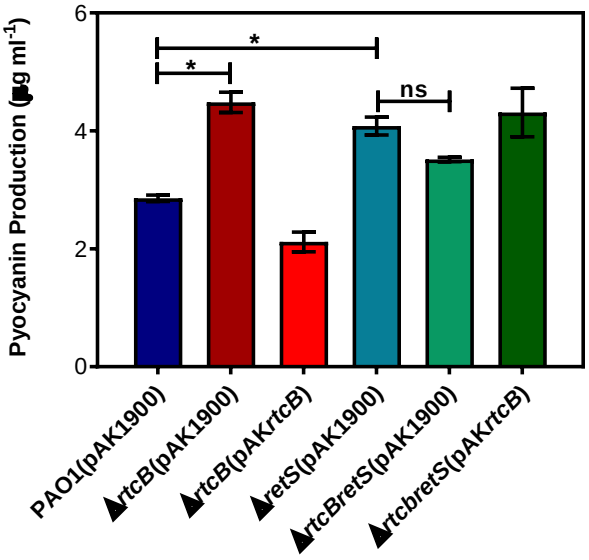
Pyocyanin Production (µg ml-1)
6
4
2
0
*
*
ns
PAO1(pAK1900)
ΔrtcB(pAK1900)
ΔrtcB(pAKrtcB)
ΔretS(pAK1900)
ΔrtcBretS(pAK1900)
ΔrtcbretS(pAKrtcB)

C

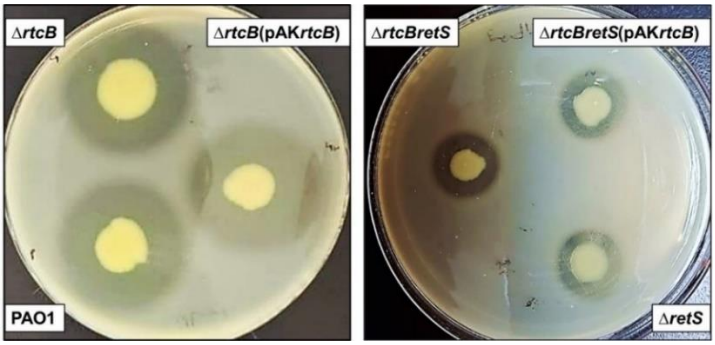
ΔrtcB
ΔrtcB(pAKrtcB)
PAO1
ΔrtcBretS
ΔrtcBretS(pAKrtcB)
ΔretS

D

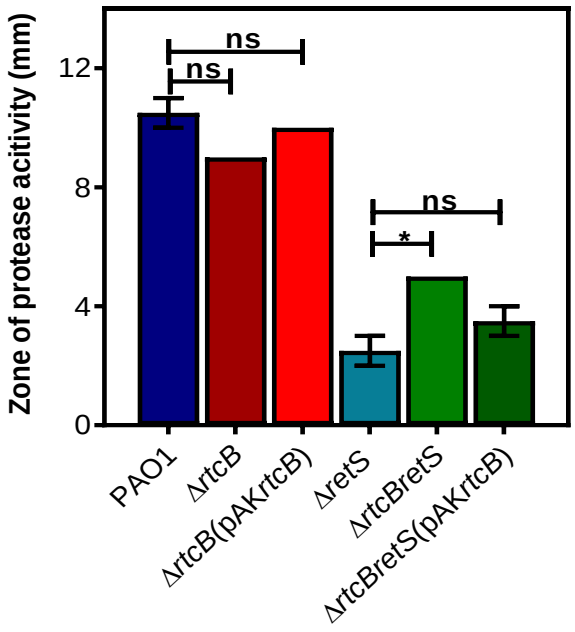
Zone of protease acitivity (mm)
12
8
4
0
ns
ns
ns
*
PAO1
ΔrtcB
ΔrtcB(pAKrtcB)
ΔretS
ΔrtcBretS
ΔrtcBretS(pAKrtcB)

Figure 4.2 Comparative analysis of PAO1, PAO1(Δ*rtcB*), PAO1(Δ*retS*), and PAO1(Δ*rtcB*Δ*retS*) on QS and PYO transcriptomes. A. The gene expression levels were quantified by row Z-score and represented in heatmap graph by the color-coded box; blue-code: downregulation and red-code: upregulation. **B.** Measurement of pyocyanin production in PAO1, PAO1(Δ*rtcB*), PAO1(Δ*retS*), and PAO1(Δ*rtcB*Δ*retS*)and the complemented strains. Pyocyanin was produced significantly higher in PAO1(Δ*rtcB*) compared to PAO1. **C, D.** PAO1(Δ*rtcB*) Showed slightly lower proteolytic activity than PAO1, where PAO1(Δ*rtcB*Δ*retS*) showed a considerably larger proteolytic zone than PAO1(Δ*retS*). The experiments were performed independently three times. Data were analyzed with an unpaired student's *t*-test. *p<0.01.

4.3.4 **RtcB controls the transcription profile of T6SSs and T3SS in *P. aeruginosa***

The transcriptome of bacterial secretion systems T2, T3, T5, T6, and Sec-SRP were markedly affected by the deletion of *rtcB*. The affected T2SS, T5SS, and Sec-SRP genes are listed in **Table 4.2**.

Previous results showed that T3SS and T6SS were altered and activated in both PAO1(Δ*rtcB*) and PAO1(Δ*rtcB*Δ*retS*) strains. The secretory and structural-related genes that were differentially expressed are presented in **Figure 4.3A, B**. In PAO1(Δ*rtcB*), T3SS is expressed slightly lower than the wild type, where T6SS is highly upregulated. Interestingly, in PAO1(Δ*rtcB*Δ*retS*), the expression pattern of T3SS genes is reversed, with the restoration of T3SS and activation of T6SS. However, the transcriptomics show downregulation of T6SS in PAO1(Δ*rtcB*Δ*retS*), the expression level has remained high that the luminescence reader could not detect the difference (studied in the previous chapter). Among the highly transcribed genes of H1-T6SS in PAO1(Δ*rtcB*), an essential HIS-I component, *clpV1*, showed a 2.37-fold change. ClpV1 has adenosine triphosphate (ATP) hydrolytic activity, functions as an energy provider for H1-T6SS and the secretion of Hcp1 (Mougous et al., 2006).

Moreover, in PAO1(Δ*rtcB*Δ*retS*), an increased expression of *exsA* was seen with a 22.47 fold change than PAO1(Δ*retS*). Upregulation of *clpV1* and *exsA* in PAO1(Δ*rtcB*) and PAO1(Δ*rtcB*Δ*retS*), respectively, explain the route of activation of H1-T6SS in PAO1(Δ*rtcB*) and restoration of T3SS in PAO1(Δ*rtcB*Δ*retS*). The altered expression of H2-, H3-T6SS in PAO1(Δ*rtcB*), and T3SS in PAO1(Δ*rtcB*Δ*retS*) suggest that *rtcB*

deletion strains pose more virulence toward eukaryotic host in compared with their background strains PAO1 and PAO1(Δ*retS*). To test if deletion of *rtcB* increases the pathogenicity of *P. aeruginosa*, I performed the lettuce infection assay. The lettuce midribs inoculated with PAO1(Δ*rtcB*) were highly infected, shown by a darker infection site than PAO1. Also, PAO1(Δ*rtcB*Δ*retS*) showed slightly higher virulence toward the plant is compared with PAO1(Δ*retS*) (**Figure 4.3C**).

Table4.2 Differential expression of secretory proteins of T2SS and T5SS

Gene Locus	Secretion System	Secreted Protein	Log 2 Fold Change
PAO1(Δ*rtcB*)			
PA2939	T2SS	PaAP	1
PA4625	T5SS	CdrA	2.1
PAO1(Δ*rtcB*Δ*retS*)			
PA0572	T2SS	Protease	-1.5
PA0852	T2SS	CbpD	-1.6
PA1249	T2SS	AprA	-1.2
PA1948	T2SS	ToxA	1.1
PA2862	T2SS	LipA	4.8
PA2939	T2SS	PepB	-1.5
PA2676	T2SS	HplS	-1.8

PA2677	T2SS	HplR	-3
PA2678	T2SS	HP*	-3.3
PA3105	T2SS	XcpQ	-2.1
PA3724	T2SS	LasB	1.2
PA3822	Sec-SRP	HP*	1
PA4082	T5SS	CupB5	-2.3
PA4624	T5SS	CdrB	-1.3
PA5210	T2SS	Probable ATPase	-1.1

HP*, Hypothetical protein

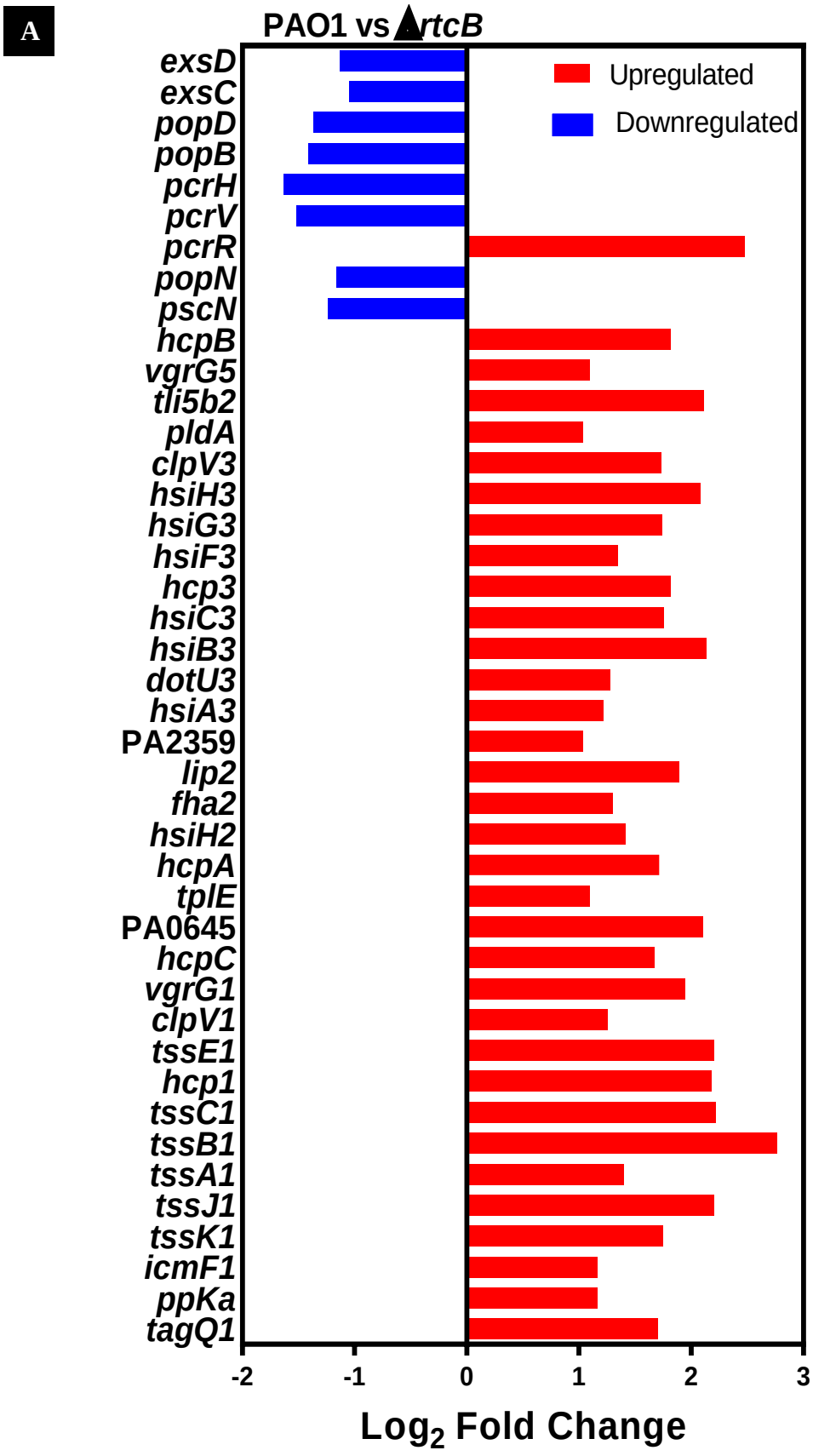
A
PAO1 vs ΔrtcB
exsD
exsC
popD
popB
pcrH
pcrV
pcrR
popN
pscN
hcpB
vgrG5
tli5b2
pldA
clpV3
hsiH3
hsiG3
hsiF3
hcp3
hsiC3
hsiB3
dotU3
hsiA3
PA2359
lip2
fha2
hsiH2
hcpA
tplE
PA0645
hcpC
vgrG1
clpV1
tssE1
hcp1
tssC1
tssB1
tssA1
tssJ1
tssK1
icmF1
ppKa
tagQ1
Upregulated
Downregulated
-2
-1
0
1
2
3
Log2 Fold Change

B

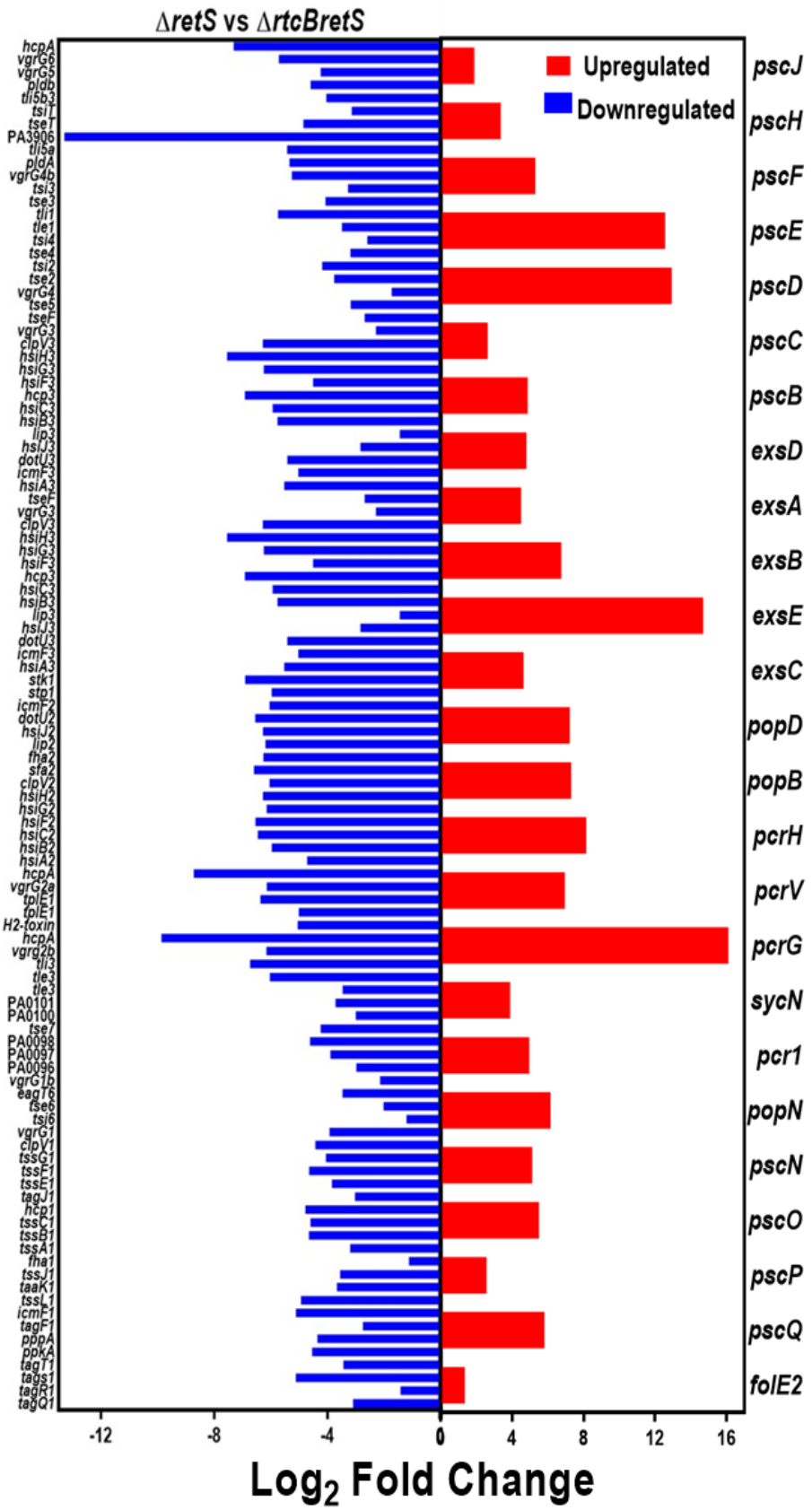
ΔretS vs ΔrtcBretS
Upregulated
Downregulated
hcpA
vgrG6
vgrG5
pldb
tli5b3
tsiT
tseT
PA3906
tli5a
pldA
vgrG4b
tsi3
tse3
tli1
tle1
tsi4
tse4
tsi2
tse2
vgrG4
tse5
tseF
vgrG3
clpV3
hsiH3
hsiG3
hsiF3
hcp3
hsiC3
hsiB3
lip3
hsiJ3
dotU3
icmF3
hsiA3
tseF
vgrG3
clpV3
hsiH3
hsiG3
hsiF3
hcp3
hsiC3
hsiB3
lip3
hsiJ3
dotU3
icmF3
hsiA3
stk1
stp1
icmF2
dotU2
hsiJ2
lip2
fha2
sfa2
clpV2
hsiH2
hsiG2
hsiF2
hsiC2
hsiB2
hsiA2
hcpA
vgrG2a
tplE1
tplE1
H2-toxin
hcpA
vgrg2b
tli3
tle3
tle3
PA0101
PA0100
tse7
PA0098
PA0097
PA0096
vgrG1b
eag16
tse6
tsi6
vgrG1
clpV1
tssG1
tssF1
tssE1
tagJ1
hcp1
tssC1
tssB1
tssA1
fha1
tssJ1
taaK1
tssL1
icmF1
tagF1
pppA
ppkA
tagT1
tags1
tagR1
tagQ1
pscJ
pscH
pscF
pscE
pscD
pscC
pscB
exsD
exsA
exsB
exsE
exsC
popD
popB
pcrH
pcrV
pcrG
sycN
pcr1
popN
pscN
pscO
pscP
pscQ
folE2
-12
-8
-4
0
4
8
12
16
Log2 Fold Change

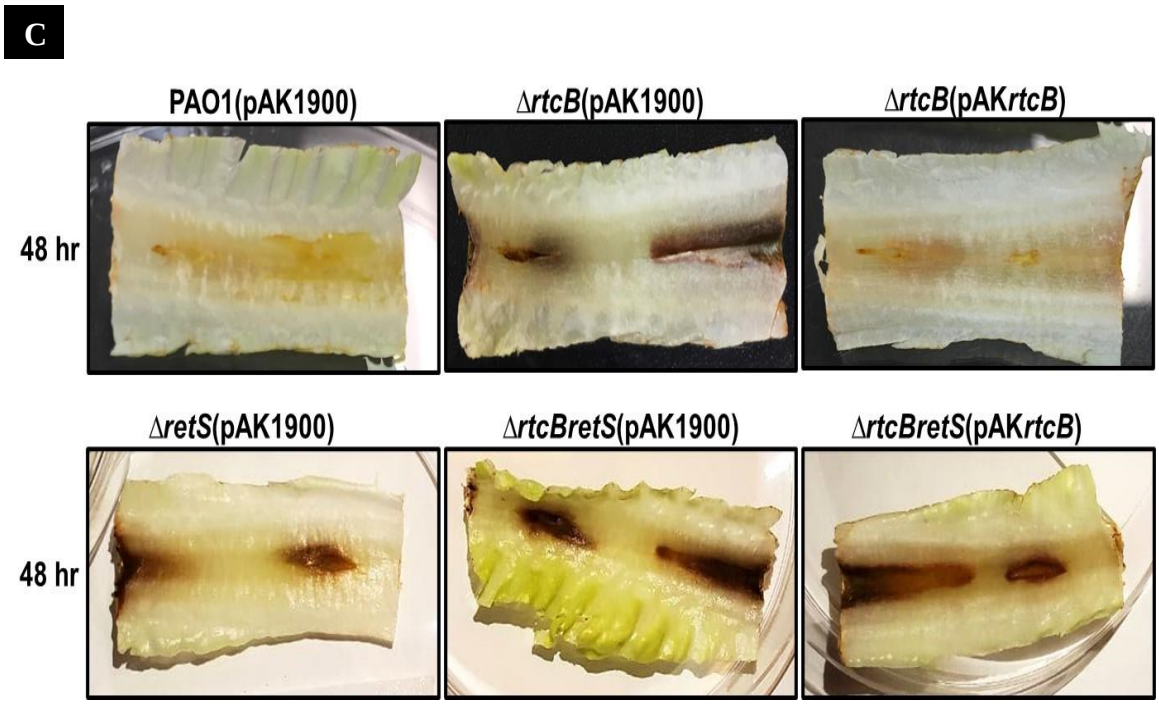

Figure 4.3 Alteration in secretion system-related gene expression and virulence of *P. aeruginosa* by deletion of *rtcB*. A, B Differential T3 and T6SS gene expression in the two studied groups PAO1 vs. PAO1(Δ*rtcB*) (B) and PAO1(Δ*retS*) vs. PAO1(Δ*rtcB*Δ*retS*) **C.** Photographed lettuce midribs show the infection sites after 48 hr. PAO1(Δ*rtcB*) and PAO1(Δ*rtcB*Δ*retS*) cause a higher infection rate than PAO1 and PAO1(Δ*retS*), respectively.

4.3.5 **Intracellular levels of c-di-GMP were significantly increased in *rtcB* deletion mutant**

Cyclic-di-GMP is a signaling molecule playing essential roles in regulating virulence factors like biofilm formation, type IV pili, motility (Valentini and Filloux, 2019), and chemotaxis (Alexandre, 2015) in *P. aeruginosa* and other bacteria. The synthesis and degradation of c-di-GMP are catalyzed reversely by the enzymatic activity of DGC and PDE proteins, which contain the GGDEF and EAL or HD-GYP domains, respectively (Römling, Galperin, and Gomelsky, 2013). To elucidate the involvement of c-di-GMP in the phenotypic changes and virulence of PAO1(Δ*rtcB*), we compared the genes involved in c-di-GMP metabolism using transcriptomes. As the heatmap graph represents (**Figure 4.4A**), a higher anabolic and catabolic activity are seen in PAO1(Δ*rtcB*) than PAO1. More hybrid proteins (harboring both GGDEF and EAL domains) and GGDEF domain-containing proteins are upregulated in PAO1(Δ*rtcB*). In contrast, a lower expression in several GGDEF-containing genes was reported in PAO1(Δ*rtcB*Δ*retS*) than PAO1(Δ*retS*) strain. To confirm whether c-di-GMP levels have contributed to the changed bacterial phenotypes, I quantified the intracellular content of c-di-GMP by ELISA kit (Cayman Chemical). The result is shown in **Figure 4.4B**. The concentration of c-di-GMP was significantly higher in PAO1(Δ*rtcB*) than PAO1, where no significant change was observed in the c-di-GMP content of PAO1(Δ*rtcB*Δ*retS*) than PAO1(Δ*retS*), probably due to the equal synthesis and degradation of c-di-GMP or generally lower availability of c-di-GMP for degradation. Higher concentrations of c-di-GMP may explain the behavioral effect of deletion of RtcB demonstrated in the previous chapter and this study.

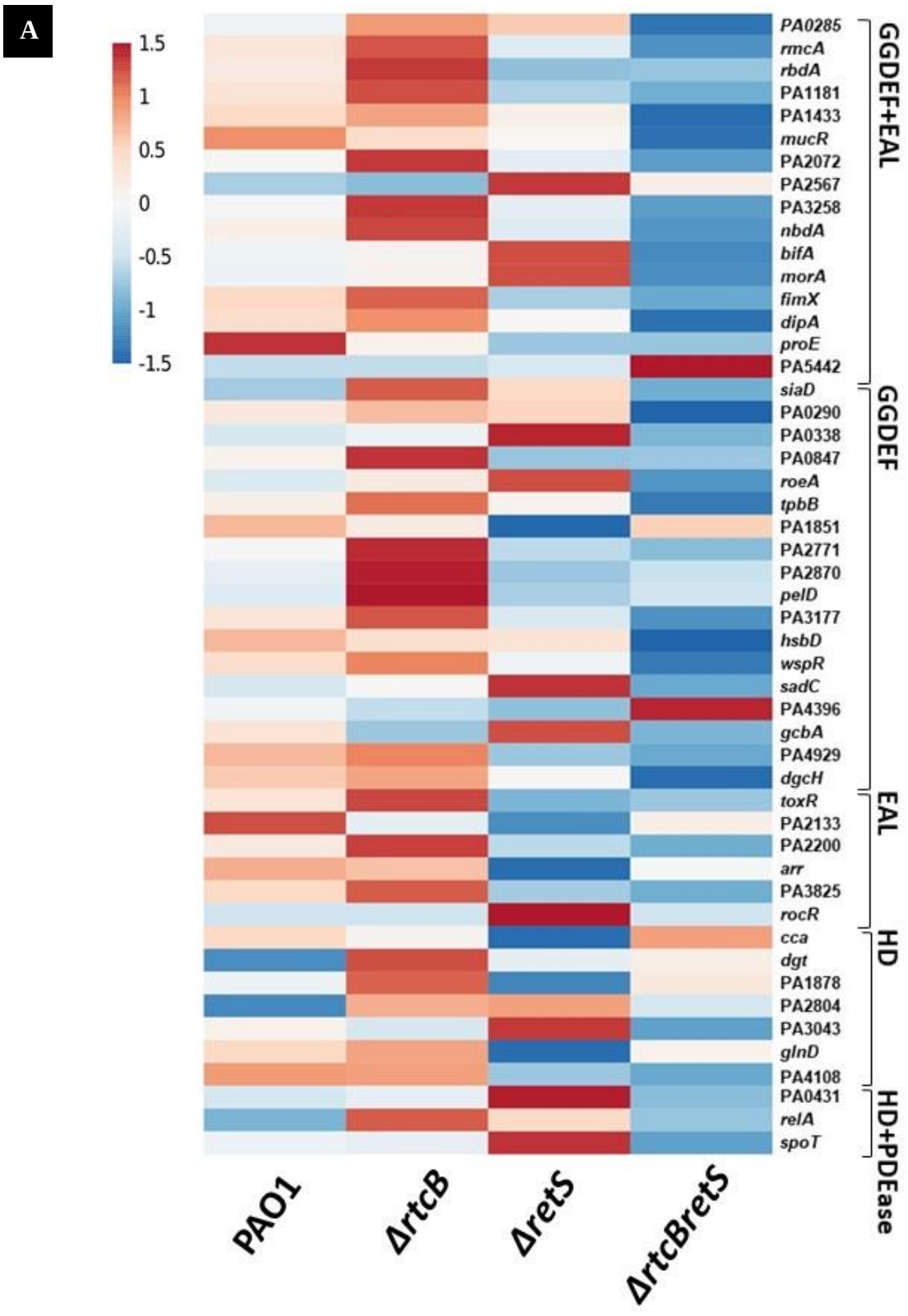
A
1.5
1
0.5
0
-0.5
-1
-1.5
PA0285
rmcA
rbdA
PA1181
PA1433
mucR
PA2072
PA2567
PA3258
nbdA
bifA
morA
fimX
dipA
proE
PA5442
siaD
PA0290
PA0338
PA0847
roeA
tpbB
PA1851
PA2771
PA2870
pelD
PA3177
hsbD
wspR
sadC
PA4396
gcbA
PA4929
dgcH
toxR
PA2133
PA2200
arr
PA3825
rocR
cca
dgt
PA1878
PA2804
PA3043
glnD
PA4108
PA0431
relA
spoT
GGDEF+EAL
GGDEF
EAL
HD
HD+PDEase
PAO1
ΔrtcB
ΔretS
ΔrtcBretS

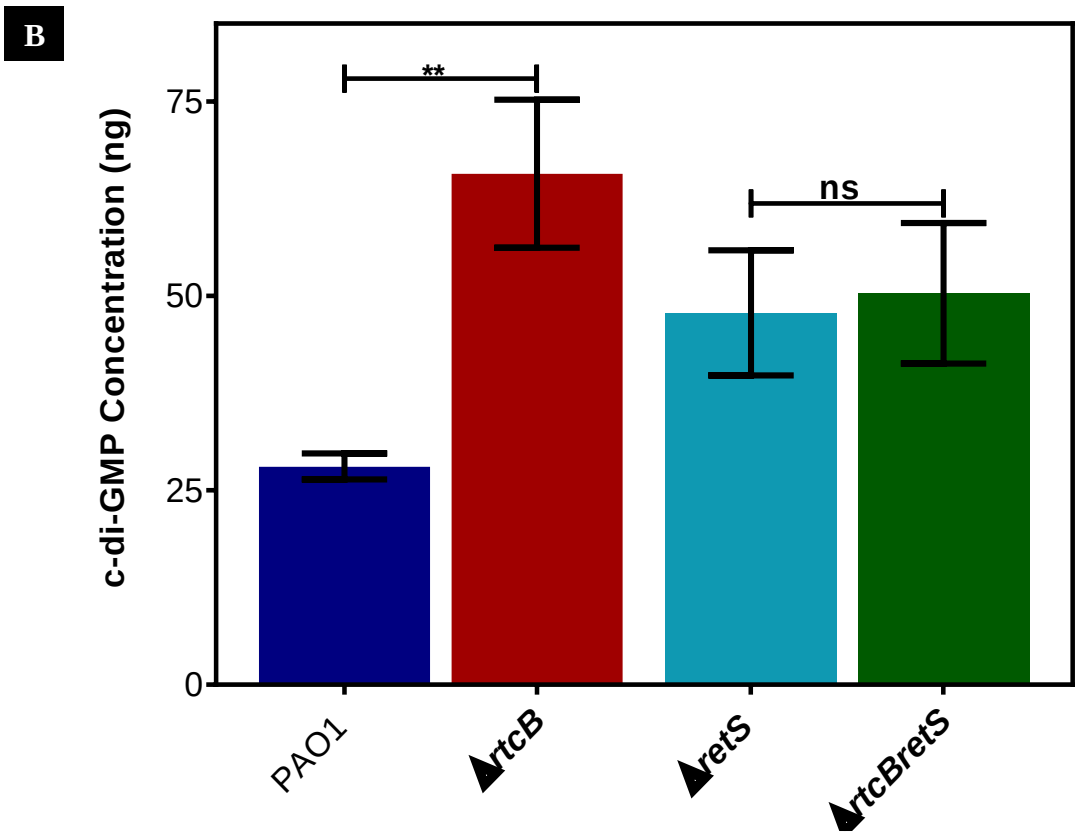

Figure 4.4 Comparison of c-di-GMP-related transcriptome and its concentration in PAO1, PAO1(Δ*rtcB*), PAO1(Δ*retS*), and PAO1(Δ*rtcB*Δ*retS*). A. The transcription level of the genes involved in the c-di-GMP secondary metabolite's metabolism was calculated from FPKM values and represented at heatmap graph by the color-coded box; blue-code: down and red-code: upregulation. **B.** Intracellular concentration of c-di-GMP was significantly increased by deleting *rtcB*, indicating the role of *rtcB* in the modulation of c-di-GMP metabolite. The experiments were performed independently three times. Error bars shows standard deviation. Data were analyzed with an unpaired student's *t*-test, $^{**}p<0.001$.

4.4 Discussion

Multiple distinct T6SS exist in *P. aeruginosa* controlled by various regulatory elements and mechanisms (Bernard et al., 2010), including QS, sRNAs, TCS (Bernard et al., 2010). These modulators have a multifactorial effect on the survival and fitness of the bacterium. Expanding our knowledge on the regulation of T6SS, RtcB was found to have a vital role in controlling the T6SS, T3SS, T2SS, and Sec-SRP. RtcB is a highly conserved protein and part of the RNA repair operon in bacteria that seals the damaged RNA, nicked by ribotoxins (Manwar et al., 2020).

To identify the effect of RtcB on the whole transcriptome of the cell, RNA-sequencing was performed and compared with PAO1 and PAO1(Δ*rteS*) backgrounds. In PAO1(Δ*rtcB*), 271 genes were upregulated, and 99 genes were downregulated compared to PAO1. In PAO1(Δ*rtcB*Δ*retS*), 498 genes showed lower expression where 532 genes were upregulated. The obtained results showed that RtcB involves modulating the cell's global and metabolic pathways, the metabolism of carbohydrates, amino acids, lipids, cofactors, and vitamins. Transmembrane proteins were of those positively affected transcripts, which includes the members of secretion systems. Also, several virulence factors beyond the secretion system partners were affected by the deletion of *rtcB*. These include but are not limited to quorum sensing pathways, proteases, pyocyanin, and secondary messenger c-di-GMP.

The four secretion systems, T2SS, Sec-SRP, T3SS, and T6SS, showed varied RNAseq data expression. T2SS and T3SS in *P. aeruginosa* exert the greatest number of toxins. Exotoxin A, Las A, and LasB proteases, phospholipase H, Type IV protease, and lipolytic

enzymes are secreted by T2SS (Cianciotto, 2005). These effectors serve in favor of the bacterium's pathogenicity (Green and Mecsas, 2016; Sijbrandi et al., 2003). Among them, secretion of LasB and phospholipase C cause the most harm in the periods of lung infections (Ostroff, Wretlind, and Vasil, 1989; Elsheikh et al., 1987). These exocellular proteins are translocated through the Sec or Tat system's inner membrane and are secreted by T2SS or T5SS (Alain Filloux, 2004). T2SS is encoded by two operons, *xcp*, and *hxc* (Ball et al., 2002), and an orphan *xqhA*, expressed when *xcpQ* is mutated (Martínez, Ostrovsky, and Nunn, 1998). Sec pathway functions as SecB and Sec-SRP modules (Hartl et al., 1990). Sec-SRP pathway secrets the proteins in their unfolded state through the inner membrane with the aid of SRP particle and FtsY docking protein. T3SS is the hallmark of acute-phase infections of *P. aeruginosa* and exerts ExoSTUY to the eukaryotic host (J. Engel and Balachandran, 2009). T5SS is formed from small autotransporters spanned in the cell's outer membrane (Klauser, Pohlner, and Meyer 1993), organized in 5 subclasses of Va to Vf (Grijpstra et al., 2013).

In PAO1(Δ*rtcB*), the expression of *pepB* and *cdrA*, members of T2 and T5SS, respectively, were increased. CdrA is a biofilm protein released to the biofilm matrix and promotes biofilm adherence and aggregation even when Psl exopolysaccharide is not present (Reichhardt et al., 2018). In PAO1(Δ*rtcB*Δ*retS*), the T2SS proteins were decreased except lasB, ToxA, and LipA. The probable Sec-SRP pathway protein, PA3822, showed higher expression, and T5SS-related proteins were downregulated.

The exciting finding on the role of RtcB is its modulatory role on both T3SS and T6SS genes. The results from RNAseq shows that RtcB modulates all three type of T6SS and not only H1-T6SS. It was established in chapter 3 that the deletion of *rtcB* led to the

simultaneous presence of active T3SS and T6SS in *rtcB* deletion mutants. This concludes that RtcB represses the expression of T6SS in PAO1 besides suppression of T3SS in Δ*retS.* Moreover, PcrR, the member of T3SS, showed to be a negative regulator of the T3SS. The higher expression of H2 and H3-T6SS in PAO1(Δ*rtcB*)contributed to the higher virulence of the strain toward the eukaryotic host, and the lettuce midribs were highly infected compared to PAO1.

The *xcp* of T2SS, ExsA of T3SS, and T6SS are regulated by QS-related genes. The QS genes were differentially expressed, as depicted in **Figure 5.2A**. Generally, the expressions of Las, RhlI, and PQS proteins were increased in PAO1(Δ*rtcB*). LasI and RhlI showed higher expression in PAO1(Δ*rtcB*Δ*retS*), where PQS system was repressed. Also, the transcription of *phz* operons was inversely regulated in PAO1(Δ*rtcB*) and PAO1(Δ*rtcB*Δ*retS*) compared to their background. The production of pyocyanin was manipulated by deletion of RtcB and increased in PAO1(Δ*rtcB*). Multiple factors could contribute to the observed higher expression of pyocyanin, which Are the increased expression of QS, T2SS, or *phz* operons. Also, the protease activity was significantly higher in PAO1(Δ*rtcB*Δ*retS*) under the control of QS, Sec-SRP, and T2SS. The higher proteolytic activity of PAO1(Δ*rtcB*Δ*retS*) is touched by the increased expression of LasB and AprA.

Interestingly, the c-di-GMP profile of the cell showed a significant alteration by deletion of RtcB. The metabolism of c-di-GMP was increased in PAO1(Δ*rtcB*Δ*retS*). The higher expression of GGDEF domain-containing protein was contributed to the overall higher intracellular concentration of c-di-GMP in a given strain. For instance, *siaD* showed an increase of 2.6-fold in PAO1(Δ*rtcB*) compare to PAO1. SiaD protein contains a GGDEF

domain, functioning in synthesizing c-di-GMPs. Previously, it was demonstrated that siaD deletion lowered the cell's c-di-GMP content (Colley et al., 2016). Contrary to PAO1(Δ*rtcB*), the synthesis and degradation of c-di-GMP were remarkably decreased in PAO1(Δ*rtcB*Δ*retS*) compared to PAO1(Δ*retS*). The secondary messenger c-di-GMP plays a crucial role in multiple virulence factors like motility and biofilms and transition between the sessile and motile lifestyle in bacteria. There is no doubt the considerable elevation in the metabolism of c-di-GMP is contributed to the notable shift of the bacterium in genotypic and phenotypic features in PAO1(Δ*rtcB*) and PAO1(Δ*rtcB*Δ*retS*).

Collectively, the data obtained in this study revealed the novel regulatory role of RtcB in the modulation of virulence factors besides its role as an RNA-repair system of the bacterium. The complex network and array of toxins and effectors affected by deletion of *rtcB* suggest the importance of RtcB contributing to the forming biofilms and motility, QS, stress response, and secondary metabolite regulation.

The functionality of RtcB ultimately contributes to the survival, pathogenicity, and fitness of the bacteria, which needs to be more investigated.

Chapter 5

5 Long-chain-fatty-acid-CoA--ligase FadD1 modulates T6SS and T3SS through c-di-GMP and cAMP

5.1 Introduction

Thriving in different ecological niches with a wide array of nutrient compositions, *Pseudomonas aeruginosa* requires diverse metabolic pathways. Many virulence factors in *P. aeruginosa* contribute to the bacterium's pathogenicity and its survival and nutrient acquisition (Matz et al., 2008; Rahme et al., 1995; Weir et al., 2008).

One of the nutrient sources for *P. aeruginosa* in CF individuals' lungs is phosphatidylcholine (PC) that induces PC-degradation genes (Son et al., 2007). The bacterium twitches toward phospholipids (Miller et al., 2008) and long-chain fatty acids (LCFA) by type IV pili (TFP). Degradation of fatty acids is under the control of Fad regulons in the bacterium (Miller et al., 2008).

The gene *fadD1*, encoding for Long-chain-fatty-acid--CoA ligase, was detected by transposon mutagenesis as a modulator of H1-T6SS in my previous study. Fad genes' importance for the nutrient utilization and survival fitness of bacteria in the host and its role in modulating virulence determinants like swarming (Yun Kang et al., 2010) and H1-T6SS motivated us for the future investigation on its function and characteristics. This is to elaborate through which pathway FadD1 deactivated the T6SS, the signaling partners involved in its role, and whether it affects other virulence factors and the secretion systems.

5.2 Materials and methods

5.2.1 **Bacterial strains, plasmid**

Bacterial strains and plasmids used in this study are listed in **Table 5.1**. *P. aeruginosa* and *E. coli* were routinely grown at 37˚C on LB agar or LB broth unless explained. Antibiotics concentrations are explained in chapter 2.

Table 5.1 Bacterial strains and plasmids of this study

Bacterial strains and plasmids	**Relevant characteristics/sequence**	**Source**
***E. coli* strains**		
DH5α	F^- φ80*lac*ZΔM15 Δ(*lacZYA-argF*) U169 *recA*1 *endA*1 *hsdR*17 (r_k^-, m_k^+) phoA supE44 λ^- *thi*-1 *gyrA*96 *relA*1	Invitrogen
SM10-λ *pir*	Mobilizing strain, RP4 integrated in the chromosome; Kn^r	(Simon et al., 1983)
***P. aeruginosa* strains**		
PAO1	Wild type, lab strain	This lab
PAO1 (Δ*retS*)	*retS* replacement mutant of PAO1	This lab
PAO1 (Δ*fadD1*)	*fadD1* replacement mutant of PAO1	This study
PAO1 (Δ*fadD1*Δ*retS*)	*retS fadD1* replacement mutant of PAO1	This study
Plasmids		

pMS402	Expression reporter plasmid carrying the promoterless *luxCDABE*; Kn^r,Tmp^r	(Duan et al. 2003)
CTX-6.1	Integration plasmid origins of plasmid mini-CTX-*lux*; Tc^r	This lab
pRK2013	Broad-host-range helper vector; Tra^+, Kn^r	(Ditta et al. 1980)
pEX18Tc	*oriT*$^+$ *sacB*$^+$ gene replacement vector with multiple-cloning site from pUC18; Tc^r	(Hoang et al. 1998b)
pAK1900	*E. coli-P. aeruginosa* shuttle cloning vector, Amp^r	(Sharp et al. 1996)
pAK- *fadD1*	pAK1900 with an 1869 bp fragment of *fadD1* between BamHI and HindIII; Amp^r, Cb^r	This study
pEX18Tc- *fadD1*	pEX18Tc carrying the upstream and downstream fragment of *fadD1*	This study
pKD-H1T6SS	pMS402 containing H1-T6SS promoter region; Kn^r, Tmp^r	This lab

CTX-*rsmY*	Integration plasmid, CTX6.1 with a fragment of pKD-*rsmY* containing *rsmY* promoter region and *luxCDABE* gene;Kn^r ,Tmp^r ,Tc^r	This lab
CTX-*rsmZ*	Integration plasmid, CTX6.1 with a fragment of pKD-*rsmZ* containing *rsmZ* promoter region and *luxCDABE* gene;Kn^r ,Tmp^r ,Tc^r	This lab
CTX-*exoS*	Integration plasmid, CTX6.1 with a fragment of pKD-*exoS* containing *exoS* promoter region and *luxCDABE* gene; Kn^r ,Tmp^r ,Tc^r	This lab
CTX-H1T6SS	Integration plasmid, CTX6.1 with a fragment of pKD-H1T6SS containing H1 promoter region and *luxCDABE* gene; Kn^r ,Tmp^r ,Tc^r	This study

5.2.2 **Construction of unmarked gene knockout mutants**

To construct the *fadD1* knockout mutant the *sacB*-based method (Hoang et al., 1998) was used**.** Approximately 1kb upstream of *fadD1* was amplified with the insertion of restriction sites. Amplicons were digested and ligated into the vector pEX18TC. The resultant suicide plasmid was transferred to the *Pseudomonas* wild type and PAO1(Δ*retS*) by triparental mating (Ditta et al., 1980). Triparental mating was set up with *E. coli* strains carrying helper plasmid pRK2013, pEX18Tc-*fadD1*$^{up+down}$ donor, and *Pseudomonas* PAO1 wild type or PAO1(Δ*retS*) (Ditta et al., 1980). PCR and agarose gel electrophoresis confirmed the mutants PAO1(Δ*fadD1*) and PAO1(Δ*fadD1*Δ*retS*). Primer sequences are listed in **Table 5.2.**

Table 5.2 Primers used in this study

Primer	Sequence (5'→3') [a]	Restriction site
fadD1-UP-S	acagcgGAATTCTCTGGTCCTCGAAGCGCAC	*Eco*RI
fadD1-UP-As	acagcg*CCCGGG*TGGAGTTCCGCGACAGCCT	*Sma*I
fadD1-DW-S	acagcgCCCGGGGCTTGAGATCGGTGTGCTGC	*Sma*I
fadD1-DW-As	acagcgAAGCTTAGGCTATGGCCTCACCGAATGC	*Hin*dIII
pAK-*fadD1*-S	acagcgAAGCTTGTTGCTTAGGAGTGGGCTTCC	*Hin*dIII
pAK-*fadD1*-As	acagcgGGATCCCTTCTTCAGGCAACGGCGGAC	*Bam*HI
rpoD-S	GATCTCCATGGAAACCCCGATC	
rpoD-As	GAGGACTTCGCGGGTGGATTC	
rsmA-S	TCCAGATGATCTCCACCTCGGA	
rsmA-As	TCGCCTGTCAGCGTCACTCA	

Note: [a], underlined are restriction site sequences

The over-hanged base pairs are shown with lower case

5.2.3 **Generation of complementing vectors**

The multi-copy-number shuttle vector pAK1900 of *E. coli-P. aeruginosa* was used to generate the complementing vector of *fadD1* (Poole et al., 1993). The primers for the *fadD1* region were designed in-frame with the incorporation of restriction sites and were amplified by PCR. The amplicons were cloned into the *Bam*HI and *Hin*dIII site of pAK1900. The resulted pAK*fadD1* vector was transferred into *Pseudomonas* by electroporation.

5.2.4 **Gas-chromatography-FID**

The bacteria were grown in trypticase soy broth at 28℃ for 24 hr. The bacteria were harvested and washed 3 times with cold PBS. Accurately, 40 mg of each sample was transferred to a fresh, clean tube. The samples were processed in five steps; saponification, methylation, extraction, and base wash following Sasser's protocol (Sasser, 1990). Man-U-Lab performed the GC-FID at Richardson center for functional foods and nutraceuticals, university of Manitoba.

5.2.5 **Quantification of intracellular cyclic-di-GMP levels**

The concertation of intracellular c-di-GMP content was obtained using CdiGMP Elisa Kit (MyBioSource #MBS288159) with modifications following Irie's protocol (Irie and Parsek, 2014). Bacterial strains were grown for 24 h in 5 ml LB at 37°C. The next day, bacterial optical density was adjusted to OD_{600}=1.8. Three milliliters of bacterial cells were harvested for 7 min at 1540 xg. Each sample was washed 3 times with cold PBS buffer. 250 µl of 0.6 M perchloric acid was added to the samples and incubated for 30

min at 4°C on the rotatory shaker. The samples were centrifugated at 18879 xg for 10 min. The supernatant was transferred to a fresh tube. A 200 µl of 1M KOH was added to each tube, and the salt was pelleted by centrifuging at 14000 for 10 min. The kit standards and salt-free supernatant was used to load the supplied 96-well plate for quantification of c-di-GMP concentration according to the manufacturer protocol. After incubation and development of the samples, the plate was read at OD 450 nm. The obtained equation calculated the intracellular c-di-GMP concentration in each sample from the standard curve plot.

5.2.6 **Quantification of intracellular cAMP content**

The cAMP level of the wild type and mutants of this study were quantified using Cyclic AMP ELISA Kit from Cayman (#581001). Bacteria were grown in LB broth at 37°C overnight. OD600 was adjusted to 8 and was harvested by centrifugation. The bacterial pellet was washed three times with ice-cold PBS buffer and mixed with 500µl of 0.1 N HCL, sonicated for 30 seconds. The supernatant was collected into a fresh tube by centrifugation for 10 min at 10000 g. Preparation of standards and bacterial samples were carried according to the manufacturer protocol and loaded into a 96-well calorimetric plate (supplied). The plate was incubated until developed and read at a wavelength between OD 405 and 420 nm. The acquired equation calculated the concentration of cAMP in each sample from the standard curve plot.

5.3 Results

5.3.1 *fadD1* influences the H1-T6SS in *P. aeruginosa*

To confirm the effect of *fadD1* on the expression of H1-T6SS, I constructed the marker-less deletion mutant of *fadD1* in both *P. aeruginosa* wild-type strain and PAO1(Δ*retS*). The H1-T6SS reporter (CTX::H1) was then introduced into these *fadD1* mutants. The reporter activity of H1-T6SS was compared in PAO1, PAO1(Δ*fadD1*), PAO1(Δ*retS*), and PAO1(Δ*fadD1*Δ*retS*). As shown in **Figure 5.1**, the results demonstrated that the activity of H1-T6SS was abolished in PAO1(Δ*fadD1*Δ*retS*). The complementation of PAO1(Δ*fadD1*Δ*retS*) using the overexpression vector pAK*fadD1* restored the expression of H1-T6SS to that in the PAO1(Δ*retS*). However, the activity of H1-T6SS showed no change in PAO1(Δ*fadD1*) compared to PAO1 and remained repressed. The result indicated that in the PAO1(Δ*retS*) mutant, the deletion of *fadD1* negatively affected the expression of H1-T6SS, confirming the observation with the transposon mutant where Tn insertion in the *fadD1* region led to inactivation of H1-T6SS (data presented in chapter 3).

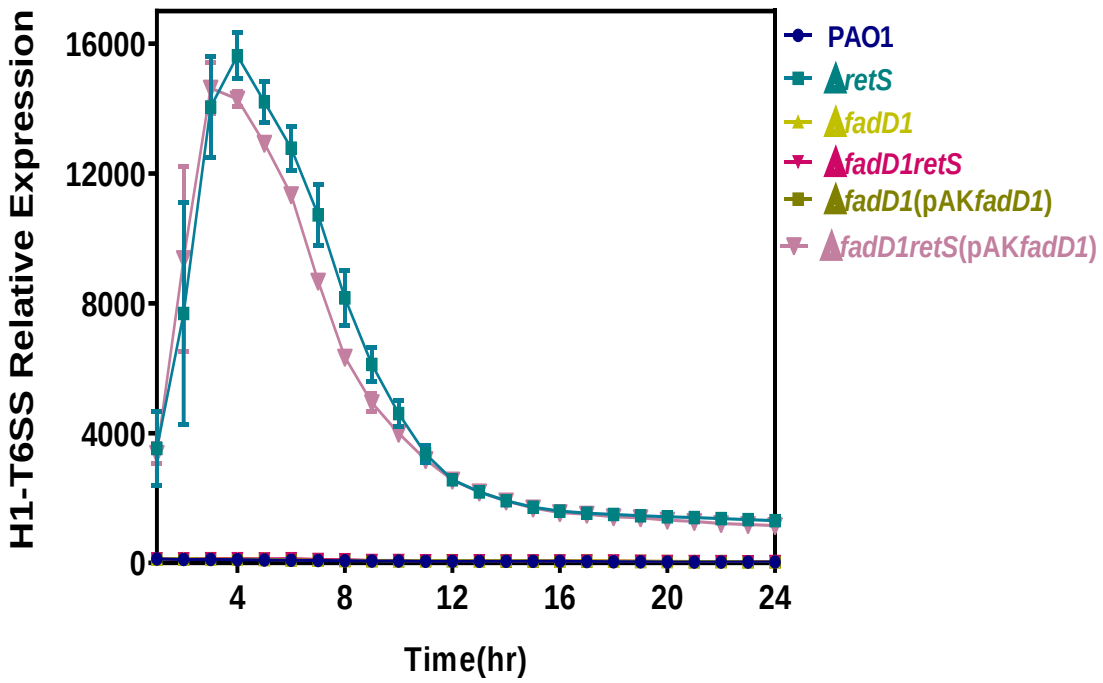

Figure 5.1 Lower transcriptional activity of H1-T6SS in PAO1(Δ*fadD1*Δ*retS*)

CTX::H1-T6SS reporter fusion was integrated into the PAO1, and mutant strains were used to record the promoter activity of H1-T6SS. Data represents significant repression in PAO1(Δ*fadD1*Δ*retS*) compared with PAO1(Δ*retS*). Deletion of *fadD1* from wildtype background did not affect the expression of H1-T6SS and it remained repressed. The data was plotted as a relative expression of luminescence to growth and represented the average of three independent experiments in triplicates. The error bars indicate standard deviations.

5.3.2 **FadD1 affects the expression of sRNAs RsmY and RsmZ**

The Gac-Rsm pathway is known to regulate the expression of T6SS through RsmA and the antagonist sRNAs RsmYZ in *P. aeruginosa*. To learn whether the Gac-Rsm pathway is involved in the repression of H1-T6SS in PAO1(Δ*fadD1*Δ*retS*), we introduced the RsmY and RsmZ reporter into wild-type, PAO1(Δ*fadD1*), PAO1(Δ*retS*), and PAO1(Δ*fadD1*Δ*retS*). The reporter activity of sRNAs was measured and compared. The result showed both sRNAs RsmYZ were entirely repressed PAO1(Δ*fadD1*Δ*retS*) and significantly reduced in PAO1(Δ*fadD1*) (**Figure 5.2 A, B**). The results suggest that *fadD1* exerts its function on the expression of H1-T6SS through the Gac-Rsm pathway. T3SS is also known to be regulated through the Gac-Rsm pathway, and its transcription is activated when sRNAs *rsmY* and *rsmZ* are not expressed (Diaz, King, and Yahr, 2011). To verify if the expression of T3SS in PAO1(Δ*fadD1*Δ*retS*) was affected by the downregulation of RsmYZ in the mutant, I transferred the *exoS* reporter into PAO1 Δ*fadD1*, PAO1(Δ*retS*), and PAO1(Δ*fadD1*Δ*retS*) mutants. ExoS is an effector of T3SS, and its expression represents T3SS activity. The expression of *exoS* showed a dramatic increase in PAO1(Δ*fadD1*Δ*retS*). (**Figure 5.2C**). However, no significant change was seen in the expression of *exoS* in PAO1(Δ*fadD1*) compared to the wild type (PAO1).

The complementation of PAO1(Δ*fadD1*Δ*retS*) with pAK*fadD1* repressed the expression of *exoS*. The results indicate that deletion of *fadD1* modulates the expression of H1-T6SS and affects the activation of T3SS, showing a significant and broad role in the modulation of secretion systems in this bacterium.

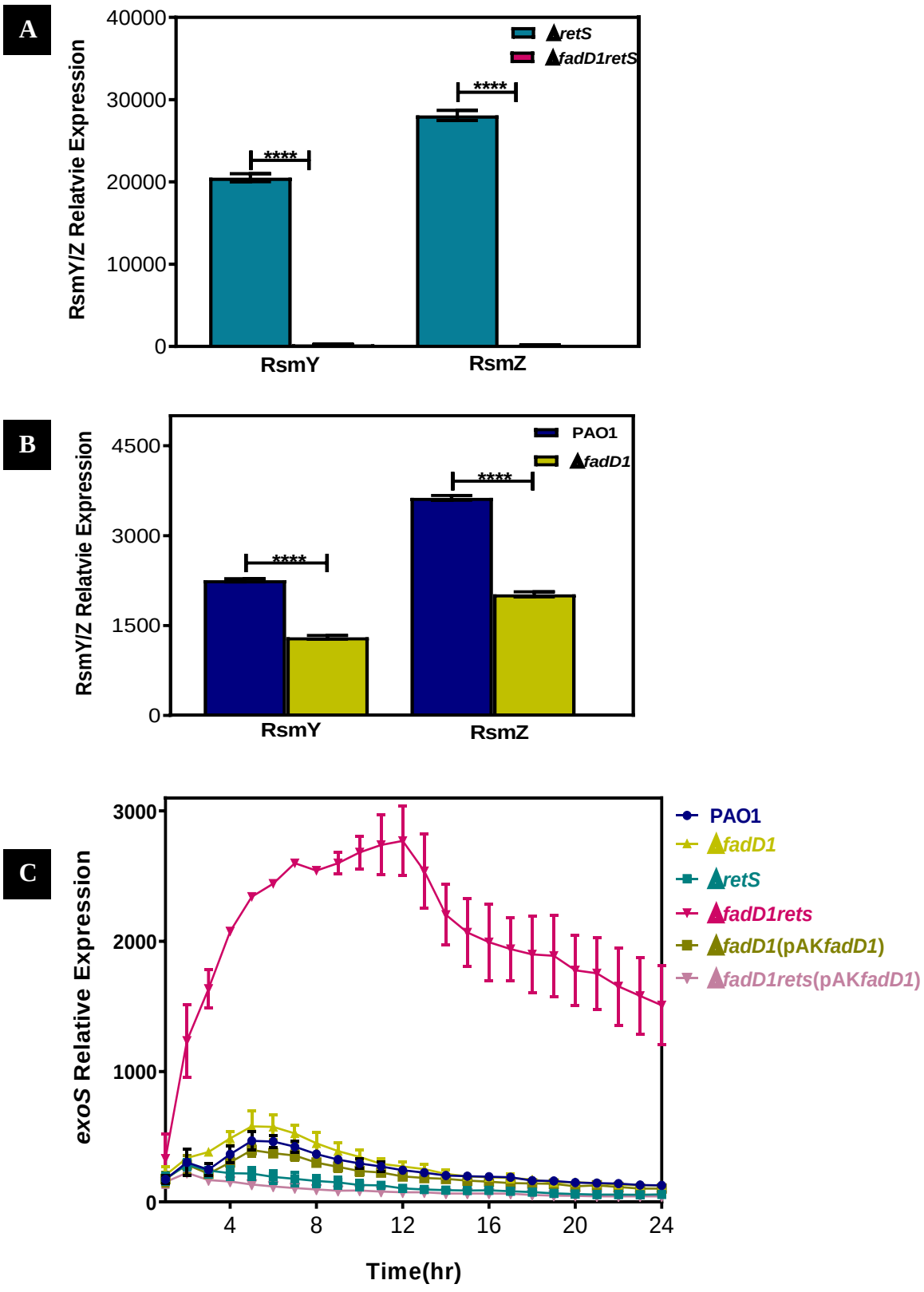
A
40000
30000
20000
10000
0
RsmY/Z Relatvie Expression
ΔretS
ΔfadD1retS
****
****
RsmY
RsmZ
B
4500
3000
1500
0
RsmY/Z Relatvie Expression
PAO1
ΔfadD1
****
****
RsmY
RsmZ
C
3000
2000
1000
0
exoS Relative Expression
4
8
12
16
20
24
Time(hr)
PAO1
ΔfadD1
ΔretS
ΔfadD1rets
ΔfadD1(pAKfadD1)
ΔfadD1rets(pAKfadD1)

Figure 5.2 Expression of *rsmY* and *rsmZ* was reduced in PAO1(Δ*fadD1*Δ*retS*) and resulted in increased *exoS* transcription. A, B. Expression of RsmYZ in PAO1(Δ*fadD1*Δ*retS*) and PAO1(Δ*fadD1*) was reduced compared to their background strains. The graphs were plotted after 12 h of growth and as a relative expression of luminescence to growth. **C.** The transcriptional activity of *exoS* was restored in PAO1(Δ*fadD1*Δ*retS*) significantly. Data represent the average of three biological replicates in triplicates. Error bars show the standard deviations. ****$p < 0.0001$.

5.3.3 **Cellular content of RsmA mRNA was increased in PAO1(Δ*fadD1*Δ*retS*)**

As described earlier, in PAO1(Δ*retS*), the expression of T3SS is repressed via sequestration of RsmA by RsmYZ. In PAO1(Δ*fadD1*Δ*retS*), *exoS* was restored, and its expression was higher than the wild-type strain. I speculated that RsmYZ might not be the only role player in the higher transcription of *exoS*. Perhaps the expression of *rsmA* could be affected by the deletion of *fadD1*. To confirm, RNA was isolated from PAO1(Δ*retS*) and PAO1(Δ*fadD1*Δ*retS*) following a quantitative PCR. Interestingly, the result showed a significant upregulation of *rsmA* in PAO1(Δ*fadD1*Δ*retS*) compares to PAO1(Δ*retS*) (**Figure 5.3**) and confirmed the role of *fadD1* in modulating the expression of *rsmA*. Together, lower expression of RsmYZ and higher expression of RsmA restored the expression of T3SS in PAO1(Δ*fadD1*Δ*retS*) and contributed to the significantly higher expression of T3SS, higher than PAO1.

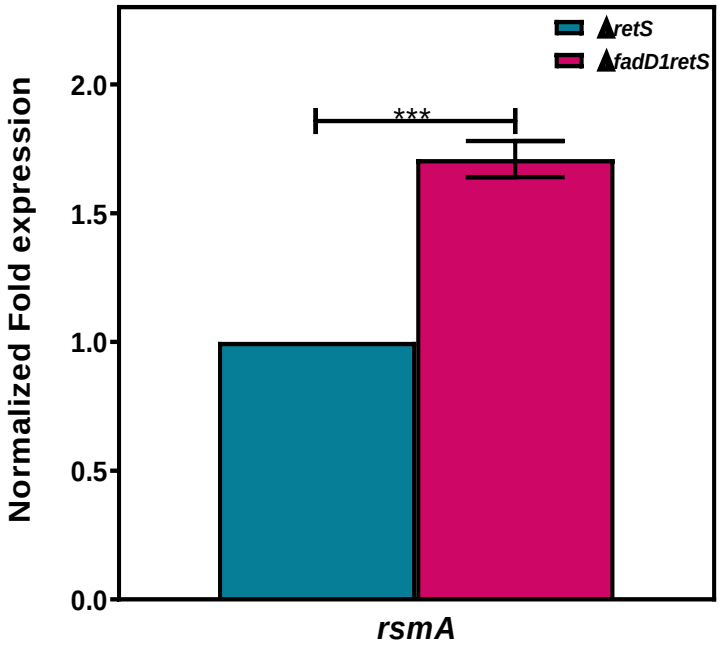

Figure 5.3 Effect of the deletion of *fadD1* on *rsmA* gene expression. The mRNA levels of *rsmA* in PAO1(Δ*fadD1*Δ*retS*) were significantly higher than PAO1(Δ*retS*). The expression of *rsmA* is presented as a normalized value to the housekeeping gene *rpoD* of PAO1(Δ*retS*) and PAO1(Δ*fadD1*Δ*retS*). Data are shown as a normalized fold change between samples and represent the average of triplicate experiments. Error bar indicates the standard deviations. ****p* < 0. 001.

5.3.4 **Deletion of *fadD1* in PAO1(Δ*retS*) decreased biofilm formation and promoted motility**

As shown above, the deletion of *fadD1* markedly altered the expression of virulence factors T3SS and T6SS. To examine the potential broader effect of the *fadD*1 on the regulation of other virulence factors and probable phenotypic alteration of PAO1(Δ*fadD1*Δ*retS*), I examined biofilm formation and motility. The result showed that biofilm formation was not affected in PAO1(Δ*fadD1*), wherein PAO1(Δ*fadD1*Δ*retS*) was significantly lower than PAO1(Δ*retS*). Moreover, all three types of motilities, swarming, swimming, and twitching increased in PAO1(Δ*fadD1*Δ*retS*) with no significant change in PAO1(Δ*fadD1*). In turn, overexpression of *fadD1* reduced swarming and swimming motility in a wild-type background. This result suggests a turnover in the expression of biofilm and motility-related genes. Biofilm formation and motility are presented in **Figure 5.4**.

A

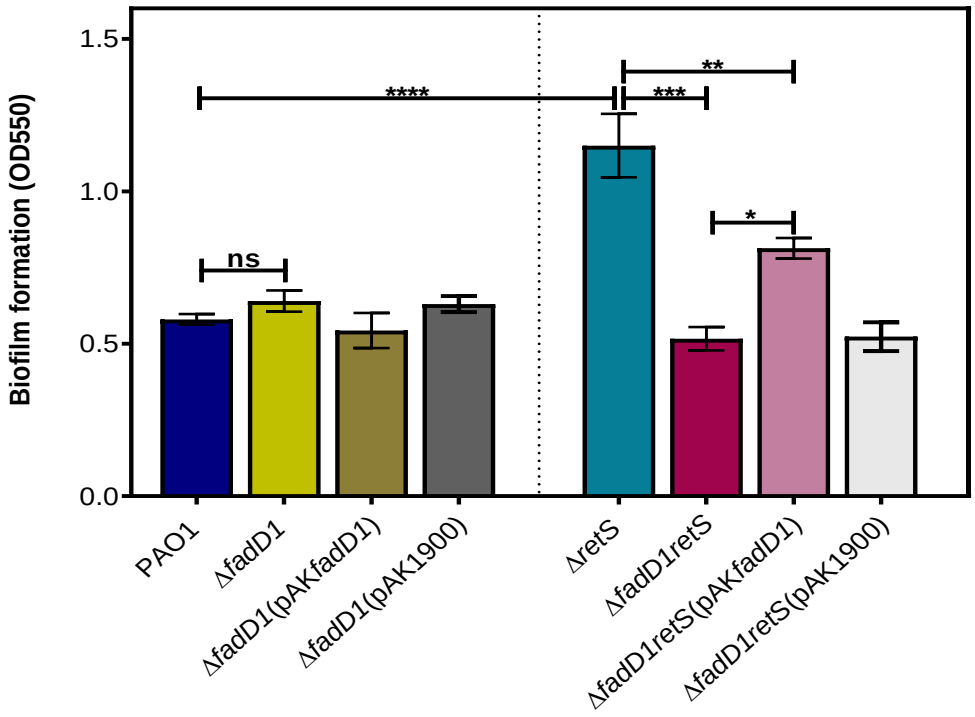
Biofilm formation (OD550)
1.5
1.0
0.5
0.0
****
**
***
*
ns
PAO1
ΔfadD1
ΔfadD1(pAKfadD1)
ΔfadD1(pAK1900)
ΔretS
ΔfadD1retS
ΔfadD1retS(pAKfadD1)
ΔfadD1retS(pAK1900)

B

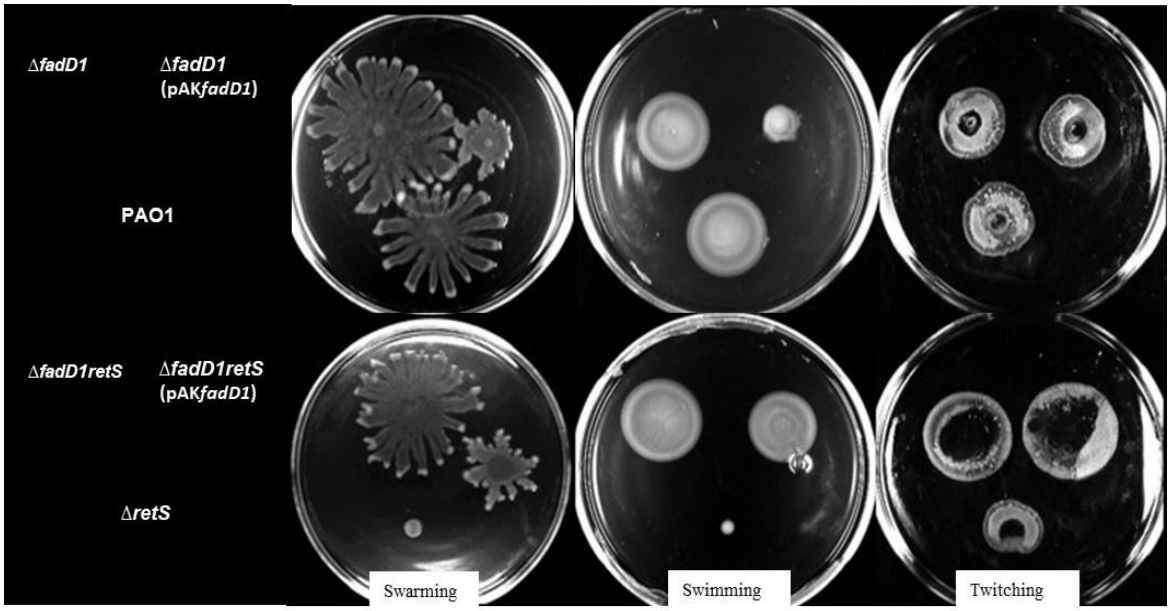
ΔfadD1
ΔfadD1 (pAKfadD1)
PAO1
ΔfadD1retS
ΔfadD1retS (pAKfadD1)
ΔretS
Swarming
Swimming
Twitching

Figure 5.4 Effect of *fadD1* on biofilm formation and motility. A. Deletion of *fadD1* in *P. aeruginosa* did not show a significant change in biofilm formation wherein PAO1(Δ*fadD1*Δ*retS*) an upregulated biofilm formation was observed. **B.** Swarming, swimming, and twitching motilities of PAO1(Δ*fadD1*Δ*retS*) were increased. In PAO1(Δ*fadD1*), swarming was slightly increased were swimming and twitching showed no significant change. The experiments were performed in three biological replicates, and the error bars indicate standard deviations. ****$p < 0.0001$; ***$p < 0.001$; **$p < 0.01$; *$p < 0.05$.

5.3.5 **T3SS was not activated through free PsrA in PAO1(Δ*fadD1*Δ*retS*)**

The transcriptional regulator PsrA is a modulator of T3SS related genes (Shen et al., 2006). It binds directly to the upstream region of the *exsC* gene and positively regulates the T3SS operon. PsrA is a fatty acid sensor, especially senses $C_{14:0}$, $C_{16:0}$, and $C_{18:1}^{\Delta 9}$ (Y. Kang et al., 2008). It is binding to the *exsC* upstream region is prevented in long-chain fatty acids (Diaz, King, and Yahr, 2011; Yun Kang et al., 2009). The FadD1 is a long-chain-fatty acid degradase and is proposed to be involved in the transport of exogenous LCFA into the cell (Yun Kang et al., 2010). Therefore, it is possible the FadD1 supplies the cell with LCFAs. I tested if the lack of FadD1 leads to an LCFA depletion in the cell, which non-sequestered PsrA and resulted in activation of T3SS. To elaborate if PsrA, in addition to RsmA, played a role in the upregulation of T3SS in PAO1(Δ*fadD1*Δ*retS*), GC-FID was performed. The result obtained from GC-FID was used to compare the total fatty acid profile of PAO1(Δ*fadD1*Δ*retS*) and PAO1(Δ*retS*). The total fatty acid of the cell did not show a significant difference between the two bacterial strains. The sole fatty acid with a considerably varied concentration was C18:1n7c, with higher intracellular levels in PAO1(Δ*fadD1*Δ*retS*). The maximum and minimum mean differences were plotted. The highest mean difference belongs to C18:1n7c. The second highest mean difference is reported for C18:3n6, which, however, is not statistically significant between the two samples (**Figure 5.5 A, B**).

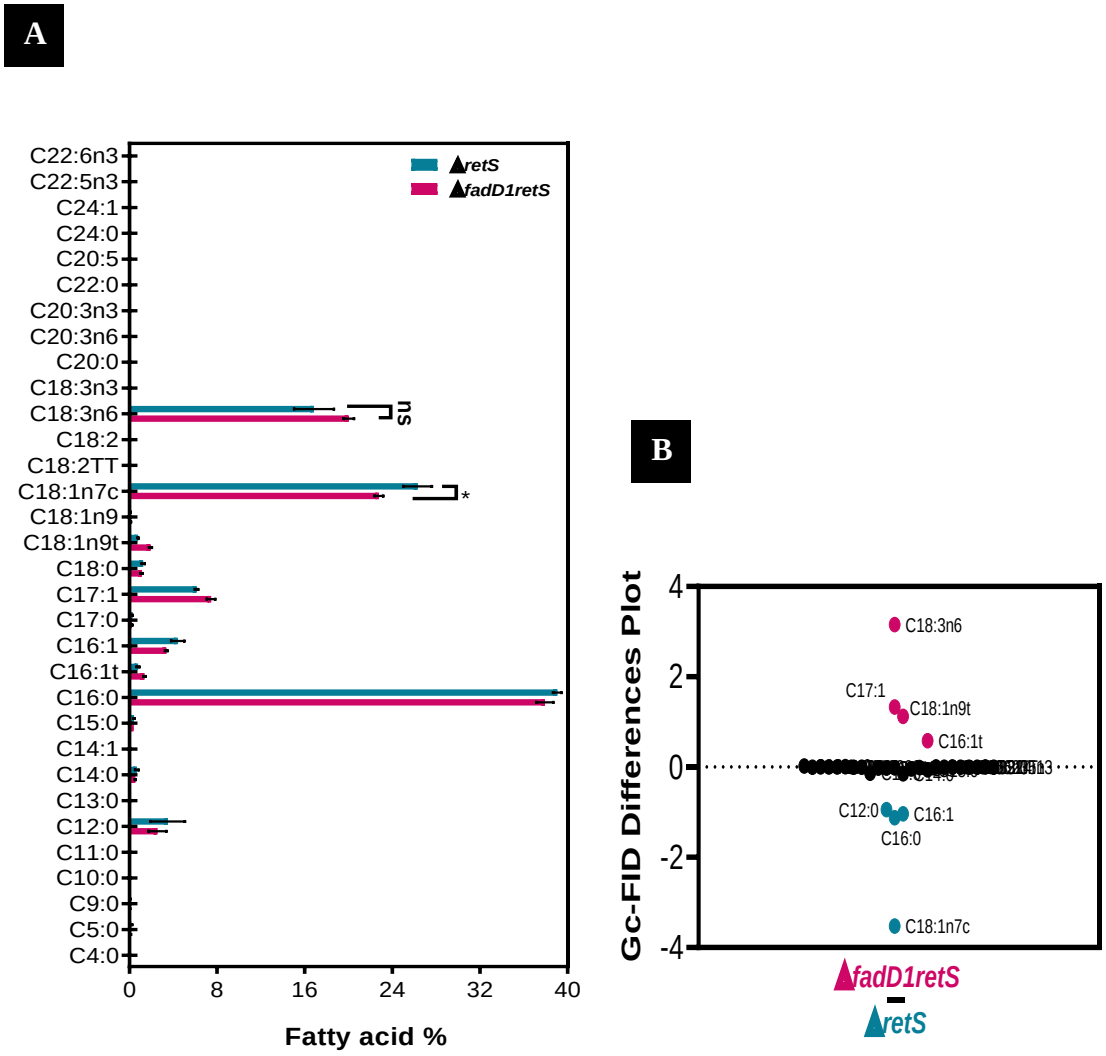

Figure 5.5 Comparison of the fatty acid profile of PAO1(Δ*retS*) and PAO1(Δ*fadD1*Δ*retS*) by GC-FID. A. GC-FID profiled the intracellular level of fatty acids of PAO1(Δ*fadD1*Δ*retS*) and PAO1(Δ*retS*). Fatty acids are presented as a percentage of total fatty acids. Data are shown as a percent of each fatty acid compared to the total content. **B.** The means difference plot represents the associated mean with each Fatty acid, profiled by GC-FID in the two strains PAO1(Δ*fadD1*Δ*retS*) and PAO1(Δ*retS*). The experiment was performed three times independently. The error bars indicate standard deviations. ***$p < 0.001$; *$p < 0.05$.

5.3.6 **FadD1 influences the intracellular levels of c-di-GMP and cAMP**

Secondary metabolite c-di-GMP plays a vital role in the transition between a sessile or motile bacterial lifestyle (Römling, Galperin, and Gomelsky, 2013). The lifestyle change under the control of c-di-GMP is Gac-Rsm-dependent. The optimum physiological level at which c-di-GMP exerts its function is unclear (Moscoso et al., 2011). Previously, it was shown that overexpression of RsmA resulted in lower c-di-GMP concentrations, and RsmA and c-di-GMP inversely regulate phenotypes and virulence factors (Colley et al., 2016).

The results of this study indicated that the PAO1(Δ*fadD1*Δ*retS*) strain shows lower biofilm, higher motility, de-repression of T3SS, downregulation of H1-T6SS, and RsmYZ, and higher expression of RsmA. To examine if c-di-GMP is a potential player in those observations, I quantified cellular c-di-GMP content by the ELISA approach. Interestingly, c-di-GMP concentrations in both PAO1(Δ*fadD1*) and PAO1(Δ*fadD1*Δ*retS*) were significantly downregulated (**Figure 5.6A)**. The result elaborated the modulatory role of *fadD1* on RsmA, directly or indirectly affected the intracellular concentrations of c-di-GMP signaling molecules.

Besides, it is reported that a higher concentration of c-di-GMP lowers the intracellular cAMP level. The transition between secondary messengers' cAMP and c-di-GMP results in transition between the acute and chronic *Pseudomonas* infection phases. To test if lower c-di-GMP led to an increased cAMP and, consequently, elevated the expression of T3SS and motile phenotypes of PAO1(Δ*fadD1*Δ*retS*), I quantified the cAMP concentrations between the bacterial strains of this study. The concertation of cAMP is

lower in PAO1(Δ*retS*); as was shown earlier, PAO1(Δ*retS*) bears high concentrations of c-di-GMP and lower cAMP (Moscoso et al., 2014; Almblad et al., 2015). The result showed that in PAO1(Δ*fadD1*Δ*retS*), cAMP concentration elevated significantly while no significant change was seen in PAO1(Δ*fadD1*). Data representing the cAMP quantification is plotted in **Figure 5.6 B**. The result suggests a complete turnover in the bacterium's homeostasis occurred in PAO1(Δ*fadD1*Δ*retS*). A repressed T3SS, lower c-di-GMP, and higher cAMP resulted from the deletion of *fadD1* in PAO1(Δ*retS*).

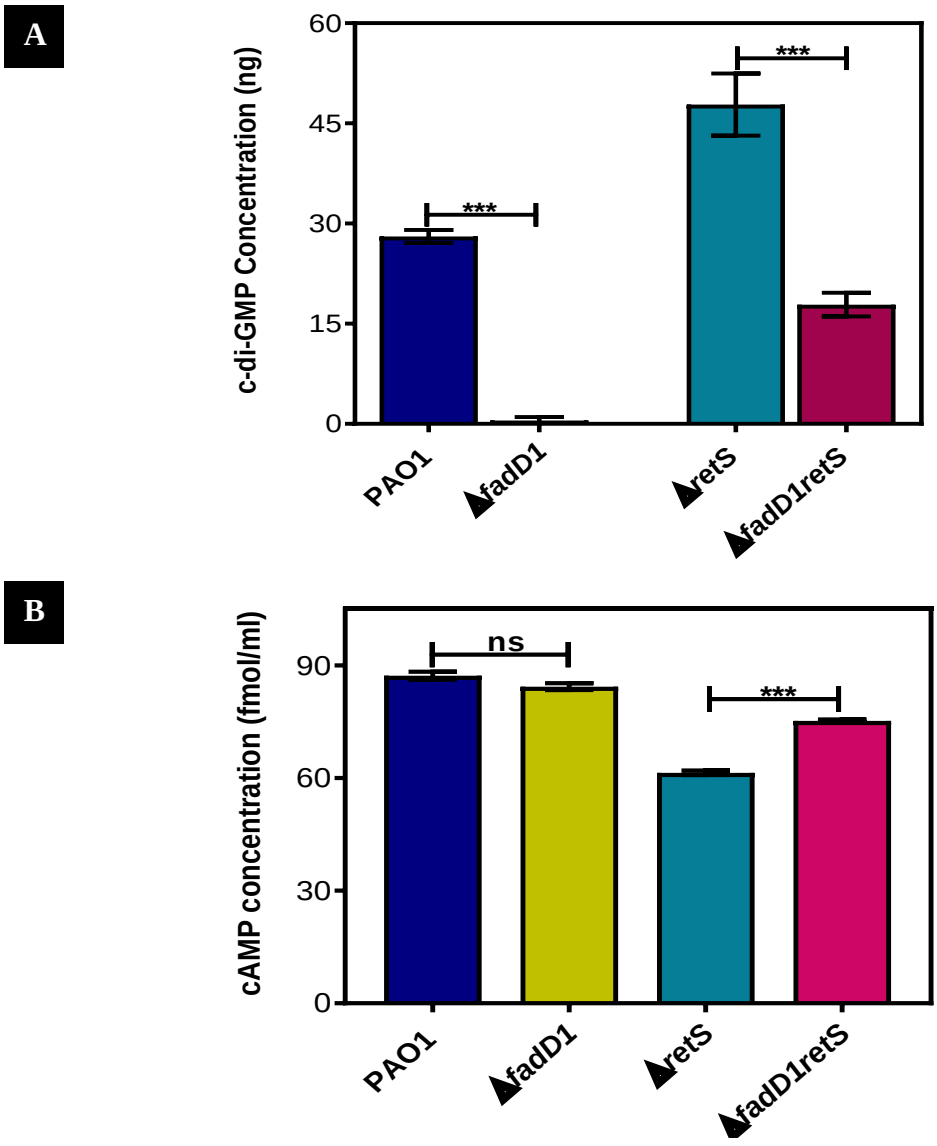

Figure 5.6 Deletion of *fadD1* resulted in a lower concentration of c-di-GMP and higher levels of cAMP. A. c-di-GMP was measured after 24 hr of growth. The test was performed by c-di-GMP ELISA kit by Cayman. Higher expression of the c-di-GMP was observed in PAO1(Δ*fadD1*Δ*retS*). **B.** Concentration of cAMP in PAO1, PAO1(Δ*fadD1*), PAO1(Δ*retS*), and PAO1(Δ*fadD1*Δ*retS*) was measured. PAO1(Δ*fadD1*Δ*retS*) Showed higher levels of cAMP compared to PAO1(Δ*retS*). The experiments were performed twice independently, and error bars indicate standard deviations ***p<0.001.

5.4 Discussion

The acute-phase bacterium is a free-living cell and motile with higher virulence to the host (Bhagirath et al., 2016). In chronic infections, biofilm production is increased, and bacteria live in a sessile lifestyle with activated T6SS (Mikkelsen et al., 2009; Moscoso et al., 2011; Schaber et al., 2007). Several modulatory elements are known, controlling the transition between bacterial lifestyle and fitness of the bacterium in the host. The role of T6SS is confirmed in pathogenic bacteria (Depluverez, Devos, and Devreese, 2016). In non-pathogenic bacteria that T6SS can have a cooperative action toward other prokaryotes and eukaryotes (Jani and Cotter, 2010). This promotes the importance of T6SS as a polytrophic tool for competition or to limit virulence (Parsons and Heffron, 2005). This study indicates that FadD1 is a new role player in the regulation of H1-T6SS in *P. aeruginosa*.

Previously, It was reported that FadD1 is involved in lipid metabolism for bacterial replication in the lungs of CF patients during infection (Son et al., 2007). In *Escherichia coli*, FadD1 degrades fatty acids and catalyzes acyl-CoA formation, a precursor for the β-oxidation cycle (Yun Kang et al., 2010). In *E. coli*, *fad* genes' expression was repressed by the addition of glucose through downregulation of the cell's cAMP levels, confirming cAMP's effect on Fad genes (Feng and Cronan, 2010; 2009). *P. aeruginosa* harbors two redundant *fad* genes, *fadD1* and *fadD2*, located in separate operons (Yun Kang et al., 2010). These *fad* proteins have substrate specificity and preference. FadD1 is more involved in the degradation of long-chain fatty acids (LCFA), whereas FadD2 degrades short and medium-chain length fatty acids (SCFAs, MCFAs). Fad proteins are not of the same function, and their role in the cell is not equivalent (Yun Kang et al., 2010). It has

been shown previously that the *fadD1fadD2* mutant strain had lower growth than the single *fad* mutant on a medium complemented with all chain-length fatty acids (Yun Kang et al., 2010). Also, *fadD1* deletion has led to higher motility and inefficient consumption of fatty acids for bacterial growth, resulting in lower bacteria fitness in-vivo (Yun Kang et al., 2010).

Here, our results showed, for the first time, that *fadD1* modulates the expression of H1-T6SS and T3SS reciprocally. Deletion of *fadD1* downregulated H1-T6SS and repressed the expression of sRNAs RsmY and RsmZ. It also upregulated the transcription of RsmA RNA binding protein. RsmA is an RNA binding protein that alters more than 500 genes in *P. aeruginosa* post-transcriptionally (Brencic and Lory, 2009)**.** RsmYZ has multiple recognition motif for RsmA (GGA motif), which RsmA detects to bind. This results in the titration of RsmA and blocking its function on acute phase-related genes (Brencic et al., 2009)**.** Together, repressed sRNAs RsmYZ and higher intracellular RsmA contributed to the restoration of T3SS in PAO1(Δ*fadD1*Δ*retS*). Moreover, the fatty acid profile of the PAO1(Δ*fadD1*Δ*retS*) was not significantly different from PAO1(Δ*retS*), voiding the potential role of free transcriptional regulator PsrA on the expression of T3SS.

The biofilm and motility assays showed a turnover in the bacterium's gene expression, with lower biofilm formation and higher motility in PAO1(Δ*fadD1*Δ*retS*). Biofilm formation is positively regulated by higher concentrations of c-di-GMP and lower cAMP signaling molecules (Almblad et al., 2019). The secondary metabolite c-di-GMP involves switching between bacteria's motile and sessile lifestyle (Moscoso et al., 2011). In *P. aeruginosa,* levels of cAMP and c-di-GMP are regulated inversely, and the mechanism that controls this turnover is not fully understood yet (Almblad et al., 2019; 2015). High

levels of cAMP reduce the intracellular content of c-di-GMP and result in the inhibition of biofilm formation (Almblad et al., 2019). Besides, the genes *pel* and *psl* are those negatively regulated by RsmA (Irie et al., 2010). Pel and Psl are required for the formation of biofilms, and higher levels of RsmA decrease the expression of *pel* and *psl*, resulting in lower biofilms. I found that FadD1 modulates the intracellular concentrations of c-di-GMP and cAMP secondary messengers. Although lower cAMP concentrations were reported to repress the expression of *fadD1* (Feng and Cronan, 2010; 2009), deletion of *fadD1* did not have the same positive relation with cAMP. The result shows a decrease in c-di-GMP, and inversely, cAMP an increase by deletion of *fadD1*. It is possible that higher expression of RsmA positively increased the transcription of Vfr, which led to higher cAMP levels (Wolfgang et al., 2003; Coggan and Wolfgang, 2012; Janssen et al., 2020; Marden et al., 2013). RsmA and Vfr are the activator of ExsA and can promote the expression of T3SS (Marden et al., 2013; Diaz, King, and Yahr, 2011). As an extension to this study, the role of Vfr, Pel, and Psl and the connection with FadD1 need to be further investigated. Data obtained from this study presents the aspects of FadD1 function to the pathogenicity of *P. aeruginosa* by modulation of cell signaling and virulence factors of the bacterium.

Chapter 6

6 Conclusion and future directions

6.1 Conclusion

A bacterium's adaptivity influences bacterial fitness and pathogenicity in a polymicrobial environment where other bacteria exist. Besides, the host defense mechanism, nutrient availability, and antibacterial affect the survival of the bacteria. The adaptivity is promoted by some virulence factors and the regulatory elements that control virulence factors' expression. Secretion systems are of those virulence determinants developed to deliver bacterial toxins to the extracellular milieu, host, or other competitive bacteria. In this study, additional regulatory pathways of H1-T6SS and several other virulence factors are discovered and characterized.

P. aeruginosa PAO1(Δ*retS*) containing an H1-T6SS reporter was subjected to transposon mutagenesis to screen for potential regulatory elements of H1-T6SS. Twelve genes and one RsmA binding region were identified. Our data indicate that the RNA ligase RtcB protein is a modulator of both H1-T6SS and T3SS. While the activation of T6SS and T3SS is reversely controlled, deleting RtcB removes this switch. The T6SS and T3SS are expressed in PAO1(Δ*rtcB*) simultaneously, and their master regulators, ClpV1 and ExsA, were upregulated in the mutant. This resulted in increased survival advantage of *P. aeruginosa* in competition with *E. coli*. Higher concentrations of RsmA protein contributed to the restoration of T3SS in PAO1(Δ*rtcB*Δ*retS*). When we exogenously overexpressed RsmY and RsmZ in PAO1(Δ*rtcB*Δ*retS*), RsmA was titrated and diminished T3SS. Not only RtcB affects the secretion systems, but it also altered several phenotypes of the bacterium, including motility and biofilm formation. Motility was restored in PAO1(Δ*rtcB*Δ*retS*), and biofilms were decreased in this mutant.

The expression of *rtcB* was elevated when the bacterium was coping with the low pH stress-inducing condition. The result suggested a role of *rtcB* in stress response through RNA repair and/or RNA processing. Hence, RNA's circularization was tested and showed *P. aeruginosa* bears circularized RNA in an RNA transcriptional stage which is modified by five cytosines in the back-splicing region (Chapter 3).

The long-chain-fatty-acid—CoA ligase FadD1 was found to be a novel modulator of H1-T6SS and T3SS. Deleting *fadD1* in the absence of *retS* in PAO1(Δ*retS*) resulted in higher transcription of RsmA and deactivation of RsmY and RsmZ. . This led to the re-activation of T3SS. H1-T6SS was repressed in PAO1(Δ*fadD1*Δ*retS*). Deletion of *fadD1* changed the intracellular levels of c-di-GMP and cAMP in favor of motile lifestyle in PAO1(Δ*fadD1*Δ*retS*) (Chapter 4).

Transcriptomic analysis of RtcB revealed that RtcB is a global regulator affecting bacterial metabolism, several virulence elements, and secondary metabolites. QS proteins, proteinases, and pyocyanin production were found to be influenced by the deletion of RtcB. It also showed to affect several secretion systems. Several DGS and PDEs were indeed differentially expressed in PAO1(Δ*rtcB*) and PAO1(Δ*rtcB*Δ*retS*) strains (Chapter 5). In conclusion, although extensive studies have elaborated on the regulation of H1-T6SS, there are unknown modulators that play pivotal roles in controlling this secretion system. The findings suggest that T6SS, T3SS, and other virulence factors are linked and connectively used by the bacterium to fight for survival in the host and the environment. The complex regulatory pathways need to be studied further.

6.2 Future directions

6.2.1 Characterization of the upstream regulation of RtcB protein

RtcR controls the regulation of RtcB. The regulatory domain of RtcR is the N-terminal divergent CARF domain. It is not clear through which cues or environmental signals the CARF domain is activated. Proteomic approaches like affinity purification-mass spectrometry on this domain, under different conditions, is appropriate to learn what stresses regulate the expression of RtcB.

6.2.2 Characterization of RtcB beyond virulence factors

Bacterial RtcB acts as a ribosomal/translational stress response system. Translational stressors activate RtcB, led to the survival of the bacterium. On the other hand, RtcB and endonuclease MazF have opposing functions on mRNAs and rRNAs. RtcB and MazF control ribosome heterogeneity and the pool of RNAs that are translated. It will be interesting to find; 1) if deletion of MazF, reverse the phenotype of PAO1(Δ*rtcB*); 2) is there a MazF binding region in the H1-T6SS or T3SS that could be regulated by this endonuclease; 3) the ribosome heterogeneity comparison between PAO1 and PAO1(Δ*rtcB*); 4) if deletion of RtcB in clinical isolates renders the same phenotypes as the laboratory strain PAO1.

6.2.3 Identification of the role of RtcB in bacterial RNA homeostasis

RtcB is an RNA processing protein that ligates the 2',3'-cyclic phosphate to the 5'-OH of the 3' fragment. To further understand the role of RtcB on non-coding RNAs, RNA deep sequencing or microarray will help navigate discontinued sequences. This should identify

the trans-ligation events or sequence-missing internal regions, elaborating the role of RtcB on ncRNAs. Also, by RNA immunoprecipitation (RIP), CRAC, or CLIP approach, RNA partners of RtcB protein can be identified.

6.2.4 **To further investigate the mechanism by which RtcB upregulated the H1-T6SS**

The RtcB protein modulates H1-T6SS. Considering that RtcB is an RNA processing protein, perhaps the RNA stability was affected upon deleting this gene, resulting in the altered gene expression of the PAO1(Δ*rtcB*). To determine through which mechanism the deletion of RtcB affected the bacterium's virulence, several approaches can be applied; 1) by measuring the mRNA half-life (for example, mRNAs of H1-T6SS) to find out the transcriptional shut-off and monitor the levels of mRNA over a time course; 2) measure RNA polymerase density along a gene like ClpV1 (by, e.g., ChIP) for transcription; 3) measure which fractions of the mRNAs of H1-T6SS eluted, in a ribosome gradient and compared between PAO1 and PAO1(Δ*rtcB*); 4) to determine if the upregulation of H1-T6SS is observed even in the presence of transcriptional inhibitors; 5) monitor the change in the affected proteins' half-life by inhibition of protein degradation or by measuring protein levels over a time course after translation inhibition.

6.2.5 **Further investigation on the role of FadD1 in survival fitness and metabolome of the bacterium**

RsmA is a modulator of several DGCs and PDEs; it will be interesting to understand if RsmA is involved in modulating the c-di-GMP content of the PAO1(Δ*fadD1*), for

example, by controlling SiaD. This will support the dissection of the modulatory effect of FadD1 in the pathogenicity of *P. aeruginosa*.

Besides, a transcriptome analysis will give a powerful insight into the differentially expressed genes affected by the deletion of *fadD1*.

References

Automatic citation updates are disabled. To see the bibliography, click Refresh in the Zotero tab.**Appendix**

Appendix 1. Differentially expressed genes in PAO1 vs PAO1(Δ*rtcB*)

Gene ID	Gene name	Gene product	log2 (fold change)	*p*-value
Downregulated genes				
PA5183	PA5183	glycine zipper 2TM domain protein	-10.213	0.004
PA4583	*rtcB*	RNA-splicing ligase RtcB	-5.162	0.000
PA0521	*qoxC*	cytochrome C oxidase subunit	-4.702	0.000
PA0525	*norD*	nitric oxide reductase activation protein NorD	-4.359	0.000
PA0524	*norB*	nitric oxide reductase subunit B	-4.032	0.000
PA4613	*katB*	catalase	-4.022	0.000

PA3390	*lsrG*	antibiotic biosynthesis monooxygenase	-3.612	0.001
PA3392	*nosZ*	nitrous-oxide reductase	-3.567	0.000
PA0517	*nirC*	cytochrome c55X	-3.376	0.000
PA0140	*ahpF*	alkyl hydroperoxide reductase	-3.195	0.000
PA0523	*norC*	nitric oxide reductase subunit C	-3.167	0.000
PA0516	*nirF*	protein nirF	-2.945	0.000
PA3393	*nosD*	copper-binding periplasmic protein	-2.607	0.000
PA0515	*nirD*	heme d1 biosynthesis protein NirD	-2.562	0.000
PA0513	*nirG*	heme d1 biosynthesis protein NirG	-2.541	0.000
PA3394	*nosF*	Daunorubicin/doxorubicin resistance ATP-binding protein DrrA	-2.438	0.000

PA0518	*nirM*	cytochrome C-551	-2.378	0.000
PA0519	*nirS*	nitrite reductase	-2.326	0.000
PA0848	*tsaA*	alkyl hydroperoxide reductase	-2.225	0.000
PA4212	*phzC*	phenazine biosynthesis protein PhzC	-2.085	0.000
PA3941	PA3941	HAD hydrolase, family IA	-2.083	0.001
PA4759	*dapB*	dihydrodipicolinate reductase	-2.075	0.000
PA0514	*nirL*	heme d1 biosynthesis protein NirL	-2.058	0.000
PA0446	PA0446	CoA transferase	-1.898	0.000
PA4760	*dnaJ*	molecular chaperone DnaJ	-1.845	0.000
PA3391	*nosR*	regulatory protein NosR	-1.838	0.000
PA0512	*nirH*	heme d1 biosynthesis protein NirH	-1.824	0.000

PA4181	PA4181	B3/4 domain protein	-1.763	0.000
PA4209	*sfmM3*	phenazine-specific methyltransferase	-1.701	0.000
PA3126	*ibpB*	heat-shock protein IbpA	-1.687	0.000
PA1707	*pcrH*	CesD/SycD/LcrH family type III secretion system chaperone	-1.633	0.000
PA1597	PA1597	dienelactone hydrolase	-1.625	0.000
PA4610	PA4610	copper transporter	-1.618	0.002
PA1722	*yscI*	preprotein translocase I	-1.613	0.001
PA4761	*dnaK*	molecular chaperone DnaK	-1.531	0.000
PA1706	*pcrV*	type III secretion protein PcrV	-1.518	0.000
PA0447	*Gcdh*	glutaryl-CoA dehydrogenase	-1.494	0.000
PA1183	*dctA2*	C4-dicarboxylate transport protein	-1.485	0.000

PA3842	*yerA*	chaperone	-1.477	0.000
PA3749	*yhjE*	major facilitator superfamily transporter	-1.445	0.007
PA1596	*htpG*	chaperone protein HtpG	-1.431	0.000
PA4211	*phzB1*	phenazine biosynthesis protein phzB 1	-1.428	0.000
PA2034	PA2034	SAM-dependent methyltransferase	-1.421	0.000
PA1708	*yopB*	translocator protein PopB	-1.415	0.000
PA0520	*nirQ*	denitrification regulatory protein NirQ	-1.411	0.000
PA3841	*aexT*	exoenzyme S	-1.402	0.000
PA1709	*yopD*	translocator outer membrane protein PopD	-1.369	0.000
PA1190	*yohC*	MULTISPECIES: YIP1 family protein	-1.357	0.000
PA0044	*aexT*	exoenzyme T	-1.335	0.000

PA5436	*cfiB*	acetyl-CoA carboxylase subunit A	-1.332	0.000
PA0511	*pqqE*	heme d1 biosynthesis protein NirJ	-1.332	0.000
PA0150	PA0150	transmembrane sensor	-1.324	0.007
PA0849	PA0849	thioredoxin reductase	-1.315	0.000
PA4385	*groL*	molecular chaperone GroEL	-1.297	0.000
PA3287	*Tanc2*	ankyrin domain-containing protein	-1.291	0.000
PA4471	PA4471	FagA	-1.289	0.000
PA4470	*fumC1*	class II fumarate hydratase	-1.282	0.000
PA0880	*glod5*	ring-cleaving dioxygenase	-1.280	0.003
PA0110	*shY1*	SURF1 family protein	-1.280	0.000
PA0051	*asnO*	phenazine-modifying protein	-1.272	0.000
PA4217	*hpxO*	flavin-dependent oxidoreductase	-1.268	0.000

PA3911	*yhbT*	SCP2 domain-containing protein	-1.262	0.004
PA2027	PA2027	Uncharacterized protein	-1.260	0.000
PA3634	*ftsB*	cell division protein FtsB	-1.240	0.000
PA1697	*yscN*	EscN/YscN/HrcN family type III secretion system ATPase	-1.235	0.000
PA4469	PA4469	FOG: TPR repeat	-1.226	0.000
PA1911	*fecR*	iron dicitrate transport regulator FecR	-1.226	0.000
PA5216	*fbpB2*	iron ABC transporter substrate-binding protein	-1.211	0.002
PA4570	PA4570	hypothetical protein	-1.206	0.000
PA3880	PA3880	zinc-binding protein	-1.194	0.005
PA2126	*ybdM*	transcriptional regulator	-1.182	0.000
PA1912	*fecI*	ECF sigma factor FemI	-1.180	0.000

PA0734	PA0734	cysteine rich CWC family protein	-1.180	0.000
PA1364	PA1364	sensor	-1.169	0.001
PA1698	*yopN*	type III secretion outer membrane protein PopN	-1.161	0.006
PA4386	*groS*	co-chaperonin	-1.160	0.000
PA4553	PA4553	type 4 fimbrial biogenesis protein	-1.152	0.000
PA4349	PA4349	acyl-CoA dehydrogenase	-1.138	0.000
PA4814	*fadH*	2,4-dienoyl-CoA reductase	-1.136	0.004
PA0108	*ctaE*	cytochrome c oxidase, subunit III	-1.135	0.000
PA1714	PA1714	ExsD	-1.135	0.000
PA2033	*viuB*	siderophore-interacting protein	-1.134	0.000
PA4588	*gdhA*	glutamate dehydrogenase	-1.127	0.000

PA0028	PA0028	Uncharacterized protein	-1.125	0.004
PA4806	PA4806	helix-turn-helix transcriptional regulator	-1.115	0.004
PA0139	*ahpC*	alkyl hydroperoxide reductase	-1.109	0.000
PA5054	*hslU*	ATP-dependent protease ATP-binding subunit HslU	-1.097	0.000
PA3584	*glpD*	glycerol-3-phosphate dehydrogenase	-1.079	0.000
PA4468	*sodA*	superoxide dismutase	-1.068	0.000
PA2191	*cya*	adenylate cyclase	-1.065	0.000
PA3927	*yeaM*	transcriptional regulator	-1.055	0.004
PA1710	*exsC*	exoenzyme S synthesis protein ExsC	-1.052	0.000
PA4896	*fecI*	RNA polymerase sigma factor	-1.049	0.000

PA4690	*pqiA*	paraquat-inducible protein A-like protein	-1.043	0.001
PA4762	*grpE*	heat shock protein GrpE	-1.041	0.000
PA3578	PA3578	isomerase	-1.028	0.000
PA5435	*pycB*	pyruvate carboxylase subunit B	-1.016	0.000
PA2857	*ybbA*	ABC transporter ATP-binding protein	-1.015	0.000
PA5427	*adhA*	Alcohol dehydrogenase	-1.004	0.000
Upregulated genes				
PA4586	PA4586	lipoprotein	14.565	0.000
PA0474	*Acot13*	esterase	11.324	0.002
PA4582	PA4582	SPFH domain / Band 7 family protein	9.331	0.000
PA4585	*rtcA*	RNA 3'-terminal-phosphate cyclase	7.291	0.000

PA4584	*ycgL*	nucleotidyltransferase	6.915	0.000
PA1633	*kdpA*	potassium-transporting ATPase subunit A	4.021	0.000
PA2508	*catC*	muconolactone delta-isomerase	3.858	0.000
PA3608	*potB*	polyamine ABC transporter permease PotB	3.709	0.000
PA1320	*cyoD*	cytochrome o ubiquinol oxidase subunit IV	3.695	0.000
PA2509	*catB*	muconate cycloisomerase I	3.547	0.000
PA2514	*antC*	anthranilate dioxygenase reductase	3.521	0.000
PA2513	*antB*	anthranilate dioxygenase small subunit	3.503	0.000
PA0281	*cysW*	sulfate transporter CysW	3.501	0.000
PA2512	*antA*	anthranilate dioxygenase large subunit	3.499	0.000

PA2507	*catA*	catechol 1,2-dioxygenase	3.438	0.000
PA5388	*gbuC*	glycine/betaine ABC transporter substrate-binding protein	3.433	0.000
PA4820	PA4820	membrane protein	3.309	0.002
PA3661	PA3661	Uncharacterized protein	3.303	0.000
PA5387	PA5387	carnitine dehydrogenase	3.295	0.000
PA1845	PA1845	Uncharacterized protein	3.218	0.000
PA3936	*tauC*	taurine ABC transporter permease	3.188	0.000
PA2682	*tcbE*	carboxymethylenebutenolidase	3.162	0.000
PA0280	*cysA*	sulfate.thiosulfate ABC transporter ATP-binding protein CysA	3.16	0.000
PA1634	*kdpB*	potassium-transporting ATPase subunit B	2.97	0.000

PA5385	*lcdH*	carnitine dehydrogenase	2.963	0.000
PA0985	*cib*	pyocin S5	2.956	0.000
PA0284	PA0284	organosulfur compounds A	2.902	0.000
PA1168	PA1168	Uncharacterized protein	2.823	0.000
PA0083	PA0083	type VI secretion protein	2.765	0.000
PA2768	PA2768	membrane protein	2.672	0.002
PA4139	PA4139	Uncharacterized protein	2.602	0.000
PA5098	*hutH*	histidine ammonia-lyase	2.52	0.000
PA1704	*pcrR*	transcriptional regulator PcrR	2.479	0.001
PA4106	PA4106	Uncharacterized protein	2.417	0.008
PA5386	*lcdH*	3-hydroxybutyryl-CoA dehydrogenase	2.357	0.000
PA0909	PA0909	Uncharacterized protein	2.346	0.007
PA0283	*sbp*	sulfate-binding protein	2.32	0.000

PA5282	PA5282	MFS transporter	2.294	0.004
PA0440	*sudA*	oxidoreductase	2.286	0.000
PA0282	*cysT*	sulfate transporter CysT	2.264	0.000
PA0646	PA0646	phage tail protein	2.253	0.000
PA2511	*andR*	transcriptional regulator	2.239	0.000
PA3935	*tauD*	taurine dioxygenase	2.229	0.000
PA0084	PA0084	EvpB/family type VI secretion protein	2.219	0.000
PA0080	PA0080	lipoprotein	2.208	0.000
PA0087	PA0087	type VI secretion system lysozyme	2.208	0.007
PA1317	*cyoA*	cytochrome o ubiquinol oxidase subunit II	2.202	0.000
PA0171	PA0171	PA0171-like protein	2.201	0.000
PA0085	*hcp1*	protein secretion apparatus assembly protein	2.18	0.000

PA0439	*preA*	dihydropyrimidine dehydrogenase subunit B	2.159	0.000
PA5256	*dsbB2*	disulfide bond formation protein	2.151	0.000
PA2365	PA2365	type VI secretion protein	2.134	0.000
PA1635	*kdpC*	potassium-transporting ATPase subunit C	2.128	0.000
PA5087	PA5087	sel1 repeat family protein	2.113	0.000
PA0645	PA0645	phage protein	2.108	0.000
PA4625	*hxuA*	hemagglutination protein	2.107	0.000
PA2203	*gltJ*	amino acid permease	2.104	0.002
PA5097	*proY*	amino acid permease	2.086	0.000
PA0695	PA0695	TonB family domain-containing protein	2.083	0.003
PA2370	PA2370	type VI secretion protein	2.082	0.000

PA2036	PA2036	methyltransferase domain protein	2.079	0.007
PA1369	PA1369	hypothetical protein	2.078	0.000
PA4191	PA4191	iron oxidase	2.027	0.000
PA5181	PA5181	oxidoreductase	2.004	0.000
PA5180	*fdhD*	sulfurtransferase FdhD	1.993	0.000
PA1319	PA1319	cytochrome o ubiquinol oxidase subunit III	1.99	0.000
PA0644	PA0644	MULTISPECIES: hypothetical protein	1.979	0.000
PA2459	PA2459	Uncharacterized protein	1.967	0.002
PA0091	PA0091	type VI secretion system protein VgrG	1.943	0.000
PA1318	*cyoB*	cytochrome ubiquinol oxidase subunit I	1.939	0.000
PA1274	*bluB*	5,6-dimethylbenzimidazole synthase	1.893	0.005

PA1666	PA1666	Type VI secretion lipoprotein/VasD	1.891	0.000
PA1873	*zntB*	corA-like Mg2+ transporter family protein	1.89	0.005
PA1421	*gbuA*	guanidinobutyrase	1.889	0.000
PA1837	PA1837	Oxidoreductase probably involved in sulfite reduction	1.878	0.000
PA1838	*sir1*	sulfite reductase	1.876	0.000
PA0441	*dht*	D-hydantoinase/dihydropyrimidinase	1.865	0.000
PA3866	*pys2*	pyocin protein	1.848	0.000
PA5267	*hcpA*	major exported protein, partial	1.817	0.000
PA2367	*hcp1*	Hcp1 family type VI secretion system effector	1.814	0.000
PA2260	PA2260	KguE	1.776	0.000

PA2204	*glnH*	ABC transporter	1.771	0.000
PA1370	PA1370	Uncharacterized protein	1.76	0.000
PA2366	PA2366	type VI secretion protein, EvpB/ family	1.756	0.000
PA5482	PA5482	probable exported protein	1.753	0.002
PA2262	*pht1*	2-ketogluconate transporter	1.75	0.000
PA0079	PA0079	type VI secretion protein	1.748	0.000
PA2263	*ghrB*	bifunctional glyoxylate/hydroxypyruvate reductase B	1.748	0.000
PA0643	PA0643	phage tail protein	1.746	0.000
PA0197	*tonB2*	transporter TonB	1.743	0.006
PA2369	PA2369	type VI secretion system protein ImpG	1.742	0.000
PA5410	*antA*	Rieske (2Fe-2S) protein	1.733	0.000
PA2371	*clpV1*	ClpA/B-type protease	1.732	0.000

PA5506	PA5506	MurR/RpiR family transcriptional regulator	1.725	0.000
PA5397	PA5397	hydrocarbon binding protein	1.722	0.000
PA0648	PA0648	Uncharacterized protein	1.722	0.001
PA1512	*hcpA*	major exported protein, partial	1.714	0.000
PA0613	PA0613	Uncharacterized protein	1.709	0.000
PA2083	*cbdA*	aromatic-ring-hydroxylating dioxygenase subunit alpha	1.706	0.000
PA0070	PA0070	Autotransporter adhesin	1.704	0.000
PA1169	*loxA*	arachidonate 15-lipoxygenase	1.7	0.000
PA0911	PA0911	Uncharacterized protein	1.698	0.000
PA3486	PA3486	type VI secretion system Vgr family protein	1.696	0.000
PA2085	*bphE*	ring-hydroxylating dioxygenase small subunit	1.687	0.002

PA3444	*ssuD*	alkanesulfonate monooxygenase	1.68	0.000
PA0647	PA0647	Uncharacterized protein	1.672	0.000
PA1419	PA1419	transporter	1.671	0.000
PA0981	PA0981	Uncharacterized protein	1.67	0.000
PA0263	*hcpA*	major exported protein, partial	1.67	0.002
PA0198	*exbB*	transporter ExbB	1.661	0.000
PA4140	PA4140	FAD-linked oxidase	1.656	0.000
PA0443	*pucI*	transporter	1.655	0.000
PA3293	PA3293	Uncharacterized protein	1.649	0.004
PA2792	PA2792	Uncharacterized protein	1.639	0.001
PA4321	PA4321	DUF4350 domain-containing protein	1.638	0.000
PA0898	*astD*	N-succinylglutamate 5-semialdehyde dehydrogenase	1.636	0.000

PA0612	*traR*	repressor PtrB	1.633	0.001
PA0098	PA0098	3-oxoacyl-ACP synthase	1.632	0.006
PA1321	*cyoE2*	protoheme IX farnesyltransferase	1.631	0.000
PA0897	*aruG*	arginine N-succinyltransferase subunit beta	1.616	0.000
PA4442	*cysNC*	bifunctional sulfate adenylyltransferase subunit 1/adenylylsulfate kinase	1.616	0.000
PA3450	PA3450	antioxidant protein	1.614	0.000
PA0172	*resE*	histidine kinase	1.608	0.000
PA3938	*tauA*	taurine-binding protein	1.586	0.000
PA2261	*kdgK*	2-ketogluconate kinase	1.581	0.000
PA4121	*hpaG*	4-hydroxyphenylacetate degradation bifunctional isomerase/decarboxylase	1.566	0.003

PA3152	*hisH2*	imidazole glycerol phosphate synthase	1.55	0.001
PA0910	PA0910	Uncharacterized protein	1.546	0.000
PA4443	*cysD*	sulfate adenylyltransferase subunit 2	1.531	0.000
PA3467	*pcaK*	major facilitator superfamily transporter	1.521	0.003
PA3154	PA3154	O-antigen polymerase	1.516	0.001
PA0622	PA0622	bacteriophage protein	1.506	0.000
PA4100	*alkJ*	dehydrogenase	1.491	0.000
PA2328	*nrtA*	ABC transporter substrate-binding protein	1.472	0.000
PA0040	*cdiB*	hemolysin activation/secretion protein	1.464	0.000
PA3236	*gbuC*	glycine betaine-binding protein	1.463	0.000

PA2518	*xylX*	toluate 1,2-dioxygenase subunit alpha	1.459	0.000
PA0896	*astA*	arginine N-succinyltransferase subunit alpha	1.454	0.000
PA4023	*yhdG*	transporter	1.453	0.000
PA1256	*glnQ*	amino acid ABC transporter ATP-binding protein	1.433	0.000
PA0718	PA0718	Uncharacterized protein	1.433	0.000
PA3443	*tauC*	aliphatic sulfonates ABC transporter permease	1.423	0.004
PA0169	*pleD*	GGDEF domain-containing protein	1.417	0.001
PA1661	PA1661	type VI secretion protein	1.411	0.002
PA1150	*pys2*	pyocin-S2	1.405	0.000
PA5099	PA5099	transporter	1.401	0.000

PA0082	PA0082	ImpA family type VI secretion-associated protein	1.399	0.000
PA2118	PA2118	topoisomerase II	1.395	0.005
PA3907	PA3907	restriction endonuclease fold toxin 5 family protein	1.39	0.001
PA2786	PA2786	FOG: GAF domain	1.385	0.000
PA2095	PA2095	methyltransferase	1.38	0.000
PA3445	PA3445	sulfonate ABC transporter substrate-binding protein	1.378	0.000
PA0097	PA0097	Uncharacterized protein	1.375	0.000
PA2762	PA2762	cupin	1.369	0.000
PA0563	*yhaI*	DUF805 domain-containing protein	1.367	0.000
PA2441	PA2441	myb-like DNA-binding domain protein	1.359	0.003
PA3149	PA3149	ORF_15; similar to Glycosyl transferases group 1	1.351	0.000

PA2368	PA2368	type VI secretion system lysozyme-like protein	1.347	0.001
PA2650	*ybaJ*	methyltransferase domain protein	1.346	0.002
PA4122	*hpaG*	4-hydroxyphenylacetate degradation bifunctional isomerase/decarboxylase	1.345	0.000
PA2598	*ssuD*	alkanesulfonate monooxygenase	1.342	0.000
PA2111	*kipI*	allophanate hydrolase	1.338	0.000
PA0899	*astB*	N-succinylglutamate 5-semialdehyde dehydrogenase	1.335	0.000
PA5415	*glyA1*	serine hydroxymethyltransferase	1.335	0.000
PA0895	*aruC*	bifunctional succinylornithine transaminase/acetylornithine aminotransferase	1.333	0.000

PA4195	*glnH*	ABC transporter	1.325	0.004
PA4151	*acoB*	acetoin catabolism protein AcoB	1.321	0.000
PA0776	PA0776	Uncharacterized protein	1.315	0.000
PA1257	PA1257	amino acid ABC transporter permease	1.309	0.003
PA4587	*ccpA*	cytochrome C551 peroxidase	1.309	0.000
PA5411	*hcr*	protein GbcB	1.309	0.000
PA3905	PA3905	Uncharacterized protein	1.306	0.000
PA4986	PA4986	oxidoreductase	1.305	0.000
PA3932	*flbD*	transcriptional regulator	1.303	0.000
PA1665	PA1665	signal peptide protein	1.299	0.008
PA0623	PA0623	Probable bacteriophage protein	1.29	0.000
PA2062	*iscS*	pyridoxal-phosphate dependent protein	1.286	0.000

PA2361	PA2361	type VI secretion system protein ImpL	1.282	0.000
PA2330	PA2330	acyl-CoA dehydrogenase	1.273	0.000
PA4642	PA4642	aminopeptidase	1.273	0.006
PA5419	*soxG*	sarcosine oxidase subunit gamma	1.263	0.000
PA0961	*cspA*	cold-shock protein	1.262	0.001
PA0090	*clpV1*	secretion protein ClpV1	1.256	0.000
PA2331	PA2331	alkylhydroperoxidase	1.254	0.000
PA5396	PA5396	membrane dipeptidase family protein	1.251	0.000
PA5398	*stcD*	dimethylglycine catabolism protein DgcA	1.241	0.000
PA2228	*nylB*	beta-lactamase family protein	1.239	0.006
PA2409	*mntC*	ABC transporter permease	1.233	0.007

PA2037	PA2037	Uncharacterized protein	1.233	0.000
PA1172	*napC*	cytochrome C protein NapC	1.231	0.000
PA2265	PA2265	gluconate dehydrogenase	1.225	0.000
PA0633	PA0633	VF2	1.224	0.000
PA1888	PA1888	Uncharacterized protein	1.223	0.000
PA3266	*cspA*	major cold shock protein CspA	1.222	0.000
PA2360	PA2360	ImpA family type VI secretion-associated protein	1.222	0.000
PA5375	*betT*	transporter, betaine/carnitine/choline transporter family protein	1.222	0.005
PA4918	*pcnA*	nicotinamidase	1.22	0.000
PA1174	*napA*	nitrate reductase catalytic subunit	1.22	0.000
PA5024	*ytnM*	anion permease	1.219	0.004

PA1646	*mcpS*	chemotaxis transducer	1.216	0.000
PA4123	*hpcC*	5-carboxy-2-hydroxymuconate semialdehyde dehydrogenase	1.216	0.000
PA2086	PA2086	epoxide hydrolase	1.215	0.000
PA0199	*exbD*	biopolymer transport protein ExbD	1.212	0.002
PA0634	PA0634	Uncharacterized protein	1.205	0.000
PA5316	*rpmB*	50S ribosomal protein L28	1.205	0.000
PA2395	*pvdO*	pyoverdine biosynthesis protein	1.203	0.000
PA5264	PA5264	Uncharacterized protein	1.199	0.000
PA2114	*mmlH*	MFS transporter	1.198	0.000
PA2089	*btuB*	TonB-dependent receptor	1.195	0.000
PA0807	*amiD*	protein AmpDh3	1.192	0.000
PA4563	*rpsT*	30S ribosomal protein S20	1.19	0.000

PA1818	*adiA*	lysine-specific pyridoxal 5'-phosphate-dependent carboxylase LdcA	1.189	0.000
PA3186	*oprB*	porin B	1.187	0.000
PA5399	*hdrD*	(Fe-S)-binding protein	1.186	0.000
PA1258	*occM*	ABC transporter permease	1.178	0.003
PA5420	*purU*	formyltetrahydrofolate deformylase	1.171	0.000
PA0077	PA0077	type VI secretion protein IcmF	1.167	0.000
PA0074	*pknB*	serine/threonine protein kinase	1.166	0.003
PA4838	PA4838	membrane protein	1.161	0.006
PA3934	PA3934	possible membrane protein	1.151	0.000
PA2540	PA2540	Phospholipase	1.146	0.000

PA4152	*acoC*	branched-chain alpha-keto acid dehydrogenase subunit E2	1.143	0.000
PA2329	*ssuB1*	ABC transporter ATP-binding protein	1.141	0.000
PA1218	PA1218	phytanoyl-CoA dioxygenase family protein	1.141	0.000
PA0444	*hyuC*	allantoate amidohydrolase	1.139	0.000
PA0907	PA0907	Uncharacterized protein	1.129	0.001
PA2327	*cmpB*	ABC transporter permease	1.129	0.000
PA3484	PA3484	Uncharacterized protein	1.128	0.000
PA3761	*nagE*	N-acetyl-D-glucosamine phosphotransferase system transporter	1.119	0.000
PA0719	PA0719	Pf1-like phage protein	1.114	0.001
PA3453	PA3453	UPF0502 protein	1.113	0.000

PA3930	*cydA*	cyanide insensitive terminal oxidase	1.113	0.000
PA5416	*soxB*	sarcosine oxidase subunit beta	1.112	0.000
PA0916	*rimO*	ribosomal protein S12 methylthiotransferase RimO	1.109	0.000
PA3315	*ptxC*	ABC transporter permease	1.108	0.007
PA1483	*cycH*	cytochrome c-type biogenesis protein CycH	1.107	0.001
PA5418	*soxA*	sarcosine oxidase subunit alpha	1.104	0.000
PA3955	PA3955	membrane protein	1.1	0.006
PA5090	PA5090	type VI secretion system Vgr family protein	1.099	0.000
PA1510	PA1510	PGAP1-like family protein	1.095	0.000
PA4091	*hpaB*	4-hydroxyphenylacetate 3-monooxygenase	1.089	0.000

PA1519	*adeP*	transporter	1.086	0.009
PA3928	PA3928	DUF2474 domain-containing protein	1.078	0.003
PA0624	PA0624	mu-like prophage FluMu gp41 family protein	1.077	0.000
PA0794	*acnM*	aconitate hydratase	1.076	0.000
PA2264	PA2264	gluconate 2-dehydrogenase	1.073	0.000
PA2259	*kdgR*	transcriptional regulator PtxS	1.069	0.000
PA2454	*ubiG*	SAM-dependent methyltransferase	1.069	0.005
PA4868	*ureC*	urease subunit alpha, partial	1.061	0.000
PA4810	*fdoI*	nitrate-inducible formate dehydrogenase, gamma subunit	1.059	0.000
PA2340	PA2340	binding-protein-dependent maltose/mannitol transport protein	1.058	0.001

PA4150	*acoA*	dehydrogenase E1 component	1.058	0.000
PA1601	*nicB*	aldehyde dehydrogenase	1.054	0.000
PA0201	PA0201	alpha/beta hydrolase	1.054	0.000
PA3495	PA3495	endonuclease III	1.047	0.003
PA0422	*yceJ*	Nickel-dependent hydrogenase B-type cytochrome subunit	1.044	0.000
PA5285	PA5285	Uncharacterized protein	1.041	0.006
PA0805	PA0805	Uncharacterized protein	1.039	0.000
PA3487	*pldA*	phospholipase D	1.034	0.000
PA2359	*zraR*	transcriptional regulator	1.033	0.002
PA0438	*codB*	cytosine permease	1.03	0.000
PA2317	*puuB*	oxidoreductase	1.026	0.000
PA2939	*lap*	aminopeptidase	1.026	0.000
PA1951	PA1951	Fap amyloid fiber secretin	1.024	0.000

PA3150	PA3150	WbpG	1.024	0.000
PA4092	*hpaC*	4-hydroxyphenylacetate 3-monooxygenase small subunit	1.024	0.003
PA5533	PA5533	COG0649: NADH:ubiquinone oxidoreductase 49 kD subunit 7	1.023	0.002
PA3931	*metQ*	YaeC family lipoprotein	1.02	0.000
PA4635	*mgtC*	Mg (2+) transport ATPase protein C	1.017	0.000
PA3492	PA3492	electron transport complex subunit D	1.012	0.000
PA4317	PA4317	probable proline and glycine rich transmembrane protein	1.001	0.000

Appendix 2. Differentially expressed genes in PAO1(Δ*retS*) vs PAO1(Δ*rtcB*Δ*retS*)

Gene ID	Gene name	Gene product	log2 (fold change)	*p* value
Downregulated genes				
PA4583	*rtcB*	RNA-splicing ligase RtcB	-14.715	0.000
PA3906	PA3906	Uncharacterized protein	-13.298	0.001
PA0263	*hcpA*	major exported protein	-9.869	0.000
PA2512	*antA*	anthranilate dioxygenase large subunit	-9.758	0.000
PA2514	*antC*	anthranilate dioxygenase reductase	-9.446	0.000
PA2513	*antB*	anthranilate dioxygenase small subunit	-9.330	0.000
PA1512	*hcpA*	major exported protein, partial	-8.732	0.000
PA2370	PA2370	type VI secretion protein	-7.556	0.000
PA5267	*hcpA*	major exported protein, partial	-7.325	0.000

PA0993	*yadV*	chaperone CupC2	-7.142	0.000
PA2367	*hcp1*	Hcp1 family type VI secretion system effector	-6.929	0.000
PA1671	*pkaA*	serine-threonine kinase Stk1	-6.917	0.000
PA0992	*fimA*	fimbrial subunit CupC1	-6.878	0.000
PA0261	PA0261	Uncharacterized protein	-6.747	0.000
PA1663	*zraR*	transcriptional regulator	-6.605	0.000
PA1668	PA1668	membrane protein	-6.560	0.000
PA1659	PA1659	type VI secretion system lysozyme-like protein	-6.552	0.000
PA1658	PA1658	EvpB/family type VI secretion protein	-6.468	0.000
PA1510	PA1510	PGAP1-like family protein	-6.379	0.000
PA2371	*clpV1*	ClpA/B-type protease	-6.291	0.000

PA1667	PA1667	type VI secretion protein	-6.289	0.000
PA1661	PA1661	type VI secretion protein	-6.289	0.000
PA1665	PA1665	signal peptide protein	-6.272	0.000
PA2369	PA2369	type VI secretion system protein ImpG	-6.257	0.000
PA1666	PA1666	Type VI secretion lipoprotein/VasD	-6.199	0.000
PA0262	PA0262	Rhs element Vgr family protein	-6.163	0.000
PA1660	PA1660	type VI secretion protein	-6.157	0.000
PA1511	PA1511	type VI secretion system Vgr family protein	-6.154	0.000
PA2509	*catB*	muconate cycloisomerase I	-6.134	0.000
PA1662	*clpV2*	ClpA/B-type protease	-6.058	0.000
PA1669	PA1669	type VI secretion protein IcmF	-6.052	0.000

PA0260	PA0260	DUF3274 domain-containing protein	-6.044	0.000
PA1670	*prpC*	serine/threonine phosphoprotein phosphatase Stp1	-5.981	0.000
PA1657	PA1657	type VI secretion protein	-5.973	0.000
PA2366	PA2366	type VI secretion protein, EvpB/ family	-5.943	0.000
PA2508	*catC*	muconolactone delta-isomerase	-5.838	0.000
PA2365	PA2365	type VI secretion protein	-5.777	0.000
PA3291	PA3291	DUF3304 domain-containing protein	-5.759	0.000
PA5266	PA5266	Rhs element Vgr family protein	-5.727	0.000
PA2091	*ybfB*	MFS transporter	-5.639	0.001

PA2360	PA2360	ImpA family type VI secretion-associated protein	-5.535	0.000
PA3488	PA3488	Uncharacterized protein	-5.432	0.000
PA2362	PA2362	type VI secretion system protein ImpK	-5.425	0.000
PA3487	*pldA*	phospholipase D	-5.351	0.000
PA3486	PA3486	type VI secretion system Vgr family protein	-5.267	0.000
PA3293	PA3293	Uncharacterized protein	-5.213	0.000
PA0072	PA0072	ABC transporter permease	-5.132	0.000
PA0077	PA0077	type VI secretion protein IcmF	-5.125	0.000
PA3294	PA3294	Rhs element Vgr family protein	-5.116	0.000
PA2204	*glnH*	ABC transporter	-5.101	0.000

PA1508	PA1508	PAAR motif family protein	-5.060	0.000
PA2361	PA2361	type VI secretion system protein ImpL	-5.043	0.000
PA1509	PA1509	membrane protein	-5.024	0.000
PA0078	*motB*	DotU family type IV/VI secretion system protein	-4.946	0.000
PA4962	*ybcI*	inner membrane protein ybcI	-4.930	0.008
PA4298	PA4298	Protein of Uncharacterized function	-4.901	0.001
PA2507	*catA*	catechol 1,2-dioxygenase	-4.891	0.000
PA3907	PA3907	restriction endonuclease fold toxin 5 family protein	-4.858	0.000
PA0050	PA0050	Uncharacterized protein	-4.833	0.000
PA4489	PA4489	Uncharacterized protein	-4.823	0.000
PA4487	*yfaP*	signal peptide protein	-4.799	0.000

PA0085	*hcp1*	protein secretion apparatus assembly protein	-4.789	0.000
PA1656	PA1656	type VI secretion-associated protein	-4.730	0.000
PA0083	PA0083	type VI secretion protein	-4.664	0.000
PA0088	PA0088	type VI secretion system protein ImpG	-4.660	0.000
PA4490	PA4490	Uncharacterized protein	-4.654	0.000
PA0985	*cib*	pyocin S5	-4.634	0.000
PA0098	PA0098	3-oxoacyl-ACP synthase	-4.627	0.000
PA0084	PA0084	EvpB/family type VI secretion protein	-4.610	0.000
PA5089	PA5089	phospholipase D family protein	-4.607	0.000
PA0074	pknB	serine/threonine protein kinase	-4.555	0.000

PA0173	*cheB2*	chemotaxis response regulator protein-glutamate methylesterase	-4.526	0.000
PA2368	PA2368	type VI secretion system lysozyme-like protein	-4.517	0.000
PA1914	PA1914	halovibrin	-4.467	0.000
PA4650	PA4650	Sigma-fimbriae uncharacterized subunit	-4.452	0.000
PA2538	PA2538	Uncharacterized protein	-4.447	0.000
PA4306	PA4306	type IVb pilin Flp	-4.445	0.000
PA0090	*clpV1*	secretion protein ClpV1	-4.439	0.000
PA2791	PA2791	Uncharacterized protein	-4.421	0.002
PA3292	PA3292	DUF3304 domain-containing protein	-4.402	0.000
PA4651	PA4651	pili assembly chaperone	-4.397	0.000
PA2792	PA2792	Uncharacterized protein	-4.388	0.000

PA3947	*cph2*	DNA-binding response regulator RocR	-4.380	0.000
PA0075	*prpC*	serine/threonine phosphatase	-4.365	0.000
PA2729	PA2729	Uncharacterized protein	-4.325	0.000
PA0174	*cheD*	chemotaxis protein CheD	-4.301	0.000
PA0099	PA0099	GHH signature containing protein	-4.253	0.000
PA5090	PA5090	type VI secretion system Vgr family protein	-4.252	0.000
PA2703	PA2703	Uncharacterized protein	-4.195	0.000
PA1891	PA1891	Uncharacterized protein	-4.184	0.004
PA4652	*sfmD*	outer membrane usher family protein	-4.168	0.000
PA3484	PA3484	Uncharacterized protein	-4.078	0.000
PA0089	PA0089	type VI secretion protein	-4.071	0.000

PA3948	*fimZ*	two-component response regulator RocA1	-4.057	0.000
PA5088	PA5088	lipoprotein	-4.052	0.000
PA3905	PA3905	Uncharacterized protein	-4.006	0.000
PA4649	*pru*	spore coat protein U	-3.996	0.000
PA2539	*ynbD*	ser/threonine protein phosphatase	-3.952	0.000
PA5265	PA5265	Uncharacterized protein	-3.938	0.000
PA0091	PA0091	type VI secretion system protein VgrG	-3.938	0.000
PA5113	PA5104	membrane protein	-3.938	0.000
PA2726	*nrdG*	radical activating enzyme	-3.919	0.000
PA0097	PA0097	Uncharacterized protein	-3.909	0.000
PA1887	PA1887	Uncharacterized protein	-3.892	0.000
PA5181	Mb2924c	oxidoreductase	-3.877	0.000
PA5180	*fdhD*	sulfurtransferase FdhD	-3.863	0.000

		type VI secretion system		
PA0087	PA0087	lysozyme	-3.852	0.000
PA2725	*clpB1*	chaperone	-3.798	0.000
PA1888	PA1888	Uncharacterized protein	-3.797	0.000
PA5100	*hutU*	urocanate hydratase	-3.788	0.000
		DUF2138 domain-		
PA4491	*yfaA*	containing protein	-3.779	0.000
PA2702	PA2702	Uncharacterized protein	-3.777	0.000
PA0126	PA0126	Uncharacterized protein	-3.765	0.000
		HEAT repeat-containing		
PA0101	PA0101	protein	-3.725	0.000
PA3450	PA3450	antioxidant protein	-3.677	0.000
PA0079	PA0079	type VI secretion protein	-3.677	0.000
		non-ribosomal peptide		
PA2302	*lgrC*	synthetase	-3.675	0.000

PA2536	*cdsA*	phosphatidate cytidylyltransferase	-3.673	0.000
PA1893	*quiP*	penicillin acylase family protein	-3.639	0.000
PA1791	PA1791	membrane protease subunit, stomatin/prohibitin	-3.623	0.000
PA0277	*loiP*	peptidase M48 family protein	-3.597	0.000
PA0080	PA0080	lipoprotein	-3.566	0.000
PA2540	PA2540	Phospholipase YtpA	-3.555	0.000
PA4648	PA4648	Spore coat protein U	-3.553	0.000
PA0175	*cheR2*	chemotaxis protein methyltransferase	-3.547	0.000
PA3619	*tolB*	WD40-like Beta Propeller Repeat family protein	-3.535	0.000
PA3290	PA3290	Rhs element Vgr protein	-3.500	0.000

PA3728	PA3728	AAA domain family protein	-3.490	0.000
PA0094	PA0094	Uncharacterized conserved protein	-3.484	0.000
PA0259	PA0259	PA2540	-3.474	0.000
PA0073	*lolD2*	ABC transporter ATP-binding protein	-3.455	0.000
PA0040	*cdiB*	hemolysin activation/secretion protein	-3.453	0.000
PA0499	*fimB*	pili assembly chaperone	-3.410	0.000
PA4085	*fimB*	chaperone CupB2	-3.404	0.000
PA1894	PA1894	2OG-Fe(II) oxygenase superfamily protein	-3.401	0.000
PA3367	*ydcA*	Uncharacterized protein	-3.394	0.000
PA2678	*rfbA*	sugar ABC transporter permease	-3.385	0.000

PA5136	PA5136	Uncharacterized protein	-3.385	0.000
PA3727	PA3727	nuclease	-3.384	0.000
PA0177	*cheW*	purine-binding chemotaxis protein	-3.376	0.000
PA2780	PA2780	transcriptional regulator	-3.376	0.000
PA2560	PA2560	Uncharacterized protein	-3.372	0.000
PA5106	*mtaD*	N-formimino-L-glutamate deiminase	-3.359	0.000
PA0047	PA0047	lipoprotein	-3.345	0.000
PA3335	PA3335	SAM-dependent methyltransferase	-3.333	0.000
PA2570	*lecA*	PA-I galactophilic lectin	-3.329	0.000
PA0041	*cdiA*	hemagglutinin	-3.326	0.000
PA5099	PA5099	transporter	-3.315	0.002
PA2303	PA2303	protein AmbD	-3.301	0.000

PA3361	PA3361	fucose-binding lectin PA-IIL	-3.295	0.000
PA3485	PA3485	Uncharacterized protein	-3.285	0.000
PA5087	PA5087	sel1 repeat family protein	-3.283	0.000
PA0563	*yhaI*	DUF805 domain-containing protein	-3.278	0.000
PA4653	PA4653	Sigma-fimbriae tip adhesin	-3.264	0.000
PA5264	PA5264	Uncharacterized protein	-3.244	0.000
PA4302	*trbB*	ATPase TadA	-3.243	0.000
PA0082	PA0082	ImpA family type VI secretion-associated protein	-3.208	0.000
PA2774	PA2774	Uncharacterized protein	-3.203	0.000
PA2684	*rhsA*	RHS repeat-associated core domain protein	-3.189	0.000
PA4086	PA4086	fimbrial subunit CupB1	-3.167	0.000

PA2062	*iscS*	pyridoxal-phosphate dependent protein	-3.166	0.000
PA3661	PA3661	Uncharacterized protein	-3.162	0.000
PA0045	PA0045	curli production assembly protein CsgG	-3.159	0.000
PA3908	PA3908	immunity 32 family protein	-3.157	0.000
PA5098	*hutH*	histidine ammonia-lyase	-3.147	0.000
PA3333	*fabH*	3-oxoacyl-ACP synthase	-3.136	0.000
PA2455	PA2455	GNAT family N-acetyltransferase	-3.131	0.000
PA0178	*cheA*	chemotaxis protein CheA	-3.120	0.000
PA0070	PA0070	Autotransporter adhesin	-3.111	0.000
PA1451	*ygcG*	TLP18.3, Psb32 and MOLO-1 founding s of phosphatase family protein	-3.106	0.000

PA0176	*tcp*	aerotaxis transducer Aer2	-3.097	0.000
PA0007	PA0007	Uncharacterized protein	-3.086	0.000
PA2677	*hxcR*	type II secretion protein	-3.085	0.000
PA2463	*cdiB*	hemolysin secretion/activation ShlB/FhaC/HecB family protein	-3.075	0.000
PA4303	PA4303	TadZ	-3.074	0.000
PA3045	*fimZ*	LuxR family transcriptional regulator	-3.063	0.000
PA4299	PA4299	type II secretion system protein TadD	-3.052	0.000
PA0086	PA0086	virulence protein SciE type	-3.043	0.000
PA2682	*tcbE*	carboxymethylenebutenolidase	-3.032	0.000
PA2781	PA2781	Uncharacterized protein	-3.027	0.000

PA2462	*cdiA*	hemagglutinin	-3.019	0.000
PA4488	*yfaQ*	stage II sporulation family protein	-3.017	0.000
PA0100	PA0100	Beta-propeller repeat TECPR	-3.013	0.000
PA2537	PA2537	acyltransferase	-2.999	0.000
PA0096	PA0096	Uncharacterized protein	-2.994	0.000
PA1276	*cobC*	threonine-phosphate decarboxylase	-2.992	0.006
PA2304	PA2304	protein AmbC	-2.981	0.000
PA2328	*nrtA*	ABC transporter substrate-binding protein	-2.970	0.000
PA1895	PA1895	tRNA (adenosine(37)-N6)-threonylcarbamoyltransferase complex dimerization subunit type 1 TsaB	-2.952	0.000
PA1396	*rpfC*	two-component sensor	-2.926	0.000

PA2511	*andR*	transcriptional regulator	-2.925	0.000
PA3329	*ppsB*	Malonyl CoA-acyl carrier protein transacylase	-2.905	0.000
PA2444	*glyA2*	serine hydroxymethyltransferase	-2.900	0.000
PA1892	PA1892	Uncharacterized protein	-2.894	0.000
PA2327	*cmpB*	ABC transporter permease	-2.882	0.000
PA3336	*ytbD*	major facilitator superfamily transporter	-2.877	0.000
PA1370	PA1370	Uncharacterized protein	-2.864	0.000
PA3729	*yqiK*	Inner membrane protein YqiK	-2.858	0.000
PA2363	PA2363	type VI secretion protein	-2.848	0.000
PA2301	PA2301	tRNA synthetase	-2.829	0.000
PA2464	PA2464	Uncharacterized protein	-2.828	0.000
PA3332	PA3332	putative isomerase	-2.817	0.000

PA3331	PA3331	cytochrome P450	-2.816	0.000
PA2329	*ssuB1*	ABC transporter ATP-binding protein	-2.794	0.000
PA3021	PA3021	Uncharacterized protein	-2.777	0.000
PA2445	*gcvP1*	glycine dehydrogenase	-2.765	0.000
PA0076	PA0076	type VI secretion system protein ImpM	-2.758	0.001
PA3715	PA3715	ABC-type multidrug transport system, ATPase and permease component	-2.756	0.000
PA3334	PA3334	acyl carrier protein	-2.744	0.000
PA0234	PA0234	nucleoside-binding protein	-2.738	0.000
PA2299	*yvoA*	transcriptional regulator	-2.738	0.000
PA2300	*chiD*	chitinase	-2.737	0.000
PA2581	PA2581	lipoprotein	-2.713	0.000

PA2240	PA2240	biofilm formation protein PslJ	-2.699	0.000
PA2374	PA2374	MORN repeat variant family protein	-2.698	0.000
PA1612	PA1612	ABC transporter substrate-binding protein	-2.682	0.002
PA4123	*hpcC*	5-carboxy-2-hydroxymuconate semialdehyde dehydrogenase	-2.681	0.000
PA3328	*hpxO*	FAD-dependent monooxygenase	-2.667	0.000
PA3330	*Rdh7*	short-chain dehydrogenase	-2.647	0.000
PA2285	PA2285	peptidase M48, Ste24p	-2.644	0.011
PA2330	PA2330	acyl-CoA dehydrogenase	-2.643	0.000
PA5033	PA5033	Uncharacterized protein	-2.636	0.000
PA1091	*rfbC*	flagellar glycosyl transferase FgtA	-2.625	0.000

PA1613	*btuB*	tonB dependent receptor family protein	-2.624	0.000
PA2775	PA2775	Uncharacterized protein	-2.608	0.000
PA2242	PA2242	possible acetyltransferase	-2.587	0.000
PA1898	*solR*	quorum-sensing control repressor	-2.580	0.007
PA1395	PA1395	lipoprotein	-2.556	0.000
PA1896	PA1896	Uncharacterized protein	-2.551	0.000
PA2432	PA2432	bistable expression regulator BexR	-2.534	0.000
PA2331	PA2331	alkylhydroperoxidase	-2.532	0.000
PA2083	*cbdA*	aromatic-ring-hydroxylating dioxygenase subunit alpha	-2.527	0.000
PA4304	*exeD*	type II/III secretion system protein	-2.517	0.000
PA3850	PA3850	Uncharacterized protein	-2.517	0.000

PA0989	PA0989	Uncharacterized protein	-2.504	0.001
PA3730	PA3730	ubiquinone biosynthesis hydroxylase	-2.499	0.000
PA3188	PA3188	sugar ABC transporter permease	-2.497	0.000
PA1277	*cobQ*	cobyric acid synthase	-2.495	0.004
PA1845	PA1845	Uncharacterized protein	-2.473	0.000
PA2895	PA2895	Uncharacterized protein	-2.461	0.001
PA0735	PA0735	Uncharacterized protein	-2.455	0.000
PA3983	*corC*	magnesium transporter	-2.446	0.000
PA2454	*ubiG*	SAM-dependent methyltransferase	-2.435	0.000
PA4492	*yfaP*	signal peptide protein	-2.433	0.000
PA2239	*rfbU*	biofilm formation protein PslI	-2.400	0.000

PA2541	*ynbA*	CDP-alcohol phosphatidyltransferase	-2.398	0.000
PA5097	*proY*	amino acid permease	-2.396	0.000
PA1798	*rstB*	two-component sensor histidine kinase	-2.388	0.009
PA0730	*phaG*	(R)-3-hydroxydecanoyl-ACP:CoA transacylase	-2.381	0.000
PA4082	*hxuA*	adhesive protein CupB5	-2.367	0.000
PA3679	PA3679	cytochrome P450	-2.363	0.000
PA3212	*mkl*	ABC transporter ATP-binding protein	-2.358	0.000
PA2503	PA2503	SMI1/KNR4 family protein	-2.355	0.000
PA4122	*hpaG*	4-hydroxyphenylacetate degradation bifunctional isomerase/decarboxylase	-2.345	0.000
PA1939	PA1939	ATP-dependent endonuclease	-2.343	0.000

PA1107	SPA0883	FOG: GGDEF domain	-2.339	0.000
PA1069	PA1069	tetratrico peptide repeat family protein	-2.334	0.000
PA5059	PA5059	transcriptional regulator	-2.330	0.000
PA3946	*bvgS*	two-component sensor	-2.327	0.000
PA5441	PA5441	outer membrane assembly lipoprotein YfiO	-2.311	0.000
PA4222	*irtB*	ABC transporter ATP-binding protein	-2.309	0.000
PA2373	PA2373	Rhs element Vgr family protein	-2.304	0.000
PA3930	*cydA*	cyanide insensitive terminal oxidase	-2.265	0.000
PA2237	PA2237	biofilm formation protein PslG	-2.256	0.000
PA4141	PA4141	Uncharacterized protein	-2.242	0.000
PA2628	PA2628	membrane protein	-2.239	0.004

PA2260	PA2260	KguE	-2.215	0.002
PA4332	*ydaM*	GGDEF domain-containing protein	-2.207	0.000
PA2793	PA2793	lipoprotein	-2.204	0.000
PA0338	*ydaM*	GGDEF domain-containing protein	-2.195	0.000
PA1174	*napA*	nitrate reductase catalytic subunit	-2.189	0.000
PA3866	*pys2*	pyocin protein	-2.189	0.000
PA1874	PA1874	Ig-like domain repeat protein	-2.185	0.000
PA0226	*catI*	CoA transferase subunit A	-2.175	0.000
PA1940	PA1940	catalase family protein	-2.162	0.000
PA3105	*xcpQ*	type II secretion system protein GspD	-2.160	0.000
PA0046	PA0046	Uncharacterized protein	-2.160	0.004

PA0095	PA0095	Rhs element Vgr family protein	-2.155	0.000
PA1941	PA1941	cytochrome c family protein	-2.146	0.000
PA5160	*emrB*	MFS transporter	-2.138	0.001
PA5290	*comM*	ATP-dependent protease	-2.138	0.000
PA2782	PA2782	Uncharacterized protein	-2.137	0.000
PA5104	PA5104	histidine utilization protein	-2.133	0.000
PA1897	*sur2*	Sterol desaturase	-2.131	0.000
PA3327	*dhbF*	non-ribosomal peptide synthetase	-2.116	0.000
PA0227	*catJ*	CoA transferase subunit B	-2.103	0.000
PA4229	PA4229	pyochelin biosynthetic protein PchC	-2.089	0.000
PA0064	PA0064	Uncharacterized protein	-2.075	0.000

PA3791	PA3791	Uncharacterized protein	-2.074	0.000
PA4317	PA4317	probable proline and glycine rich transmembrane protein	-2.072	0.000
PA2380	PA2380	Uncharacterized protein	-2.068	0.007
PA1331	*yegH*	TerC family protein	-2.064	0.000
PA0498	PA0498	fimbrial family protein	-2.049	0.000
PA2238	*pimA*	biofilm formation protein PslH	-2.044	0.000
PA3213	PA3213	ABC-type transporter, periplasmic component	-2.039	0.000
PA3190	PA3190	sugar ABC transporter substrate-binding protein	-2.036	0.000
PA0093	*rhsB*	PAAR motif family protein	-2.034	0.000
PA4300	PA4300	type II secretion system protein TadC	-2.027	0.010

PA0994	*fimD*	usher CupC3	-2.007	0.000
PA0534	*puuB*	Oxidoreductase	-2.004	0.000
PA4323	PA4323	DUF58 domain-containing protein	-2.003	0.012
PA1175	*napD*	NapD protein of periplasmic nitrate reductase	-2.002	0.000
PA3919	PA3919	PhoH family protein	-2.001	0.000
PA4224	PA4224	pyochelin biosynthetic protein PchG	-1.989	0.000
PA1472	PA1472	acetyltransferase, GNAT family	-1.988	0.007
PA2234	*amsH*	polysaccharide biosynthesis/export protein	-1.974	0.000
PA3789	PA3789	peptidase	-1.973	0.000
PA3042	PA3042	Uncharacterized protein	-1.959	0.000

PA2564	*tam*	trans-aconitate 2-methyltransferase	-1.959	0.000
PA5362	*yhdP*	CBS domain protein	-1.951	0.000
PA4518	PA4518	glyoxalase	-1.948	0.000
PA4225	*irp2*	pyochelin synthetase	-1.931	0.000
PA3748	*yfjD*	hemolysin	-1.928	0.002
PA3722	PA3722	Uncharacterized protein	-1.926	0.000
PA2441	PA2441	myb-like DNA-binding domain protein	-1.923	0.011
PA4112	*dhkJ*	transcriptional regulator	-1.908	0.000
PA2592	*spuE*	spermidine/putrescine-binding protein	-1.905	0.000
PA2622	*cspD*	cold shock domain protein CspD	-1.903	0.000
PA4218	PA4218	MFS transporter, partial	-1.888	0.000

PA1806	*fabI*	NADH-dependent enoyl-ACP reductase	-1.881	0.000
PA4331	*ndoR*	probable ferredoxin reductase	-1.876	0.000
PA0228	*pcaF*	beta-ketoadipyl CoA thiolase	-1.875	0.000
PA4015	PA4015	(R)-specific enoyl-CoA hydratase	-1.863	0.000
PA2676	*pilC*	type II secretion system protein	-1.862	0.011
PA4034	*aqpZ*	aquaporin Z	-1.855	0.008
PA4230	*pchB*	pchB	-1.838	0.000
PA3929	*cydB*	cyanide insensitive terminal oxidase	-1.835	0.000
PA2326	*dmoA*	5,10-methylene tetrahydromethanopterin reductase	-1.828	0.001

PA2236	PA2236	biofilm formation protein PslF	-1.827	0.000
PA3187	*ugpC*	ABC transporter ATP-binding protein	-1.823	0.000
PA0034	*fimZ*	two-component response regulator	-1.820	0.002
PA0706	*cat*	chloramphenicol acetyltransferase	-1.819	0.000
PA2298	PA2298	oxidoreductase	-1.818	0.000
PA2760	*oprD*	probable outer membrane protein precursor	-1.816	0.000
PA0938	PA0938	chain length determinant family protein	-1.803	0.000
PA2565	PA2565	Uncharacterized protein	-1.798	0.000
PA1173	*napB*	cytochrome C protein NapB	-1.793	0.000
PA2235	PA2235	biofilm formation protein PslE	-1.787	0.000

PA3726	*yaeQ*	yaeQ family protein	-1.785	0.007
PA4226	*irp2*	dihydroaeruginoic acid synthetase	-1.785	0.000
PA4571	*adhB*	cytochrome c	-1.783	0.000
PA4221	*fptA*	Fe(III)-pyochelin outer membrane receptor	-1.779	0.000
PA5169	*siaT*	C4-dicarboxylate transporter	-1.778	0.000
PA1089	PA1089	HAD phosphoserine phosphatase-like hydrolase, family IB	-1.775	0.000
PA2075	PA2075	Chromosome segregation ATPase	-1.774	0.000
PA0855	PA0855	Protein of Uncharacterized function	-1.755	0.000
PA2685	PA2685	type VI secretion protein ImpA	-1.749	0.000

		chromosome segregation		
PA4686	PA4686	ATPase	-1.747	0.000
		glucose-1-phosphate		
PA5163	*rmlA*	thymidylyltransferase	-1.743	0.000
		salicylate biosynthesis		
PA4231	*pchA*	isochorismate synthase	-1.736	0.000
		biofilm formation protein		
PA2231	*wcaJ*	PslA	-1.724	0.000
		dTDP-4-dehydrorhamnose		
PA5164	*rmlC*	3,5-epimerase	-1.723	0.000
		pepSY-associated TM		
PA4219	PA4219	helix family protein	-1.723	0.000
		malto-oligosyltrehalose		
PA2162	*treY*	synthase	-1.719	0.009
		biofilm formation protein		
PA2233	*rfbN*	PslC	-1.719	0.000
		histidine utilization		
PA5105	*hutC*	repressor HutC	-1.716	0.000

PA4532	PA4532	membrane protein	-1.716	0.000
PA1967	PA1967	Uncharacterized protein	-1.708	0.000
PA3982	*ybeY*	metalloprotease	-1.704	0.001
PA2475	*pksS*	cytochrome P450	-1.704	0.000
PA2696	*btr*	transcriptional regulator	-1.693	0.000
PA5280	*xerC*	site-specific tyrosine recombinase XerC	-1.688	0.001
PA1951	PA1951	Fap amyloid fiber secretin	-1.680	0.000
PA1172	*napC*	cytochrome C protein NapC	-1.679	0.000
PA0054	*kptA*	RNA 2'-phosphotransferase-like protein	-1.666	0.010
PA0852	*cbpD*	chitin-binding protein CbpD	-1.651	0.000
PA0546	*metK*	methionine adenosyltransferase	-1.646	0.000

PA2717	*cpo*	chloroperoxidase	-1.636	0.000
PA4296	*algB*	two-component response regulator, PprB	-1.634	0.000
PA2067	PA2067	probable hydrolase	-1.629	0.000
PA2305	*lgrB*	non-ribosomal peptide synthetase	-1.627	0.000
PA4223	*msbA*	ABC transporter ATP-binding protein	-1.616	0.000
PA4305	PA4305	RcpC	-1.606	0.010
PA1104	*fliI*	flagellum-specific ATP synthase	-1.603	0.000
PA5114	PA5104	membrane protein	-1.598	0.000
PA2939	*lap*	aminopeptidase	-1.593	0.000
PA3267	*lplT*	MFS transporter	-1.578	0.000
PA3086	*glpG*	rhomboid family protein	-1.568	0.003
PA0418	PA0418	Uncharacterized protein	-1.566	0.000

PA1086	*flgK*	flagellar hook-associated protein FlgK	-1.561	0.000
PA4442	PA4442	bifunctional sulfate adenylyltransferase subunit 1/adenylylsulfate kinase	-1.561	0.000
PA4580	PA4580	Swarming motility protein YbiA	-1.556	0.000
PA3214	PA3214	ABC transporter	-1.555	0.000
PA0399	*Cbs*	cystathionine beta-synthase	-1.555	0.000
PA2232	*manC*	biofilm formation protein PslB	-1.555	0.000
PA0523	*norC*	nitric oxide reductase subunit C	-1.549	0.007
PA1068	*htpG*	heat-shock protein	-1.547	0.000
PA4297	PA4297	TadG	-1.545	0.002

PA5273	PA5273	Uncharacterized conserved protein	-1.538	0.003
PA1461	*motB*	flagellar motor protein MotD	-1.532	0.000
PA0572	PA0572	peptidase M60-like family protein	-1.529	0.000
PA5168	PA5168	dicarboxylate transporter	-1.526	0.000
PA1837	PA1837	Oxidoreductase probably involved in sulfite reduction	-1.511	0.000
PA0659	*yhaI*	membrane protein	-1.507	0.000
PA3044	*bvgS*	two-component sensor	-1.502	0.000
PA1090	*glmU*	Possible sugar nucleotidyltransferase	-1.497	0.003
PA0429	PA0429	Uncharacterized protein	-1.490	0.000
PA3732	PA3732	Uncharacterized protein	-1.480	0.000
PA4601	PA1727	motility regulator	-1.478	0.000

PA1369	PA1369	Uncharacterized protein	-1.467	0.004
PA5178	*xkdP*	peptidoglycan-binding protein LysM	-1.465	0.001
PA3790	*pfeA*	copper transporter porin	-1.463	0.000
PA0257	PA0257	transposase	-1.463	0.000
PA2364	PA2364	type VI secretion protein	-1.462	0.000
PA3981	*ybeZ*	PhoH-like protein	-1.459	0.000
PA1202	PA1202	hydrolase	-1.453	0.000
PA0179	*cheY*	two-component response regulator	-1.445	0.000
PA4443	*cysD*	sulfate adenylyltransferase subunit 2	-1.443	0.000
PA5053	*hslV*	heat shock protein HslV	-1.441	0.000
PA4684	PA4684	Uncharacterized protein	-1.440	0.013
PA2068	*hcaT*	MFS transporter	-1.438	0.000

PA1799	*rstA*	two-component response regulator ParR	-1.438	0.000
PA0071	PA0071	type VI secretion protein	-1.437	0.000
PA0613	PA0613	Uncharacterized protein	-1.437	0.006
PA5058	*phaC*	poly(3-hydroxyalkanoic acid) synthase	-1.433	0.000
PA2003	PA2003	3-hydroxybutyrate dehydrogenase	-1.420	0.000
PA0820	PA0820	restriction endonuclease	-1.419	0.000
PA4810	*fdoI*	nitrate-inducible formate dehydrogenase, gamma subunit	-1.416	0.000
PA3198	*scpA*	segregation/condensation protein A	-1.404	0.000
PA2160	*glgX*	glycosyl hydrolase	-1.392	0.000
PA2446	*gcvH1*	glycine cleavage system protein H	-1.391	0.002

PA1119	*ompA*	YfiB	-1.390	0.000
PA5025	*cysD*	O-acetylhomoserine aminocarboxypropyltransferase	-1.376	0.000
PA2066	PA2066	Uncharacterized protein	-1.375	0.000
PA2165	*glgA*	glycogen synthase	-1.374	0.000
PA4624	PA4624	surface antigen variable number repeat family protein	-1.371	0.000
PA2291	*oprB*	carbohydrate porin	-1.358	0.001
PA4632	PA4632	peptidase M48	-1.356	0.000
PA2147	*katE*	catalase HPII	-1.354	0.000
PA3189	PA3189	sugar ABC transporter permease	-1.349	0.010
PA2004	*yxjC*	citrate transporter family protein	-1.348	0.000

PA3456	*mnmC*	tRNA 5-methylaminomethyl-2-thiouridine biosynthesis bifunctional protein MnmC	-1.345	0.000
PA4375	PA4375	multidrug efflux protein	-1.344	0.000
PA2450	PA2450	Uncharacterized protein	-1.343	0.000
PA3705	PA3705	CheW domain protein	-1.343	0.008
PA1549	*copA*	heavy metal translocating P-type ATPase	-1.341	0.000
PA2072	PA2072	bifunctional diguanylate cyclase/phosphodiesterase	-1.335	0.000
PA2698	PA2698	hydrolase	-1.328	0.000
PA2608	*tusE*	sulfurtransferase TusE	-1.328	0.010
PA3794	PA3794	Permeases of the major facilitator superfamily	-1.323	0.003
PA1611	*barA*	sensor/response regulator hybrid protein	-1.322	0.001

		flagellar hook protein		
PA1080	*flgE*	FlgE	-1.316	0.000
PA1639	PA1639	Uncharacterized protein	-1.315	0.000
PA4495	PA4495	Uncharacterized protein	-1.314	0.000
PA3041	PA3041	membrane protein	-1.307	0.000
		phosphoglucosamine		
PA4749	*glmM*	mutase	-1.307	0.000
		chemotaxis sensor/effector		
PA3704	*cheA*	fusion protein	-1.301	0.000
PA2047	*yqhC*	transcriptional regulator	-1.289	0.000
PA1597	PA1597	dienelactone hydrolase	-1.280	0.000
PA1130	*rfbF*	rhamnosyltransferase	-1.280	0.000
PA0646	PA0646	phage tail protein	-1.277	0.001
		probable outer membrane		
PA2525	*ttgF*	protein precursor	-1.274	0.002
PA1176	*napF*	ferredoxin protein NapF	-1.273	0.000

PA0851	*ilvA*	serine/threonine dehydratase	-1.271	0.000
PA3460	*cphA*	acetyltransferase	-1.266	0.000
PA4283	*recD*	exodeoxyribonuclease V subunit alpha	-1.259	0.001
PA2573	*tar*	chemotaxis transducer	-1.256	0.000
PA1486	PA1486	D-aminopeptidase	-1.254	0.000
PA5291	*betT*	choline transporter	-1.251	0.000
PA2579	*kynA*	tryptophan 2,3-dioxygenase	-1.249	0.000
PA3326	*clpP2*	ATP-dependent Clp protease proteolytic subunit	-1.247	0.000
PA5495	*thrB*	homoserine kinase	-1.243	0.000
PA1838	*sir1*	sulfite reductase	-1.241	0.000

PA4206	*mdtA*	resistance-nodulation-cell division (RND) efflux membrane fusion protein	-1.234	0.000
PA4465	PA4465	RNase adaptor protein RapZ	-1.227	0.000
PA3311	PA3311	bifunctional diguanylate cyclase/phosphodiesterase	-1.224	0.000
PA0547	PA0547	transcriptional regulator	-1.222	0.000
PA1077	*flgB*	flagellar basal-body rod protein FlgB	-1.221	0.005
PA1249	*aprA*	alkaline metalloproteinase	-1.220	0.000
PA0092	PA0092	Phosphoglycerate dehydrogenase	-1.220	0.004
PA4228	*dhbE*	pyochelin biosynthesis protein PchD	-1.216	0.000
PA4367	PA1727	diguanylate cyclase domain protein	-1.215	0.000
PA5340	PA5340	lipoprotein	-1.215	0.000

PA0180	*mpcT*	trichloroethylene chemotactic transducer CttP	-1.208	0.000
PA1254	*dapA1*	dihydrodipicolinate synthetase	-1.198	0.000
PA1085	*flgJ*	peptidoglycan hydrolase FlgJ	-1.193	0.000
PA0431	*spoT*	HD domain protein	-1.193	0.000
PA0927	*ddh*	D-lactate dehydrogenase	-1.193	0.000
PA1088	PA1088	methyltransferase domain protein	-1.191	0.000
PA3940	PA3940	DNA binding protein	-1.186	0.000
PA1766	PA1766	alpha-L-glutamate ligase	-1.183	0.000
PA5338	*spoT*	guanosine-3',5'-bis(diphosphate) 3'-pyrophosphohydrolase	-1.183	0.000
PA4238	*rpoA*	DNA-directed RNA polymerase subunit alpha	-1.161	0.000

PA3920	*copA*	copper-translocating P-type ATPase	-1.160	0.000
PA3483	PA3483	UDP-N-acetylglucosamine enolpyruvyl transferase	-1.159	0.004
PA5272	*cyaA*	adenylate cyclase	-1.158	0.000
PA1865	*fan1*	Fanconi-associated nuclease	-1.150	0.000
PA3943	PA3943	nitroreductase family protein	-1.147	0.002
PA5258	PA5258	heme biosynthesis operon protein HemX	-1.145	0.000
PA5065	*ubiB*	ubiquinone biosynthetic protein UbiB	-1.141	0.000
PA2755	*eco*	ecotin	-1.140	0.000
PA0081	PA0081	phosphopeptide-binding protein	-1.139	0.002
PA0998	*fabH*	beta-keto-ACP synthase	-1.117	0.000

PA1137	PA1137	oxidoreductase	-1.111	0.002
PA0290	PA2817	GGDEF domain-containing protein	-1.111	0.000
PA2289	*yncD*	tonB dependent receptor family protein	-1.109	0.007
PA0400	*metC*	cystathionine gamma-lyase	-1.109	0.000
PA4142	*mchE*	secretion protein	-1.107	0.003
PA4322	*moxR*	AAA family ATPase	-1.107	0.001
PA4387	*ytzA*	phage exclusion suppressor FxsA	-1.106	0.000
PA0746	PA0746	acyl-CoA dehydrogenase	-1.106	0.000
PA5210	*xcpR*	secretion pathway ATPase	-1.105	0.000
PA4124	*hpcB*	3,4-dihydroxyphenylacetate 2,3-dioxygenase	-1.104	0.000
PA0360	*podJ*	Sel1 repeat protein	-1.104	0.000

PA0575	PA1727	bifunctional diguanylate cyclase/phosphodiesterase	-1.102	0.000
PA0288	*gpuA*	guanidinopropionase	-1.100	0.008
PA3003	PA3003	Peptidoglycan-binding protein, CsiV	-1.096	0.003
PA4811	*fdoH*	nitrate-inducible formate dehydrogenase subunit beta	-1.093	0.000
PA4216	*phzD*	pyridoxamine 5'-phosphate oxidase	-1.090	0.000
PA5446	PA5446	DUF1127 domain-containing protein	-1.078	0.003
PA3706	*wspC*	biofilm formation methyltransferase WspC	-1.075	0.001
PA2815	*fadE*	acyl-CoA dehydrogenase	-1.069	0.000
PA4205	PA4205	DoxX family protein	-1.065	0.000
PA0736	PA0736	membrane protein	-1.064	0.000

PA4258	*rplV*	50S ribosomal protein L22	-1.059	0.005
PA4091	*hpaB*	4-hydroxyphenylacetate 3-monooxygenase	-1.055	0.000
PA3186	*oprB*	porin B	-1.050	0.000
PA5257	PA5257	heme biosynthesis protein HemY	-1.047	0.000
PA1123	PA1123	Uncharacterized protein	-1.045	0.000
PA2896	*rpoE*	RNA polymerase sigma factor	-1.044	0.006
PA1927	*metE*	5-methyltetrahydropteroyltriglutamate--homocysteine methyltransferase	-1.044	0.012
PA1842	PA1842	Uncharacterized protein	-1.041	0.012
PA3205	PA3205	LTXXQ domain protein	-1.040	0.001
PA3317	PA3317	membrane protein	-1.038	0.001

PA1218	PA1218	phytanoyl-CoA dioxygenase family protein	-1.030	0.003
PA1215	*sauT*	AMP-binding protein	-1.027	0.008
PA2973	*nhaA*	peptidase	-1.025	0.003
PA0430	*metF*	methylenetetrahydrofolate reductase [NAD(P)H]	-1.025	0.000
PA5159	*emrA*	multidrug resistance protein	-1.017	0.008
PA5158	*mdtP*	probable outer membrane protein precursor	-1.008	0.002
PA2609	*trpD*	Anthranilate phosphoribosyltransferase like protein	-1.007	0.000
PA0788	PA0788	glycosyl transferase family 51	-1.003	0.000
PA1705	*lcrG*	type III secretion regulator	16.098	0.000
PA1711	PA1711	ExsE	14.690	0.000

PA2146	*ymdF*	Conidiation-specific protein 10	13.685	0.002
PA1717	*yscD*	type III export protein PscD	12.933	0.000
PA1718	*pscE*	type III export protein PscE	12.564	0.001
PA4637	PA4637	lipoprotein	11.110	0.012
Upregulated genes				
PA1971	*braZ*	branched-chain amino acid transport system 3 carrier protein	9.512	0.005
PA1707	*lcrH*	CesD/SycD/LcrH family type III secretion system chaperone	8.140	0.000
PA4826	PA4826	Uncharacterized protein	7.648	0.000
PA1708	*yopB*	translocator protein PopB	7.299	0.000
PA1709	*yopD*	translocator outer membrane protein PopD	7.222	0.000

PA4824	PA4824	Uncharacterized protein	7.149	0.000
PA4825	*mgtB*	magnesium-translocating P-type ATPase	6.946	0.000
PA1706	*lcrV*	type III secretion protein PcrV	6.940	0.000
PA1712	*exsB*	exoenzyme S synthesis protein ExsB	6.743	0.000
PA4822	*yjbB*	na+/Pi-cotransporter family protein	6.667	0.000
PA1698	*yopN*	type III secretion outer membrane protein PopN	6.150	0.000
PA4823	PA4823	Uncharacterized protein	6.073	0.000
PA3842	*yerA*	chaperone	5.975	0.000
PA1298	*rcnR*	Transcriptional repressor RcnR	5.969	0.000
PA2191	*cya*	adenylate cyclase	5.819	0.000

PA1694	*yscQ*	type III secretion system protein	5.804	0.000
PA1696	*yscO*	translocation protein in type III secretion	5.501	0.001
PA1719	*pscF*	type III export protein PscF	5.294	0.000
PA1974	PA1974	membrane protein	5.224	0.001
PA0044	*aexT*	exoenzyme T	5.126	0.000
PA1697	*yscN*	EscN/YscN/HrcN family type III secretion system ATPase	5.117	0.000
PA1699	*tyeA*	Pcr1	4.953	0.000
PA4364	PA4364	ACT domain protein	4.895	0.000
PA1715	*yscB*	type III export apparatus protein	4.875	0.000
PA4582	PA4582	SPFH domain / Band 7 family protein	4.829	0.000

PA2862	*lip*	lactonizing lipase	4.821	0.000
PA1714	PA1714	ExsD	4.794	0.000
PA3841-exos	*aexT*	exoenzyme S	4.746	0.000
PA0753	PA0753	tripartite tricarboxylate transporter TctB family protein	4.668	0.001
PA1710	*exsC*	exoenzyme S synthesis protein ExsC	4.631	0.000
PA2868	PA2868	terminase	4.518	0.001
PA1713	*exsA*	exoenzyme S transcriptional regulator ExsA	4.496	0.000
PA2913	*btuF*	iron ABC transporter substrate-binding protein	4.445	0.003
PA4677	PA4677	acyl-coenzyme A:6-aminopenicillanic acid	4.303	0.000

		acyl-transferase family protein		
PA3358	*yvbV*	EamA family transporter	4.302	0.012
PA4365	*argO*	transporter	4.285	0.000
PA1019	*mucK*	cis,cis-muconate transporter MucK	4.248	0.001
PA1983	*qgdA*	cytochrome c-550 PedF	4.181	0.013
PA0125	PA0125	Ribbon-helix-helix protein, CopG family	4.138	0.001
PA2863	*lifO*	lipase chaperone, partial	4.118	0.000
PA4789	PA4789	pyrophosphatase	4.085	0.007
PA3396	PA3396	acessory protein NosL	4.022	0.008
PA1428	*yjaB*	GNAT family N-acetyltransferase	3.934	0.005
PA1700	*sycN*	type III secretion chaperone SycN	3.886	0.001
PA3912	*yhbV*	U32 family peptidase	3.875	0.001

PA2689	*besA*	esterase	3.704	0.013
PA4599	*acrA*	resistance-nodulation-cell division (RND) multidrug efflux membrane fusion protein MexC	3.700	0.000
PA0734	PA0734	cysteine-rich CWC family protein	3.639	0.000
PA3518	PA3518	iron-containing redox enzyme family protein	3.613	0.001
PA2027	PA2027	Uncharacterized protein	3.595	0.000
PA0758	PA0758	HDOD domain protein	3.557	0.000
PA3038	*nicP*	porin	3.549	0.000
PA1721	*yscH*	type III export protein PscH	3.369	0.003
PA0843	*plcR*	phospholipase C accessory protein PlcR	3.349	0.011
PA4550	*epsG*	type 4 fimbrial biogenesis protein FimU	3.272	0.000

PA0111	PA0111	probable transmembrane protein	3.265	0.000
PA4181	PA4181	B3/4 domain protein	3.250	0.000
PA3578	PA3578	isomerase	3.231	0.000
PA0240	*galP*	porin	3.229	0.008
PA4635	*mgtC*	Mg(2+) transport ATPase protein C	3.206	0.000
PA0913	*mgtE*	Mg transporter MgtE	3.195	0.000
PA5440	*yegQ*	peptidase	3.189	0.000
PA0476	*pucI*	permease	3.170	0.000
PA5315	*rpmG*	50S ribosomal protein L33	3.144	0.009
PA4552	PA4552	type 4 fimbrial biogenesis protein PilW	3.109	0.000
PA2429	PA2429	Uncharacterized protein	3.104	0.006
PA3390	*lsrG*	antibiotic biosynthesis monooxygenase	3.103	0.012

PA5137	PA5137	amino acid ABC transporter substrate-binding protein	3.009	0.000
PA3781	*siaT*	transporter	2.956	0.013
PA4551	PA4551	type 4 fimbrial biogenesis protein PilV	2.950	0.000
PA5388	*gbuC*	glycine/betaine ABC transporter substrate-binding protein	2.944	0.000
PA3519	PA3519	Pyrroloquinoline quinone (Coenzyme PQQ) biosynthesis protein C	2.939	0.006
PA0733	*rsuA*	ribosomal small subunit pseudouridine synthase A	2.919	0.005
PA0931	*pfeA*	TonB-dependent siderophore receptor	2.917	0.000
PA0110	PA0110	SURF1 family protein	2.894	0.001
PA1146	*dhaT*	amino acid permease	2.890	0.009

PA0144	PA0144	nucleoside 2-deoxyribosyltransferase family protein	2.873	0.010
PA0755	*nicP*	cis-aconitate porin OpdH	2.873	0.006
PA5387	*kce*	carnitine dehydrogenase	2.861	0.002
PA0834	*yihG*	acyltransferase	2.858	0.004
PA4882	*yedY*	oxidoreductase molybdopterin binding domain protein	2.855	0.005
PA0112	*ctaA*	cytochrome B561	2.848	0.002
PA0241	*exuT*	major facilitator superfamily transporter	2.753	0.013
PA1946	*rbsB*	ribose ABC transporter substrate-binding protein	2.727	0.000
PA4209	*sfmM3*	phenazine-specific methyltransferase	2.717	0.000
PA4168	*fpvA*	second ferric pyoverdine receptor FpvB	2.701	0.000

PA2322	*gnuT*	gluconate permease	2.700	0.003
PA0165	*ompK*	membrane protein	2.658	0.006
PA1716	*yscC*	Type III secretion outer membrane protein	2.630	0.000
PA1501	*hyi*	hydroxypyruvate isomerase	2.627	0.000
PA5545	PA5545	C4-dicarboxylate ABC transporter	2.626	0.000
PA4553	PA4553	type 4 fimbrial biogenesis protein PilX	2.615	0.000
PA5462	PA5462	Holliday junction resolvase	2.613	0.001
PA3514	PA3514	ABC transporter ATP-binding protein	2.609	0.009
PA1190	*yohC*	Uncharacterized protein	2.600	0.000
PA4158	*fepC*	ferric enterobactin transporter FepC	2.580	0.013

PA1695	*yscP*	type III secretion system needle length determinant	2.571	0.002
PA3410	*fecI*	DNA-directed RNA polymerase sigma-70 factor	2.549	0.013
PA3913	*yhbU*	protease	2.546	0.010
PA1852	PA1852	Uncharacterized protein	2.546	0.000
PA1502	*gcl*	glyoxylate carboligase	2.543	0.000
PA0105	*ctaC*	cytochrome C oxidase subunit II	2.507	0.000
PA2127	*ybdN*	phosphoadenosine phosphosulfate reductase	2.464	0.000
PA5081	PA5081	pyrophosphatase	2.464	0.013
PA4731	*panD*	aspartate 1-decarboxylase	2.427	0.008
PA0153	*pcaH*	protocatechuate 3,4-dioxygenase subunit beta	2.410	0.000

PA4554	*pilY1*	type IV pilus biogenesis factor PilY1	2.410	0.000
PA4710	*hpuB*	heme/hemoglobin uptake outer membrane receptor PhuR	2.402	0.000
PA4182	*paiB*	transcriptional regulator	2.373	0.000
PA0478	PA0478	acetyltransferase, GNAT family	2.360	0.000
PA2126	*ybdM*	transcriptional regulator	2.356	0.007
PA4055	*ribE*	riboflavin synthase subunit alpha	2.340	0.000
PA2704	*oruR*	transcriptional regulator	2.336	0.006
PA1947	*rbsA3*	ribose transporter RbsA	2.334	0.000
PA1507	*uacT*	transporter	2.322	0.008
PA0887	*acsA1*	acetyl-CoA synthetase	2.316	0.000
PA1016	PA1016	thiolase	2.312	0.008

PA3925	*thlA*	acyl-CoA thiolase	2.295	0.000
PA1607	PA1607	HxlR family transcriptional regulator	2.293	0.000
PA3888	*osmY*	ABC transporter permease	2.289	0.009
PA4290	*dcrA*	chemotaxis transducer	2.283	0.000
PA4584	*ycgL*	nucleotidyltransferase	2.246	0.000
PA3584	*glpD*	glycerol-3-phosphate dehydrogenase	2.239	0.000
PA3233	PA3233	cyclic nucleotide-binding domain protein	2.214	0.013
PA4709	*hmuS*	hemin degrading factor	2.211	0.000
PA4567	*rpmA*	50S ribosomal protein L27	2.208	0.000
PA4198	PA4198	acyl-CoA synthetase	2.206	0.000
PA5543	PA5543	Uncharacterized protein	2.182	0.000
PA1592	PA1592	lipoprotein	2.179	0.000

PA2190	*gsiB*	glucose starvation-inducible protein B	2.157	0.000
PA0754	*yflP*	C4-dicarboxylate ABC transporter substrate-binding protein	2.131	0.000
PA5209	*ygiF*	CYTH domain-containing protein	2.111	0.000
PA3927	*yeaM*	transcriptional regulator	2.106	0.003
PA5233	PA5233	flagellar basal body-associated protein FliL	2.102	0.000
PA3890	*osmW*	ABC transporter permease	2.094	0.000
PA4134	PA4134	cytochrome Cbb oxidase CcoQ	2.092	0.008
PA4054	*ribB*	bifunctional 3,4-dihydroxy-2-butanone 4-phosphate synthase/GTP cyclohydrolase II-like protein	2.092	0.000

PA5372	*betA*	choline dehydrogenase	2.070	0.000
PA0833	*yiaD*	Outer membrane protein	2.069	0.000
PA0108	*ctaE*	cytochrome c oxidase, subunit III	2.061	0.000
PA0106	*ctaD*	cytochrome C oxidase subunit I	2.060	0.000
PA0301	*spuE*	spermidine ABC transporter substrate-binding protein SpuE	2.041	0.000
PA4341	*yagI*	transcriptional regulator	2.036	0.000
PA3891	*osmV*	ABC transporter ATP-binding protein	2.028	0.000
PA2426	PA2426	extracytoplasmic-function sigma-70 factor	2.023	0.000
PA3889	*osmX*	ABC transporter	2.019	0.000
PA0752	PA0752	tripartite tricarboxylate transporter TctA family protein	2.016	0.000

		Fe(III) dicitrate transporter		
PA3901	*fecA*	FecA	2.006	0.000
PA1500	*glxR*	oxidoreductase	2.000	0.000
PA4377	PA4377	Uncharacterized protein	1.978	0.000
PA3779	*yiaO*	bacterial extracellular solute-binding, 7 family protein	1.944	0.000
PA4170	*ahpF*	thioredoxin reductase	1.934	0.000
PA0107	*ctaG*	cytochrome C oxidase assembly protein	1.921	0.000
PA1835	PA1835	phenylacetic acid degradation protein	1.919	0.000
PA0756	*tctD*	two-component response regulator	1.913	0.000
PA3672	*nodI*	ABC transporter ATP-binding protein	1.904	0.000

PA2747	PA2747	MULTISPECIES: DUF3509 domain-containing protein	1.895	0.000
PA4556	*pilE*	type 4 fimbrial biogenesis protein PilE	1.893	0.000
PA1830	PA1830	SCP-2 sterol transfer family protein	1.893	0.000
PA5274	*rnk*	nucleoside diphosphate kinase regulator	1.887	0.001
PA4396	*cheY*	response regulator	1.883	0.000
PA1723	*yscJ*	type III export protein PscJ	1.881	0.003
PA4963	PA4963	lipoprotein	1.877	0.000
PA5348	*hupA*	DNA-binding protein	1.877	0.002
PA5116	*soxR*	transcriptional regulator	1.851	0.007
PA5076	*fliY*	ABC transporter	1.850	0.000
PA4979	*acdA*	acyl-CoA dehydrogenase	1.849	0.000

PA3581	*glpF*	glycerol uptake facilitator protein	1.838	0.009
PA1432	*lasI*	acyl-homoserine-lactone synthase	1.832	0.000
PA1571	PA1571	Uncharacterized protein	1.825	0.000
PA2417	*yafC*	transcriptional regulator	1.825	0.000
PA4785	*fadI*	acetyl-CoA acetyltransferase	1.825	0.000
PA2433	PA2433	tmRNA	1.817	0.000
PA4325	PA4325	DUF4124 domain-containing protein	1.815	0.000
PA5491	PA5491	cytochrome C-type protein	1.803	0.000
PA2821	PA2821	glutathione S-transferase	1.791	0.000
PA4427	*sspB*	stringent starvation protein B	1.791	0.000
PA3509	*mhpC2*	hydrolase	1.790	0.001

PA2633	PA2633	secretin	1.790	0.000
PA2134	PA2134	membrane protein	1.789	0.001
PA0937	*yaiL*	Nucleoprotein/polynucleotide-associated enzyme	1.788	0.010
PA0797	*ydhC*	transcriptional regulator	1.780	0.000
PA3530	PA3530	(2Fe-2S)-binding protein	1.773	0.001
PA4573	PA4573	cation transporter	1.772	0.013
PA4676	*can*	carbonic anhydrase	1.770	0.000
PA0113	*cyoE1*	protoheme IX farnesyltransferase	1.756	0.000
PA2877	*yhjC*	transcriptional regulator	1.749	0.000
PA4337	PA4337	Uncharacterized protein	1.735	0.002
PA4626	*hprA*	glycerate dehydrogenase	1.731	0.000
PA0409	*pilH*	twitching motility protein PilH	1.730	0.000

PA5138	PA5138	amino acid ABC transporter substrate-binding protein	1.722	0.000
PA0740	PA0740	SDS hydrolase SdsA1	1.717	0.001
PA3234	*actP*	acetate permease	1.716	0.000
PA1998	*ybhD*	transcriptional regulator DhcR	1.714	0.000
PA5502	PA5502	lipoprotein	1.702	0.000
PA4784	*lrpC*	transcriptional regulator	1.700	0.000
PA3819	*ycfJ*	glycine zipper 2TM domain protein	1.695	0.000
PA2660	PA2660	alpha/beta superfamily hydrolase	1.689	0.000
PA1336	*dctB*	two-component sensor	1.684	0.000
PA4500	*dppA*	ABC transporter	1.683	0.000
PA4978	PA4978	acyl-CoA synthetase	1.681	0.000

PA4611	PA4611	GTP-binding protein	1.680	0.000
PA4555	PA4555	type 4 fimbrial biogenesis protein PilY2	1.675	0.000
PA4468	*sodA*	superoxide dismutase	1.666	0.000
PA2691	PA2691	NADH dehydrogenase	1.665	0.000
PA2481	*tsdA*	Cytochrome c family protein	1.662	0.000
PA0954	*acyP*	acylphosphatase	1.658	0.013
PA3116	*usg*	aspartate-semialdehyde dehydrogenase	1.651	0.001
PA0782	*putA*	bifunctional proline dehydrogenase/pyrroline-5-carboxylate dehydrogenase	1.636	0.000
PA0359	PA0359	Cation/multidrug efflux pump	1.635	0.000
PA2744	*thrS*	threonine--tRNA ligase	1.634	0.000

PA4469	PA4469	FOG: TPR repeat	1.633	0.000
PA0206	*potA1*	spermidine/putrescine ABC transporter ATP-binding protein	1.627	0.008
PA0672	PA0672	heme oxygenase	1.626	0.000
PA4977	*aruI*	2-ketoarginine decarboxylase, AruI	1.625	0.000
PA0500	*bioB*	biotin synthase	1.622	0.000
PA5542	*nylB*	beta-lactamase family protein	1.604	0.000
PA1017	PA1017	pimeloyl-CoA synthetase	1.601	0.003
PA1519	*adeP*	transporter	1.600	0.011
PA4010	*Mpg*	3-methyladenine DNA glycosylase	1.598	0.000
PA4421	*mraZ*	cell division protein MraZ	1.595	0.000
PA2033	*viuB*	siderophore-interacting protein	1.594	0.000

PA5544	PA5544	C4-dicarboxylate ABC transporter	1.590	0.000
PA1025	*nicP*	porin	1.589	0.005
PA0982	*nhaA1*	DSBA-like thioredoxin domain protein	1.586	0.008
PA0763	*mucA*	sigma factor AlgU negative regulator MucA	1.583	0.000
PA4738	PA4738	Protein yjbJ	1.582	0.001
PA5528	PA5528	membrane protein	1.580	0.000
PA0302	*potG*	polyamine transporter PotG	1.576	0.000
PA3550	*algF*	alginate o-acetyltransferase AlgF	1.572	0.000
PA2708	PA2708	protein involved in outer membrane biogenesis	1.568	0.005
PA5442	PA3311	GGDEF domain-containing protein	1.566	0.000

PA0983	PA0983	transposase family protein	1.566	0.013
PA1832	*sohB*	protease	1.563	0.000
PA5518	*ybaL*	potassium efflux transporter	1.549	0.000
PA4523	PA4523	thymidine phosphorylase	1.543	0.000
PA1141	*lrhA*	transcriptional regulator	1.535	0.002
PA4846	*aroQ1*	3-dehydroquinate dehydratase	1.535	0.000
PA4674	*vapI*	HigA family addiction module antidote protein	1.532	0.000
PA0391	PA0391	50S ribosome binding GTPase family protein	1.529	0.000
PA2968	*fabD*	malonyl CoA-ACP transacylase	1.517	0.000
PA4496	*dppA*	ABC transporter	1.517	0.000
PA5464	PA5464	Uncharacterized protein	1.514	0.007

PA4904	*vanA*	Vanillate O-demethylase oxygenase subunit	1.511	0.003
PA4075	PA4075	methyltransferase domain protein	1.504	0.000
PA4356	*nemA*	xenobiotic reductase	1.489	0.001
PA0737	PA0737	Uncharacterized protein	1.484	0.000
PA2551	*nagR*	LysR substrate binding domain protein	1.482	0.000
PA1035	PA1035	late embryogenesis abundant family protein	1.479	0.000
PA4729	*panB2*	3-methyl-2-oxobutanoate hydroxymethyltransferase	1.475	0.000
PA2561	*ctpH*	methyl-accepting chemotaxis protein CtpH	1.474	0.004
PA0200	PA0200	DUF3079 domain-containing protein	1.470	0.008
PA3876	*narK*	nitrite extrusion protein 2	1.461	0.013

PA3079	*ydfJ*	patched family protein	1.456	0.000
PA2182	PA2182	hypothetical protein	1.454	0.002
PA0203	*spuE*	ABC transporter	1.454	0.000
PA1373	*fabF*	beta-ketoacyl-[acyl-carrier-protein] synthase II	1.453	0.000
PA0899	*astB*	N-succinylglutamate 5-semialdehyde dehydrogenase	1.451	0.000
PA3766	*tyrP*	aromatic amino acid transporter	1.446	0.001
PA2776	*puuB*	gamma-glutamylputrescine oxidoreductase	1.446	0.000
PA5229	PA5229	EVE domain-containing protein	1.445	0.000
PA1157	*ompR*	two-component response regulator	1.443	0.000

PA0898	*astD*	N-succinylglutamate 5-semialdehyde dehydrogenase	1.441	0.000
PA1542	PA1542	metal-dependent hydrolase	1.434	0.000
PA0208	*madA*	malonate decarboxylase subunit alpha	1.432	0.000
PA4481	*mreB*	rod shape-determining protein MreB	1.432	0.000
PA0357	*mutM*	formamidopyrimidine-DNA glycosylase	1.428	0.000
PA1414	PA1414	Uncharacterized protein	1.425	0.001
PA3015	PA3015	ATP synthase subunit beta	1.421	0.000
PA4831	PA4831	transcriptional regulator	1.418	0.007
PA4708	*hmuT*	heme-transporter PhuT	1.414	0.000
PA5196	*rimK*	ATP-dependent zinc protease family protein	1.413	0.007

PA0351	PA0351	metallophosphatase family protein	1.410	0.005
PA1309	*cysL*	probable transcriptional regulator	1.407	0.001
PA0884	*dctP*	C4-dicarboxylate-binding protein	1.406	0.002
PA3427	PA3427	short-chain dehydrogenase	1.405	0.004
PA3479	*rhlA*	rhamnosyltransferase 1 subunit A	1.405	0.000
PA3125	PA3125	GDSL-like Lipase/Acylhydrolase family protein	1.400	0.003
PA3081	PA3922	outer membrane lipoprotein-sorting protein	1.398	0.000
PA4199	*mmgC*	acyl-CoA dehydrogenase	1.397	0.000
PA4675	*iutA*	TonB-dependent receptor	1.397	0.000
PA3684	PA3684	Uncharacterized protein	1.394	0.006

PA3923	PA3923	adhesin	1.389	0.000
PA4524	*nadC*	nicotinate-nucleotide pyrophosphorylase	1.389	0.000
PA5523	*hemL*	aminotransferase	1.387	0.000
PA3698	PA3698	lipoprotein	1.379	0.000
PA4581	*rtcR*	transcriptional regulator RtcR	1.375	0.003
PA2817	PA2817	dehydrogenase	1.374	0.000
PA2020	*ttgR*	transcriptional regulator	1.374	0.000
PA0155	*pcaR*	transcriptional regulator PcaR	1.373	0.000
PA5039	*aroK*	shikimate kinase	1.373	0.001
PA3899	*fecI*	RNA polymerase sigma factor	1.370	0.000
PA4995	*Acads*	acyl-CoA dehydrogenase	1.370	0.004
PA0055	PA0055	Uncharacterized protein	1.367	0.000

PA3875	*narG*	respiratory nitrate reductase subunit alpha	1.363	0.000
PA3604	*agmR*	response regulator ErdR	1.362	0.006
PA0217	*mauR*	transcriptional regulator	1.354	0.010
PA1674	*folE2*	GTP cyclohydrolase I	1.354	0.000
PA3872	*narV*	respiratory nitrate reductase subunit gamma	1.353	0.012
PA2746	PA2746	putative membrane protein	1.353	0.001
PA1051	PA1051	transporter	1.351	0.000
PA3220	*exsA*	transcriptional regulator	1.347	0.000
PA4428	*sspA*	stringent starvation protein A	1.343	0.000
PA3682	*Dml*	2-methylisocitrate lyase	1.342	0.006
PA4286	*lipL*	lipoate--protein ligase	1.342	0.002
PA1375	*pdxB*	erythronate-4-phosphate dehydrogenase	1.339	0.001

PA4786	*fabG*	3-oxoacyl-ACP reductase	1.338	0.000
PA4912	*livH*	branched-chain amino acid ABC transporter	1.337	0.002
PA3270	PA3270	N-acetyltransferase	1.336	0.000
PA4277	*tufA*	translation elongation factor Tu	1.336	0.000
PA1580	*gltA*	citrate synthase	1.335	0.000
PA3516	*purB*	adenylosuccinate lyase	1.335	0.004
PA3031	*ygdR*	lipoprotein	1.332	0.000
PA3009	PA3009	ABC transporter ATP-binding protein	1.331	0.002
PA2816	PA2816	Uncharacterized protein	1.330	0.000
PA4090	PA4090	cytochrome b561	1.329	0.000
PA5554	*atpD*	ATP synthase subunit beta	1.327	0.000
PA3582	*glpK2*	glycerol kinase	1.324	0.000

PA4309	*pctA*	methyl-accepting chemotaxis protein PctA	1.318	0.000
PA0376	*rpoH*	RNA polymerase sigma factor RpoH	1.315	0.000
PA0355	*pfpI*	protease PfpI	1.313	0.005
PA1263	PA1263	transcriptional regulator	1.308	0.000
PA5320	*coaBC*	bifunctional phosphopantothenoylcysteine decarboxylase/phosphopantothenate synthase	1.306	0.000
PA0882	PA0882	predicted acyl-CoA transferases/carnitine dehydratase	1.306	0.008
PA1041	*oprF*	probable outer membrane protein precursor	1.303	0.000
PA3880	PA3880	zinc-binding protein	1.301	0.004
PA0060	PA0060	protein YnfD	1.299	0.002

PA2860	PA2816	Uncharacterized protein	1.291	0.004
PA4585	*rtcA*	RNA 3'-terminal-phosphate cyclase	1.290	0.000
PA0762	*algU*	RNA polymerase sigma factor AlgU	1.290	0.000
PA5558	*atpF*	ATP synthase subunit B	1.286	0.000
PA2883	PA2883	Protein of Uncharacterized function	1.286	0.006
PA5309	*puuB*	oxidoreductase	1.285	0.000
PA4635a	PA4635a	Uncharacterized protein	1.282	0.009
PA2002	*atoE*	Short chain fatty acid transporter	1.281	0.003
PA5560	*atpB*	ATP synthase subunit A	1.280	0.000
PA4994	*bcd*	acyl-CoA dehydrogenase	1.280	0.000
PA3881	PA3881	multidrug transporter	1.279	0.010
PA5300	PA5300	cytochrome c5	1.279	0.000

PA2482	*tsdB*	cytochrome C	1.277	0.002
PA5275	*cyaY*	iron donor protein CyaY	1.277	0.003
PA3048	*rlmL*	ribosomal RNA large subunit methyltransferase K/L	1.276	0.000
PA3896	*ghrB*	2-hydroxyacid dehydrogenase	1.274	0.004
PA2471	*nagK*	5-carboxymethyl-2-hydroxymuconate isomerase	1.274	0.007
PA4798	PA4798	Uncharacterized protein	1.270	0.000
PA1920	*nrdD*	anaerobic ribonucleoside triphosphate reductase	1.269	0.005
PA0154	*pcaG*	protocatechuate 3,4-dioxygenase subunit alpha	1.268	0.000
PA5427	*adhA*	Alcohol dehydrogenase	1.265	0.000

PA4911	*braE*	branched-chain amino acid ABC transporter permease	1.263	0.011
PA1297	*czcD*	metal transporter	1.262	0.013
PA4827	*nat*	arylamine N-acetyltransferase	1.261	0.008
PA5555	*atpG*	ATP synthase subunit gamma	1.255	0.000
PA1158	*rstB*	two-component sensor	1.255	0.007
PA3874	*narY*	respiratory nitrate reductase subunit beta	1.254	0.000
PA1562	*acnA*	aconitate hydratase	1.252	0.000
PA3798	*ybdL*	aminotransferase	1.248	0.000
PA1337	*ansB*	glutaminase-asparaginase	1.248	0.000
PA4983	*aruR*	DNA-binding response regulator	1.246	0.000

PA0599	PA0599	hydrolase or acyltransferase	1.245	0.000
PA2550	PA2550	acyl-CoA dehydrogenase	1.239	0.006
PA0508	*mmgC*	acyl-CoA dehydrogenase	1.239	0.000
PA3421	PA3922	outer membrane lipoprotein-sorting protein	1.234	0.011
PA3551	*algA*	mannose-1-phosphate guanylyltransferase/mannose-6-phosphate isomerase	1.231	0.000
PA5430	*yedE*	sulfur transport family protein	1.230	0.001
PA2634	PA2634	isocitrate lyase	1.230	0.000
PA0953	*resA*	thioredoxin	1.228	0.000
PA4515	*piuC*	PKHD-type hydroxylase piuC	1.221	0.000
PA0196	*pntB*	pyridine nucleotide transhydrogenase subunit beta	1.212	0.001

PA3046	*yggL*	YggL protein	1.212	0.003
PA0209	*mdcB*	triphosphoribosyl-dephospho-CoA synthase	1.209	0.000
PA1773	*zntB*	transporter	1.209	0.000
PA2009	*hmgA*	homogentisate 1,2-dioxygenase	1.208	0.000
PA3321	*nahR*	transcriptional regulator	1.208	0.002
PA0865	*hpd*	4-hydroxyphenylpyruvate dioxygenase	1.206	0.000
PA3724	*lasB*	elastase LasB	1.202	0.000
PA0550	*hyi*	hydroxypyruvate isomerase	1.200	0.004
PA3712	*yebE*	protein YebE	1.200	0.000
PA2624	*icd*	isocitrate dehydrogenase, NADP-dependent	1.199	0.000
PA3529	*tsaA*	peroxidase	1.197	0.000

PA0506	*mmgC*	acyl-CoA dehydrogenase	1.191	0.000
PA4739	*osmY*	Osmotically inducible protein Y precursor	1.191	0.000
PA3299	*fadD*	long-chain-fatty-acid--CoA ligase	1.189	0.000
PA3236	*gbuC*	glycine betaine-binding protein	1.184	0.000
PA3027	*oruR*	transcriptional regulator	1.183	0.000
PA4344	*hipO*	hydrolase	1.183	0.003
PA5051	*argS*	arginine--tRNA ligase	1.180	0.000
PA2030	PA2030	Uncharacterized protein	1.179	0.000
PA3508	*pcaR*	transcriptional regulator	1.177	0.011
PA4200	*ytnP*	beta-lactamase	1.173	0.004
PA2813	*gstB*	glutathione S-transferase	1.172	0.000
PA4930	*alr*	alanine racemase biosynthetic	1.172	0.003

PA5556	*atpA*	ATP synthase subunit alpha	1.171	0.000
PA2273	*soxR*	redox-sensitive transcriptional activator SoxR	1.169	0.002
PA5122	PA5122	Uncharacterized protein	1.168	0.001
PA2402	*lgrC*	non-ribosomal peptide synthetase	1.162	0.000
PA1563	*rlmM*	ribosomal RNA large subunit methyltransferase M	1.159	0.003
PA5380	*cdhR*	protein GbdR	1.159	0.000
PA1570	*cmpR*	transcriptional regulator	1.157	0.000
PA1948	*rbsC*	ABC transporter permease	1.157	0.000
PA5421	*fdhA*	glutathione-independent formaldehyde dehydrogenase	1.155	0.000
PA0766	PA0766	serine protease MucD	1.153	0.000

PA1538	PA1538	Baeyer-Villiger monooxygenase	1.153	0.000
PA5557	*atpH*	ATP synthase subunit delta	1.152	0.000
PA0943	PA0943	dehydrogenase	1.150	0.000
PA1033	*yfcG*	glutathione S-transferase	1.149	0.000
PA1338	*ggt*	gamma-glutamyltranspeptidase	1.148	0.000
PA3510	PA3510	cupin domain protein	1.146	0.011
PA2998	*nqrB*	Na(+)-translocating NADH-quinone reductase subunit B	1.144	0.000
PA5553	*atpC*	ATP synthase subunit epsilon	1.141	0.000
PA5239	*rho*	transcription termination factor Rho	1.141	0.000
PA5212	PA5212	Ribonucleotide reductase, alpha subunit	1.140	0.000

PA0831	*oruR*	ornithine utilization transcriptional regulator OruR	1.135	0.010
PA2467	*fecR*	peptide ABC transporter substrate-binding protein	1.134	0.000
PA4577	PA4577	COG1734: DnaK suppressor protein	1.126	0.004
PA3686	*adk*	adenylate kinase	1.125	0.000
PA0381	*thiG*	thiazole synthase	1.124	0.000
PA5490	*cc4*	cytochrome C4	1.119	0.000
PA0897	*aruG*	arginine N-succinyltransferase subunit beta	1.115	0.000
PA1748	*fadJ*	enoyl-CoA hydratase	1.111	0.000
PA4188	*dapA*	dihydrodipicolinate synthase family protein	1.109	0.013
PA3471	*maeA*	NAD-dependent malic enzyme	1.108	0.000

PA3506	PA3506	probable decarboxylase	1.106	0.000
PA5073	PA5073	UPF0158 protein	1.105	0.002
PA5522	*puuA*	glutamine synthetase	1.104	0.000
PA4734	PA4734	histidine kinase	1.103	0.001
PA3080	PA3080	photosynthesis system II assembly factor YCF48 family protein	1.102	0.000
PA2468	*fecI*	ECF sigma factor FoxI	1.099	0.001
PA1863	*modA*	molybdenum ABC transporter substrate-binding protein ModA	1.098	0.000
PA0300	*spuD*	putrescine-binding periplasmic protein SpuD	1.096	0.000
PA4588	*gdhA*	glutamate dehydrogenase	1.094	0.001
PA4359	*feoA*	ferrous iron transporter A	1.092	0.001
PA1050	*cdaR*	CdaR family transcriptional regulator	1.089	0.000

PA3124	*yafC*	transcriptional regulator	1.088	0.001
PA1178	PA1178	PhoP/Q and low Mg2+ inducible outer membrane protein H1	1.086	0.000
PA1821	*Ech1*	enoyl-CoA hydratase	1.085	0.000
PA5152	*aotP*	ABC transporter ATP-binding protein	1.082	0.000
PA5435	*pycB*	pyruvate carboxylase subunit B	1.082	0.000
PA4993	PA4993	Cation transport ATPase	1.082	0.000
PA3942	*tesB*	acyl-CoA thioesterase	1.080	0.001
PA3194	*edd*	phosphogluconate dehydratase	1.079	0.000
PA2601	*czcR*	transcriptional regulator	1.078	0.003
PA4358	*feoB*	ferrous iron transporter B	1.076	0.000
PA0167	*rutR*	transcriptional regulator	1.073	0.001

PA0247	*pobA*	p-hydroxybenzoate hydroxylase	1.073	0.004
PA4418	*ftsI*	penicillin-binding protein 3	1.073	0.000
PA0780	*lumQ*	proline utilization regulator	1.072	0.000
PA0921	PA0921	Uncharacterized protein	1.071	0.002
PA0935	*mazG*	nucleoside triphosphate pyrophosphohydrolase	1.070	0.000
PA0212	*madD*	malonate decarboxylase subunit gamma	1.068	0.000
PA0459	*clpB*	chaperone protein ClpB	1.068	0.000
PA4345	PA4345	yceI-like domain protein	1.063	0.001
PA4643	PA4643	Uncharacterized protein PAE221_00460	1.061	0.001
PA5045	*mrcA*	penicillin-binding protein 1A	1.060	0.000

PA3822	*yajC*	preprotein translocase subunit YajC	1.056	0.000
PA1196	*rocR*	transcriptional regulator	1.054	0.000
PA3082	PA3082	glycine betaine transmethylase	1.053	0.001
PA1226	PA1226	transcriptional regulator	1.050	0.003
PA1853	*hdfR*	transcriptional regulator	1.049	0.004
PA3158	*wbpB*	UDP-N-acetyl-2-amino-2-deoxy-D-glucuronate oxidase	1.045	0.000
PA1796	*folD*	bifunctional 5,10-methylene-tetrahydrofolate dehydrogenase/ 5,10-methylene-tetrahydrofolate cyclohydrolase	1.043	0.003
PA5516	*pdxY*	pyridoxamine kinase	1.043	0.002

PA3053	*dhmA*	hydrolase	1.042	0.000
PA0449	PA0449	acyl-CoA thioesterase	1.041	0.000
PA3535	PA3535	serine protease	1.039	0.000
PA5305	*ydbL*	Uncharacterized conserved protein	1.039	0.004
PA1850	*cdhR*	transcriptional regulator	1.038	0.001
PA3539	PA3539	protein YaaA	1.037	0.000
PA4381	*czcR*	two-component response regulator	1.035	0.000
PA4788	PA4788	(R)-specific enoyl-CoA hydratase	1.034	0.000
PA3026	*eapA*	FAD binding domain protein	1.032	0.001
PA0872	*phhA*	phenylalanine 4-monooxygenase	1.031	0.000
PA1284	*bcd*	acyl-CoA dehydrogenase	1.028	0.004

PA0501	*bioF*	8-amino-7-oxononanoate synthase	1.026	0.002
PA4572	*fklB*	peptidyl-prolyl cis-trans isomerase FklB	1.024	0.000
PA5312	*puuC*	aldehyde dehydrogenase PuuC	1.024	0.000
PA0544	PA0544	metallo-dependent phosphatase	1.022	0.010
PA0140	*ahpF*	alkyl hydroperoxide reductase	1.018	0.000
PA0901	*astE*	succinylglutamate desuccinylase	1.018	0.000
PA2849	*ohrR*	OhrR	1.017	0.001
PA0810	PA0810	haloacid dehalogenase	1.016	0.004
PA4412	*murG*	UDP-N-acetylglucosamine-N-acetylmuramyl-(pentapeptide) pyrophosphoryl-	1.015	0.009

		undecaprenol N-acetylglucosamine transferase		
PA3195	*gap*	glyceraldehyde 3-phosphate dehydrogenase	1.014	0.000
PA1043	PA1043	Collagen pro alpha-chain precursor	1.013	0.002
PA0035	*trpA*	tryptophan synthase subunit alpha	1.013	0.000
PA1513	PA1513	membrane protein	1.013	0.000
PA4516	PA4516	sel1 repeat family protein	1.012	0.005
PA4370	PA4370	insulin-cleaving metalloproteinase outer membrane protein	1.011	0.000
PA5521	*fabG*	short-chain dehydrogenase	1.008	0.000
PA3895	PA3895	transcriptional regulator	1.007	0.002
PA4956	*rhdA*	thiosulfate:cyanide sulfurtransferase	1.007	0.000

PA5445	*cat1*	coenzyme A transferase	1.007	0.005
PA3637	*pyrG*	CTP synthetase	1.005	0.000